OCULAR PHARMACOLOGY: RECENT BREAKTHROUGHS AND UNMET NEEDS

EDITED BY: Claudio Bucolo, Chiara M. Eandi and Mario Damiano Toro
PUBLISHED IN: Frontiers in Pharmacology

frontiers Research Topics

ISSN 1664-8714
ISBN 978-2-88974-644-6
DOI 10.3389/978-2-88974-644-6

About Frontiers

Frontiers is more than just an open-access publisher of scholarly articles: it is a pioneering approach to the world of academia, radically improving the way scholarly research is managed. The grand vision of Frontiers is a world where all people have an equal opportunity to seek, share and generate knowledge. Frontiers provides immediate and permanent online open access to all its publications, but this alone is not enough to realize our grand goals.

Frontiers Journal Series

The Frontiers Journal Series is a multi-tier and interdisciplinary set of open-access, online journals, promising a paradigm shift from the current review, selection and dissemination processes in academic publishing. All Frontiers journals are driven by researchers for researchers; therefore, they constitute a service to the scholarly community. At the same time, the Frontiers Journal Series operates on a revolutionary invention, the tiered publishing system, initially addressing specific communities of scholars, and gradually climbing up to broader public understanding, thus serving the interests of the lay society, too.

Dedication to Quality

Each Frontiers article is a landmark of the highest quality, thanks to genuinely collaborative interactions between authors and review editors, who include some of the world's best academicians. Research must be certified by peers before entering a stream of knowledge that may eventually reach the public - and shape society; therefore, Frontiers only applies the most rigorous and unbiased reviews.
Frontiers revolutionizes research publishing by freely delivering the most outstanding research, evaluated with no bias from both the academic and social point of view. By applying the most advanced information technologies, Frontiers is catapulting scholarly publishing into a new generation.

What are Frontiers Research Topics?

Frontiers Research Topics are very popular trademarks of the Frontiers Journals Series: they are collections of at least ten articles, all centered on a particular subject. With their unique mix of varied contributions from Original Research to Review Articles, Frontiers Research Topics unify the most influential researchers, the latest key findings and historical advances in a hot research area! Find out more on how to host your own Frontiers Research Topic or contribute to one as an author by contacting the Frontiers Editorial Office: frontiersin.org/about/contact

OCULAR PHARMACOLOGY: RECENT BREAKTHROUGHS AND UNMET NEEDS

Topic Editors:
Claudio Bucolo, University of Catania, Italy
Chiara M. Eandi, Università degli Studi di Torino, Italy
Mario Damiano Toro, Medical University of Lublin, Poland

The research on ocular pharmacology has increased significantly, over the past decade. More recently, the discovery and approval of eye disease modifying treatments is considered an unbelievable scientific breakthrough. Anti-VEGF molecules, cell therapy and gene therapy for age-related retinal degeneration, autologous corneal cells replacement, and Leber's congenital amaurosis to name a few as some impressive examples.

New drugs have been recently introduced for the treatment of glaucoma focusing on new pharmacological targets, such as Rho kinase inhibitors. For example, such novel treatments have been approved for optic neuromyelitis spectrum disorders. Regarding diseases of the front of the eye, advances have been reached with approval of recombinant Nerve Growth Factor (cenegermin) for treatment of neurotrophic keratitis. New discoveries and treatments recently introduced in ophthalmology should promote new efforts and encourage research in ocular pharmacology.

It is noteworthy that several medical unmet needs remain in the field of ocular diseases, particularly for glaucoma, diabetic retinopathy (DR) and age-related macular degeneration (AMD). Early stages of DR or dry AMD need a cure and glaucoma deserves a new therapeutic approach in terms of retinal ganglion cells protection. Furthermore, current pharmacological treatments of glaucoma do not address one major issue underlying the pathology: neuroinflammation. When it comes to dry eye disorders, novel ophthalmic formulations and research findings focusing on immunomodulatory responses are welcomed to provide new insights on these conditions. Finally, one of the most challenging aspects in ocular pharmacology is related to ocular drug delivery. This Research Topic would like to address and discuss important medical unmet needs, and include a tangible contribution to handle sight threatening diseases that have a devastating impact not only for the patients but also for the healthcare system.

This Research Topic aims to translate new basic science into clinically breakthrough therapies to help patients faced with debilitating ocular diseases. The Topic welcomes submissions of Original Research, Reviews, Clinical trials, and Case Reports articles that cover the following topics, but not limited to:

- Diagnostic and prognostic biomarkers as potential pharmacological target of eye diseases (glaucoma, retinal diseases, ocular surface diseases).
- Investigation on novel pharmacological targets for treatment of diabetic retinopathy, age related macular degeneration, glaucoma and dry eye.
- New ocular drug delivery systems.

Citation: Bucolo, C., Eandi, C. M., Toro, M. D., eds. (2023). Ocular Pharmacology: Recent Breakthroughs and Unmet Needs. Lausanne: Frontiers Media SA. doi: 10.3389/978-2-88974-644-6

Table of Contents

frontiers in Pharmacology

EDITORIAL
published: 14 February 2022
doi: 10.3389/fphar.2022.848332

Editorial: Ocular Pharmacology: Recent Breakthroughs and Unmet Needs

Claudio Bucolo[1]*, *Mario Damiano Toro*[2,3] *and Chiara M. Eandi*[4,5]

[1]Department of Biomedical and Biotechnological Sciences, School of Medicine, University of Catania, Catania, Italy, [2]Chair and Department of General and Pediatric Ophthalmology, Medical University of Lublin, Lublin, Poland, [3]Eye Clinic, Public Health Department, University of Naples "Federico II", Naples, Italy, [4]Department of Ophthalmology, University of Lausanne, Fondation Asile des Aveugles, Jules Gonin Eye Hospital, Lausanne, Switzerland, [5]Department of Surgical Sciences, University of Torino, Torino, Italy

Keywords: ocular pharmacology, diabetic retinopathy, glaucoma, age-related macular degeneration (AMD), retinoblastoma, cornea

Editorial on the Research Topic

Ocular Pharmacology: Recent Breakthroughs and Unmet Needs

OPEN ACCESS

Edited and reviewed by:
Cesare Mancuso,
Catholic University of the Sacred Heart, Italy

***Correspondence:**
Claudio Bucolo
bucocla@unict.it

Specialty section:
This article was submitted to Experimental Pharmacology and Drug Discovery, a section of the journal Frontiers in Pharmacology

Received: *04 January 2022*
Accepted: *18 January 2022*
Published: *14 February 2022*

Citation:
Bucolo C, Toro MD and Eandi CM (2022) Editorial: Ocular Pharmacology: Recent Breakthroughs and Unmet Needs. Front. Pharmacol. 13:848332. doi: 10.3389/fphar.2022.848332

The research on ocular pharmacology has increased significantly over the past decade. More recently, the discovery and approval of eye disease modifying treatments is considered an unbelievable scientific breakthrough. This Research Topic "Ocular Pharmacology: Recent Breakthroughs and Unmet Needs" presents nine *original research articles*, two *reviews*, one *opinion*, and one *brief research report* from eight different Countries, and has contributions that span the field of ocular pharmacology providing new insights on recent drug breakthroughs and medical unmet needs. Most of the contributions concern the retinal conditions that have an important impact on quality-of-life and Countries health systems. Age-related macular degeneration, diabetic retinopathy and glaucoma are the diseases discussed in this Research Topic along with corneal conditions.

Four contributions are related to diabetic retinopathy and diabetic macular edema. The review by Adornetto et al. focused their work on diabetic retinopathy and autophagy, the major catabolic pathway involved in removing and recycling damaged macromolecules, suggesting that dysfunctions of this pathway contribute to the onset and progression of diabetic retinopathy and at the same time could be a good target for therapeutic approach. The authors underlined that most evidence suggests that autophagy may act with a damage/time-dependent double action: under mild stress or during the initial phase of diabetic retinopathy, autophagy acts as an adaptative response with pro-survival and anti-apoptotic effects, whereas, under severe stress and in the later phase of diabetic retinopathy, dysregulated autophagy, because of the system overload due to the prolonged damage, contributes to the apoptotic retinal cell death exacerbating the damage. The high glucose impact has been studied also by Maugeri et al. who used human retinal pigment epithelial cells, to assess the role of p38 MAPK signaling pathway and its modulation by dimethyl fumarate. They demonstrated that dimethyl fumarate treatment attenuated HG-induced apoptosis and protect retinal tissue. The authors concluded that the small molecule dimethyl fumarate represents a good candidate for diabetic retinopathy treatment and warrants further *in vivo* and clinical evaluation. Another important contribution on diabetic retinopathy has been provided by Bucolo et al. who

investigated the role of vascular endothelial growth factor (VEGF) at different phases of diabetic retinopathy using *Ins2*^{Akita} (diabetic) mice at different ages. These authors showed that the retina of the diabetic *Ins2*^{Akita} mice, as expected for mice, does not develop proliferative retinopathy even after 46 weeks. However, diabetic *Ins2*^{Akita} mice recapitulate the same evolution of patients with diabetic retinopathy in terms of both retinal neurodegeneration and pro-angiogenic shift, this latter indicated by the progressive protein expression of the pro-angiogenic isoform VEGF-A_{164}, which can be sustained by the protein kinase C betaII (PKCβII)/human antigen R (HuR) pathway acting at post-transcriptional level. In agreement with this last concept, this rise in VEGF-A_{164} protein is not paralleled by an increment of the corresponding transcript. Nevertheless, the observed increase in hypoxia inducible factor-1α (HIF-1α) at 9 weeks indicates that this transcription factor may favor, in the early phase of the disease, the transcription of other isoforms, possibly neuroprotective, in the attempt to counteract the neurodegenerative effects of VEGF-A_{164}. The authors concluded that the time-dependent VEGF-A_{164} expression in the retina of diabetic *Ins2*^{Akita} mice suggests that pharmacological intervention in diabetic retinopathy might be chosen, among other reasons, based on the specific stages of the pathology to pursue the best clinical outcome. On this regards, innovative ocular drug delivery system such as nanosytems, should be considered to address unmet medical needs (Amadio et al., 2016). Finally, the COVID-19 pandemic situation imposed huge changes in the management of retinal diseases such as diabetic macular edema with a great impact on visual outcome and cost for the patient and the public health system. Iovino et al. proposed their opinion on a possible management paradigm for the treatment of diabetic macular edema in the COVID-19 Era.

Three contributions, two *original research articles* and one *brief research report*, focused on cornea. Roszkowska et al. investigated the effect of oral supplementation with amino acids on corneal nerves regrowth after excimer laser refractive surgery with photorefractive keratectomy (PRK). These authors reported that oral supplementation with eleven amino acids improved significantly corneal nerve restoration after PRK and could thus be considered as an additional treatment during corneal surgical procedures. In an original research study, Du et al. described the corneal protective effects of a water-soluble and biocompatible small molecule, dihydropyrimidinthione derivative, against UV-B damage. Finally, *brief research report* by Bonzano et al. deals with an appropriate method, optical coherence tomography, to monitor the wound healing elicited by cenegermin, a novel recombinant human nerve growth factor, to handle neurotrophic keratitis, a rare orphan condition that affects fewer than 65,000 persons in the United States.

The study from Yousef et al. investigate the safety and efficacy of intravitreal melphalan chemotherapy as a treatment for recurrent and refractory vitreous seeds in patients with retinoblastoma. They concluded that melphalan chemotherapy is an effective and relatively safe treatment modality for retinoblastomas and has changed the outcome of eyes with vitreous seeds, significantly improving the ocular oncologists' capability to save eyes. However, there are side effects on both the anterior and posterior segments of the eye, and unexpected serious adverse reaction may occur with the standard dose of melphalan.

Two contributions deal with retinal protection and glaucoma. The first is a review leaded by Jassim et al. at University of Pennsylvania regarding the crosstalk between dysfunctional mitochondria and inflammation in glaucomatous neurodegeneration. The review discussed evidence for the interaction between mitochondrial damage and inflammation, with a focus on glaucomatous neurodegeneration, and proposed that positive feedback resulting from this crosstalk drives pathology. The authors underlined that damaged mitochondrial DNA is a damage-associated molecular pattern, which activates the nucleotide-binding domain (NOD)-like receptor protein 3 (NLRP3) inflammasome. They hypothesize that crosstalk between damaged mitochondria and increased inflammatory signaling enhances pathology in glaucomatous neurodegeneration, with implications for other complex age-dependent neurodegenerations like Alzheimer's and Parkinson's disease. The second contribution on retinal protection and glaucoma is an original research article on brimonidine, an α_{2A}-adrenergic receptor agonist approved for lowering intraocular pressure (IOP) in patients with open-angle glaucoma. The authors investigated the neuroprotective effect of the drug after retinal ischemia damage on mouse eye. They concluded that brimonidine was effective in preventing loss of function of retinal ganglion cells and in regulating inflammatory biomarkers elicited by retinal ischemia/reperfusion injury.

The retrospective study by Fasler et al. confirmed the lack of efficacy of eplerenone, an aldosterone antagonist, versus observation on resolution of subretinal fluid in patients with acute and chronic central serous chorioretinopathy in the real life. These findings are in accordance with previous report (Lotery et al., 2020). Finally, an original research contribution on brolucizumab, the new approved drug for the treatment of neovascular age-related macular degeneration, was published on the present Research Topic. The clinical pharmacological profile and safety has been demonstrated by the HAWK and HARRIER trials (Dugel et al., 2021). However, a few reports so far describe its efficacy in a routine clinical practice. Montesel et al. reported short term real-life experiences of brolucizumab intravitreal injection in a single referral center and showed very good outcomes in fluid control with similar inflammatory side effects as reported in the HAWK and HARRIER trials.

AUTHOR CONTRIBUTIONS

All authors listed have made a substantial, direct, and intellectual contribution to the work and approved it for publication.

REFERENCES

Amadio, M., Pascale, A., Cupri, S., Pignatello, R., Osera, C., D'Agata, V., et al. (2016). Nanosystems based on siRNA silencing HuR expression counteract diabetic retinopathy in rats. *Pharmacol. Res.* 111, 713–720. doi:10.1016/j.phrs.2016.07.042

Dugel, P. U., Singh, R. P., Koh, A., Ogura, Y., Weissgerber, G., Gedif, K., et al. (2021). HAWK and HARRIER: Ninety-Six-Week Outcomes from the Phase 3 Trials of Brolucizumab for Neovascular Age-Related Macular Degeneration. *Ophthalmology* 128 (1), 89–99. doi:10.1016/j.ophtha.2020.06.028

Lotery, A., Sivaprasad, S., O'Connell, A., Harris, R. A., Culliford, L., Ellis, L., et al. (2020). Eplerenone for Chronic Central Serous Chorioretinopathy in Patients with Active, Previously Untreated Disease for More Than 4 Months (VICI): A Randomised, Double-Blind, Placebo-Controlled Trial. *Lancet* 395 (10220), 294–303. doi:10.1016/S0140-6736(19)32981-2

Conflict of Interest: The authors declare that the research was conducted in the absence of any commercial or financial relationships that could be construed as a potential conflict of interest.

frontiers in Pharmacology

OPINION
published: 12 April 2021
doi: 10.3389/fphar.2021.670468

Evolving Treatment Paradigm in the Management of Diabetic Macular Edema in the Era of COVID-19

*Claudio Iovino[1], Enrico Peiretti[2], Giuseppe Giannaccare[3], Vincenzo Scorcia[3] and Adriano Carnevali[3]**

[1]Multidisciplinary Department of Medical, Surgical and Dental Sciences, University of Campania Luigi Vanvitelli, Naples, Italy, [2]Department of Surgical Sciences, Eye Clinic, University of Cagliari, Cagliari, Italy, [3]Department of Ophthalmology, University of Magna Graecia, Catanzaro, Italy

Keywords: COVID-19, intravitreal injection, diabetic macular edema, dexamethason implant, pandemic (COVID19)

OPEN ACCESS

Edited by:
Mario Damiano Toro, Medical University of Lublin, Poland

Reviewed by:
Sibel Demirel, Ankara University, Turkey
Dinah Zur, Tel Aviv Sourasky Medical Center, Israel

***Correspondence:**
Adriano Carnevali
adrianocarnevali@live.it

Specialty section:
This article was submitted to Experimental Pharmacology and Drug Discovery, a section of the journal Frontiers in Pharmacology

Received: *21 February 2021*
Accepted: *10 March 2021*
Published: *12 April 2021*

Citation:
Iovino C, Peiretti E, Giannaccare G, Scorcia V and Carnevali A (2021) Evolving Treatment Paradigm in the Management of Diabetic Macular Edema in the Era of COVID-19. Front. Pharmacol. 12:670468. doi: 10.3389/fphar.2021.670468

Intravitreal therapy is widely recognized as a major milestone in ophthalmology being one of the most commonly performed ocular procedures (He et al., 2018). The spread of coronavirus disease (COVID-19) still represents an important public health problem worldwide (Ferrara et al., 2020; Wang et al., 2020). This novel virus infection, is causing a significant downsizing of non-urgent treatments provided for ocular disorders (Tognetto et al., 2020; Toro M. D. et al., 2020, Toro M. et al., 2020), including intravitreal therapy (Elfalah et al., 2021).

Since diabetic retinopathy (DR) still remains the leading cause of blindness among working-age adults (Ting et al., 2016), ophthalmologists should be aware of the potential negative effects of COVID-19 restrictions in the management of diabetic patients in the next months.

The global COVID-19 pandemic led many governments from different nations to adopt protective and strict measures to reduce its spread. In these unprecedented circumstances, many healthcare systems are overwhelmed and under stress.

In this scenario, there is an urgent need to support ophthalmologists who are treating patients with intravitreal injections in decision-making protocols. In order to provide continuity of care, and to reduce the risk of contamination, series of protection measures have been proposed (Iovino et al., 2020a; Borrelli et al., 2020; Korobelnik et al., 2020). Nevertheless, many patients cannot receive a prompt therapy due to all public health restriction measures. During COVID-19 outbreak Carnevali et al. proposed treatment priority levels to treat the most urgent patients, although a drop of 91.7% of the injections performed compared to the same period of 2019 was registered (Carnevali et al., 2020).

Diabetic patients are considered at high risk for COVID-19 complications and should not be exposed to avoidable risks, including the injections procedure itself. However, continuation of care, where possible, is important to avoid irreversible vision loss.

For non-monocular patients with diabetic macular edema (DME), postponement (>4–6 months) of appointments has been proposed (Korobelnik et al., 2020). As recently reported, postponing treatment in patients with good visual acuity does not affect the prognosis at 1 year, regardless of whether the DME was treated or not (Busch et al., 2019). Conversely, in patients with more advanced DR and worse visual acuity, a delay in treatments could cause irreversible visual loss (Ting et al., 2016; Elfalah et al., 2021).

Anti-vascular endothelial growth factor (VEGF) injections represent generally a first-line therapy for several retinal disorders including DME (Heier et al., 2012; Reibaldi et al., 2014; Schmidt-Erfurth et al., 2017; Plyukhova et al., 2020), but monthly injections are needed at least during the loading dose (Schmidt-Erfurth et al., 2017). Of note, intravitreal dexamethasone (DEX) implant 0.7 mg (Ozurdex®, Allergan, Inc. Irvine, CA, United States) is considered a valid alternative for both refractory to anti-VEGF treatment eyes and treatment naïve ones (Iglicki et al., 2019; Iovino et al.,

2020b). Intravitreal DEX implant releases active ingredients within the vitreous chamber over a 3–6 months period, and its efficacy and safety in various retinal diseases have been proved in clinical trials and real-life studies (Maturi et al., 2016; Rajesh et al., 2020). Several authors also reported significant anatomical and functional effects of DEX implant in vitrectomized eyes in different conditions (Boyer et al., 2011; Reibaldi et al., 2012; Iovino et al., 2019). Corticosteroids have multiple levels of action, modifying tight junction integrity, inhibiting different molecules involved in vascular permeability and inflammation processes including interleukin-6, stroma-derived factor-1, Intercellular adhesion molecule-1, as well as VEGF (Iovino et al., 2020b).

All these mechanisms of action work in aggregate, resulting in decreased macular edema and VEGF production, fibrin deposition, capillary leakage and migration of inflammatory cells (Gagliano et al., 2015). There is evidence that oxidative stress, ischemia and inflammation promote the initiation and progression of DR (Toro et al., 2019), further supporting the role of DEX implant in controlling the progression of the DME (Ceravolo et al., 2020).

Cataract progression and intraocular pressure rise are the most common side effects, but often rather easily manageable (Iovino et al., 2020b; Rajesh et al., 2020). Additionally, several optical coherence tomography (OCT) biomarkers were identified as functional outcome predictors in DME eyes treated with DEX implant including the presence of submacular fluid, absence of hyperreflective intraretinal foci and integrity of the ellipsoid zone (Zur et al., 2018).

On this background, a good selection of patients with DME who can benefit from observation or a single intravitreal DEX injection rather than monthly anti-VEGF injections, could be of great importance in reducing the burden of injections of clinics and hospitals. Treating eligible subjects with DME showing the previously mentioned OCT biomarkers, could indeed reduce the burden of care delivery for patients and health system. Considering that the IOP increase after the injection is typically noticed within the first 2 weeks, IOP lowering eye drops together with a post-injection visit should be taken into account for patients with high risk for glaucoma.

Almost one year is gone since the WHO declared the global pandemic and new more contagious virus variants are now emerging. Physicians may be dealing with this emergency status for the next 1 or 2 years.

In our opinion, by tailoring the treatment to patients in most need, equity can be considered the ethical value that support the decisionmaking by the treating provider.

Although an evidence-based clinical practice guideline for intravitreal injections is not yet available, we believe that these considerations about management of diabetic patients with DME, could be useful for ophthalmologists from most affected countries who will be under public health COVID-19 measures and restrictions for the next months. Saving costs, resources and time is an important goal for all health workers who are facing this common enemy in first line.

AUTHOR CONTRIBUTIONS

CI wrote the first draft of the manuscript. EP, GG, VS, and AC checked and revised the draft manuscript. All authors contributed read, revised, and approved the submitted version.

REFERENCES

Borrelli, E., Sacconi, R., Querques, L., Zucchiatti, I., Prascina, F., Bandello, F., et al. (2020). Taking the right measures to control COVID-19 in ophthalmology: the experience of a tertiary eye care referral center in Italy. *Eye* 34, 1175. doi:10.1038/s41433-020-0880-6

Boyer, D. S., Faber, D., Gupta, S., Patel, S. S., Tabandeh, H., Li, X.-Y., et al. (2011). Dexamethasone intravitreal implant for treatment OF diabetic macular edema IN vitrectomized patients. *Retina* 31, 915–923. doi:10.1097/IAE.0b013e318206d18c

Busch, C., Fraser-Bell, S., Iglicki, M., Lupidi, M., Couturier, A., Chaikitmongkol, V., et al. (2019). Real-world outcomes of non-responding diabetic macular edema treated with continued anti-VEGF therapy versus early switch to dexamethasone implant: 2-year results. *Acta Diabetol.* 56, 1341–1350. doi:10.1007/s00592-019-01416-4

Carnevali, A., Giannaccare, G., Gatti, V., Scuteri, G., Randazzo, G., and Scorcia, V. (2020). Intravitreal injections during COVID-19 outbreak: real-world experience from an Italian tertiary referral center. *Eur. J. Ophthalmol.* 31. doi:10.1177/1120672120962032

Ceravolo, I., Oliverio, G. W., Alibrandi, A., Bhatti, A., Trombetta, L., Rejdak, R., et al. (2020). The application of structural retinal biomarkers to evaluate the effect of intravitreal ranibizumab and dexamethasone intravitreal implant on treatment of diabetic macular edema. *Diagnostics* 10. doi:10.3390/diagnostics10060413

Elfalah, M., AlRyalat, S. A., Toro, M. D., Rejdak, R., Zweifel, S., Nazzal, R., et al. (2021). Delayed intravitreal anti-VEGF therapy for patients during the COVID-19 lockdown: an ethical endeavor. *Clin. Ophthalmol.* 15, 661–669. doi:10.2147/OPTH.S289068

Ferrara, M., Romano, V., Steel, D. H., Gupta, R., Iovino, C., van Dijk, E. H. C., et al. (2020). Reshaping ophthalmology training after COVID-19 pandemic. *Eye* 34, 2089. doi:10.1038/s41433-020-1061-3

Gagliano, C., Toro, M., Avitabile, T., Stella, S., and Uva, M. (2015). Intravitreal steroids for the prevention of PVR after surgery for retinal detachment. *Curr. Pharm. Des.* 21, 4698–4702. doi:10.2174/1381612821666150909100212

He, Y., Ren, X. J., Hu, B. J., Lam, W. C., and Li, X. R. (2018). A meta-analysis of the effect of a dexamethasone intravitreal implant versus intravitreal anti-vascular endothelial growth factor treatment for diabetic macular edema. *BMC Ophthalmol.* 18, 121. doi:10.1186/s12886-018-0779-1

Heier, J. S., Brown, D. M., Chong, V., Korobelnik, J. F., Kaiser, P. K., Nguyen, Q. D., et al. (2012). Intravitreal aflibercept (VEGF trap-eye) in wet age-related macular degeneration. *Ophthalmology* 119, 2537–2548. doi:10.1016/j.ophtha.2012.09.006

Iglicki, M., Busch, C., Zur, D., Okada, M., Mariussi, M., Chhablani, J. K., et al. (2019). Dexamethasone implant for diabetic macular edema in naive compared with refractory eyes: the international retina group real-life 24-month multicenter study: the irgrel-dex study. *Retina* 39, 44–51. doi:10.1097/IAE.0000000000002196

Iovino, C., Caporossi, T., and Peiretti, E. (2020a). Vitreoretinal surgery tip and tricks in the era of COVID-19. *Graefes Arch. Clin. Exp. Ophthalmol.* 258, 2869. doi:10.1007/s00417-020-04800-x

Iovino, C., Giannaccare, G., Pellegrini, M., Bernabei, F., Braghiroli, M., Caporossi, T., et al. (2019). Efficacy and safety of combined vitrectomy with intravitreal dexamethasone implant for advanced stage epiretinal membrane. *Drug Des. Devel. Ther.* 13, 4107–4114. doi:10.2147/DDDT.S229031

Iovino, C., Mastropasqua, R., Lupidi, M., Bacherini, D., Pellegrini, M., Bernabei, F., et al. (2020b). Intravitreal dexamethasone implant as a sustained release Drug delivery device for the treatment of ocular diseases: a comprehensive review of the literature. *Pharmaceutics* 12, 703. doi:10.3390/pharmaceutics12080703

Korobelnik, J.-F., Loewenstein, A., Eldem, B., Joussen, A. M., Koh, A., Lambrou, G. N., et al. (2020). Guidance for anti-VEGF intravitreal injections during the COVID-19 pandemic. *Graefe's Arch. Clin. Exp. Ophthalmol.* 258, 1–8. doi:10.1007/s00417-020-04703-x

Maturi, R. K., Pollack, A., Uy, H. S., Varano, M., Gomes, A. M. V., Li, X. Y., et al. (2016). Intraocular pressure in patients with diabetic macular edema treated with dexamethasone intravitreal implant in the 3-year mead study. *Retina* 36, 1143–1152. doi:10.1097/IAE.0000000000001004

Plyukhova, A. A., Budzinskaya, M. V., Starostin, K. M., Rejdak, R., Bucolo, C., Reibaldi, M., et al. (2020). Comparative safety of bevacizumab, ranibizumab, and aflibercept for treatment of neovascular age-related macular degeneration (amd): a systematic review and network meta-analysis of direct comparative studies. *J. Clin. Med.* 9, 1522. doi:10.3390/jcm9051522

Rajesh, B., Zarranz-Ventura, J., Fung, A. T., Busch, C., Sahoo, N. K., Rodriguez-Valdes, P. J., et al. (2020). Safety of 6000 intravitreal dexamethasone implants. *Br. J. Ophthalmol.* 104, 39–46. doi:10.1136/bjophthalmol-2019-313991

Reibaldi, M., Russo, A., Avitabile, T., Uva, M. G., Franco, L., Longo, A., et al. (2014). Treatment of persistent serous retinal detachment in vogt-koyanagi-harada syndrome with intravitreal bevacizumab during the systemic steroid treatment. *Retina* 34, 490–496. doi:10.1097/IAE.0b013e3182a0e446

Reibaldi, M., Russo, A., Zagari, M., Toro, M., De Grande, V., Cifalinò, V., et al. (2012). Resolution of persistent cystoid macular edema due to central retinal vein occlusion in a vitrectomized eye following intravitreal implant of dexamethasone 0.7 mg. *Case Rep. Ophthalmol.* 3, 30–34. doi:10.1159/000336273

Schmidt-Erfurth, U., Garcia-Arumi, J., Bandello, F., Berg, K., Chakravarthy, U., Gerendas, B. S., et al. (2017). Guidelines for the management of diabetic macular edema by the European Society of Retina Specialists (EURETINA). *Ophthalmologica* 237, 185–222. doi:10.1159/000458539

Ting, D. S. W., Cheung, G. C. M., and Wong, T. Y. (2016). Diabetic retinopathy: global prevalence, major risk factors, screening practices and public health challenges: a review. *Clin. Exp. Ophthalmol.* 44, 260–277. doi:10.1111/ceo.12696

Tognetto, D., Brézin, A. P., Cummings, A. B., Malyugin, B. E., Evren Kemer, O., Prieto, I., et al. (2020). Rethinking elective cataract surgery diagnostics, assessments, and tools after the COVID-19 pandemic experience and beyond: insights from the EUROCOVCAT group. *Diagnostics* 10, 1035. doi:10.3390/diagnostics10121035

Toro, M., Choragiewicz, T., Posarelli, C., Figus, M., and Rejdak, R. (2020). Early impact of covid-19 outbreak on the availability of cornea donors: warnings and recommendations. *Clin. Ophthalmol.* 14, 2879–2882. doi:10.2147/OPTH.S260960

Toro, M. D., Brézin, A. P., Burdon, M., Cummings, A. B., Evren Kemer, O., Malyugin, B. E., et al. (2020). Early impact of COVID-19 outbreak on eye care: insights from EUROCOVCAT group. *Eur. J. Ophthalmol.* 31. doi:10.1177/1120672120960339

Toro, M. D., Nowomiejska, K., Avitabile, T., Rejdak, R., Tripodi, S., Porta, A., et al. (2019). Effect of resveratrol on *in vitro* and *in vivo* models of diabetic retinopathy: a systematic review. *Int. J. Mol. Sci.* 20. doi:10.3390/ijms20143503

Wang, C., Horby, P. W., Hayden, F. G., and Gao, G. F. (2020). A novel coronavirus outbreak of global health concern. *Lancet* 395, 470–473. doi:10.1016/S0140-6736(20)30185-9

Zur, D., Iglicki, M., Busch, C., Invernizzi, A., Mariussi, M., Loewenstein, A., et al. (2018). "OCT biomarkers as functional outcome predictors in diabetic macular edema treated with dexamethasone implant," in *Ophthalmology* (Elsevier Inc.)), 267–275. doi:10.1016/j.ophtha.2017.08.031

Conflict of Interest: The authors declare that the research was conducted in the absence of any commercial or financial relationships that could be construed as a potential conflict of interest.

frontiers in Pharmacology

ORIGINAL RESEARCH
published: 07 May 2021
doi: 10.3389/fphar.2021.684680

Attenuation of High Glucose-Induced Damage in RPE Cells through p38 MAPK Signaling Pathway Inhibition

Grazia Maugeri[1], Claudio Bucolo[2,3], Filippo Drago[2,3], Settimio Rossi[4], Michelino Di Rosa[1], Rosa Imbesi[1], Velia D'Agata[1] and Salvatore Giunta[1]*

[1]Section of Anatomy, Histology and Movement Sciences, Department of Biomedical and Biotechnological Sciences, University of Catania, Catania, Italy, [2]Pharmacology Section, Department of Biomedical and Biotechnological Sciences, University of Catania, Catania, Italy, [3]Center for Research in Ocular Pharmacology (CERFO), University of Catania, Catania, Italy, [4]Eye Clinic, Multidisciplinary Department of Medical, Surgical and Dental Sciences, University of Campania "Luigi Vanvitelli", Napoli, Italy

This study aimed to investigate the high glucose damage on human retinal pigment epithelial (RPE) cells, the role of p38 MAPK signaling pathway and how dimethyl fumarate can regulate that. We carried out *in vitro* studies on ARPE-19 cells exposed to physiological and high glucose (HG) conditions, to evaluate the effects of DMF on cell viability, apoptosis, and expression of inflammatory and angiogenic biomarkers such as COX-2, iNOS, IL-1β, and VEGF. Our data have demonstrated that DMF treatment attenuated HG-induced apoptosis, as confirmed by reduction of BAX/Bcl-2 ratio. Furthermore, in RPE cells exposed to HG we observed a significant increase of iNOS, COX-2, and IL-1β expression, that was reverted by DMF treatment. Moreover, DMF reduced the VEGF levels elicited by HG, inhibiting p38 MAPK signaling pathway. The present study demonstrated that DMF provides a remarkable protection against high glucose-induced damage in RPE cells through p38 MAPK inhibition and the subsequent down-regulation of VEGF levels, suggesting that DMF is a small molecule that represents a good candidate for diabetic retinopathy treatment and warrants further *in vivo* and clinical evaluation.

Keywords: retinal pigment epithelial cells, diabetic retinopathy, VEGF, dimethyl fumarate, p38 MAPK, retina

OPEN ACCESS

Edited by:
Cesare Mancuso, Catholic University of the Sacred Heart, Italy

Reviewed by:
Tamas Atlasz, University of Pécs, Hungary
Germano Guerra, University of Molise, Italy

****Correspondence:***
Claudio Bucolo
claudio.bucolo@unict.it

Specialty section:
This article was submitted to Experimental Pharmacology and Drug Discovery, a section of the journal Frontiers in Pharmacology

Received: *23 March 2021*
Accepted: *26 April 2021*
Published: *07 May 2021*

Citation:
Maugeri G, Bucolo C, Drago F, Rossi S, Di Rosa M, Imbesi R, D'Agata V and Giunta S (2021) Attenuation of High Glucose-Induced Damage in RPE Cells through p38 MAPK Signaling Pathway Inhibition. Front. Pharmacol. 12:684680. doi: 10.3389/fphar.2021.684680

INTRODUCTION

Diabetic retinopathy (DR) is the leading cause of visual impairment and preventable blindness, and it represents an important cost in terms of social and economic issues for health care systems worldwide. Vision loss is associated with retinal pigment epithelial (RPE) damage, these retinal cells play a key role in terms of protection and functional maintenance of photoreceptors (Plafker et al., 2012). Pre-clinical studies and clinical trials showed that hyperglycemia represents the primary risk factor leading to DR (Cade, 2008). It has been observed that sustained hyperglycemia promotes the activation of both apoptotic (Kowluru et al., 2004) and inflammatory mechanisms (Yuuki et al., 2001) as well as dysregulation of growth factors and hypoxia-inducible factors (Grant et al., 2004; Schlingemann, 2004; D'Amico et al., 2015). Upregulation of cytokines and other proinflammatory mediators inducing chronic inflammation, is believed to actively contribute to the DR-associated damage to the retinal vasculature (Zheng and Kern, 2009; Boss et al., 2017) also by triggering apoptosis of RPE cells and promotion of retinal neovascularization (Kim et al., 2015; Xiao et al., 2017).

The vascular endothelial growth factor (VEGF) triggers the angiogenesis modulating vascular permeability, and it is hypothesized as the key factor in the pathogenesis of DR and diabetic macular edema (Giurdanella et al., 2015; Platania et al., 2015; Bolinger and Antonetti, 2016; Bucolo et al., 2018). The expression of VEGF by RPE cells has been analyzed in different studies, and the results have contributed to our knowledge on the involvement RPE cells in the pathophysiology of DR (Saishin et al., 2003; Campochiaro, 2013). Elevated VEGF levels were obtained in vitreous, aqueous, and subretinal fluid of patients with DR and other retinal disorders, even though VEGF levels were different in patients affected by proliferative and non-proliferative DR (Aiello et al., 1994; Rubio and Adamis, 2016). Angiogenesis and inflammation are two important components implicated in the pathogenesis of DR (Bucolo et al., 2013; D'Amico et al., 2015; Platania et al., 2017). Recent studies provided evidence that dimethyl-fumarate (DMF) has a strong anti-inflammatory action, although the effect of DMF on angiogenesis is unknown. Interestingly, Zhao et al. (2014) has demonstrated that DMF can affect the release of VEGF.

DMF is an efficient immunomodulatory drug, approved in clinical practice for the treatment of relapsing–remitting multiple sclerosis and psoriasis. The primary pharmacodynamic response to DMF treatment is activation of HO-1 gene through the regulation of nuclear factor erythroid-2–related factor-2 (Nrf2). However, DMF seems to have several biological effects as it has been shown to also inhibit the phosphorylated p38 MAPK (Nishioku et al., 2020; Kortam et al., 2021) thus blocking downstream targets that may be involved in the development and progression of inflammatory cascades leading to numerous diseases. In fact, it has been demonstrated that the activation of p38 MAPK signaling is required for VEGF expression in response to growth factors and cytokines stimulation (Gomes and Rockwell, 2008; Sakai et al., 2017).

In the present study we explored the hypothesis that the DMF is able to interfere with p38 MAPK signaling and consequently down-regulate VEGF levels in RPE cells exposed to high glucose damage. To address this issue, we carried out *in vitro* studies on human RPE cells exposed to normal (NG) or high (HG) glucose conditions, in order to figure out the effects of DMF on cell viability, apoptosis and expression of inflammatory and angiogenic biomarkers such as COX-2, iNOS, IL-1β, and VEGF.

MATERIALS AND METHODS

Cells

This study was performed on human retinal pigment epithelial cell culture (ARPE-19) purchased from the American Type Culture Collection (Rockville, United States). Cells cultured in DMEM:F12 medium containing 10% fetal bovine serum (FBS), 100 U/ml penicillin, 10 μg/ml streptomycin, were incubated at 37°C in a humidified atmosphere with 5% CO_2. Once cells reached confluence, they were exposed to normal glucose condition (NG, 5.5 mM D-glucose) or to high glucose (HG, 25 mM D-glucose) in order to mimic physiological or hyperglycemic conditions, respectively (Maugeri et al., 2017). To exclude any potential bias by an osmotic effect, a separate control group of cells were also grown in NG medium plus mannitol (5.5 mM D-glucose and 19.5 mM mannitol vs. 25mM D-glucose). All experiments and measurements described below were performed in parallel in NG and HG conditions.

Chemicals and Reagents

Dimethyl fumarate (DMF) was obtained by Sigma-Aldrich (St. Louis, MO, United States). A selective p38 MAP kinase inhibitor SB202190 was purchased from Abcam (Cambridge, United Kingdom). All other chemicals and reagents were purchased by Sigma-Aldrich unless otherwise stated. The stock solution of DMF was prepared using DMSO and diluted with cell culture medium to obtain final dose for each treatment. As indicated, vehicle (0.2% v/v DMSO) corresponds to the amount present in the highest dosage and was used in all experiments to exclude unspecific and toxic effects.

Cell Viability

Cell viability was measured using the cell proliferation kit I (MTT) according to manufacturer's procedures (Roche, Basel, Switzerland) (Maugeri et al., 2018a). Cells were seeded into 96-well plates at a density of 1×10^4 cells/well. After the treatments, medium containing 0.5 mg/ml 3-[4,5-dimethylthiazol-2-yl]-2,5-diphenyltetrazolium bromide (MTT) (Sigma Aldrich, St. Louis, MO, United States) was added in each well. Following incubation for 4 h at 37°C, medium was removed, and 100 μL of DMSO was added. Formazan generated by the cleavage of the yellow tetrazolium salt MTT was measured at 570 nm using a microplate reader (BioRad Laboratories, Milan, Italy).

Apoptotis

The effects of HG and DMF on apoptosis and nuclear morphology in the cells were assessed by the use of fluorescence microscopy with the nuclear dye Hoechst 33,258 as previously described (Bucolo et al., 2019). After indicated treatment, cells were fixed with a solution of methanol/acetic acid (3:1 v/v) for 30 min, washed with ice-cold PBS and stained for 15 min at 37°C with 0.4 μg/ml Hoechst 33,258 dye. After being rinsed in water, cells were observed under an Axiovert 40 fluorescence microscope (Carl Zeiss Inc., Thornwood, NY, United States). Apoptosis and nuclear morphology were identified by condensation of nuclear chromatin and its fragmentation. Each condition was reproduced in three dishes per experiment. Both apoptotic and normal cells were determined by analyzing at least three different fields per dish in a fixed pattern.

ELISA

IL-1ß and VEGF levels were assessed by ELISA analysis, performed in fresh supernatant derived from serum-free media of cells cultured with or without treatments. Briefly, cell supernatant was collected through centrifugation (500 Å~ g, 5 min, 4°C). The levels of IL-1β and VEGF in the supernatant (100 μL) of ARPE-19 cells were detected using sandwich ELISA kits according to the manufacturer's protocol of each kit (DY201, R&D Systems, Minneapolis, United States, and ENZ-KIT156-0001, Enzo Life Science, Milano, Italy, respectively).

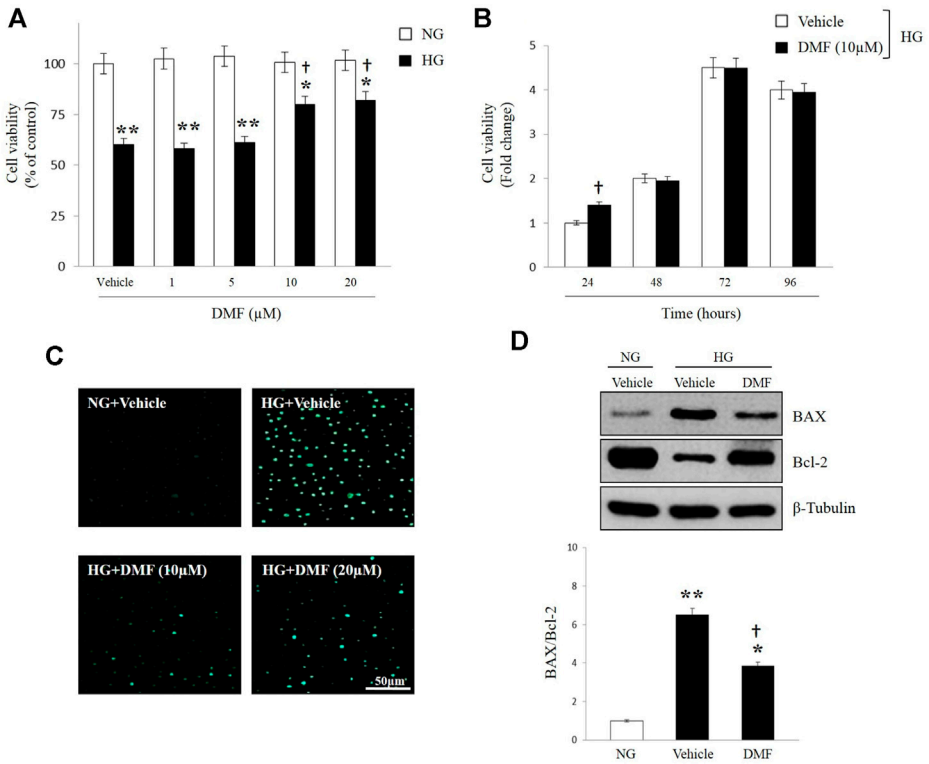

FIGURE 1 | Effects of DMF on RPE cells viability. ARPE-19 cells exposed to normal glucose (NG) or high glucose (HG) w/or w/o DMF. Cell viability **(A,B)**, DNA damage **(C)** BAX and Bcl-2 protein expression **(D)** were assessed. **(A,B)** MTT analyses: values are expressed as percentage of cell viability of NG treated-vehicle group (Vehicle/NG) or Fold change ± SEM. (n = 6; *p < 0.05 or **p < 0.01 vs. Vehicle/NG; †p < 0.05 vs. Vehicle/HG. **(C)** Apoptotic assay by nuclear staining: Representative photomicrographs of ARPE cells exposed to NG and HG and treated with 10 or 20 μM DMF up to 24 h. Cells were stained with the fluorescent nuclear dye Hoechst 33,258 and observed at ×40 magnification. Scale bar = 50 μm. (**D**) Western blot analyses of BAX and Bcl-2 in ARPE cells exposed to HG w/or w/o DMF (10 μM) for 24 h. Band densities were quantified by ImageQuantTL software and normalized values were indicated below each corresponding band. Normalized band density values in control groups (NG) were set to 1. *p < 0.05 or **p < 0.01 vs. NG; †p < 0.01 vs. Vehicle/HG; n = 6.

Western Blot

Protein extracts were detected by western blot as previously described by D'Amico et al. (2018). Primary antibodies: BAX (sc-493, Santa Cruz Biotechnology, Inc, CA, United States), Bcl-2 (sc-509, Santa Cruz Biotechnology, Inc, CA, United States), COX-2 (sc-19999, Santa Cruz Biotechnology, Inc, CA, United States), iNOS (sc-651, Santa Cruz Biotechnology, Inc, CA, United States), p38 MAPK (#9212, Cell Signaling Technology, United States), p-p38 MAPK (Thr180/Tyr182) (#9211, Cell Signaling Technology, United States) and β-tubulin (sc-9104, Santa Cruz Biotechnology, Inc, CA, United States). Secondary antibodies: goat anti-Rabbit IRDye 680 (cat #926-68021, LI-COR Biosciences, Lincoln, NE, United States) and goat anti-Mouse IRDye 800CW (cat #926-32210, LI-COR Biosciences, Lincoln, NE, United States).

Immunolocalization

The cellular distribution of VEGF was detected by immunofluorescence assay as described in a previous study (Maugeri et al., 2018b). Cells cultured on slides, were rinsed with PBS and then fixed in 4% paraformaldehyde in PBS, permeabilized with 0.2% Triton X100, blocked with 0.1% BSA in PBS, and then incubated with anti-VEGFA antibody (ab1316, Abcam, Cambridge United Kingdom). The fixed cells were then washed, and Alexa Fluor 594-conjugated secondary antibodies (Thermo, United States) were used to stain the corresponding primary antibodies for 1.5 h at 37°C. After a sequence of washes, the fixed cells were cover-slipped with vecta-shield mounting medium (Vector Laboratories, Inc, Burlingame, CA, United States). Ten fields from randomly selected slides were visualized using an Axiovert 40 epifluorescence microscope (Carl Zeiss Inc, Thornwood, NY, United States) at ×40 magnification and images of each field were captured using a digital camera (Canon, Ōta, Tokyo, Japan).

Semi-Quantitative Reverse Transcription–Polymerase Chain Reaction (RT-PCR)

Semi-quantitative RT-PCR was performed as described in detail in an earlier report (Castorina et al., 2010). Total cellular RNA was isolated through the use of 1 ml TRIzol reagent (Invitrogen), 0.2 ml chloroform and precipitated with 0.5 ml isopropanol. Aliquots of cDNA were amplified using specific primers

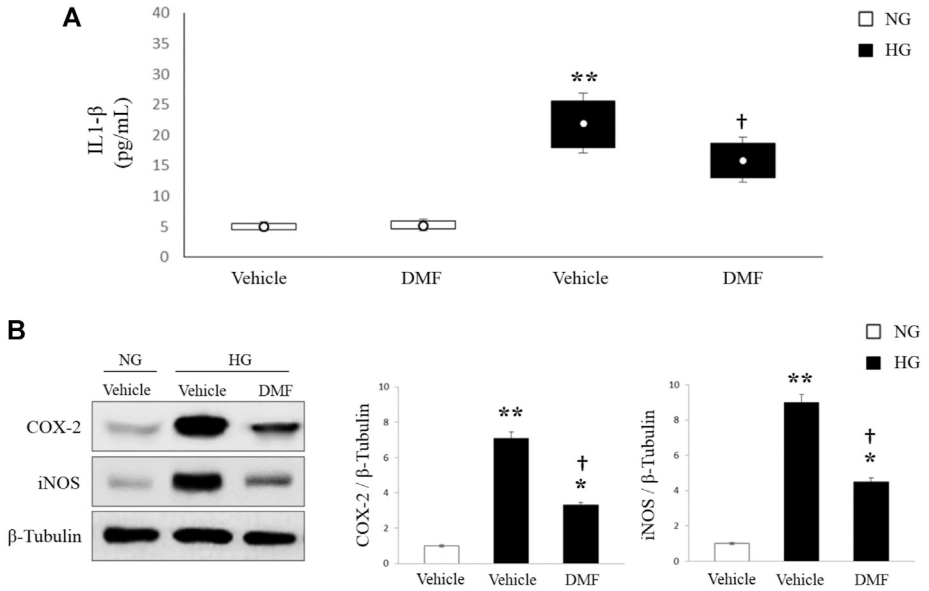

FIGURE 2 | Effects of DMF on inflammatory cascade of ARPE-19 cells. ARPE-19 cells exposed to normal glucose (NG) or high glucose (HG) w/or w/o DMF for 24 h. **(A)** IL-1ß production was measured through ELISA. (n = 6, $^{**}p < 0.01$ vs. Vehicle/NG; †$p < 0.05$ vs. Vehicle/HG). (**B**) Western blot: COX-2 and iNOS expression proteins. Band densities were quantified by ImageQuantTL software and normalized values were indicated below each corresponding band. $^{*}p < 0.05$ or $^{**}p < 0.01$ vs. Vehicle/NG; †$p < 0.05$ vs. Vehicle/HG; n = 6.

matching the reported sequence of human VEGF and ribosomal protein S18 (RPS18), used as reference gene. The primers used were the following: VEGF (forward: 5′-GAAGTGGTGAAGTTC ATGGA-3′; reverse: 3′-GCCTTGCAACGCGAGTCTGT-5′) and RPS18 (forward: 5′-GAGGATGAGGTGGAACGTGT-3′; reverse: 3′-GGACCTGGCTGTATTTTCCA-5′). Semi-quantification of the density of each band was done by ImageJ software (US National Institutes of Health).

Statistical Analysis

GraphPad InStat version 3.00 (GraphPad Software Inc, San Diego CA, United States) was used to analyze the experimental data. All the data are expressed as mean ± SEM. The data from multiple groups were analyzed by one-way ANOVA and statistical significance was assessed by Tukey-Kramer post-hoc test, unless otherwise indicated. The level of significance accepted for all statistical tests was $p \leq 0.05$.

RESULTS

Anti-Apoptotic Effect of DMF on RPE Cells Exposed to High Glucose

DMF effect on human RPE cells survival exposed to HG insult, was evaluated through MTT assay. ARPE-19 cells were cultured in NG or HG and exposed to different concentration of DMF (1, 5, 10, and 20 μM) for 24 h. As shown in **Figure 1A**, HG exposure significantly reduced cells viability as compared to cells grown in NG ($p < 0.01$ vs. Vehicle/NG). Treatment with DMF attenuated this effect in a dose-dependent manner with significant values at concentrations of 10 and 20 μM ($p < 0.05$ vs. Vehicle/HG). The effect of DMF was also studied in a time-dependent manner. ARPE-19 cells were incubated for 24, 48, 72, and 96 h in HG condition and treated with 10 μM of DMF. As shown in **Figure 1B**, DMF significantly increased cells viability at 24 h as compared to vehicle ($p < 0.05$ vs. Vehicle/HG).

In order to evaluate if high glucose levels induced the activation of apoptotic process and to investigate the possible protective role of DMF, ARPE-19 cells were exposed to NG or HG with or without DMF and assayed for DNA fragmentation. Representative images in **Figure 1C** showed the morphological signs of nuclear damage (as determined by Hoechst 33,258 staining) in response to HG exposure for 24 h. On the contrary, cells cultured under high glucose insult and treated with 10 or 20 μM of DMF generated only slight DNA damage, which was greatest at 10 μM of concentration. The anti-apoptotic effect of DMF was confirmed by western blot analysis. **Figure 1D** showed that BAX (proapoptotic)/Bcl-2 (antiapoptotic) ratio was significantly increased in HG exposed cells as compared to ARPE-19 cultured in NG ($p < 0.05$ or $p < 0.01$ vs. NG). As expected, DMF treatment significantly reduced BAX/Bcl-2 ratio ($p < 0.05$ vs. Vehicle/HG).

Effect of DMF on Inflammatory Process of RPE Cells

Increase of inflammatory process and production of pro-inflammatory cytokines was largely demonstrated in the vitreous of diabetic patients, in the retina of STZ-induced diabetic rats and also in the RPE cells under high glucose conditions. According with these findings (**Figure 2A**) we found high levels of IL-1ß in ARPE-19 cells exposed to HG

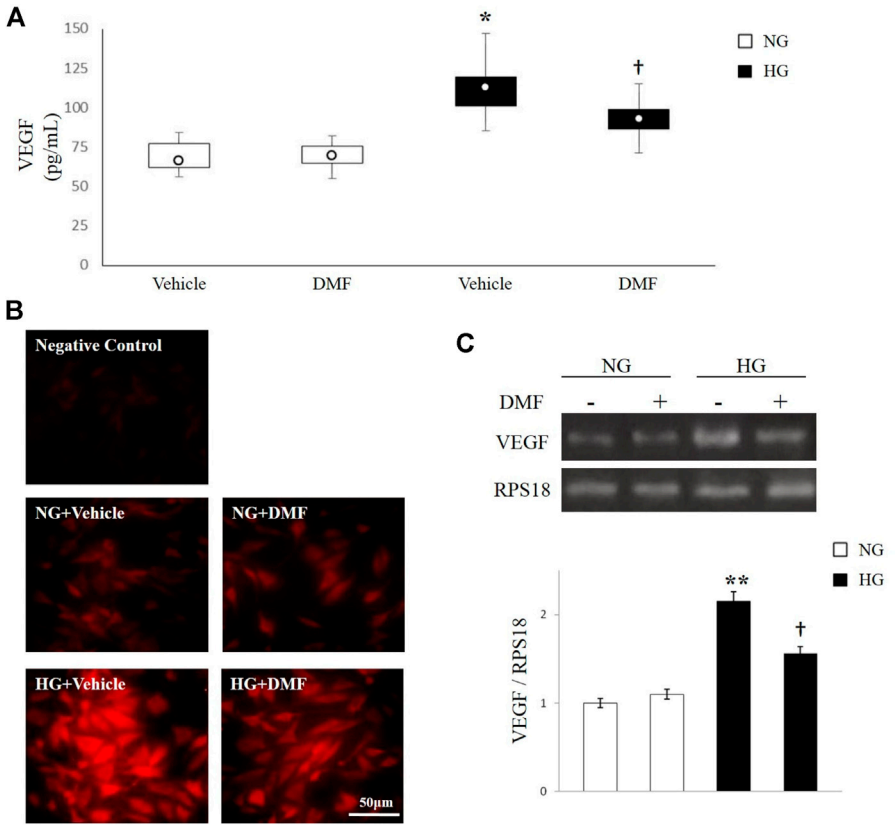

FIGURE 3 | Effects of DMF on VEGF levels. ARPE-19 cells exposed to normal glucose (NG) or high glucose (HG) w/or w/o DMF (10 μM) for 24 h. **(A)** VEGF production was measured through ELISA. *$p < 0.05$ vs. Vehicle/NG; †$p < 0.05$ vs. Vehicle/HG; $n = 6$. **(B)** Representative photomicrographs showing VEGF expression (red). Photomicrographs are representative results of fields taken randomly from each slide and observed by Axiovert 40 epifluorescence microscope (magnification ×40). **(C)** Semi-quantitative RT-PCR shows VEGF mRNA expression normalized to the ribosomal protein S18 (RPS18, housekeeping gene). **$p < 0.01$ vs. NG untreated cells, †$p < 0.05$ vs. untreated/HG; $n = 6$.

($p < 0.01$ vs. Vehicle/NG). Interestingly, treatment of HG-cultured cells with DMF (10 μM) significantly reduced the release of this pro-inflammatory cytokine ($p < 0.05$ vs. Vehicle/HG).

Considering that IL-1ß is a trigger of the neuroinflammatory cascade stimulating COX enzymes and iNOS, we analyzed through western blot the expression levels of iNOS and COX-2 proteins. As shown in **Figure 2B**, iNOS and COX-2 expression levels were significantly increased in ARPE-19 cells grown in HG as compared to NG cultured cells ($p < 0.01$ vs. NG). Interestingly, treatment with 10 μM of DMF significantly reduced the expression of both inflammatory mediators ($p < 0.05$ vs. Vehicle/HG).

Effect of DMF on VEGF Expression in ARPE-19 Cells

It is well known that hyperglycemia triggers angiogenesis in RPE cells. Here, we evaluated the effect of DMF on VEGF production in ARPE-19 cells exposed to high glucose insult through ELISA, immunofluorescence analysis and semi-quantitative RT-PCR. As shown in **Figure 3A**, the levels of VEGF in the culture media of ARPE-19 cells exposed to high glucose conditions significantly increased in comparison with NG exposed cells ($p < 0.05$ vs. Vehicle/NG). Conversely, DMF treatment significantly reduced the production of VEGF ($p < 0.05$ vs. Vehicle/HG). These data were also confirmed through immunofluorescence analysis. In fact, as shown in **Figure 3B**, VEGF was weakly expressed in NG with or without DMF treatment. On the contrary, HG exposure induced a dramatic increase of VEGF expression in ARPE-19; this effect was significantly attenuated by DMF treatment.

The reduction of VEGF levels mediated by DMF treatment was further demonstrated by analyzing the expression of VEGF mRNA through semiquantitative RT-PCR, by using specific primers recognizing the angiogenic factor. Consistent with the results of ELISA and immunofluorescence analysis, the mRNA levels of VEGF were significantly increased after HG stimulation compared to NG grown cells ($p < 0.01$ vs. NG). As expected, DMF partially decreased VEGF expression ($p < 0.05$ vs. Vehicle/HG).

Effects of DMF on p38 MAPK Activation

In order to investigate the molecular mechanisms involved in DMF protection, we have analyzed the activation of p38 MAPK signaling cascades, given that literature shown that activation of

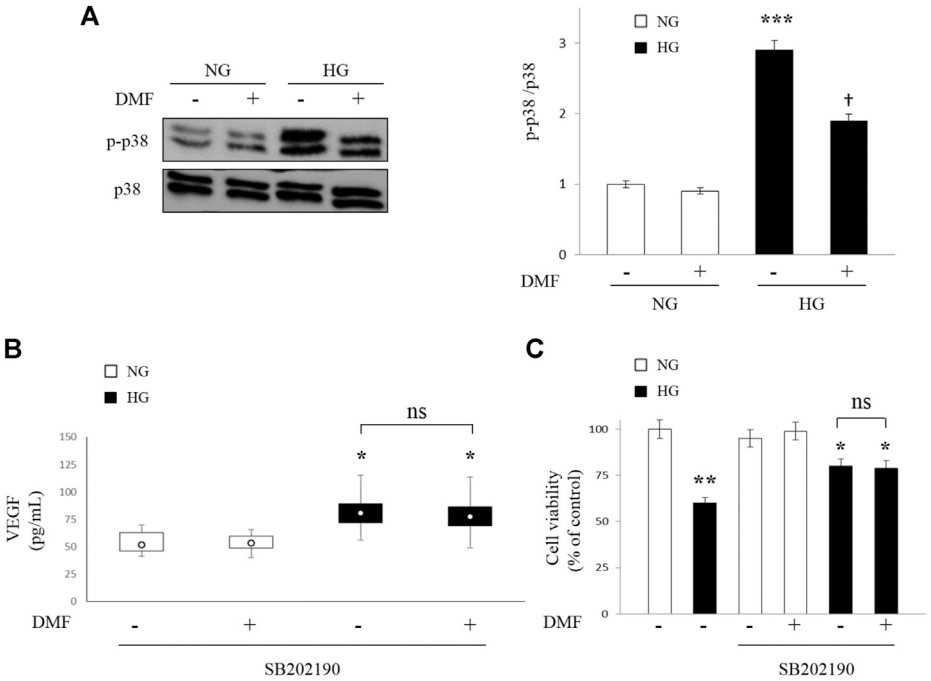

FIGURE 4 | Effects of DMF on p38 MAPK pathway. ARPE-19 cells exposed to normal glucose (NG) or high glucose (HG) w/or w/o DMF (10 μM) for 24 h **(A)** p38 MAPK was measured by western blot analysis; band densities were quantified by ImageQuantTL software and normalized values were plotted in the histogram shown on the right (***$p < 0.001$ vs. NG; †$p < 0.05$ vs. untreated/HG; $n = 6$). **(B)** ARPE-19 cells exposed to normal glucose (NG) or high glucose (HG) were pretreated with SB202190 (10 μM), a p38 MAPK inhibitor for 30 min and then treated with DMF (10 μM) for 24 h. VEGF levels were measured through ELISA. *$p < 0.05$ vs. NG untreated cells; $n = 6$. (**C**) MTT analysis: values are expressed as percentage of cell viability in NG untreated cells. *$p < 0.05$ or **$p < 0.01$ vs. NG untreated cells; $n = 6$.

this signaling pathway affect the expression of VEGF. To address this issue, we performed western blot analyses to assess any changes in p38 MAPK protein levels as well as in its phosphorylated forms in ARPE-19 cells exposed to NG or HG conditions with or without DMF (10 μM) up to 24 h. The results of **Figure 4A** indicated that HG exposure significantly increased the phosphorylation of p38 MAPK levels ($p < 0.001$ vs. NG). Interestingly, DMF administration partially counteracted HG-induced p38 MAPK activation ($p < 0.05$ vs. untreated/HG).

ARPE-19 cells, both in NG and HG conditions, were pre-treated with the specific p38 MAPK inhibitor (SB202190, 10 μM) for 30 min prior to DMF treatment for 24 h and VEGF production (ELISA) and cell viability (MTT analysis) were measured. We chose these experimental conditions based on previous data (Saika et al., 2005; Cheng et al., 2019). As shown in **Figure 4B**, the previously observed HG-induced VEGF increase (see **Figure 3A**) were partially reversed by SB202190 pre-treatment and, more important, any significant differences in the levels of VEGF were detected in HG grown cells after DMF administration (n.s. vs. untreated/HG), confirming that the protective effect of DMF is attributable to p38 MAPK pathway inhibition.

We confirmed that the effect of DMF is attributable to p38 MAPK pathway inhibition through MTT assay. In fact, as shown in **Figure 4C**, no significant difference was observed between cells pre-treated with SB202190 with or without DMF (n.s. vs. DMF-untreated/HG).

DISCUSSION

In the present study, we showed that DMF counteracts high glucose-induced damage in RPE cells through the attenuation of inflammatory cascades that involves p38 MAPK pathway-mediated VEGF inhibition suggesting a protective role in the pathologic events associated to hyperglycemia. The protective role of DMF in nervous system has been extensively demonstrated in several paradigms of neuroinflammation both *in vitro* and *in vivo*. In particular, DMF counteracted the apoptotic cascade by increasing cells survival and reducing the inflammatory process (Wilms et al., 2010; Linker et al., 2011; Scannevin et al., 2012; Wang et al., 2015). The beneficial role of DMF was also demonstrated in the retina (Cho et al., 2015). In particular, DMF down-regulated inflammatory genes expression, counteracted reactive Müller cell gliosis and reduced cell loss by promoting the physiological functions of the retina against ischemia-reperfusion injury (Cho et al., 2015). Moreover, DMF protected retinal tissue in streptozotocin-induced diabetic rats (Patil et al., 2008; Fan et al., 2012). On this regards it could be useful develop in the future a biodegradable deliver system to administer DMF into the eye (Conti et al., 1997). Recently, antioxidant and wound healing properties of DMF were demonstrated in RPE cells challenged with high glucose (Foresti et al., 2015). Based on these previous results, the present study was designed to further confirm the protective effects exerted by DMF on outer BRB during HG exposure. It is

well known that outer BRB is impaired under sustained hyperglycemia, and RPE cell loss is a key event in the progression of DR (Chen et al., 2016; Xia and Rizzolo, 2017). According with these data, we observed a dramatic reduction of RPE cells viability, up to 50%, compared to RPE cells exposed to physiological levels of glucose (5mM, NG). Interestingly, DMF treatment protects RPE cells exposed to high glucose, maintaining their viability in a dose-dependent manner. Further, we showed that DMF decreased the expression of apoptotic gene (Bax) and increased the expression of anti-apoptotic genes (Bcl-2) in RPE cells. This result leads to a decrease in the ratio of pro-apoptotic Bax/anti-apoptotic Bcl2 genes, which causes apoptosis reduction. These observations suggest that DMF has the potential to attenuate apoptotic events associated to hyperglycemia. The HG-induced damage to RPE layer is also due to a severe inflammation sustained by the release of inflammatory cytokines including IL-1β (Joussen et al., 2004; Kern, 2007; Wang et al., 2019). IL-1ß is known to induce vascular dysfunction as well as apoptosis cell death during DR progression (Vincent and Mohr, 2007; Zhang et al., 2019). The immunomodulation role of DMF has already been reported in literature; in fact, previous studies displayed that DMF increases anti-inflammatory cytokines and reduces the pro-inflammatory cytokines like tumor necrosis factor-alpha, IL-2 and IL-17 (Albrecht et al., 2012). In the present study, we showed that DMF treatment decreased the IL-1β levels in HG-cultured RPE cells. The evidence that DMF plays an anti-inflammatory role was further supported by the analysis of COX-2 and iNOS, two inflammatory markers over-expressed by different retinal cell types in response to high levels of glucose (Du et al., 2013; Shin et al., 2014). The present findings showed a significant decrease expression of COX-2 and iNOS in RPE exposed to high glucose when treated with DMF.

It has been demonstrated that the hyperglycemic insult promotes release and activation of the VEGF (Yancopoulos et al., 2000) and RPE cells exposed to high glucose synthetized high levels of this angiogenic factor (Sone et al., 1996). Here, we have shown for the first time that DMF attenuates expression of VEGF mRNA and its release from RPE cells exposed to HG. Since the p38 MAPK pathway promotes and regulates the expression of pro-angiogenesis factors, including VEGF (Gomes and Rockwell, 2008; Sakai et al., 2017) we sought to determine whether VEGF decrease could rely on a DMF-induced p38 MAPK down-regulation. Therefore, we performed Western blot and ELISA assay to further explore the role of DMF on the modulation of p38 MAPK pathway and VEGF levels production. Our results showed that the expression of phosphorylated form of p38 MAPK, was significantly down-regulated by DMF in HG exposed cells. The inhibitory effect of DMF on p38 MAPK phosphorylation was consistent with other studies in human cells stimulated with IL-8 and tumor necrosis factor-α (Nishioku et al., 2020; Kortam et al., 2021). Moreover, the SB202190 reduced the release of VEGF at comparable levels to reduction induced by DMF, and co-treatment of SB202190 with DMF did not alter VEGF secretion.

CONCLUSION

The present data demonstrated that DMF provides protection against high glucose-induced damage in human RPE cells counteracting inflammation and angiogenesis *via* p38 MAPK/VEGF pathway. In conclusion these findings suggested that DMF represents a potential good candidate for diabetic retinopathy treatment and warrants further *in vivo* and clinical evaluation.

DATA AVAILABILITY STATEMENT

The raw data supporting the conclusions of this article will be made available by the authors, without undue reservation.

AUTHOR CONTRIBUTIONS

Conceptualization SG, GM, and CB; methodology, analysis, investigation SG, GM, MD, RI; writing—review and editing CB, VD'A; supervision, CB, VD'A; funding acquisition, SG, FD.

FUNDING

This work was funded by Italian Ministry of Education, University and Research (MIUR) (grant number PRIN 2017TSHBXZ_003) and Grant from University of Catania, PIAno inCEntivi RIcerca Ateneo 2020/2022 - Linea Intervento 2.

REFERENCES

Aiello, L. P., Avery, R. L., Arrigg, P. G., Keyt, B. A., Jampel, H. D., Shah, S. T., et al. (1994). Vascular Endothelial Growth Factor in Ocular Fluid of Patients with Diabetic Retinopathy and Other Retinal Disorders. *N. Engl. J. Med.* 331, 1480–1487. doi:10.1056/nejm199412013312203

Albrecht, P., Bouchachia, I., Goebels, N., Henke, N., Hofstetter, H. H., Issberner, A., et al. (2012). Effects of Dimethyl Fumarate on Neuroprotection and Immunomodulation. *J. Neuroinflamm.* 9, 163. doi:10.1186/1742-2094-9-163

Bolinger, M., and Antonetti, D. (2016). Moving Past Anti-VEGF: Novel Therapies for Treating Diabetic Retinopathy. *Ijms* 17, 1498. doi:10.3390/ijms17091498

Boss, J. D., Singh, P. K., Pandya, H. K., Tosi, J., Kim, C., Tewari, A., et al. (2017). Assessment of Neurotrophins and Inflammatory Mediators in Vitreous of Patients with Diabetic Retinopathy. *Invest. Ophthalmol. Vis. Sci.* 58, 5594–5603. doi:10.1167/iovs.17-21973

Bucolo, C., Marrazzo, G., Platania, C. B., Drago, F., Leggio, G. M., and Salomone, S. (2013). Fortified Extract of Red Berry, Ginkgo Biloba, and White Willow Bark in Experimental Early Diabetic Retinopathy. *J. Diabetes Res.* 2013, 432695. doi:10.1155/2013/432695

Bucolo, C., Drago, F., Maisto, R., Romano, G. L., D'Agata, V., Maugeri, G., et al. (2019). Curcumin Prevents High Glucose Damage in Retinal Pigment Epithelial Cells through ERK1/2-mediated Activation of the Nrf2/HO-1 Pathway. *J. Cel. Physiol.* 234, 17295–17304. doi:10.1002/jcp.28347

Bucolo, C., Gozzo, L., Longo, L., Mansueto, S., Vitale, D. C., and Drago, F. (2018). Long-term Efficacy and Safety Profile of Multiple Injections of Intravitreal Dexamethasone Implant to Manage Diabetic Macular Edema: A Systematic Review of Real-World Studies. *J. Pharmacol. Sci.* 138 (4), 219–232. doi:10.1016/j.jphs.2018.11.001

Cade, W. T. (2008). Diabetes-Related Microvascular and Macrovascular Diseases in the Physical Therapy Setting. *Phys. Ther.* 88, 1322–1335. doi:10.2522/ptj.20080008

Campochiaro, P. A. (2013). Ocular Neovascularization. *J. Mol. Med.* 91, 311–321. doi:10.1007/s00109-013-0993-5

Castorina, A., Tiralongo, A., Giunta, S., Carnazza, M. L., Scapagnini, G., and D'Agata, V. (2010). Early Effects of Aluminum Chloride on Beta-Secretase mRNA Expression in a Neuronal Model of SS-Amyloid Toxicity. *Cell. Biol. Toxicol.* 26, 367–377. doi:10.1007/s10565-009-9149-3

Chen, M., Wang, W., Ma, J., Ye, P., and Wang, K. (2016). High Glucose Induces Mitochondrial Dysfunction and Apoptosis in Human Retinal Pigment Epithelium Cells via Promoting SOCS1 and Fas/FasL Signaling. *Cytokine* 78, 94–102. doi:10.1016/j.cyto.2015.09.014

Cheng, S.-C., Huang, W.-C., S. Pang, J.-H., Wu, Y.-H., and Cheng, C.-Y. (2019). Quercetin Inhibits the Production of IL-1β-Induced Inflammatory Cytokines and Chemokines in ARPE-19 Cells via the MAPK and NF-κB Signaling Pathways. *Ijms* 20, 2957. doi:10.3390/ijms20122957

Cho, H., Hartsock, M. J., Xu, Z., He, M., and Duh, E. J. (2015). Monomethyl Fumarate Promotes Nrf2-Dependent Neuroprotection in Retinal Ischemia-Reperfusion. *J. Neuroinflamm.* 12, 239. doi:10.1186/s12974-015-0452-z

Conti, B., Bucolo, C., Giannavola, C., Puglisi, G., Giunchedi, P., and Conte, U. (1997). Biodegradable Microspheres for the Intravitreal Administration of Acyclovir: *In vitro*/in vivo Evaluation. *Eur. J. Pharm. Sci.* 5 (5), 287–293. doi:10.1016/S0928-0987(97)00023-7

D'Amico, A. G., Maugeri, G., Reitano, R., Bucolo, C., Saccone, S., Drago, F., et al. (2015). PACAP Modulates Expression of Hypoxia-Inducible Factors in Streptozotocin-Induced Diabetic Rat Retina. *J. Mol. Neurosci.* 57, 501–509. doi:10.1007/s12031-015-0621-7

D'Amico, A. G., Maugeri, G., Rasà, D. M., La Cognata, V., Saccone, S., Federico, C., et al. (2018). NAP Counteracts Hyperglycemia/hypoxia Induced Retinal Pigment Epithelial Barrier Breakdown through Modulation of HIFs and VEGF Expression. *J. Cel. Physiol.* 233, 1120–1128. doi:10.1002/jcp.25971

Du, Y., Veenstra, A., Palczewski, K., and Kern, T. S. (2013). Photoreceptor Cells Are Major Contributors to Diabetes-Induced Oxidative Stress and Local Inflammation in the Retina. *Proc. Natl. Acad. Sci.* 110, 16586–16591. doi:10.1073/pnas.1314575110

Fan, J., Xu, G., Jiang, T., and Qin, Y. (2012). Pharmacologic Induction of Heme Oxygenase-1 Plays a Protective Role in Diabetic Retinopathy in Rats. *Invest. Ophthalmol. Vis. Sci.* 53, 6541–6556. doi:10.1167/iovs.11-9241

Foresti, R., Bucolo, C., Platania, C. M. B., Drago, F., Dubois-Randé, J.-L., and Motterlini, R. (2015). Nrf2 Activators Modulate Oxidative Stress Responses and Bioenergetic Profiles of Human Retinal Epithelial Cells Cultured in Normal or High Glucose Conditions. *Pharmacol. Res.* 99, 296–307. doi:10.1016/j.phrs.2015.07.006

Giurdanella, G., Anfuso, C. D., Olivieri, M., Lupo, G., Caporarello, N., Eandi, C. M., et al. (2015). Aflibercept, Bevacizumab and Ranibizumab Prevent Glucose-Induced Damage in Human Retinal Pericytes in vitro, through a PLA2/COX-2/VEGF-A Pathway. *Biochem. Pharmacol.* 96 (3), 278–287. doi:10.1016/j.bcp.2015.05.017

Gomes, E., and Rockwell, P. (2008). p38 MAPK as a Negative Regulator of VEGF/VEGFR2 Signaling Pathway in Serum Deprived Human SK-N-SH Neuroblastoma Cells. *Neurosci. Lett.* 431, 95–100. doi:10.1016/j.neulet.2007.11.068

Grant, M. B., Afzal, A., Spoerri, P., Pan, H., Shaw, L. C., and Mames, R. N. (2004). The Role of Growth Factors in the Pathogenesis of Diabetic Retinopathy. *Expert Opin. Investig. Drugs* 13, 1275–1293. doi:10.1517/13543784.13.10.1275

Joussen, A. M., Poulaki, V., Le, M. L., Koizumi, K., Esser, C., Janicki, H., et al. (2004). A Central Role for Inflammation in the Pathogenesis of Diabetic Retinopathy. *FASEB J.* 18, 1450–1452. doi:10.1096/fj.03-1476fje

Kern, T. S. (2007). Contributions of Inflammatory Processes to the Development of the Early Stages of Diabetic Retinopathy. *Exp. Diabetes Res.* 2007, 1–14. doi:10.1155/2007/95103

Kim, D. I., Park, M. J., Choi, J. H., Lim, S. K., Choi, H. J., and Park, S. H. (2015). Hyperglycemia-Induced GLP-1R Downregulation Causes RPE Cell Apoptosis. *Int. J. Biochem. Cel. Biol.* 59, 41–51. doi:10.1016/j.biocel.2014.11.018

Kortam, M. A., Ali, B. M., and Fathy, N. (2021). The Deleterious Effect of Stress-Induced Depression on Rat Liver: Protective Role of Resveratrol and Dimethyl Fumarate via Inhibiting the MAPK/ERK/JNK Pathway. *J. Biochem. Mol. Toxicol.* 35 (1), e22627. doi:10.1002/jbt.22627

Kowluru, R. A., Chakrabarti, S., and Chen, S. (2004). Re-institution of Good Metabolic Control in Diabetic Rats and Activation of Caspase-3 and Nuclear Transcriptional Factor (NF-kB) in the Retina. *Acta Diabetol.* 41 (4), 194–199. doi:10.1007/s00592-004-0165-8

Linker, R. A., Lee, D.-H., Ryan, S., van Dam, A. M., Conrad, R., Bista, P., et al. (2011). Fumaric Acid Esters Exert Neuroprotective Effects in Neuroinflammation via Activation of the Nrf2 Antioxidant Pathway. *Brain* 134, 678–692. doi:10.1093/brain/awq386

Maugeri, G., D'Amico, A. G., Rasà, D. M., La Cognata, V., Saccone, S., Federico, C., et al. (2017). Nicotine Promotes Blood Retinal Barrier Damage in a Model of Human Diabetic Macular Edema. *Toxicol. Vitro* 44, 182–189. doi:10.1016/j.tiv.2017.07.003

Maugeri, G., D'Amico, A. G., Rasà, D. M., Saccone, S., Federico, C., Cavallaro, S., et al. (2018b). PACAP and VIP Regulate Hypoxia-Inducible Factors in Neuroblastoma Cells Exposed to Hypoxia. *Neuropeptides* 69, 84–91. doi:10.101610.1016/j.npep.2018.04.009

Maugeri, G., Longo, A., D'Amico, A. G., Rasà, D. M., Reibaldi, M., Russo, A., et al. (2018a). Trophic Effect of PACAP on Human Corneal Endothelium. *Peptides* 99, 20–26. doi:10.1016/j.peptides.2017.11.003

Nishioku, T., Kawamoto, M., Okizono, R., Sakai, E., Okamoto, K., and Tsukuba, T. (2020). Dimethyl Fumarate Prevents Osteoclastogenesis by Decreasing NFATc1 Expression, Inhibiting of erk and p38 MAPK Phosphorylation, and Suppressing of HMGB1 Release. *Biochem. Biophys. Res. Commun.* 530, 455–461. doi:10.1016/j.bbrc.2020.05.088

Patil, K., Bellner, L., Cullaro, G., Gotlinger, K. H., Dunn, M. W., and Schwartzman, M. L. (2008). Heme Oxygenase-1 Induction Attenuates Corneal Inflammation and Accelerates Wound Healing after Epithelial Injury. *Invest. Ophthalmol. Vis. Sci.* 49, 3379–3386. doi:10.1167/iovs.07-1515

Plafker, S. M., O'Mealey, G. B., and Szweda, L. I. (2012). Mechanisms for Countering Oxidative Stress and Damage in Retinal Pigment Epithelium. *Int. Rev. Cel. Mol. Biol.* 298, 135–177. doi:10.1016/B978-0-12-394309-5.00004-3

Platania, C. B. M., Di Paola, L., Leggio, G. M., Romano, G. L., Drago, F., Salomone, S., et al. (2015). Molecular Features of Interaction between VEGFA and Anti-angiogenic Drugs Used in Retinal Diseases: a Computational Approach. *Front. Pharmacol.* 6, 248. doi:10.3389/fphar.2015.00248

Platania, C. B. M., Giurdanella, G., Di Paola, L., Leggio, G. M., Drago, F., Salomone, S., et al. (2017). P2X7 Receptor Antagonism: Implications in Diabetic Retinopathy. *Biochem. Pharmacol.* 138, 130–139. doi:10.1016/j.bcp.2017.05.001

Rubio, R. G., and Adamis, A. P. (2016). Ocular Angiogenesis: Vascular Endothelial Growth Factor and Other Factors. *Dev. Ophthalmol.* 55, 28–37. doi:10.1159/000431129

Saika, S., Yamanaka, O., Ikeda, K., Kim-Mitsuyama, S., Flanders, K. C., Yoo, J., et al. (2005). Inhibition of p38MAP Kinase Suppresses Fibrotic Reaction of Retinal Pigment Epithelial Cells. *Lab. Invest.* 85, 838–850. doi:10.1038/labinvest.3700294

Saishin, Y., Saishin, Y., Takahashi, K., Melia, M., Vinores, S. A., and Campochiaro, P. A. (2003). Inhibition of Protein Kinase C Decreases Prostaglandin-Induced Breakdown of the Blood-Retinal Barrier. *J. Cel. Physiol.* 195, 210–219. doi:10.1002/jcp.10238

Sakai, G., Tokuda, H., Fujita, K., Kainuma, S., Kawabata, T., Matsushima-Nishiwaki, R., et al. (2017). Heat Shock Protein 70 Negatively Regulates TGF-β-Stimulated VEGF Synthesis via p38 MAP Kinase in Osteoblasts. *Cell Physiol. Biochem.* 44, 1133–1145. doi:10.1159/000485418

Scannevin, R. H., Chollate, S., Jung, M.-y., Shackett, M., Patel, H., Bista, P., et al. (2012). Fumarates Promote Cytoprotection of Central Nervous System Cells against Oxidative Stress via the Nuclear Factor (Erythroid-derived 2)-like 2 Pathway. *J. Pharmacol. Exp. Ther.* 341, 274–284. doi:10.1124/jpet.111.190113210.1124/jpet.111.190132

Schlingemann, R. O. (2004). Role of Growth Factors and the Wound Healing Response in Age-Related Macular Degeneration. *Graefe's Arch. Clin. Exp. Ophthalmol.* 242, 91–101. doi:10.1007/s00417-003-0828-0

Shin, E. S., Huang, Q., Gurel, Z., Sorenson, C. M., and Sheibani, N. (2014). High Glucose Alters Retinal Astrocytes Phenotype through Increased Production of

Inflammatory Cytokines and Oxidative Stress. *PLoS One* 9, e103148. doi:10.1371/journal.pone.0103148

Sone, H., Kawakami, Y., Okuda, Y., Kondo, S., Hanatani, M., Suzuki, H., et al. (1996). Vascular Endothelial Growth Factor Is Induced by Long-Term High Glucose Concentration and Up-Regulated by Acute Glucose Deprivation in Cultured Bovine Retinal Pigmented Epithelial Cells. *Biochem. Biophys. Res. Commun.* 221, 193–198. doi:10.1006/bbrc.1996.0568

Vincent, J. A., and Mohr, S. (2007). Inhibition of Caspase-1/Interleukin-1 Signaling Prevents Degeneration of Retinal Capillaries in Diabetes and Galactosemia. *Diabetes* 56, 224–230. doi:10.2337/db06-0427

Wang, P., Chen, F., Wang, W., and Zhang, X.-D. (2019). Hydrogen Sulfide Attenuates High Glucose-Induced Human Retinal Pigment Epithelial Cell Inflammation by Inhibiting ROS Formation and NLRP3 Inflammasome Activation. *Mediators Inflamm.* 2019, 1–13. doi:10.1155/2019/8908960

Wang, Q., Chuikov, S., Taitano, S., Wu, Q., Rastogi, A., Tuck, S., et al. (2015). Dimethyl Fumarate Protects Neural Stem/Progenitor Cells and Neurons from Oxidative Damage through Nrf2-ERK1/2 MAPK Pathway. *Ijms* 16, 13885–13907. doi:10.3390/ijms160613885

Wilms, H., Sievers, J., Rickert, U., Rostami-Yazdi, M., Mrowietz, U., and Lucius, R. (2010). Dimethylfumarate Inhibits Microglial and Astrocytic Inflammation by Suppressing the Synthesis of Nitric Oxide, IL-1β, TNF-α, and IL-6 in an in-vitro Model of Brain Inflammation. *J. Neuroinflamm.* 7, 30. doi:10.1186/1742-2094-7-30

Xia, T., and Rizzolo, L. J. (2017). Effects of Diabetic Retinopathy on the Barrier Functions of the Retinal Pigment Epithelium. *Vis. Res.* 139, 72–81. doi:10.1016/j.visres.2017.02.006

Xiao, J., Yao, J., Jia, L., Lin, C., and Zacks, D. N. (2017). Protective Effect of Met12, a Small Peptide Inhibitor of Fas, on the Retinal Pigment Epithelium and Photoreceptor after Sodium Iodate Injury. *Invest. Ophthalmol. Vis. Sci.* 58, 1801–1810. doi:10.1167/iovs.16-21392

Yancopoulos, G. D., Davis, S., Gale, N. W., Rudge, J. S., Wiegand, S. J., and Holash, J. (2000). Vascular-Specific Growth Factors and Blood Vessel Formation. *Nature* 407, 242–248. doi:10.1038/35025215

Yuuki, T., Kanda, T., Kimura, Y., Kotajima, N., Tamura, J. i., Kobayashi, I., et al. (2001). Inflammatory Cytokines in Vitreous Fluid and Serum of Patients with Diabetic Vitreoretinopathy. *J. Diabetes its Complications* 15, 257–259. doi:10.1016/s1056-8727(01)00155-6

Zhang, Y., Xi, X., Mei, Y., Zhao, X., Zhou, L., Ma, M., et al. (2019). High-Glucose Induces Retinal Pigment Epithelium Mitochondrial Pathways of Apoptosis and Inhibits Mitophagy by Regulating ROS/PINK1/Parkin Signal Pathway. *Biomed. Pharmacother.* 111, 1315–1325. doi:10.1016/j.biopha.2019.01.034

Zhao, G., Liu, Y., Fang, J., Chen, Y., Li, H., and Gao, K. (2014). Dimethyl Fumarate Inhibits the Expression and Function of Hypoxia-Inducible Factor-1α (HIF-1α). *Biochem. Biophys. Res. Commun.* 448, 303–307. doi:10.1016/j.bbrc.2014.02.062

Zheng, L., and Kern, T. S. (2009). Role of Nitric Oxide, Superoxide, Peroxynitrite and PARP in Diabetic Retinopathy. *Front. Biosci.* 14, 3974–3987. doi:10.2741/3505

Conflict of Interest: The authors declare that the research was conducted in the absence of any commercial or financial relationships that could be construed as a potential conflict of interest.

frontiers in Pharmacology

ORIGINAL RESEARCH
published: 10 May 2021
doi: 10.3389/fphar.2021.675295

Routine Clinical Practice Treatment Outcomes of Eplerenone in Acute and Chronic Central Serous Chorioretinopathy

Katrin Fasler[1,2], *Jeanne M. Gunzinger*[1,2], *Daniel Barthelmes*[1,2,3] *and Sandrine A. Zweifel*[1,2]*

[1]Department of Ophthalmology, University Hospital Zurich, Zurich, Switzerland, [2]University of Zurich, Zurich, Switzerland, [3]Save Sight Institute, The University of Sydney, Sydney, NSW, Australia

Purpose: To evaluate efficacy of eplerenone therapy vs. observation on resolution of subretinal fluid (SRF) in patients with acute and chronic central serous chorioretinopathy (CSCR) in routine clinical practice.

Methods: Retrospective comparative case series of eyes diagnosed with CSCR treated with eplerenone or observation. Primary outcome measure was maximum height of SRF at 12 months. Secondary outcome was percentage of eyes with complete resolution of SRF, percentage of eyes with reduction of SRF ≥50%, and best corrected visual acuity (VA) at 12 months. Separate analysis was conducted for eyes with acute and chronic CSCR.

Results: Sixty-eight eyes of 60 patients (82% male) were included. Eleven of the 38 eyes with acute CSCR, and seven of the 30 eyes with chronic CSCR, received eplerenone. Subretinal fluid decreased from baseline to 12 months in acute (287 ± 221 to 31 ± 63 µm) and chronic (148 ± 134 to 40 ± 42 µm) CSCR. Kaplan-Meier curves were similar for treated and observed eyes and COX regression analysis did not show a significant difference in SRF resolution in treated vs. observed eyes (p = 0.6 for acute, p = 0.2 for chronic CSCR).

Conclusion: This routine clinical practice outcome study did not show evidence of efficacy of eplerenone on resolution of SRF in acute nor chronic CSCR.

Keywords: aldosterone antagonists, central serous chorioretinopathy, eplerenone, medical retina, retinal disease

OPEN ACCESS

Edited by:
Claudio Bucolo,
University of Catania, Italy

Reviewed by:
Riccardo Sacconi,
San Raffaele Hospital (IRCCS), Italy
Yutaka Imamura,
Teikyo University Mizonokuchi Hospital, Japan

***Correspondence:**
Sandrine A. Zweifel
sandrine.zweifel@usz.ch.

Specialty section:
This article was submitted to Experimental Pharmacology and Drug Discovery, a section of the journal Frontiers in Pharmacology

Received: *02 March 2021*
Accepted: *21 April 2021*
Published: *10 May 2021*

Citation:
Fasler K, Gunzinger JM, Barthelmes D and Zweifel SA (2021) Routine Clinical Practice Treatment Outcomes of Eplerenone in Acute and Chronic Central Serous Chorioretinopathy. Front. Pharmacol. 12:675295. doi: 10.3389/fphar.2021.675295

INTRODUCTION

Central serous chorioretinopathy (CSCR) is a retinal disease characterized by subretinal fluid (SRF) accumulation causing a neurosensory detachment and alterations of the retinal pigment epithelium (RPE) (Liew et al., 2013; Mehta et al., 2017). The precise pathophysiology of CSCR remains unknown, but advances in retinal imaging, particularly enhanced-depth optical coherence tomography (EDI-OCT) improved understanding of retinal and choroidal changes observed in CSCR. Increased choroidal thickness (pachychoroid) was correlated with CSCR, supporting the important role of choroidal abnormalities as underlying cause of RPE dysfunction and SRF leakage leading to neurosensory detachment (Dansingani et al., 2016). Recently, a new classification was proposed, embedding CSCR into the spectrum of pathology with increased choroidal vascularity index or "pachychoroid diseases" (Dansingani et al., 2016; Singh et al., 2019).

Two subtypes of CSCR are distinguished: Acute CSCR is usually self-limited and has a favorable visual prognosis (Liew et al., 2013). Chronic CSCR however, is often associated with progressive visual impairment due to persistent SRF and subsequent damage to the neuroretina and RPE resulting in atrophy of both (Loo et al., 2002).

There is no evidence-based consensus for the management of either acute or chronic CSCR. For acute CSCR, the most common initial approach is observation (Salehi et al., 2015; Mehta et al., 2017). For chronic CSCR, a variety of interventions has been proposed, among them aldosterone antagonists, subthreshold laser therapy, and photodynamic therapy (Salehi et al., 2015; Scholz et al., 2016; Cakir et al., 2019; Iacono et al., 2018; Zola et al., 2018; Fusi-Rubiano et al., 2019; Lee et al., 2019; Wang et al., 2019).

Preclinical studies reported that CSCR may result from over-activation of the mineralocorticoid receptor pathway in the choroid (Zhao et al., 2012; Daruich et al., 2015). Based on these findings, a pilot study demonstrated potential clinical efficacy of eplerenone (Bousquet et al., 2013). Following this, several studies assessed aldosterone-antagonist treatment with variable outcomes (Behar-Cohen and Zhao 2016; Bertan Cakir et al., 2016; Daruich et al., 2016; Ghadiali et al., 2016; Kapoor and Wagner 2016; Pichi et al., 2016; Rahimy et al., 2017; Schwartz et al., 2017). In 2019, the first sufficiently powered prospective study did not find a clinically significant benefit of eplerenone over placebo in chronic CSCR (Lotery et al., 2020b).

In this study, we evaluated eplerenone therapy vs. observation for acute and chronic CSCR in routine clinical practice.

MATERIALS AND METHODS

Ethics

Institutional review board approval (Ethics Committee of the University of Zurich, BASEC-No. PB_2016-00264) was obtained and all patients gave informed consent to publish their clinical data. The study adheres to the tenets of the Declaration of Helsinki.

Data Collection

Patients aged 18 years and older who were diagnosed with acute or chronic CSCR and were consecutively seen at the Department of Ophthalmology, University Hospital Zurich between July 2008 and March 2017, were included in this retrospective study. Diagnosis of CSCR was made by multimodal imaging: Spectral domain EDI-OCT, autofluorescence, fluorescein- and indocyanine green angiography. The distinction between acute and chronic CSCR was based on the duration of symptoms and signs of chronicity in multimodal imaging (symptoms ≥3 months and descending tracts/hypoautofluorescence on autofluorescence/outer retinal or pigment epithelium atrophy = chronic). Exemplary cases of acute and chronic CSCR are shown in **Supplementary Figures S1,S2**.

Exclusion criteria were secondary choroidal neovascularization, pachychoroid neovasculopathy, history of photodynamic therapy (PDT)/thermal laser/anti-VEGF therapy, or history of mineralocorticoid-antagonist therapy. Exogenous steroid therapy was not an exclusion criteria. Excluded were 8 eyes with secondary choroidal neovascularization (CNV), 10 eyes receiving PDT, and 61 eyes with signs of CSCR that never had any SRF during the observation period (inactive or so called non exudative CSCR), 1 eye with only baseline visit, and 1 eye with history of PDT treatment. Consort style flow diagram of data collection is shown in **Figure 1**. The duration of eplerenone therapy was measured in weeks. There was no matching of patients/eyes.

Baseline and Outcome Measures

Baseline time point for the observation only group was defined as date of first presentation, for the treatment group as date of initiation of eplerenone therapy. There was a minimum follow-up of 48 weeks for SRF analysis at 12 months, but no minimum follow-up for survival analysis. Primary outcome measure was maximum height of SRF at 12 months as detected on EDI-OCT imaging. 12 month date was defined as date closest to 365 days after baseline of eyes having at least 48 weeks of follow-up. Secondary outcome was percentage of eyes with complete resolution of SRF and reduction of SRF ≥50% at 12 months, time to reach 0 SRF, and best corrected decimal VA at 12 months. Choroidal thickness could not be measured consistently due to errors in image centration at acquisition and indiscernible sclera-choroidal junction, precluding reasonable statistical analysis. Reasons for discontinuation of eplerenone were assessed.

Imaging/Image Grading

Fluorescein angiography images were obtained using a Zeiss camera (FF450 Plus - Version 4.5.2) or Heidelberg Spectralis (Heidelberg Engineering, Heidelberg, Germany), EDI-OCT and autofluorescence images were obtained with Heidelberg Spectralis (version 1.9.13.0) and viewed with the contained Heidelberg software (Spectralis Viewing Module 6.5.2.0; Heidelberg Engineering, Heidelberg, Germany). Grading was carried out by a retina specialist (KF). SRF was measured in μm manually at the maximal level of the neurosensory detachment from the RPE to the outer border of the hyperreflectivity of the outer retinal layers perpendicular to the RPE.

Statistics

Data were coded in Excel and analyzed in SPSS statistics software (IBM Corp. Released 2017. IBM SPSS Statistics for Windows, Version 25.0. Armonk, NY: IBM Corp). The eye was defined as unit of analysis. Mean values in text are expressed with ± standard deviation, median values with 95% confidence interval, unless otherwise specified. Kaplan Meier Curves and Cox Regression were used to assess the effect of eplerenone therapy on resolution of SRF.

RESULTS

Demographics and Baseline Characteristics

Sixty-eight eyes of 60 patients (82% male) qualified for inclusion in this study. Details of in-/exclusion and number of eyes up to 12 months are shown in **Figure 1**. Thirty-eight eyes were considered to be acute and 30 eyes chronic CSCR. Mean age

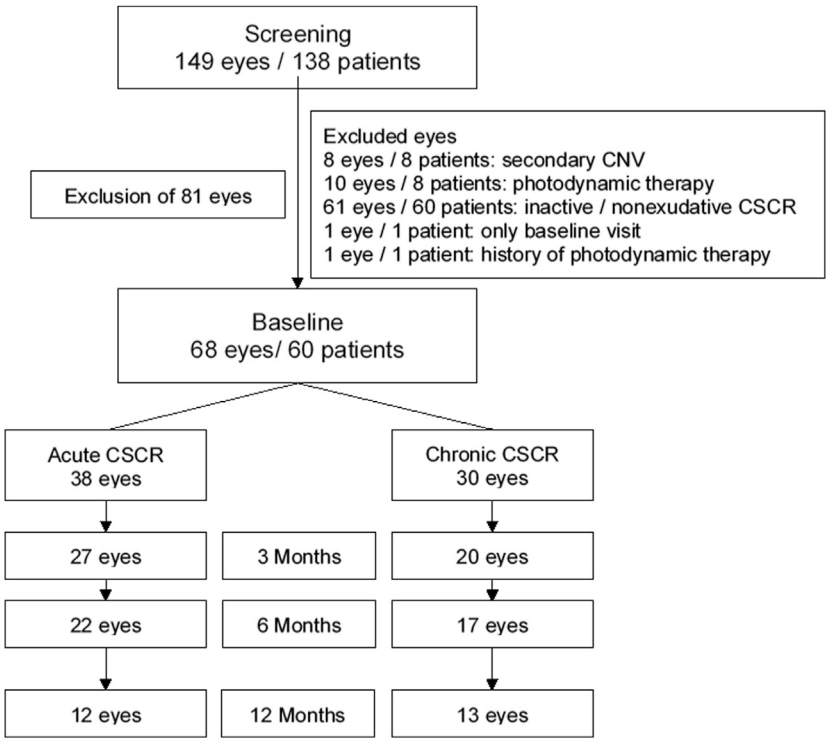

FIGURE 1 | Consort style flow diagram of data collection and follow-up. CNV–choroidal neovascular membrane, CSCR central serous chorioretinopathy.

TABLE 1 | Baseline characteristics and outcomes at 12 months of eyes with acute and chronic CSCR.

	Acute CSCR		Chronic CSCR	
—	**Baseline (n = 38)**	**12 months (n = 12)**	**Baseline (n = 30)**	**12 months (n = 13)**
SRF[a] (μm) mean ± SD (range)	—	—	—	—
All eyes	287 ± 221 (28–1,023)	31 ± 63 (0–215)	148 ± 134 (19–502)	40 ± 42 (0–143)
Observation only	326 ± 236 (28–1,023)(n = 27)	36 ± 74 (0–215)(n = 9)	147 ± 149 (19–502)(n = 23)	18 ± 25 (0–52)(n = 8)
Eyes with ≥50% SRF reduction (%)	—	7 (78%)	—	6 (75%)
Eyes with zero SRF(%)	—	4 (44%)	—	5 (63%)
Eplerenone therapy	192 ± 154 (53–570) (n = 11)	21 ± 41 (0–82) (n = 4)	150 ± 145 (45–267) (n = 7)	75 ± 42 (40–143) (n = 5)
Eyes with ≥50% SRF reduction (%)	—	4 (80%)	—	2 (40%)
Eyes with zero SRF(%)	—	3 (60%)	—	0 (0%)
Visual acuity decimal (snellen) mean ± SD (range)	—	—	—	—
All eyes	0.6 (20/32)±0.2 (0.2–1.0)	1.0 (20/20)±0.2 (0.8–1.25)	0.8 (20/25)±0.3 (0.2–1.25)	0.9 (20/22)±0.3 (0.3–1.25)
Observation only	0.6 (20/32)±0.3 (0.2–1.0); (n = 27)	1.0 (20/20) ±0.2 (0.8–1.3); (n = 8)	0.8 (20/25) ±0.3 (0.2–1.3); (n = 23)	1.0 (20/20)±0.3 (0.3–1.3); (n = 8)
Eplerenone therapy	0.7 (20/29) ±0.2 (03–1.0); (n = 11)	1.0 (20/20) ±0.2 (0.8–1.3); (n = 4)	0.8 (20/25)±0.2 (0.6–1.0); (n = 7)	0.9 (20/22)±0.3 (0.6–1.3); (n = 5)

[a]*SRF = subretinal fluid, n = number of eyes.*

at presentation was 40 ± 10 (range 27–72) years for acute and 48 ± 8 (range 36–66) years for chronic CSCR patients. Mean follow-up time was 46 ± 45 weeks (range 1–188) for eyes with acute and 81 ± 90 (range 4–266) weeks for eyes with chronic CSCR. Eleven of the 38 eyes (29%) with acute CSCR, and 7 of the 30 eyes (23%) with chronic CSCR, received eplerenone 25 mg/day for 1 week followed by 50 mg/day. Mean therapy time was 24 ± 16 (range 7–50) weeks for patients with acute and 74 ± 90 (range 10–205) weeks for patients with chronic CSCR. Baseline characteristics are shown in **table 1**.

Primary Outcome

Maximal height of SRF decreased from baseline to 12 months in acute [287 ± 221 (range 28–1,023) μm to 31 ± 63 (range

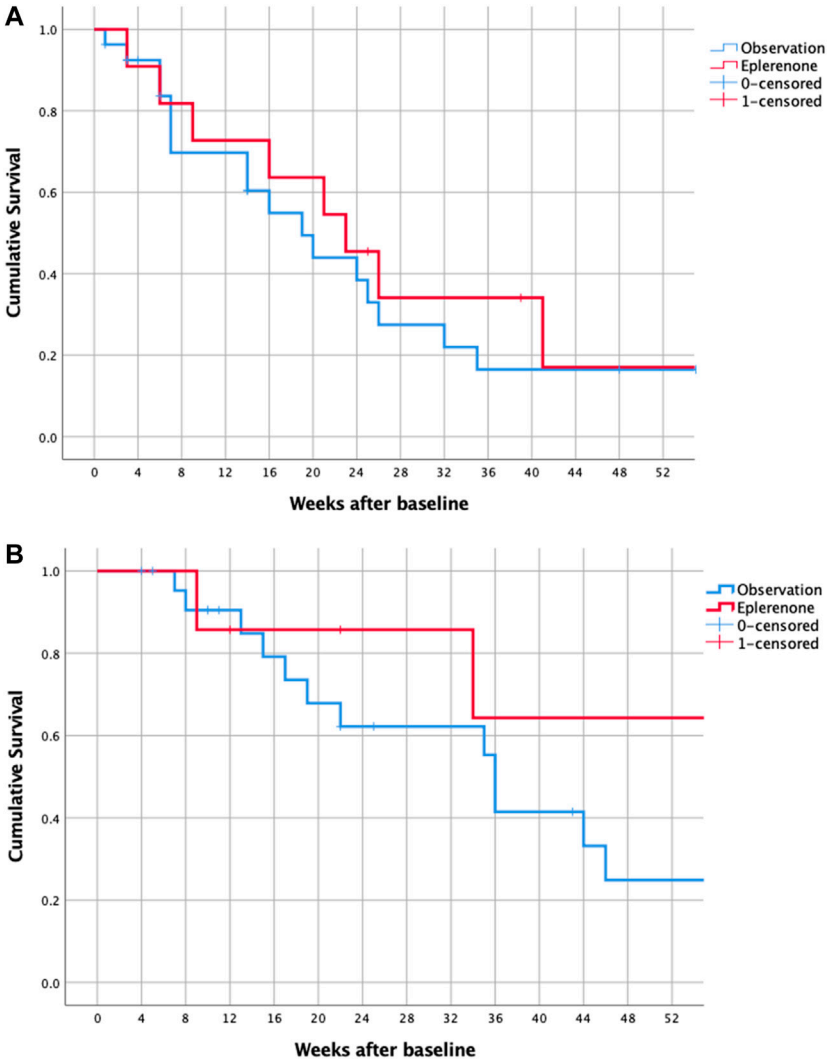

FIGURE 2 | Kaplan-Meier survival of all eyes with acute **(A)** and chronic **(B)** CSCR reaching complete resolution of SRF (event = zero SRF). CSCR—central serous chorioretinopathy, SRF–subretinal fluid.

0–215) μm] and chronic [148 ± 134 (range 19–502) μm to 40 ± 42 (range 0–143) μm] CSCR.

Secondary Outcomes

Percentages of eyes to reach complete resolution of SRF or achieve ≥50% reduction of SRF as well as VA are shown in **table 1**. Median time to complete resolution of SRF was 21 (12, 30) weeks for acute and 36 (24, 48) weeks for chronic CSCR. For both groups, acute and chronic CSCR, survival curves to reach complete resolution of SRF were similar for treated and observed eyes (**Figure 2**). COX regression analysis did not show a significant effect of eplerenone therapy on resolution of SRF: Acute CSCR [Exp(B) = 0.8 CI (0.3, 1.8)], $p = 0.6$; chronic CSCR [Exp(B) = 0.35 CI (0.1, 1.6)], $p = 0.2$.

Reasons for discontinuing eplerenone treatment included absence of anatomical or functional effect (1 eye), gastrointestinal side effects (2 eyes, 1 patient) and complete resolution of SRF (9 eyes). In 4 eyes, the reason for discontinuation could not be determined.

DISCUSSION

Aldosterone antagonists, specifically eplerenone, has been reported to be a pathophysiologically reasonable choice for treatment of CSCR(Zhao et al., 2012; Bousquet et al., 2013; Behar-Cohen and Zhao 2016). However, clinical results so far have been less convincing, and most recently, a well-designed double-blind, placebo-controlled trial (VICI) reported that eplerenone was not superior to placebo for chronic CSCR (Lotery et al., 2020b). Our real life data showing no effect of eplerenone on resolution of SRF nor improvement in VA in acute or chronic CSCR is consistent with the published data of the VICI trial.

In the majority of studies analyzing mineralocorticoid antagonists for CSCR, eplerenone was chosen due to its better safety profile compared to spironolactone. Its affinity in aldosterone-receptor blockage is 10–20-fold less than that of spironolactone *in vitro* (de Gasparo et al., 1987). However, it also has very low affinity to other steroid receptors, which significantly lowers progestational and anti-androgenic side effects and *in vivo* efficacy in blocking aldosterone-mediated changes in urinary Na:K ratio in rats is similar for both drugs (Delyani 2000). While comparative studies of eplerenone and spironolactone for its ophthalmological use are not conclusive, long lasting cardiological evidence of similar clinical efficacy and significant fewer side effects are definitely favoring eplerenone as drug of choice (Chin et al., 2015; Ghadiali et al., 2016; Kapoor and Wagner 2016; Pichi et al., 2016). Only 1 out of 18 patients in our study discontinued eplerenone due to side effects (i.e. gastrointestinal disturbance), confirming good tolerance of the medication.

The high percentage of spontaneous resolution of acute CSCR makes treatment indication in acute cases generally questionable (Liew et al., 2013). However, patients with large amounts of SRF are at higher risk for loss of photoreceptors and subsequent visual impairment, which could justify treatment for acute CSCR (Gerendas et al., 2018). In our study, all patients with acute CSCR were offered eplerenone as off-label therapy option. No difference in time to complete resolution of SRF could be shown between treated and observed eyes up to 12 months, even though baseline SRF of observed eyes was higher than baseline SRF of treated eyes (326 ± 236 vs. 192 ± 154 µm). Further, already at 3 months, zero SRF was achieved in similar proportion (36 and 30%) in treated and observed eyes respectively. This is contradictory to the only previous retrospective study comparing eplerenone treatment to observation in 22 eyes with acute CSCR (Zucchiatti et al., 2018). This study showed a higher resolution rate of SRF (80 vs. 25%) and a significant improvement in VA in the treatment group compared to observation only at 3 months (Zucchiatti et al., 2018). Further, another prospective study of 30 patients found accelerated resolution of SRF in patients treated with spironolactone compared to observation at 2 months (Sun et al., 2018). These diverging results could result from the small sample sizes, the short observation periods (2–3 months) as well as the different study drug with possible different efficacy in the study of Sun et al. Our data suggests that eplerenone does not accelerate SRF resolution in acute CSCR, however in the context of the limitations of our study (e.g. small sample size, variable follow-up time) and the sparse previous evidence, there are larger, prospective studies necessary to draw definite conclusions about eplerenone for acute CSCR.

In eyes with chronic CSCR, no difference could be detected between the treated and observed group in resolution of SRF or VA improvement. This coincides with the results of the VICI trial, where no difference in partial/complete resolution of SRF or VA was found at 12 months between eplerenone and placebo, but SRF decreased over time in both groups (Lotery et al., 2020b). Despite being the highest quality evidence on efficacy of eplerenone for CSCR, the VICI trial also has several limitations, i.e. possible introduction of bias by exclusion of eyes with secondary CNV without OCT angiography, non-balanced administration of additional PDT treatment between groups, and a possible ceiling effect on VA outcomes due to very good baseline VA (Lotery et al., 2020a; Sacconi et al., 2020; Stanescu-Segall et al., 2020;). Other smaller prospective studies with variable patient selection, choice of aldosterone antagonist, controlling with placebo, and follow-up resulted in diverging results on functional and/or anatomical efficacy (Pichi et al., 2016; Rahimy et al., 2017; Schwartz et al., 2017). Due to the spectrum of CSCR and possible different response to treatment, drawing a definite conclusion needs to be done with caution (Daruich et al., 2016). However, our data does not suggest a relevant effect of eplerenone on resolution of SRF in chronic CSCR.

In chronic and acute CSCR, VA improved in both groups over time irrespective of treatment in our study. This again reflects the results of the VICI trial results. To note that VA might not be vicarious for treatment effect, since it mostly depends on the presence of subfoveal SRF and the state of the RPE and outer retina after its resolution (Liew et al., 2013).

Limitations of our study are its retrospective design and the possibility of selection bias (e.g. patients with eplerenone had a longer follow-up period than observation only eyes, eyes with longstanding SRF are more likely to get treatment) and the fact that there was no matching of patients. Further, comparison to other studies is difficult due to the varying definition of chronic disease (e.g. based on symptom duration ≥ 4 months in the VICI trial and others) and the non-standardized visits/treatment (Daruich et al., 2016; Lotery et al., 2020b). However, we believe to have chosen a pathophysiologically and clinically relevant distinction of acute vs. chronic CSCR with a combination of functional and structural parameters. There was a high number of loss to follow-up as is to be expected in a retrospective real-life study which needs to be accounted for in interpretation of the baseline and 12 months data. However, this does not affect the survival analysis.

In conclusion, the results of this study evaluating routine clinical practice data do not show any evidence of efficacy of eplerenone in resolution of SRF in CSCR (Lotery et al., 2020b).

DATA AVAILABILITY STATEMENT

Data from this study will be shared upon request in an anonymized form.

ETHICS STATEMENT

The study involving human participants were reviewed and approved by the Ethics Committee of the University of Zurich, BASEC-No. PB_2016-00264. The patients/participants provided their written informed consent to participate in this study.

AUTHOR CONTRIBUTIONS

KF has contributed to data collection and curation, methodology and formal analysis and has written the original draft. She has approved of the final manuscript to be published and is accountable for all aspects of the work. JG has contributed to data collection and validation and has critically revised the manuscript. She has approved of the final manuscript to be published and is accountable for all aspects of the work. DB has contributed in conceptualizing and design of the study, supervising, and critical review of the manuscript. He has approved of the final manuscript to be published and is accountable for all aspects of the work. SZ has conceptualized and designed the project and contributed in critical review of the manuscript. She has approved of the final manuscript to be published and is accountable for all aspects of the work.

SUPPLEMENTARY MATERIAL

The Supplementary Material for this article can be found online at: https://www.frontiersin.org/articles/10.3389/fphar.2021.675295/full#supplementary-material

REFERENCES

Behar-Cohen, F., and Zhao, M. (2016). Corticosteroids and the Retina. *Curr. Opin. Neurol.* 29 (1), 49–54. doi:10.1097/WCO.0000000000000284

Bousquet, E., Beydoun, T., Zhao, M., Hassan, L., Offret, O., and Behar-Cohen, F. (2013). Mineralocorticoid Receptor Antagonism in the Treatment of Chronic Central Serous Chorioretinopathy. *Retina* 33 (10), 2096–2102. doi:10.1097/IAE.0b013e318297a07a

Cakir, B., Fischer, F., Ehlken, C., Bühler, A., Stahl, A., Schlunck, G., et al. (2016). Clinical Experience with Eplerenone to Treat Chronic Central Serous Chorioretinopathy. *Graefes Arch. Clin. Exp. Ophthalmol.* 254 (11), 2151–2157. doi:10.1007/s00417-016-3373-3

Cakir, B., Agostini, H., and Lange, C. (2019). Behandlung der Chorioretinopathia centralis serosa mittels Aldosteronantagonisten [Treatment of central serous chorioretinopathy with mineralocorticoid receptor antagonists]. *Ophthalmologe* 116 (2), 189–200. doi:10.1007/s00347-018-0785-y

Chin, E., Almeida, D., Roybal, C. N., Niles, P. Karen. M., Gehrs, K., Sohn, E., et al. (2015). Oral Mineralocorticoid Antagonists for Recalcitrant Central Serous Chorioretinopathy. *Opth* 9, 1449–1456. doi:10.2147/OPTH.S86778

Dansingani, K. K., Balaratnasingam, C., Naysan, J., and Freund, K. B. (2016). En Face Imaging of Pachychoroid Spectrum Disorders with Swept-Source Optical Coherence Tomography. *Retina* 36 (3), 499–516. doi:10.1097/IAE.0000000000000742

Daruich, A., Matet, A., Dirani, A., Bousquet, E., Zhao, M., Farman, N., et al. (2015). Central Serous Chorioretinopathy: Recent Findings and New Physiopathology Hypothesis. *Prog. Retin. Eye Res.* 48, 82–118. doi:10.1016/j.preteyeres.2015.05.003

Daruich, A., Matet, A., Dirani, A., Gallice, M., Nicholson, L., Sivaprasad, S., et al. (2016). Oral Mineralocorticoid-Receptor Antagonists: Real-Life Experience in Clinical Subtypes of Nonresolving Central Serous Chorioretinopathy with Chronic Epitheliopathy. *Trans. Vis. Sci. Tech.* 5 (2), 2. doi:10.1167/tvst.5.2.2https://iovs.arvojournals.org/article.aspx?articleid=2500129

de Gasparo, M., Joss, U., Ramjoué, H. P., Whitebread, S. E., Haenni, H., Schenkel, L., et al. (1987). Three New Epoxy-Spirolactone Derivatives: Characterization In Vivo and In Vitro. *J. Pharmacol. Exp. Ther.* 240 (2), 650–656. https://www.ncbi.nlm.nih.gov/pubmed/2949071.

Delyani, J. A. (2000). Mineralocorticoid Receptor Antagonists: The Evolution of Utility and Pharmacology. *Kidney Int.* 57 (4), 1408–1411. doi:10.1046/j.1523-1755.2000.00983.x

Fusi-Rubiano, W., Saedon, H., Patel, V., and Yang, Y. C. (2019). Oral Medications for Central Serous Chorioretinopathy: A Literature Review. *Eye* 34, 809–824. doi:10.1038/s41433-019-0568-y

Gerendas, B. S., Kroisamer, J.-S., Buehl, W., Rezar-Dreindl, S. M., Eibenberger, K. M., Pablik, E., et al. (2018). Correlation between Morphological Characteristics in Spectral-Domain-Optical Coherence Tomography, Different Functional Tests and a Patient's Subjective Handicap in Acute Central Serous Chorioretinopathy. *Acta Ophthalmol.* 96 (7), e776–e782. doi:10.1111/aos.13665https://onlinelibrary.wiley.com/doi/abs/10.1111/aos.13665

Ghadiali, Q., Jung, J. J., Yu, S., Patel, S. N., and Yannuzzi, L. A. (2016). Central Serous Chorioretinopathy Treated with Mineralocorticoid Antagonists. *Retina* 36 (3), 611–618. doi:10.1097/IAE.0000000000000748

Iacono, P., Toto, L., Costanzo, E., Varano, M., and Parravano, M. C. (2019). Pharmacotherapy of Central Serous Chorioretinopathy: A Review of the Current Treatments. *Cpd* 24 (41), 4864–4873. doi:10.2174/1381612825666190123165914

Kapoor, K. G., and Wagner., A. L. (2016). Mineralocorticoid Antagonists in the Treatment of Central Serous Chorioretinopathy: A Comparative Analysis. *Ophthalmic Res.* 56 (1), 17–22. doi:10.1159/000444058

Lee, J. H., Lee, S. C., Kim, H., and Lee, C. S. (2019). Comparison of Short-Term Efficacy between Oral Spironolactone Treatment and Photodynamic Therapy for the Treatment of Nonresolving Central Serous Chorioretinopathy. *Retina* 39 (1), 127–133. doi:10.1097/IAE.0000000000001913

Liew, G., Quin, G., Gillies, M., and Fraser-Bell, S. (2013). Central Serous Chorioretinopathy: A Review of Epidemiology and Pathophysiology. *Clin. Exp. Ophthalmol.* 41 (2), 201–214. doi:10.1111/j.1442-9071.2012.02848.x

Loo, R. H., Scott, I. U., Flynn, H. W., Jr, Gass, J. D., Murray, T. G., Lewis, M. L., et al. (2002). Factors Associated with Reduced Visual Acuity during Long-Term Follow-Up of Patients with Idiopathic Central Serous Chorioretinopathy. *Retina* 22 (1), 19–24. doi:10.1097/00006982-200202000-00004https://www.ncbi.nlm.nih.gov/pubmed/11884873

Lotery, A., O'Connell, A., Harris, R. A., Sivaprasad, S., and Reeves, B. C. (2020a). "Eplerenone for Chronic Central Serous Chorioretinopathy—Authors" Reply. *Lancet* 396 (10262), 1557–1558. doi:10.1016/s0140-6736(20)32321-7

Lotery, A., Sivaprasad, S., O'Connell, A., Harris, R. A., Culliford, L., Ellis, L., et al. (2020b). Eplerenone for Chronic Central Serous Chorioretinopathy in Patients with Active, Previously Untreated Disease for More Than 4 Months (VICI): A Randomised, Double-Blind, Placebo-Controlled Trial. *Lancet* 395 (10220), 294–303. doi:10.1016/S0140-6736(19)32981-2

Mehta, P. H., Meyerle, C., Sivaprasad, S., Boon, C., and Chhablani, J. (2017). Preferred Practice Pattern in Central Serous Chorioretinopathy. *Br. J. Ophthalmol.* 101 (5), 587–590. doi:10.1136/bjophthalmol-2016-309247

Pichi, F., Carrai, P., Ciardella, A., Behar-Cohen, F., and Nucci, P.Central Serous Chorioretinopathy Study Group (2016). Comparison of Two Mineralcorticosteroids Receptor Antagonists for the Treatment of Central Serous Chorioretinopathy. *Int. Ophthalmol.* 37, 1115–1125. doi:10.1007/s10792-016-0377-2

Rahimy, E., Pitcher, J. D., 3rd, Hsu, J., Adam, M. K., Shahlaee, A., Samara, W. A., et al. (2018).A Randomized Double-Blind Placebo-Control Pilot Study of Eplerenone for the Treatment of Central Serous Chorioretinopathy (Ecselsior) *Retina* 38, 962–969. doi:10.1097/IAE.0000000000001649

Sacconi, R., Borrelli, E., and Querques, G. (2020). Eplerenone for Chronic Central Serous Chorioretinopathy. *Lancet* 396 (10262), 1556. doi:10.1016/s0140-6736(20)31610-x

Salehi, M., Wenick, A. S., Law, H. A., Evans, J. R., and Gehlbach, P. (2015). Interventions for Central Serous Chorioretinopathy: A Network Meta-Analysis. *Cochrane Database Syst. Rev.* 12 (12), CD011841. doi:10.1002/14651858.CD011841.pub2

Scholz, P., Altay, L., and Fauser, S. (2016). Comparison of Subthreshold Micropulse Laser (577 Nm) Treatment and Half-Dose Photodynamic Therapy in Patients with Chronic Central Serous Chorioretinopathy. *Eye* 30 (10), 1371–1377. doi:10.1038/eye.2016.142

Schwartz, R., Habot-Wilner, Z., Martinez, M. R., Nutman, A., Goldenberg, D., Cohen, S., et al. (2017). Eplerenone for Chronic Central Serous Chorioretinopathy-A Randomized Controlled Prospective Study. *Acta Ophthalmol.* 95 (7), e610–e618. doi:10.1111/aos.13491https://onlinelibrary.wiley.com/doi/abs/10.1111/aos.13491

Singh, S. R., Vupparaboina, K. K., Goud, A., Dansingani, K. K., and Chhablani, J. (2019). Choroidal Imaging Biomarkers. *Surv. Ophthalmol.* 64 (3), 312–333. doi:10.1016/j.survophthal.2018.11.002

Stanescu-Segall, D., Touhami, S., Bodaghi, B., and LeHoang, P. (2020). Eplerenone for Chronic Central Serous Chorioretinopathy. *Lancet* 396 (10262), 1556–1557. doi:10.1016/S0140-6736(20)32327-8

Sun, X., Shuai, Y., Fang, W., Li, J., Ge, W., Yuan, S., et al. (2018). Spironolactone versus Observation in the Treatment of Acute Central Serous Chorioretinopathy. *Br. J. Ophthalmol.* 102(8) 1060-1065. doi:10.1136/bjophthalmol-2017-311096

Wang, S. K., Sun, P., Tandias, R. M., Seto, B. K., and Arroyo, J. G. (2019). Mineralocorticoid Receptor Antagonists in Central Serous Chorioretinopathy. *Ophthalmol. Retina* 3 (2), 154–160. doi:10.1016/j.oret.2018.09.003

Zhao, M., Célérier, I., Bousquet, E., Jeanny, J.-C., Jonet, L., Savoldelli, M., et al. (2012). Mineralocorticoid Receptor Is Involved in Rat and Human Ocular Chorioretinopathy. *J. Clin. Invest.* 122 (7), 2672–2679. doi:10.1172/JCI61427

Zola, M., Daruich, A., Matet, A., Mantel, I., and Behar-Cohen, F. (2018). Two-Year Follow-Up of Mineralocorticoid Receptor Antagonists for Chronic Central Serous Chorioretinopathy. *Br. J. Ophthalmol.* 103, 1184–1189. doi:10.1136/bjophthalmol-2018-312892

Zucchiatti, I., Sacconi, R., Parravano, M. C., Costanzo, E., Querques, L., Montorio, D., et al. (2018). Eplerenone Versus Observation in the Treatment of Acute Central Serous Chorioretinopathy: A Retrospective Controlled Study. *Ophthalmol. Ther.* 7 (1), 109–118. doi:10.1007/s40123-018-0121-2

Conflict of Interest: The authors declare that the research was conducted in the absence of any commercial or financial relationships that could be construed as a potential conflict of interest.

frontiers in Pharmacology

REVIEW
published: 21 June 2021
doi: 10.3389/fphar.2021.695267

Autophagy: A Novel Pharmacological Target in Diabetic Retinopathy

Annagrazia Adornetto[1]*, *Carlo Gesualdo*[2], *Maria Luisa Laganà*[1], *Maria Consiglia Trotta*[3], *Settimio Rossi*[2] and *Rossella Russo*[1]

[1]Preclinical and Translational Pharmacology, Department of Pharmacy, Health and Nutritional Sciences, University of Calabria, Rende, Italy, [2]Multidisciplinary Department of Medical, Surgical and Dental Sciences, University of Campania "Luigi Vanvitelli", Naples, Italy, [3]Department of Experimental Medicine, University of Campania "Luigi Vanvitelli", Naples, Italy

Autophagy is the major catabolic pathway involved in removing and recycling damaged macromolecules and organelles and several evidences suggest that dysfunctions of this pathway contribute to the onset and progression of central and peripheral neurodegenerative diseases. Diabetic retinopathy (DR) is a serious complication of diabetes mellitus representing the main preventable cause of acquired blindness worldwide. DR has traditionally been considered as a microvascular disease, however this concept has evolved and neurodegeneration and neuroinflammation have emerged as important determinants in the pathogenesis and evolution of the retinal pathology. Here we review the role of autophagy in experimental models of DR and explore the potential of this pathway as a target for alternative therapeutic approaches.

Keywords: autophagy, diabetic retinopathy, LC3, autophagosomes, retinal degeneration, hyperglycemia

OPEN ACCESS

Edited by:
Salvatore Salomone,
University of Catania, Italy

Reviewed by:
Elisabetta Catalani,
University of Tuscia, Italy
Giovanni Casini,
University of Pisa, Italy

***Correspondence:**
Annagrazia Adornetto
annagrazia.adornetto@unical.it

Specialty section:
This article was submitted to Experimental Pharmacology and Drug Discovery, a section of the journal Frontiers in Pharmacology

Received: *14 April 2021*
Accepted: *09 June 2021*
Published: *21 June 2021*

Citation:
Adornetto A, Gesualdo C, Laganà ML, Trotta MC, Rossi S and Russo R (2021) Autophagy: A Novel Pharmacological Target in Diabetic Retinopathy. Front. Pharmacol. 12:695267. doi: 10.3389/fphar.2021.695267

INTRODUCTION

Diabetic retinopathy (DR), a chronic and progressive complication of diabetes mellitus, is the main cause of legal blindness in working-age population (20–65 years old) (Ting et al., 2016; Simo-Servat et al., 2019). DR is prompted by hyperglycemia, which causes an increase of oxidative stress leading to an adaptive inflammatory response in microvasculature and neuroretinal tissue (Saxena et al., 2016; Al-Kharashi, 2018). The disease has long been considered as a microvascular disease, since loss of pericytes, damage of vascular endothelial cells and breakdown of blood-retinal barrier (BRB) are typical hallmarks of the early stage of the pathology (Beltramo and Porta, 2013; Mrugacz et al., 2021). However, recent and intensive research identified neurodegeneration and neuroinflammation as processes involved in the pathogenesis and evolution of DR (Kadlubowska et al., 2016). Furthermore, experimental and clinical studies have shown that neuronal apoptosis and reactive gliosis, with thinning of the nerve fiber layer often precede the typical vascular alterations (Barber et al., 2011; Gu et al., 2019). Importantly, DME (diabetic macular edema), which is due to an abnormal intraretinal fluid collection in the macular area, is the most common cause of vision loss in patients with DR (Romero-Aroca et al., 2016). Experimental and clinical studies have highlighted the role of inflammation in DME and OCT-imaging biomarkers of retinal inflammation have been identified (Ceravolo et al., 2020).

The mechanisms underlying the neurodegenerative and neuroinflammatory processes occurring in DR are common to other central and retinal diseases, like glaucoma and retinitis pigmentosa (Baumgartner, 2000; Barber, 2003; Gupta and Yücel, 2007). These mechanisms include oxidative stress and free radical formation, advanced glycation end products (AGEs) production, glutamate excitotoxicity, mitochondrial dysfunction, impaired bioenergetics, dysfunction of neurotrophin signals and autophagy (Dong et al., 2009; Jellinger, 2010; Rosa et al., 2016).

Autophagy is a major lysosomal pathway for the turnover of cytoplasmic organelles and long-lived proteins and, besides its homeostatic functions, it also acts as an adaptive response to cellular stresses (Mizushima, 2007). Dysfunctions of this process have been identified as recurrent events in neurodegenerative disorders (Frake et al., 2015) and, more recently, experimental and clinical data have shown that autophagy modulation also occurs in experimental models of DR and in the retina of diabetic patients, with or without retinopathy (Lopes de Faria et al., 2016; Dehdashtian et al., 2018).

However, the functional role of autophagy in DR remains unclear. Here we discuss the available literature on the role of autophagy in experimental models of DR and explore the potential of this pathway as a target for alternative therapeutic approaches.

DIABETIC RETINOPATHY: A NEURODEGENERATIVE RETINAL DISEASE

DR is a social disease with considerable costs, whose global incidence is strongly increasing due to the improved life expectancy and the exponential spread of diabetes (Flaxman et al., 2017). Indeed in 2015, 415 million people were affected by diabetes globally and this number is projected to reach 642 million by 2040 (Ogurtsova et al., 2017). In addition, it has been estimated that more than a third of people with diabetes worldwide have some form of DR and that nearly one in 10 develops forms of DR or complications that are particularly threatening for the sight such as proliferative DR or diabetic macular edema (Yau et al., 2012).

The diagnosis of DR is made on the bases of typical vascular abnormalities following the clinical examination of ocular fundus; it is possible to distinguish two stages: the non-proliferative DR (NPDR) and the proliferative DR (PDR). NPDR, the earliest form of DR, is divided into three stages of increasing severity, namely: 1) the mild DR characterized by rare microaneurysms and hemorrhages; 2) the moderate DR characterized by an increase in the aforementioned lesions associated with hard exudates; 3) the severe or pre-proliferating DR characterized by the coexistence of numerous microaneurysms, retinal hemorrhages, cottony nodules and venous caliber anomalies (Singh et al., 2008; Karst et al., 2018). At this stage, diabetic subjects can sometimes be asymptomatic for long time. On the other hand, in PDR, characterized by the appearance of epiretinal or epi-papillary new vessels that can sometimes invade the vitreous, patients may present a sudden vision impairment due to vitreous hemorrhages and/or tractional retinal detachment (Gotzaridis et al., 2001). Both forms of DR can be further complicated by macular edematous (DME) and/or ischemic damage, which are the main causes of severe vision impairment (Wilkinson et al., 2003; Cheung et al., 2010; Wang and Lo, 2018).

The onset of typical DR vascular changes is determined by prolonged hyperglycemic episodes resulting from suboptimal glycemic control in patients with type I or II diabetes mellitus. Elevated blood glucose levels result in aberrant regulation of a number of biochemical pathways, eventually leading to superoxide production and overload of oxidative stress in retinal tissues. Prolonged hyperglycemia has been shown to cause increased flow of the polyol pathway (Gabbay et al., 1966; Lee and Chung, 1999), increased formation of AGEs (Shinohara et al., 1998; Stitt, 2010), abnormal activation of signaling cascades like protein kinase C (PKC) pathway (Koya and King, 1998; Idris et al., 2001), increase in the flux of the hexosamine pathway (Kolm-Litty et al., 1998; Du et al., 2000) and reactive oxygen species (ROS) (Brownlee, 2005). All these changes lead to an intensification in oxidative stress and an inflammatory attack on the retina with consequent structural and functional changes (Kowluru and Chan, 2007; Hammes, 2018) (**Figure 1**).

The first responses, considered as metabolic self-regulation to increase retinal metabolism, are vessel dilation and changes in blood flow (Bek, 2017). Another hallmark of early DR is the loss of pericytes which has been demonstrated in both *in vitro* and *in vivo* studies (Romeo et al., 2002). Since pericytes provide structural support to capillaries, their loss leads to the formation of microaneurysms, which represents the first clinical characteristic sign of DR (Ejaz et al., 2008). Other pathogenetic processes found during DR include endothelial cells apoptosis and thickening of the basement membrane, which overall contribute to compromise the BRB integrity (Beltramo and Porta, 2013). Finally, the loss of pericytes and endothelial cells causes capillaries occlusion and consequent ischemia. Retinal ischemia, through the activation of hypoxia-inducible factor-1 (HIF-1) (Huang et al., 2015), determines an overproduction of vascular endothelial growth factor (VEGF), a key factor involved in both the progression of retinopathy towards PDR, and in DME development through phosphorylation of tight junction proteins such as occludin and zonula occludens-1 (Antonetti et al., 1999). Furthermore, VEGF, by the activation of the mitogen activated protein (MAP), stimulates the proliferation of endothelial cells, resulting in new vessels development (Rousseau et al., 1997). The key role of VEGF in DR has been demonstrated in multiple studies showing its increased expression in diabetic mice retina (Li et al., 2010; Rossi et al., 2016), as well as in the vitreous of patients with DME and PDR (Adamis et al., 1994). In light of these evidence, the intravitreal injection of anti-VEGF agents is currently the gold standard for both early and advanced stages DR therapy (Sun and Jampol, 2019). Other therapeutic tools aimed at managing the microvascular complications of DR are steroid intravitreal injection, laser photocoagulation and vitreous surgery (Stitt et al., 2016; Wang and Lo, 2018; Sun and Jampol, 2019). However, although these treatments demonstrate clinical benefits, no tools are effective in completely blocking clinical progression or reversing retinal damage. In fact, such therapies are often used in the more advanced stages of DR, characterized by a high risk of irreversible and severe visual impairment.

Furthermore, in many cases frequent administration of intravitreal agents is necessary with a consequent increased risk of side effects related to the injection, not to mention the high costs associated with frequent eye examinations (Donnelly et al., 2004; Gupta et al., 2013).

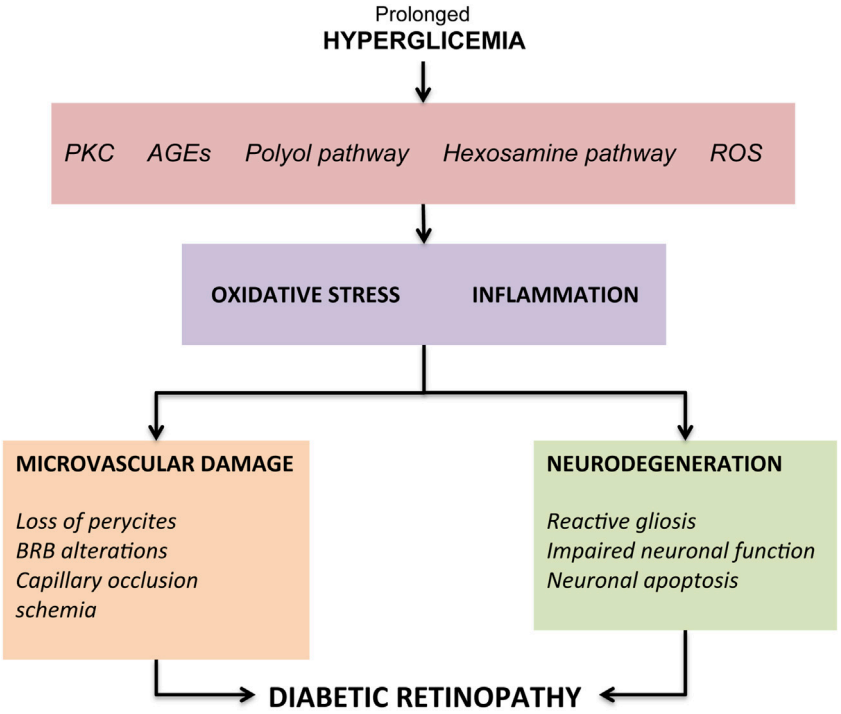

FIGURE 1 | Overview of the pathogenic mechanisms leading to diabetic retinopathy.

For many years, microangiopathic lesions were considered the exclusive cause of DR, leading to the visual loss in diabetic patients. However, the concept of DR as a microvascular disease has evolved: nowadays, it is considered a more complex diabetic complication, in which neurodegeneration has emerged as an important factor, playing a significant role in DR pathogenesis and evolution (Ola and Alhomida, 2014; Jindal, 2015). Indeed, the American Diabetes Association (ADA) recently defined DR as a diabetes neurovascular complication that involves a progressive disruption of the interdependence between multiple cell types in the retina (Solomon et al., 2017).

The hallmarks of diabetes-induced neuroglial degeneration, which include reactive gliosis, impaired retinal neuronal function and apoptosis of neural cells, have been described before typical microangiopathy in multiple experimental models of DR and also in the retina of diabetic donors (Barber et al., 1998; Lieth et al., 1998; Lung et al., 2012; Howell et al., 2013; Jindal, 2015).

The first retinal neurons affected are retinal ganglion cells (RGCs) and amacrine cells, however photoreceptors also show an increased apoptosis (Lynch and Abràmoff, 2017). The structural consequence of this early death is a reduction in the ganglion cell layer (GCL) thinning and corresponding loss of nerve fiber layer (NFL) thickness, detected by optical coherence tomography (OCT) (van Dijk et al., 2010; Sohn et al., 2016). Moreover, functional studies performed with multifocal electroretinography (mfERG) have shown a delayed implicit time P1 and a reduction in the trace's amplitude as a consequence of the early neurodegenerative process (Simão et al., 2017). These structural and functional alterations lead to reduced contrast sensitivity, delayed dark adaptation and altered visual fields, resulting overall in reduced vision-related quality of life, despite the absence of clinically detectable vascular anomalies (Wolff et al., 2015; Trento et al., 2017).

Müller cells and retinal astrocytes play an important role in the damage to retinal neurons and in linking the neurodegenerative process with vascular disease. Indeed, gliosis is associated with higher expression of VEGF and hyper-activation of pro-inflammatory pathways, with consequent overexpression of pro-inflammatory cytokines and dysfunction of the BRB (Bringmann and Wiedemann, 2012). Diabetes-induced subclinical inflammation is further amplified by the activation of immune cells resident in the retina, namely microglial cells. This microglial activation is accompanied by a phenotypic shift from the anti-inflammatory (M2) towards a pro-inflammatory amoeboid (M1) form (Coorey et al., 2012; Arroba and Valverde Á, 2017). This shift results in transcriptional changes mediated by nuclear factor-kappa B (NF-κB) and extracellular signaling mechanisms of the signal-regulated kinase (ERK) responsible for the release or activation of pro-inflammatory and neurotoxic molecules (i.e. cytokines, chemokines, glutamate) which contributes to the disruption of BRB and neuronal death (Altmann and Schmidt, 2018).

AUTOPHAGY: MECHANISMS AND FUNCTIONS

Autophagy is a highly conserved catabolic pathway by which cells remove misfolded or aggregated proteins and damaged organelles

(Klionsky et al., 2021). This process regulates essential biological functions such as cell survival, cell metabolism, development, aging, and immunity. It also represents an adaptive response to different forms of stresses, like nutrient deprivation, growth factor depletion, infection, hypoxia, ischemia/reperfusion injury, oxidative stress, endoplasmic reticulum (ER) stress and mitochondrial damage (Glick et al., 2010; Dikic and Elazar, 2018).

In mammalian cells, there are three primary types of autophagy: microautophagy, macroautophagy, and chaperone-mediated autophagy (CMA) (Yang and Klionsky, 2010). Furthermore, different selective forms of autophagy, such as mitophagy, ribophagy or aggrephagy, have also been identified (Menzies et al., 2017).

In microautophagy, cytosolic components are directly taken up by lysosomes through the invagination of their membrane (Li et al., 2012). CMA, involves the formation of a complex between target proteins (identified by bearing a CMA targeting motif) and chaperones of the Hsp70 family; these complexes are recognized by the lysosome-associated membrane protein type-2A (LAMP-2A) at the lysosomal membrane where the substrate proteins unfold and translocate in the lumen for degradation by lysosomal hydrolase (Itakura and Mizushima, 2010).

Macroautophagy (hereafter referred to as autophagy) involves the formation of a cup-shaped membrane structure, the phagophore, that elongates and closes around the cytosolic cargo; the resulted double-membrane vesicle is called autophagosome and it is selectively associated with this pathway (Yang and Klionsky, 2010). Autophagosomes are transported, along the microtubules, to the perinuclear region where they fuse with lysosomes; here the autophagic content is degraded and released for recycling into the cytoplasm (Parzych and Klionsky, 2014). Autophagy and its regulatory mechanisms are evolutionarily conserved among eukaryotic cells even if the level of complexity of the process may differ (Yang and Klionsky, 2009).

Autophagosome biogenesis is orchestrated by the sequential action of autophagy-related (Atg) proteins; most of them were originally identified in yeast but have their homologs in mammalian cells (Mizushima et al., 2011). The ULK1 complex, formed by the serine/threonine protein kinase Atg1/(unc-51-like kinase 1), FIP200 (focal adhesion kinase family interacting protein of 200 kDa), Atg13 and Atg101 is involved in the initiation of autophagy (Hara et al., 2008). Upon autophagy induction, the mammalian target of rapamycin (mTOR), one of the main negative regulators of the process, is inactivated resulting in upregulation of ULK1 kinase activity and consequent phosphorylation of Atg13 and FIP200 (Noda, 2017). ULK1 complex gathers to specific ER region engaged in autophagosome formation (Itakura and Mizushima, 2010) and regulates the recruitment of a second kinase complex, the vacuolar protein sorting 34 (Vps34) complex formed by Beclin-1, AMBRA, Vps34, Vps15 and Atg14 (Glick et al., 2010). Vps34 participates in various membrane-sorting processes but it is selectively involved in autophagy when complexed to Beclin-1 (Backer, 2008). At variance with the other PI3-kinases, Vps34 only uses phosphatidylinositol (PI) as substrate to generate phosphatidyl inositol triphosphate (PI3P), which is therefore essential for phagophore nucleation, elongation and recruitment of other Atg proteins (Xie and Klionsky, 2007). The interaction of Beclin-1 with Vps34 promotes its catalytic activity and increases PI3P levels (Glick et al., 2010).

Following the initiation step, the elongation process is undertaken by two ubiquitin like proteins: Atg12 and Atg8/LC3. In this system, the E1-like enzyme Atg7 and E2-like enzyme Atg10 catalyze the formation of the Atg12-Atg5 complex that allows the formation of the Atg12-Atg5-Atg16 (L1) complex. The latter is crucial for autophagosome formation and for efficient promotion of the microtubule-associated protein light chain 3 (LC3) lipidation (Otomo et al., 2013).

Several experimental evidences demonstrate that LC3 is involved in the selective identification of autophagy substrates (Yoshii and Mizushima, 2017; Mizushima and Murphy, 2020). Indeed, LC3-II interacts with the constitutively expressed adaptor molecule p62 (or sequestosome-1, SQSTM1) that contains both a ubiquitin binding domain and a LC3-interacting (LIR) domain to deliver sequestered proteins to the autophagosomes (Zhang et al., 2015).

The fusion of the autophagosomal membrane with lysosome results in the release of a single-membrane autophagic body into the lysosomal lumen, which is followed by the degradation of the autophagic cargo by the lysosomal acid proteases (Dikic and Elazar, 2018).

Cellular homeostasis depends on the balance between the production and removal of macromolecules and organelles. In this context, basal autophagy activity plays a key role in the maintenance of cellular integrity (Chun and Kim, 2018). As a quality control mechanism, the process is fundamental for every cell, but it is particularly important in neurons. Indeed, neuronal cells are metabolically highly active and, being post mitotic cells, cannot dilute damaged or aged organelles and misfolded proteins by cell division (Mariño et al., 2011; Russo et al., 2013). Therefore, not surprisingly, accumulation of these altered components, due to autophagy inefficiency, has been associated with neurotoxicity and neurodegeneration.

Autophagy disruption or insufficiency has been reported in a number of different ocular diseases and pathological conditions like: retinal injury (Besirli et al., 2011), retinal degenerations (Punzo et al., 2009; Rodríguez-Muela et al., 2015), light-induced stress (Kunchithapautham et al., 2011; Chen et al., 2014), hyperglycemia (Lopes de Faria et al., 2016) and hypoglycemia (Zhou et al., 2015).

In this context, autophagy is becoming an attractive target to treat neurodegenerative disorders (Zhu et al., 2013), including the ones affecting the retina (Russo et al., 2013).

THE ROLE OF AUTOPHAGY IN ANIMAL MODELS OF DIABETIC RETINOPATHY

Several groups have reported a modulation of Atg proteins in animal models of TD1 and TD2 diabetes (**Table 1**). In C57BL/6J mice, induction of type1 (T1D) diabetes by administration of

TABLE 1 | Autophagy modulation in animal models of diabetic retinopathy.

Animal Models	DR model	Autophagy markers	References
Mice			
C57BL/6J	150 mg/kg STZ (single injection)	↑ LC3-I ↑ Atg5 ↑ Beclin-1	Piano et al. (2016)
$Ins2^{+/+}$ Akita (male)		↑ Beclin-1 ↑ LC3-II ↑ Atg12-Atg5 ↑ Atg3	Wang et al. (2017)
C57BL/6J (male, 6 weeks old)	40 mg/kg STZ (5 days treatment)	↓ Atg9 ↓ Atg7 ↓ LC3 ↓ Beclin-1	Qi et al. (2020)
C57BL/KsJ-db/db (male, 8-12-16-18-25 weeks old) and -db/m (male, 8 weeks old)		Fluctuating modulation of LC3-II	Fu et al. (2020)
C57BL/6J (male, 6 weeks old)	50 mg/kg/d STZ	↓ Beclin-1 ↓ Atg7 ↓ p62 ↓ LC3-II	Wang et al. (2020)
C57BL/6J (male, 8 weeks old)	150 mg/kg STZ (single injection)	↑ Beclin-1 ↑ ATG9A	Madrakhimov et al. (2021)
db/db mice (male, 20 weeks old)		↓ LC3-II ↓ Beclin-1 ↓ Atg5 ↑ p62	Luo et al. (2021)
Rats			
Sprague-Dawley (male, 6–8 weeks old)	High sugar/fat diet + 40 mg/kg STZ (single injection)	↑ LC3-II	Cai et al. (2017)
Sprague-Dawley (male)	STZ injection	↑ Beclin-1 ↑ LC3-II ↑ Atg12-Atg5 ↑ Atg3	Wang et al. (2017)
Sprague-Dawley (male, 2 months old)	35 mg/kg STZ (single injection)	↓ LC3-II	Shruthi et al. (2017)
Sprague-Dawley (male, 7–8 weeks old)	60 mg/kg STZ (single injection)	↑ Beclin-1 ↑ LC3-II/LC3-I ↑ ph-AMPK ↓ ph-mTOR	Park et al. (2018)
Sprague-Dawley (male, 6–8 weeks old)	40 mg/kg STZ (single injection)	↓ LC3-II ↓ LC3-II/LC3-I	Mao et al. (2019)
BBZDR/Wor (male, 5 months old)	BBZDR/Wor: type 2 diabetic model	↓ Atg9 ↓ Atg7 ↓ LC3 ↓ Beclin-1	Qi et al. (2020)

(DR: diabetic retinopathy; STZ: streptozotocin).

streptozotocin (STZ) was associated with increased LC3-II immunoreactivity in the outer plexiform layer (OPL) and upregulation of the Atg related proteins, Beclin-1 and Atg5 (Piano et al., 2016). These changes occurred within the same time frame of outer retinal damage and might take part to the process of photoreceptors loss in the early phase of DR, before the appearance of evident signs of vascular damage (Piano et al., 2016). Accordingly, upregulation of Beclin-1, LC3-II, Atg12-Atg5 and Atg3 was reported in STZ-diabetic rats and $Ins2^{Akita}$ mice, a spontaneous T1D mouse model (Wang et al., 2017). In this study knockdown of Hist1h1c, a gene that encoded for Histone H1.2 protein, significantly reduced both basal and high-glucose-induced autophagy, attenuated inflammation and cell toxicity. Conversely, adeno-associated virus (AAV)-mediated histone HIST1H1C overexpression led to increased autophagy, glial activation and neuronal loss which are pathological changes identified in the early stages of DR (Wang et al., 2017). These findings suggest that over-stimulation of autophagy is associated with increased retinal cell death and takes part to the progression of DR through advanced stages.

A very recent study by Madrakhimov and colleagues demonstrated that long-term hyperglycemia causes mTOR inhibition leading to autophagy dysregulation (Madrakhimov et al., 2021). Indeed, inhibition of the mTORC1 pathway in STZ-induced diabetic mice was associated with upregulation of Beclin-1 in the entire inner retina and ATG9A in NeuN (Neuronal Nuclei) positive RGCs. These changes were accompanied with signs of neuronal cell damage, such as activation of cleaved caspase three and decrease of the total number of cells in the GCL. Interestingly, blockade of autophagy by mTOR activator-MHY1485 injections in diabetic mice resulted in a prominent rescue of neuronal cells (Madrakhimov et al., 2021).

Increased LC3-II expression was also reported by Cai and colleagues (2017) in male rats fed with sugar, high fat diet followed by STZ injection; in this model treatment with Glucagon-like peptide-1 (GLP-1), reduced oxidative stress and reverted the upregulation of LC3-II expression (Cai et al., 2017).

At variance with the previous reported results, in the retina of STZ-induced diabetic mice a decrease of Beclin-1, Atg7, p62 and LC3-II expression was reported as compared to control group; treatment with the heparanase inhibitor PG545 promoted autophagy and inhibited the secretion of pro-inflammatory cytokines alleviating diabetic retinopathy (Wang et al., 2020).Similarly, in STZ-induced diabetic C57BL/6J mice, as well as in Bio-Breeding Zucker diabetic (BBZDR/Wor) rats that spontaneously develop a T2D, Qi and colleagues reported a dramatic reduction of Atg7, Atg9, LC3 and Beclin-1 in diabetic retina as compared to controls (Qi et al., 2020).

Interestingly, in this same study the authors showed a diurnal rhythmicity of Atg proteins levels. Under basal conditions Atg9 and LC3 expression showed a biphasic diurnal cycle with two peaks of highest and lowest levels, respectively, while Atg7 and Beclin-1 had a monophasic 24 h cycle. In the retinas from both T1D and T2D mice a significant impairment of Atg proteins diurnal rhythmicity was reported (Qi et al., 2020). This suggests that in diabetic retina the molecular circuit regulating basal autophagy, in terms of intensity and duration, might be altered.

Suppression of LC3-II expression was also reported by Mao and colleagues in STZ-induced diabetic rats; the reduced level of LC3-II correlated with a significant upregulation of a specific microRNA (miRNA), miR-204-5p. Indeed, anti-miR-204-5p treatment enhanced the expression of LC3-II and increased LC3-II/LC3-I ratio, while miR-204-5p mimic treatment was associated with opposite effects thus suggesting that in DR miR-204-5p is responsible for the inhibition of the autophagy pathway (Mao et al., 2019).

The modulation of autophagy in diabetic models may vary depending on the progression of the disease and therefore on the time points analyzed. In RGCs of C57BL/KsJ-db/db mouse, a rodent model of spontaneous diabetes, Fu and co-workers (2020) observed a fluctuating modulation of LC3-II protein levels depending on the age of diabetic mice without identifying a clear trend (Fu et al., 2020). In db/db mice Luo and colleagues reported a downregulation of pro-autophagy proteins like LC3-II, Beclin-1 and Atg5 and a significant upregulation of p62 (Luo et al., 2021). More interestingly, in STZ-induced diabetic rats Shruthi and collaborators (2017) observed a biphasic modulation of LC3-II retinal expression characterized by an increase in 2 months old followed by a significant decrease in 4 months old diabetic rats when compared to control animals. The initial upregulation of the pathway could be part of the adaptive response to the damage induced by hyperglycemia. On the other hand, the later impairment of autophagy might be the consequence of the system overload due to the prolonged diabetic-related damage and contribute to the apoptotic retinal cell death (Shruthi et al., 2017).

A recent study by Park and collaborators (2018) focused on the role of autophagy on RGC survival depending on the type of triggering injury (Park et al., 2018). Autophagy was upregulated in both diabetic and glaucomatous retinas, however while autophagy inhibition, by 3-methyladenine (3-MA), an inhibitor of phosphatidylinositol 3-kinases (PI3K), decreased the apoptosis of RGCs in glaucomatous retina, it failed in rescuing RGCs in diabetic retina. The work by Park and collaborators suggests that, depending on the type of injury and the intracellular pathway engaged for cell death, autophagy could either promote RGC survival or death (Park et al., 2018).

Interestingly in a *drosophila* model of hyperglycemia developed by raising adult fruit flies under high-sucrose regimens, signs of autophagy deregulation, such as significant and progressive increase of LC3 and p62 staining, with accumulation of autophagosomes were observed in eye sections (Catalani et al., 2021).

In murine retinal explant, exposure to HG was associated with reduced LC3-II levels and upregulation of the cargo-protein p62. Treatment with octreotide, an analogue of somatostatin, prevented the autophagy changes induced by HG, and exerted anti-apoptotic effects. Co-treatment with the autophagy inhibitor chloroquine (CQ) reverted the neuroprotective effects of octreotide suggesting that a cross talk between autophagy and apoptosis occurs in the injured retina (Amato et al., 2018).

THE ROLE OF AUTOPHAGY IN *IN VITRO* MODELS OF DIABETIC RETINOPATHY

Retinal lesions observed over the course of DR are initially characterized by pericyte cell death, which generates ischemia and promotes the extravasation of plasma constituents such as low-density lipoproteins (LDLs). This generates the damage of RPE and activation of microglial and Müller cells (Fu et al., 2012). On the other hand, DR induced neuronal dysfunction, with RGCs death, apoptosis of amacrine cells in INL, loss of synapses and dendrites and alteration of synaptic activity (Ozcan et al., 2006; Oshitari et al., 2011). It is clear that a large number of cellular elements in the retina are affected by DR (Yang et al., 2020) and therefore, several *in vitro* studies have focused on the modulation of autophagy in the different cell types exposed to diabetes-related insults (**Table 2**).

Retinal Pigment Epithelial Cells

Exposure of human immortalized RPE cell, ARPE-19, to high glucose (HG) induced a significant upregulation of autophagy flux. Compared to cells cultured under normal glucose condition, cultures exposed to HG showed increased autophagosome formation, upregulation and changes in the expression pattern of LC3-II and reduction of p62 levels. HG-induced autophagy was mainly regulated through the ROS-mediated ER stress and independent of mTOR signaling pathway (Yao et al., 2014). Similarly, in the same cell line exposed to HG, Shi and colleagues (2015), showed activation of autophagy by reporting an increase of autophagosome number and upregulation of LC3-II protein expression. Under these experimental conditions, inhibition of autophagy obtained by pre-treatment with 3-MA, induced accumulation of damaged-mitochondria, increased the

TABLE 2 | Autophagy modulation in cell culture models of diabetic retinopathy.

Cell culture	DR model	Autophagy markers	References
RPE			
hTERT-RPE (telomerase-immortalized human RPE cells)	HOG-LDL -highly oxidized glycated-LDL	↑ LC3-II	Du et al. (2013)
ARPE-19 (human immortalized RPE cells)	HG: 30 mM, 48 h	↑ LC3-II ↑ autophagosomes ↓ p62	Yao et al. (2014)
ARPE-19	HG: 30 mM, 48 h	↑ autophagosomes ↑ LC3-II	Shi et al. (2015)
hiPSC-RPE (human induced pluripotent stem-cell-derived retinal pigment epithelium cell lines)	HG: 25 mM, 5 weeks	↑ p62	Kiamehr et al. (2019)
Müller cells			
rMC-1 (rat retinal Müller cells)	HG: 25 mM, 24 h	↑ LC3-II ↑ Beclin-1 ↑ p62	Lopes de Faria et al. (2016)
MIO-M1 (immortalized human Müller cell line)	HOG-LDL-highly oxidized glycated-LDL	↑ LC3-II ↑ Beclin-1 ↑ Atg5	Fu et al. (2016a)
rMCs (primary rat Müller cells)	HG: 30–60 mM, 24–48 h	↓ LC3-II ↓ Beclin-1	Chen et al. (2018)
rMCs	HG: 40 mM, 24 h	↓ Beclin-1 ↓ LC3-II ↑ p62	Wang et al. (2019b)
Pericytes			
HRCPs (human retinal capillary pericytes)	HOG-LDL-highly oxidized glycated-LDL	↑ LC3-II ↑ Beclin-1 ↑ Atg5	Fu et al. (2016b)

(DR: diabetic retinopathy; LDL: low density lipoprotein; HG: high glucose).

activity of interleukin-1β (IL-1β) and NLRP3 (a NOD-like receptor family pyrin domain containing three inflammasome responsible for the processing of pro-IL1β to the active form of IL-1β) and reduced cell survival (Shi et al., 2015). Altogether, these experimental observations would suggest that in RPE cells exposed to HG stress induction of autophagy represents a cytoprotective response.

Accordingly, treatment with fenofibrate, a peroxisome proliferator-activated receptor alpha (PPARα) agonist by preventing ER-stress and inducing autophagy, exhibited a protective effect in RPE cells exposed to hyperglycemia (25 mM, 18 days) and hypoxia (1% oxygen, for 6 h or 24 h), two components of the diabetic milieu (Miranda et al., 2012; Lazzara et al., 2020).

More recently, Kiamehr and co-workers (2019) using human induced pluripotent stem-cell-derived retinal pigment epithelium (hiPSC-RPE) cell lines, obtained from T2D and healthy control patients, evaluated the effects of hyperglycemia, in the presence of absence of added insulin, on cellular functionality and autophagy (Kiamehr et al., 2019). The authors did not detect any differences in LC3-II expression between diabetic or healthy control hiPSC-RPEs, whereas they observed a significant p62 accumulation in T2D hiPSC-RPE as compared to healthy control (Kiamehr et al., 2019). This change in p62 expression might be unrelated to the autophagy pathway, since p62 is involved in several other functions; one possible hypothesis is that this upregulation of p62 is linked to the antioxidative NRF-2ARE pathway (nuclear factor erythroid-2 related factor/antioxidant response elements) evoked by the energy depletion in diabetic cells (Jain et al., 2010; Felszeghy et al., 2019).

In addition to hyperglycemia, extravasation of plasma lipoproteins modified by oxidation and glycation are important factors driving DR and leading to cytotoxicity (Yu and Lyons, 2013). In telomerase-immortalized human RPE (hTERT-RPE) cells treated with in vitro-modified highly oxidized glycated- (HOG-) LDL, reduced viability was accompanied by the induction of LC3-II expression with no changes in Beclin-1 protein level (Du et al., 2013). Pre-treatment with either native-High-density lipoprotein (N-HDL) or HOG-HDL inhibited HOG-LDL-induced LC3-II expression and partially mitigated RPE cell death (Du et al., 2013).

Retinal Müller Cells

Retinal Müller cells (rMCs), the primary retinal glial cells, make contacts with every cell type in the retina and are necessary for both neuronal and vascular function and viability (Shen et al., 2014).

The role of autophagy in modulating rMCs response to HG was investigated by Lopes de Faria and collaborators (Lopes de Faria et al., 2016). The study showed that rMCs exposed to HG upregulated the initial steps of autophagy, as shown by increase of Beclin-1 and LC3-II protein expression levels; however, the process of cargo degradation could not be completed due to the overcome of lysosomal dysfunction. The latter caused accumulation of p62 that, in turn, led to VEGF release and

rMCs apoptosis. Inhibition of the initial stage of autophagy with 3-MA or the final stage with Bafilomycin A1 (a vacuolar-type H^+-ATPase inhibitor) increased the number of apoptotic rMCs under either normal condition or following exposure to diabetic milieu conditions. On the contrary, induction of autophagy by rapamycin, a mTOR inhibitor, upregulated Beclin-1 expression, prevented p62 accumulation by restoring autophagy cargo degradation and protected cells from apoptosis (Lopes de Faria et al., 2016).

Comparable results were reported by Wang and collaborators (2019) in a similar cell culture model of primary rat rMCs. Following exposure of rMCs to HG, the authors detected a downregulation of autophagy with reduction of Beclin-1 and LC3-II expression and accumulation of p62 (L. Wang et al., 2019a). Treatment with epigallocatechin gallate (EGCG), a polyphenol present in green tea, protected cells from apoptosis by activating autophagy and reestablishing cargo degradation (L. Wang et al., 2019a). Accordingly, in rat primary rMCs the number of autophagic/lysosomal vacuoles was reduced after exposure to HG; this observation, together with the reported decrease of LC3-II and Beclin-1 protein expression suggested that autophagy activity in rMCs was inhibited by HG conditions. Under these experimental conditions, treatments with berberine reduced HG-induced rMCs apoptosis at least in part by enhancing autophagy (Chen et al., 2018).

Upregulation of Atg5, Beclin-1 and LC3-II proteins were reported in spontaneously immortalized human Müller cell line (MIO-M1) exposed to in vitro-modified HOG-LDL. Müller cell death was partially prevented by inhibiting autophagy with 3-MA or by knocking down Atg5 and Beclin-1 suggesting that autophagy takes part to the apoptosis induced by HOG-LDL (Fu et al., 2016a).

Pericytes

Pericyte cell death is one of the early features of DR (Hammes et al., 2002). Fu and colleagues (2012, 2016) investigated the modulation of autophagy in human retinal capillary pericytes (HRCP) exposed to HOG-LDL (Fu et al., 2012; Fu et al., 2016b) showing a significant dose-dependent increase of LC3-II, Atg5 and Beclin-1 (Fu et al., 2016b). In this study, autophagy appeared to play a dual role depending of the HOG-LDL concentrations: exposure to low levels of HOG-LDL was associated with a pro-survival autophagy response, on the contrary, when the cells were exposed to higher HOG-LDL concentration autophagy promoted cell death (Fu et al., 2016b).

MITOPHAGY AND DIABETIC RETINOPATHY

Mitophagy is a specialized form of autophagy responsible for the quality and quantity control of mitochondria (Pickles et al., 2018). These organelles are the primary source of cellular energy (ATP production), involved in respiration and metabolic processes (Kowluru, 2005) and a key source of ROS in diabetes (Sivitz and Yorek, 2010; Hammes, 2018). Oxidative stress originating in mitochondria from endothelial cell has been reported to alter several independent pathways, each contributing to the development of microvascular complications in DR (Du et al., 2000; Nishikawa et al., 2000). Furthermore, the increase of oxidative stress during hyperglycemia damages itself mitochondria function and structure (Madsen-Bouterse et al., 2010). Indeed, retina of diabetic patients and diabetic rodents showed accumulation of damaged and dysfunctional mitochondria (Masser et al., 2017; Kowluru and Mishra, 2018).

Recently, Zhou and co-workers (2019) showed activation of mitophagy in the retinas of diabetic (db/db) mice (Zhou et al., 2019). Indeed, a significant increase of mitophagy associated protein, PINK-1 and Parkin, was reported in the retinas of db/db mice as compared with non-diabetic (db/m) mice together with the upregulation of LC3-II/LC3-I ratio and reduction of p62. PINK1 (PTEN induces putative kinase protein 1) is a mitochondrially localized serine/threonine protein kinase (Valente et al., 2004) responsible for activation and translocation of Parkin, an E3 ubiquitin-ligase (Kitada et al., 1998), from the cytoplasm to damaged mitochondria (Matsuda et al., 2010). Parkin then marks damaged mitochondria with ubiquitin chains targeting them to mitophagy (Bingol et al., 2014). Accordingly, to the *in vivo* data, rMC-1 cells exposed to HG displayed significant increase of PINK1, Parkin and LC3-II/LC3-I expression as compared to cells exposed to normal glucose (Zhou et al., 2019).

Zhang and collaborators (2019) demonstrated that while the exposure of ARPE-19 cell cultures to low glucose (LG) (15 mM) induced autophagy, treatment with HG (50 mM) was associated with ROS mediated inhibition of mitophagy and reduced proliferative abilities (Zhang et al., 2019). Under HG conditions PINK1 and Parkin were downregulated and exogenous overexpression of these proteins, which reestablished mitophagy, reduced apoptosis and promoted cellular proliferation (Zhang et al., 2019). Intriguingly, the study by Zhang et al. (2019) showed that LG recruit LC3 to mitochondrial fraction suggesting that this condition may specifically induce mitophagy in RPE cells (Zhang et al., 2019).

Devi and colleagues reported induction of mitochondrial damage and mitophagy in rMCs exposed to HG (Devi et al., 2017) that were mediated by the upregulation of thioredoxin-interacting protein (TXNIP), a pro-oxidative stress and pro-apoptotic protein strongly induced by diabetes and HG conditions (Singh, 2013).

In a recent study, Taki and co-workers (2020), using 661W cells, a transformed murine cone cell line, observed that HG treatment (25 mM, 48 h) induced changes in mitophagy and autophagy with mitochondria accumulation and upregulation of p62. Treatment with 3-MA caused a greater increase of p62, superoxides and caspase 3/7 activation suggesting that impairment of the autophagy pathway correlates with superoxide formation and induction of apoptosis (Taki et al., 2020).

In spontaneous $Ins2^{Akita}$ diabetic mouse model, Hombrebueno and colleagues (2019), showed a time-dependent modulation of mitophagy (Hombrebueno et al., 2019). Indeed PINK1-dependent mitophagy in both Müller cells and photoreceptors was exacerbated within the first 2 months of diabetes, while a significant impairment of the

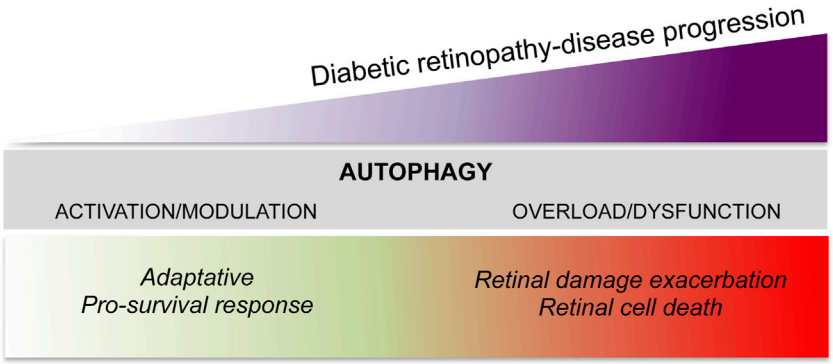

FIGURE 2 | The dual role of autophagy in diabetic retinopathy.

pathway was reported in the advanced stages of neurovascular dysfunction (8 months of diabetes). Furthermore, during prolonged diabetes, impairment of mitophagy correlated with the development of premature outer retina senescence (Hombrebueno et al., 2019).

CONCLUDING REMARKS

Autophagy in DR has become an area of intense research, however, despite the studies currently available, the question of whether autophagy is counteracting or favoring the evolution of DR remains unclear. Furthermore, controversial results have often been reported in terms of the type of autophagy modulation induced by hyperglycemia (induction *vs* impairment), in both *in vitro* and *in vivo* models (Gong et al., 2021). However, most evidence suggests that autophagy may act with a damage/time-dependent double action (**Figure 2**). Under mild stress or during the initial phase of DR, autophagy acts as an adaptative response with pro-survival and anti-apoptotic effects (Dehdashtian et al., 2018); on the other hand, under severe stress and in the later phase of DR, dysregulated autophagy, as a consequence of the system overload due to the prolonged damage, contributes to the apoptotic retinal cell death exacerbating the damage (Fu et al., 2016b; Shruthi et al., 2016).

In must also be stressed that the claim of some studies related to the induction or inhibition of autophagy are often not supported by the data. Indeed, being a dynamic process, autophagy should be studied in terms of flux. A simply increased number of autophagosomes, either by LC3 immunofluorescent staining or by transmission electron microscope (TEM), as well as changes in LC3-II/LC3-I ratio detected by western blot are not enough to drawing conclusion on the kind of autophagy activity modulation (Abudu and Acevedo-Arozena, 2021; Klionsky et al., 2021). Therefore, the use of more specific experimental settings, i.e. measurement of autophagosome substrates degradation, comparison of LC3-II accumulation in the absence or presence of lysosomal enzymatic activity inhibitors, should be performed to be able to state the occurrence of an autophagic process (Rubinsztein et al., 2009; Klionsky et al., 2021). It should be also taken into consideration that autophagy activity varies with animal age, sex or strain background and it also undergoes a diurnal rhythmicity. All these factors might affect the final results introducing a complex variability among the different experimental settings and making difficult a direct comparison of the different studies.

Based on the data accumulated so far, interpreting the contribution of autophagy in DR is still difficult and further studies are guaranteed in order to unravel the possibility that pharmacological modulation of the pathway could be exploited for DR supportive therapies.

AUTHOR CONTRIBUTIONS

Data collection and writing: AA, CG, ML, and RR; manuscript revising SR, MT, and RR; editing and figure preparation RR.

FUNDING

This work is supported by grants from the Italian Ministry of Education, University and Research: PRIN 2017 protocol number "2017TSHBXZ_002."

REFERENCES

Abudu, Y. P., and Acevedo-Arozena, A. (2021). Guidelines for the Use and Interpretation of Assays for Monitoring Autophagy (4th Edition)(1). *Autophagy* 17 (1), 1–382. doi:10.1080/15548627.2020.1797280

Adamis, A. P., Miller, J. W., Bernal, M. T., D'Amico, D. J., Folkman, J., Yeo, T. K., et al. (1994). Increased Vascular Endothelial Growth Factor Levels in the Vitreous of Eyes with Proliferative Diabetic Retinopathy. *Am. J. Ophthalmol.* 118 (4), 445–450. doi:10.1016/s0002-9394(14)75794-0

Al-Kharashi, A. S. (2018). Role of Oxidative Stress, Inflammation, Hypoxia and Angiogenesis in the Development of Diabetic Retinopathy. *Saudi J. Ophthalmol.* 32 (4), 318–323. doi:10.1016/j.sjopt.2018.05.002

Altmann, C., and Schmidt, M. H. H. (2018). The Role of Microglia in Diabetic Retinopathy: Inflammation, Microvasculature Defects and Neurodegeneration. *Int. J. Mol. Sci.* 19 (1). doi:10.3390/ijms19010110

Amato, R., Catalani, E., Dal Monte, M., Cammalleri, M., Di Renzo, I., Perrotta, C., et al. (2018). Autophagy-mediated Neuroprotection Induced by Octreotide in an *Ex Vivo* Model of Early Diabetic Retinopathy. *Pharmacol. Res.* 128, 167–178. doi:10.1016/j.phrs.2017.09.022

Antonetti, D. A., Barber, A. J., Hollinger, L. A., Wolpert, E. B., and Gardner, T. W. (1999). Vascular Endothelial Growth Factor Induces Rapid Phosphorylation of Tight junction Proteins Occludin and Zonula Occluden 1. A Potential Mechanism for Vascular Permeability in Diabetic Retinopathy and Tumors. *J. Biol. Chem.* 274 (33), 23463–23467. doi:10.1074/jbc.274.33.23463

Arroba, A. I., and Valverde Á, M. (2017). Modulation of Microglia in the Retina: New Insights into Diabetic Retinopathy. *Acta Diabetol.* 54 (6), 527–533. doi:10.1007/s00592-017-0984-z

Backer, J. M. (2008). The Regulation and Function of Class III PI3Ks: Novel Roles for Vps34. *Biochem. J.* 410 (1), 1–17. doi:10.1042/bj20071427

Barber, A. J. (2003). A New View of Diabetic Retinopathy: a Neurodegenerative Disease of the Eye. *Prog. Neuropsychopharmacol. Biol. Psychiatry* 27 (2), 283–290. doi:10.1016/s0278-5846(03)00023-x

Barber, A. J., Gardner, T. W., and Abcouwer, S. F. (2011). The Significance of Vascular and Neural Apoptosis to the Pathology of Diabetic Retinopathy. *Invest. Ophthalmol. Vis. Sci.* 52 (2), 1156–1163. doi:10.1167/iovs.10-6293

Barber, A. J., Lieth, E., Khin, S. A., Antonetti, D. A., Buchanan, A. G., and Gardner, T. W. (1998). Neural Apoptosis in the Retina during Experimental and Human Diabetes. Early Onset and Effect of Insulin. *J. Clin. Invest.* 102 (4), 783–791. doi:10.1172/jci2425

Baumgartner, W. A. (2000). Etiology, Pathogenesis, and Experimental Treatment of Retinitis Pigmentosa. *Med. Hypotheses* 54 (5), 814–824. doi:10.1054/mehy.1999.0957

Bek, T. (2017). Diameter Changes of Retinal Vessels in Diabetic Retinopathy. *Curr. Diab Rep.* 17 (10), 82. doi:10.1007/s11892-017-0909-9

Beltramo, E., and Porta, M. (2013). Pericyte Loss in Diabetic Retinopathy: Mechanisms and Consequences. *Curr. Med. Chem.* 20 (26), 3218–3225. doi:10.2174/09298673113209990022

Besirli, C. G., Chinskey, N. D., Zheng, Q. D., and Zacks, D. N. (2011). Autophagy Activation in the Injured Photoreceptor Inhibits Fas-Mediated Apoptosis. *Invest. Ophthalmol. Vis. Sci.* 52 (7), 4193–4199. doi:10.1167/iovs.10-7090

Bingol, B., Tea, J. S., Phu, L., Reichelt, M., Bakalarski, C. E., Song, Q., et al. (2014). The Mitochondrial Deubiquitinase USP30 Opposes Parkin-Mediated Mitophagy. *Nature* 510 (7505), 370–375. doi:10.1038/nature13418

Bringmann, A., and Wiedemann, P. (2012). Müller Glial Cells in Retinal Disease. *Ophthalmologica* 227 (1), 1–19. doi:10.1159/000328979

Brownlee, M. (2005). The Pathobiology of Diabetic Complications: a Unifying Mechanism. *Diabetes* 54 (6), 1615–1625. doi:10.2337/diabetes.54.6.1615

Cai, X., Li, J., Wang, M., She, M., Tang, Y., Li, J., et al. (2017). GLP-1 Treatment Improves Diabetic Retinopathy by Alleviating Autophagy through GLP-1r-Erk1/2-HDAC6 Signaling Pathway. *Int. J. Med. Sci.* 14 (12), 1203–1212. doi:10.7150/ijms.20962

Catalani, E., Silvestri, F., Bongiorni, S., Taddei, A. R., Fanelli, G., Rinalducci, S., et al. (2021). Retinal Damage in a New Model of Hyperglycemia Induced by High-Sucrose Diets. *Pharmacol. Res.* 166, 105488. doi:10.1016/j.phrs.2021.105488

Ceravolo, I., Oliverio, G. W., Alibrandi, A., Bhatti, A., Trombetta, L., Rejdak, R., et al. (2020). The Application of Structural Retinal Biomarkers to Evaluate the Effect of Intravitreal Ranibizumab and Dexamethasone Intravitreal Implant on Treatment of Diabetic Macular Edema. *Diagnostics (Basel)* 10 (6), 413. doi:10.3390/diagnostics10060413

Chen, P., Cescon, M., and Bonaldo, P. (2014). Autophagy-mediated Regulation of Macrophages and its Applications for Cancer. *Autophagy* 10 (2), 192–200. doi:10.4161/auto.26927

Chen, Z., Li, Y., Jiang, G., Yang, C., Wang, Y., Wang, X., et al. (2018). Knockdown of LRP6 Activates Drp1 to Inhibit Survival of Cardiomyocytes during Glucose Deprivation. *Biomed. Pharmacother.* 103, 1408–1414. doi:10.1016/j.biopha.2018.04.134

Cheung, N., Mitchell, P., and Wong, T. Y. (2010). Diabetic Retinopathy. *Lancet* 376 (9735), 124–136. doi:10.1016/s0140-6736(09)62124-3

Chun, Y., and Kim, J. (2018). Autophagy: An Essential Degradation Program for Cellular Homeostasis and Life. *Cells* 7 (12), 278. doi:10.3390/cells7120278

Coorey, N. J., Shen, W., Chung, S. H., Zhu, L., and Gillies, M. C. (2012). The Role of Glia in Retinal Vascular Disease. *Clin. Exp. Optom.* 95 (3), 266–281. doi:10.1111/j.1444-0938.2012.00741.x

Dehdashtian, E., Mehrzadi, S., Yousefi, B., Hosseinzadeh, A., Reiter, R. J., Safa, M., et al. (2018). Diabetic Retinopathy Pathogenesis and the Ameliorating Effects of Melatonin; Involvement of Autophagy, Inflammation and Oxidative Stress. *Life Sci.* 193, 20–33. doi:10.1016/j.lfs.2017.12.001

Devi, T. S., Somayajulu, M., Kowluru, R. A., and Singh, L. P. (2017). TXNIP Regulates Mitophagy in Retinal Müller Cells under High-Glucose Conditions: Implications for Diabetic Retinopathy. *Cell Death Dis* 8 (5), e2777. doi:10.1038/cddis.2017.190

Dikic, I., and Elazar, Z. (2018). Mechanism and Medical Implications of Mammalian Autophagy. *Nat. Rev. Mol. Cel Biol* 19 (6), 349–364. doi:10.1038/s41580-018-0003-4

Dong, X. X., Wang, Y., and Qin, Z. H. (2009). Molecular Mechanisms of Excitotoxicity and Their Relevance to Pathogenesis of Neurodegenerative Diseases. *Acta Pharmacol. Sin* 30 (4), 379–387. doi:10.1038/aps.2009.24

Donnelly, R., Idris, I., and Forrester, J. V. (2004). Protein Kinase C Inhibition and Diabetic Retinopathy: a Shot in the Dark at Translational Research. *Br. J. Ophthalmol.* 88 (1), 145–151. doi:10.1136/bjo.88.1.145

Du, M., Wu, M., Fu, D., Yang, S., Chen, J., Wilson, K., et al. (2013). Effects of Modified LDL and HDL on Retinal Pigment Epithelial Cells: a Role in Diabetic Retinopathy? *Diabetologia* 56 (10), 2318–2328. doi:10.1007/s00125-013-2986-x

Du, X. L., Edelstein, D., Rossetti, L., Fantus, I. G., Goldberg, H., Ziyadeh, F., et al. (2000). Hyperglycemia-induced Mitochondrial Superoxide Overproduction Activates the Hexosamine Pathway and Induces Plasminogen Activator Inhibitor-1 Expression by Increasing Sp1 Glycosylation. *Proc. Natl. Acad. Sci. U S A.* 97 (22), 12222–12226. doi:10.1073/pnas.97.22.12222

Ejaz, S., Chekarova, I., Ejaz, A., Sohail, A., and Lim, C. W. (2008). Importance of Pericytes and Mechanisms of Pericyte Loss during Diabetes Retinopathy. *Diabetes Obes. Metab.* 10 (1), 53–63. doi:10.1111/j.1463-1326.2007.00795.x

Felszeghy, S., Viiri, J., Paterno, J. J., Hyttinen, J. M. T., Koskela, A., Chen, M., et al. (2019). Loss of NRF-2 and PGC-1α Genes Leads to Retinal Pigment Epithelium Damage Resembling Dry Age-Related Macular Degeneration. *Redox Biol.* 20, 1–12. doi:10.1016/j.redox.2018.09.011

Flaxman, S. R., Bourne, R. R. A., Resnikoff, S., Ackland, P., Braithwaite, T., Cicinelli, M. V., et al. (2017). Global Causes of Blindness and Distance Vision Impairment 1990-2020: a Systematic Review and Meta-Analysis. *Lancet Glob. Health* 5 (12), e1221–e1234. doi:10.1016/s2214-109x(17)30393-5

Frake, R. A., Ricketts, T., Menzies, F. M., and Rubinsztein, D. C. (2015). Autophagy and Neurodegeneration. *J. Clin. Invest.* 125 (1), 65–74. doi:10.1172/jci73944

Fu, D., Wu, M., Zhang, J., Du, M., Yang, S., Hammad, S. M., et al. (2012). Mechanisms of Modified LDL-Induced Pericyte Loss and Retinal Injury in Diabetic Retinopathy. *Diabetologia* 55 (11), 3128–3140. doi:10.1007/s00125-012-2692-0

Fu, D., Yu, J. Y., Connell, A. R., Yang, S., Hookham, M. B., McLeese, R., et al. (2016a). Beneficial Effects of Berberine on Oxidized LDL-Induced Cytotoxicity to Human Retinal Müller Cells. *Invest. Ophthalmol. Vis. Sci.* 57 (7), 3369–3379. doi:10.1167/iovs.16-19291

Fu, D., Yu, J. Y., Yang, S., Wu, M., Hammad, S. M., Connell, A. R., et al. (2016b). Survival or Death: a Dual Role for Autophagy in Stress-Induced Pericyte Loss in Diabetic Retinopathy. *Diabetologia* 59 (10), 2251–2261. doi:10.1007/s00125-016-4058-5

Fu, Y., Wang, Y., Gao, X., Li, H., and Yuan, Y. (2020). Dynamic Expression of HDAC3 in Db/db Mouse RGCs and its Relationship with Apoptosis and Autophagy. *J. Diabetes Res.* 2020, 6086780. doi:10.1155/2020/6086780

Gabbay, K. H., Merola, L. O., and Field, R. A. (1966). Sorbitol Pathway: Presence in Nerve and Cord with Substrate Accumulation in Diabetes. *Science* 151 (3707), 209–210. doi:10.1126/science.151.3707.209

Glick, D., Barth, S., and Macleod, K. F. (2010). Autophagy: Cellular and Molecular Mechanisms. *J. Pathol.* 221 (1), 3–12. doi:10.1002/path.2697

Gong, Q., Wang, H., Yu, P., Qian, T., and Xu, X. (2021). Protective or Harmful: The Dual Roles of Autophagy in Diabetic Retinopathy. *Front. Med. (Lausanne)* 8, 644121. doi:10.3389/fmed.2021.644121

Gotzaridis, E. V., Lit, E. S., and D'Amico, D. J. (2001). Progress in Vitreoretinal Surgery for Proliferative Diabetic Retinopathy. *Semin. Ophthalmol.* 16 (1), 31–40. doi:10.1076/soph.16.1.31.4218

Gu, L., Zhu, Y., Zhu, X., and Li, J. (2019). [Genetic Study of a Pedigree Affected with Oculodentodigital Dysplasia]. *Zhonghua Yi Xue Yi Chuan Xue Za Zhi* 36 (12), 1191–1194. doi:10.3760/cma.j.issn.1003-9406.2019.12.010

Gupta, N., Mansoor, S., Sharma, A., Sapkal, A., Sheth, J., Falatoonzadeh, P., et al. (2013). Diabetic Retinopathy and VEGF. *Open Ophthalmol. J.* 7, 4–10. doi:10.2174/1874364101307010004

Gupta, N., and Yücel, Y. H. (2007). Glaucoma as a Neurodegenerative Disease. *Curr. Opin. Ophthalmol.* 18 (2), 110–114. doi:10.1097/ICU.0b013e3280895aea

Hammes, H. P. (2018). Diabetic Retinopathy: Hyperglycaemia, Oxidative Stress and beyond. *Diabetologia* 61 (1), 29–38. doi:10.1007/s00125-017-4435-8

Hammes, H. P., Lin, J., Renner, O., Shani, M., Lundqvist, A., Betsholtz, C., et al. (2002). Pericytes and the Pathogenesis of Diabetic Retinopathy. *Diabetes* 51 (10), 3107–3112. doi:10.2337/diabetes.51.10.3107

Hara, T., Takamura, A., Kishi, C., Iemura, S., Natsume, T., Guan, J. L., et al. (2008). FIP200, a ULK-Interacting Protein, Is Required for Autophagosome Formation in Mammalian Cells. *J. Cel Biol* 181 (3), 497–510. doi:10.1083/jcb.200712064

Hombrebueno, J. R., Cairns, L., Dutton, L. R., Lyons, T. J., Brazil, D. P., Moynagh, P., et al. (2019). Uncoupled Turnover Disrupts Mitochondrial Quality Control in Diabetic Retinopathy. *JCI Insight* 4 (23), e129760. doi:10.1172/jci.insight.129760

Howell, S. J., Mekhail, M. N., Azem, R., Ward, N. L., and Kern, T. S. (2013). Degeneration of Retinal Ganglion Cells in Diabetic Dogs and Mice: Relationship to Glycemic Control and Retinal Capillary Degeneration. *Mol. Vis.* 19, 1413–1421.

Huang, H., He, J., Johnson, D., Wei, Y., Liu, Y., Wang, S., et al. (2015). Deletion of Placental Growth Factor Prevents Diabetic Retinopathy and Is Associated with Akt Activation and HIF1α-VEGF Pathway Inhibition. *diabetes* 64 (3), 200–212. doi:10.2337/db15-er03

Idris, I., Gray, S., and Donnelly, R. (2001). Protein Kinase C Activation: Isozyme-specific Effects on Metabolism and Cardiovascular Complications in Diabetes. *Diabetologia* 44 (6), 659–673. doi:10.1007/s001250051675

Itakura, E., and Mizushima, N. (2010). Characterization of Autophagosome Formation Site by a Hierarchical Analysis of Mammalian Atg Proteins. *Autophagy* 6 (6), 764–776. doi:10.4161/auto.6.6.12709

Jain, A., Lamark, T., Sjøttem, E., Larsen, K. B., Awuh, J. A., Øvervatn, A., et al. (2010). p62/SQSTM1 Is a Target Gene for Transcription Factor NRF2 and Creates a Positive Feedback Loop by Inducing Antioxidant Response Element-Driven Gene Transcription. *J. Biol. Chem.* 285 (29), 22576–22591. doi:10.1074/jbc.M110.118976

Jellinger, K. A. (2010). Should the Word 'dementia' Be Forgotten? *J. Cel Mol Med* 14 (10), 2415–2416. doi:10.1111/j.1582-4934.2010.01159.x

Jindal, V. (2015). Neurodegeneration as a Primary Change and Role of Neuroprotection in Diabetic Retinopathy. *Mol. Neurobiol.* 51 (3), 878–884. doi:10.1007/s12035-014-8732-7

Kadlubowska, J., Malaguarnera, L., Waz, P., and Zorena, K. (2016). Neurodegeneration and Neuroinflammation in Diabetic Retinopathy: Potential Approaches to Delay Neuronal Loss. *Curr. Neuropharmacol* 14 (8), 831–839. doi:10.2174/1570159x14666160614095559

Karst, S. G., Lammer, J., Radwan, S. H., Kwak, H., Silva, P. S., Burns, S. A., et al. (2018). Characterization of *In Vivo* Retinal Lesions of Diabetic Retinopathy Using Adaptive Optics Scanning Laser Ophthalmoscopy. *Int. J. Endocrinol.* 2018, 7492946. doi:10.1155/2018/7492946

Kiamehr, M., Klettner, A., Richert, E., Koskela, A., Koistinen, A., Skottman, H., et al. (2019). Compromised Barrier Function in Human Induced Pluripotent Stem-Cell-Derived Retinal Pigment Epithelial Cells from Type 2 Diabetic Patients. *Int. J. Mol. Sci.* 20 (15). 3773. doi:10.3390/ijms20153773

Kitada, T., Asakawa, S., Hattori, N., Matsumine, H., Yamamura, Y., Minoshima, S., et al. (1998). Mutations in the Parkin Gene Cause Autosomal Recessive Juvenile Parkinsonism. *Nature* 392 (6676), 605–608. doi:10.1038/33416

Klionsky, D. J., Abdel-Aziz, A. K., Abdelfatah, S., Abdellatif, M., Abdoli, A., Abel, S., et al. (2021). Guidelines for the Use and Interpretation of Assays for Monitoring Autophagy (4th Edition)(1). *Autophagy* 17(1), 1–382. doi:10.1080/15548627.2020.1797280

Kolm-Litty, V., Sauer, U., Nerlich, A., Lehmann, R., and Schleicher, E. D. (1998). High Glucose-Induced Transforming Growth Factor Beta1 Production Is Mediated by the Hexosamine Pathway in Porcine Glomerular Mesangial Cells. *J. Clin. Invest.* 101 (1), 160–169. doi:10.1172/jci119875

Kowluru, R. A., and Chan, P. S. (2007). Oxidative Stress and Diabetic Retinopathy. *Exp. Diabetes Res.* 2007, 43603. doi:10.1155/2007/43603

Kowluru, R. A. (2005). Diabetic Retinopathy: Mitochondrial Dysfunction and Retinal Capillary Cell Death. *Antioxid. Redox Signal.* 7 (11-12), 1581–1587. doi:10.1089/ars.2005.7.1581

Kowluru, R. A., and Mishra, M. (2018). Therapeutic Targets for Altering Mitochondrial Dysfunction Associated with Diabetic Retinopathy. *Expert Opin. Ther. Targets* 22 (3), 233–245. doi:10.1080/14728222.2018.1439921

Koya, D., and King, G. L. (1998). Protein Kinase C Activation and the Development of Diabetic Complications. *Diabetes* 47 (6), 859–866. doi:10.2337/diabetes.47.6.859

Kunchithapautham, K., Coughlin, B., Lemasters, J. J., and Rohrer, B. (2011). Differential Effects of Rapamycin on Rods and Cones during Light-Induced Stress in Albino Mice. *Invest. Ophthalmol. Vis. Sci.* 52 (6), 2967–2975. doi:10.1167/iovs.10-6278

Lazzara, F., Trotta, M. C., Platania, C. B. M., D'Amico, M., Petrillo, F., Galdiero, M., et al. (2020). Stabilization of HIF-1α in Human Retinal Endothelial Cells Modulates Expression of miRNAs and Proangiogenic Growth Factors. *Front. Pharmacol.* 11, 1063. doi:10.3389/fphar.2020.01063

Lee, A. Y., and Chung, S. S. (1999). Contributions of Polyol Pathway to Oxidative Stress in Diabetic Cataract. *Faseb j* 13 (1), 23–30. doi:10.1096/fasebj.13.1.23

Li, J., Wang, J. J., Yu, Q., Chen, K., Mahadev, K., and Zhang, S. X. (2010). Inhibition of Reactive Oxygen Species by Lovastatin Downregulates Vascular Endothelial Growth Factor Expression and Ameliorates Blood-Retinal Barrier Breakdown in Db/db Mice: Role of NADPH Oxidase 4. *Diabetes* 59 (6), 1528–1538. doi:10.2337/db09-1057

Li, W. W., Li, J., and Bao, J. K. (2012). Microautophagy: Lesser-Known Self-Eating. *Cell Mol Life Sci* 69 (7), 1125–1136. doi:10.1007/s00018-011-0865-5

Lieth, E., Barber, A. J., Xu, B., Dice, C., Ratz, M. J., Tanase, D., et al. (1998). Glial Reactivity and Impaired Glutamate Metabolism in Short-Term Experimental Diabetic Retinopathy. Penn State Retina Research Group. *Diabetes* 47 (5), 815–820. doi:10.2337/diabetes.47.5.815

Lopes de Faria, J. M., Duarte, D. A., Montemurro, C., Papadimitriou, A., Consonni, S. R., and Lopes de Faria, J. B. (2016). Defective Autophagy in Diabetic Retinopathy. *Invest. Ophthalmol. Vis. Sci.* 57 (10), 4356–4366. doi:10.1167/iovs.16-19197

Lung, J. C., Swann, P. G., Wong, D. S., and Chan, H. H. (2012). Global Flash Multifocal Electroretinogram: Early Detection of Local Functional Changes and its Correlations with Optical Coherence Tomography and Visual Field Tests in Diabetic Eyes. *Doc Ophthalmol.* 125 (2), 123–135. doi:10.1007/s10633-012-9343-0

Luo, Y., Dong, X., Lu, S., Gao, Y., Sun, G., and Sun, X. (2021). Gypenoside XVII Alleviates Early Diabetic Retinopathy by Regulating Müller Cell Apoptosis and Autophagy in Db/db Mice. *Eur. J. Pharmacol.* 895, 173893. doi:10.1016/j.ejphar.2021.173893

Lynch, S. K., and Abràmoff, M. D. (2017). Diabetic Retinopathy Is a Neurodegenerative Disorder. *Vis. Res* 139, 101–107. doi:10.1016/j.visres.2017.03.003

Madrakhimov, S. B., Yang, J. Y., Kim, J. H., Han, J. W., and Park, T. K. (2021). mTOR-dependent Dysregulation of Autophagy Contributes to the Retinal Ganglion Cell Loss in Streptozotocin-Induced Diabetic Retinopathy. *Cell Commun Signal* 19 (1), 29. doi:10.1186/s12964-020-00698-4

Madsen-Bouterse, S. A., Mohammad, G., Kanwar, M., and Kowluru, R. A. (2010). Role of Mitochondrial DNA Damage in the Development of Diabetic Retinopathy, and the Metabolic Memory Phenomenon Associated with its Progression. *Antioxid. Redox Signal.* 13 (6), 797–805. doi:10.1089/ars.2009.2932

Mao, X. B., Cheng, Y. H., and Xu, Y. Y. (2019). miR-204-5p Promotes Diabetic Retinopathy Development via Downregulation of Microtubule-Associated Protein 1 Light Chain 3. *Exp. Ther. Med.* 17 (4), 2945–2952. doi:10.3892/etm.2019.7327

Mariño, G., Madeo, F., and Kroemer, G. (2011). Autophagy for Tissue Homeostasis and Neuroprotection. *Curr. Opin. Cel Biol* 23 (2), 198–206. doi:10.1016/j.ceb.2010.10.001

Masser, D. R., Otalora, L., Clark, N. W., Kinter, M. T., Elliott, M. H., and Freeman, W. M. (2017). Functional Changes in the Neural Retina Occur in the Absence of Mitochondrial Dysfunction in a Rodent Model of Diabetic Retinopathy. *J. Neurochem.* 143 (5), 595–608. doi:10.1111/jnc.14216

Matsuda, N., Sato, S., Shiba, K., Okatsu, K., Saisho, K., Gautier, C. A., et al. (2010). PINK1 Stabilized by Mitochondrial Depolarization Recruits Parkin to

Damaged Mitochondria and Activates Latent Parkin for Mitophagy. *J. Cel Biol* 189 (2), 211–221. doi:10.1083/jcb.200910140

Menzies, F. M., Fleming, A., Caricasole, A., Bento, C. F., Andrews, S. P., Ashkenazi, A., et al. (2017). Autophagy and Neurodegeneration: Pathogenic Mechanisms and Therapeutic Opportunities. *Neuron* 93 (5), 1015–1034. doi:10.1016/j.neuron.2017.01.022

Miranda, S., González-Rodríguez, Á., García-Ramírez, M., Revuelta-Cervantes, J., Hernández, C., Simó, R., et al. (2012). Beneficial Effects of Fenofibrate in Retinal Pigment Epithelium by the Modulation of Stress and Survival Signaling under Diabetic Conditions. *J. Cel Physiol* 227 (6), 2352–2362. doi:10.1002/jcp.22970

Mizushima, N. (2007). Autophagy: Process and Function. *Genes Dev.* 21 (22), 2861–2873. doi:10.1101/gad.1599207

Mizushima, N., and Murphy, L. O. (2020). Autophagy Assays for Biological Discovery and Therapeutic Development. *Trends Biochem. Sci.* 45 (12), 1080–1093. doi:10.1016/j.tibs.2020.07.006

Mizushima, N., Yoshimori, T., and Ohsumi, Y. (2011). The Role of Atg Proteins in Autophagosome Formation. *Annu. Rev. Cel Dev Biol* 27, 107–132. doi:10.1146/annurev-cellbio-092910-154005

Mrugacz, M., Bryl, A., and Zorena, K. (2021). Retinal Vascular Endothelial Cell Dysfunction and Neuroretinal Degeneration in Diabetic Patients. *J. Clin. Med.* 10 (3), 458. doi:10.3390/jcm10030458

Nishikawa, T., Edelstein, D., Du, X. L., Yamagishi, S., Matsumura, T., Kaneda, Y., et al. (2000). Normalizing Mitochondrial Superoxide Production Blocks Three Pathways of Hyperglycaemic Damage. *Nature* 404 (6779), 787–790. doi:10.1038/35008121

Noda, T. (2017). Regulation of Autophagy through TORC1 and mTORC1. *Biomolecules* 7 (3), 52. doi:10.3390/biom7030052

Ogurtsova, K., da Rocha Fernandes, J. D., Huang, Y., Linnenkamp, U., Guariguata, L., Cho, N. H., et al. (2017). IDF Diabetes Atlas: Global Estimates for the Prevalence of Diabetes for 2015 and 2040. *Diabetes Res. Clin. Pract.* 128, 40–50. doi:10.1016/j.diabres.2017.03.024

Ola, M. S., and Alhomida, A. S. (2014). Neurodegeneration in Diabetic Retina and its Potential Drug Targets. *Curr. Neuropharmacol* 12 (4), 380–386. doi:10.2174/1570159x12666140619205024

Oshitari, T., Yoshida-Hata, N., and Yamamoto, S. (2011). Effect of Neurotrophin-4 on Endoplasmic Reticulum Stress-Related Neuronal Apoptosis in Diabetic and High Glucose Exposed Rat Retinas. *Neurosci. Lett.* 501 (2), 102–106. doi:10.1016/j.neulet.2011.06.057

Otomo, C., Metlagel, Z., Takaesu, G., and Otomo, T. (2013). Structure of the Human ATG12~ATG5 Conjugate Required for LC3 Lipidation in Autophagy. *Nat. Struct. Mol. Biol.* 20 (1), 59–66. doi:10.1038/nsmb.2431

Ozcan, U., Yilmaz, E., Ozcan, L., Furuhashi, M., Vaillancourt, E., Smith, R. O., et al. (2006). Chemical Chaperones Reduce ER Stress and Restore Glucose Homeostasis in a Mouse Model of Type 2 Diabetes. *Science* 313 (5790), 1137–1140. doi:10.1126/science.1128294

Park, H. L., Kim, J. H., and Park, C. K. (2018). Different Contributions of Autophagy to Retinal Ganglion Cell Death in the Diabetic and Glaucomatous Retinas. *Sci. Rep.* 8 (1), 13321. doi:10.1038/s41598-018-30165-7

Parzych, K. R., and Klionsky, D. J. (2014). An Overview of Autophagy: Morphology, Mechanism, and Regulation. *Antioxid. Redox Signal.* 20 (3), 460–473. doi:10.1089/ars.2013.5371

Piano, I., Novelli, E., Della Santina, L., Strettoi, E., Cervetto, L., and Gargini, C. (2016). Involvement of Autophagic Pathway in the Progression of Retinal Degeneration in a Mouse Model of Diabetes. *Front Cel Neurosci* 10, 42. doi:10.3389/fncel.2016.00042

Pickles, S., Vigié, P., and Youle, R. J. (2018). Mitophagy and Quality Control Mechanisms in Mitochondrial Maintenance. *Curr. Biol.* 28 (4), R170–r185. doi:10.1016/j.cub.2018.01.004

Punzo, C., Kornacker, K., and Cepko, C. L. (2009). Stimulation of the insulin/mTOR Pathway Delays Cone Death in a Mouse Model of Retinitis Pigmentosa. *Nat. Neurosci.* 12 (1), 44–52. doi:10.1038/nn.2234

Qi, X., Mitter, S. K., Yan, Y., Busik, J. V., Grant, M. B., and Boulton, M. E. (2020). Diurnal Rhythmicity of Autophagy Is Impaired in the Diabetic Retina. *Cells* 9 (4), 905. doi:10.3390/cells9040905

Rodríguez-Muela, N., Hernández-Pinto, A. M., Serrano-Puebla, A., García-Ledo, L., Latorre, S. H., de la Rosa, E. J., et al. (2015). Lysosomal Membrane Permeabilization and Autophagy Blockade Contribute to Photoreceptor Cell Death in a Mouse Model of Retinitis Pigmentosa. *Cell Death Differ* 22 (3), 476–487. doi:10.1038/cdd.2014.203

Romeo, G., Liu, W. H., Asnaghi, V., Kern, T. S., and Lorenzi, M. (2002). Activation of Nuclear Factor-kappaB Induced by Diabetes and High Glucose Regulates a Proapoptotic Program in Retinal Pericytes. *Diabetes* 51 (7), 2241–2248. doi:10.2337/diabetes.51.7.2241

Romero-Aroca, P., Baget-Bernaldiz, M., Pareja-Rios, A., Lopez-Galvez, M., Navarro-Gil, R., and Verges, R. (2016). Diabetic Macular Edema Pathophysiology: Vasogenic versus Inflammatory. *J. Diabetes Res.* 2016, 2156273. doi:10.1155/2016/2156273

Rosa, M. D., Distefano, G., Gagliano, C., Rusciano, D., and Malaguarnera, L. (2016). Autophagy in Diabetic Retinopathy. *Curr. Neuropharmacol* 14 (8), 810–825. doi:10.2174/1570159x14666160321122900

Rossi, S., Maisto, R., Gesualdo, C., Trotta, M. C., Ferraraccio, F., Kaneva, M. K., et al. (2016). Activation of Melanocortin Receptors MC 1 and MC 5 Attenuates Retinal Damage in Experimental Diabetic Retinopathy. *Mediators Inflamm.*, 7368389. doi:10.1155/2016/7368389*2016*

Rousseau, S., Houle, F., Landry, J., and Huot, J. (1997). p38 MAP Kinase Activation by Vascular Endothelial Growth Factor Mediates Actin Reorganization and Cell Migration in Human Endothelial Cells. *Oncogene* 15 (18), 2169–2177. doi:10.1038/sj.onc.1201380

Rubinsztein, D. C., Cuervo, A. M., Ravikumar, B., Sarkar, S., Korolchuk, V., Kaushik, S., et al. (2009). In Search of an "autophagomometer. *Autophagy* 5 (5), 585–589. doi:10.4161/auto.5.5.8823

Russo, R., Berliocchi, L., Adornetto, A., Amantea, D., Nucci, C., Tassorelli, C., et al. (2013). In Search of New Targets for Retinal Neuroprotection: Is There a Role for Autophagy? *Curr. Opin. Pharmacol.* 13 (1), 72–77. doi:10.1016/j.coph.2012.09.004

Saxena, R., Singh, D., Saklani, R., and Gupta, S. K. (2016). Clinical Biomarkers and Molecular Basis for Optimized Treatment of Diabetic Retinopathy: Current Status and Future Prospects. *Eye Brain* 8, 1–13. doi:10.2147/EB.S69185

Shen, W., Lee, S. R., Araujo, J., Chung, S. H., Zhu, L., and Gillies, M. C. (2014). Effect of Glucocorticoids on Neuronal and Vascular Pathology in a Transgenic Model of Selective Müller Cell Ablation. *Glia* 62 (7), 1110–1124. doi:10.1002/glia.22666

Shi, H., Zhang, Z., Wang, X., Li, R., Hou, W., Bi, W., et al. (2015). Inhibition of Autophagy Induces IL-1β Release from ARPE-19 Cells via ROS Mediated NLRP3 Inflammasome Activation under High Glucose Stress. *Biochem. Biophys. Res. Commun.* 463 (4), 1071–1076. doi:10.1016/j.bbrc.2015.06.060

Shinohara, M., Thornalley, P. J., Giardino, I., Beisswenger, P., Thorpe, S. R., Onorato, J., et al. (1998). Overexpression of Glyoxalase-I in Bovine Endothelial Cells Inhibits Intracellular Advanced Glycation Endproduct Formation and Prevents Hyperglycemia-Induced Increases in Macromolecular Endocytosis. *J. Clin. Invest.* 101 (5), 1142–1147. doi:10.1172/jci119885

Shruthi, K., Reddy, S. S., and Reddy, G. B. (2017). Ubiquitin-proteasome System and ER Stress in the Retina of Diabetic Rats. *Arch. Biochem. Biophys.* 627, 10–20. doi:10.1016/j.abb.2017.06.006

Shruthi, K., Reddy, S. S., Reddy, P. Y., Shivalingam, P., Harishankar, N., and Reddy, G. B. (2016). Amelioration of Neuronal Cell Death in a Spontaneous Obese Rat Model by Dietary Restriction through Modulation of Ubiquitin Proteasome System. *J. Nutr. Biochem.* 33, 73–81. doi:10.1016/j.jnutbio.2016.03.008

Simão, S., Costa, M., Sun, J. K., Cunha-Vaz, J., and Simó, R. (2017). Development of a Normative Database for Multifocal Electroretinography in the Context of a Multicenter Clinical Trial. *Ophthalmic Res.* 57 (2), 107–117. doi:10.1159/000450958

Simo-Servat, O., Hernandez, C., and Simo, R. (2019). Diabetic Retinopathy in the Context of Patients with Diabetes. *Ophthalmic Res.* 62 (4), 211–217. doi:10.1159/000499541

Singh, L. P. (2013). Thioredoxin Interacting Protein (TXNIP) and Pathogenesis of Diabetic Retinopathy. *J. Clin. Exp. Ophthalmol.* 4. doi:10.4172/2155-9570.1000287

Singh, R., Ramasamy, K., Abraham, C., Gupta, V., and Gupta, A. (2008). Diabetic Retinopathy: an Update. *Indian J. Ophthalmol.* 56 (3), 178–188. doi:10.4103/0301-4738.40355

Sivitz, W. I., and Yorek, M. A. (2010). Mitochondrial Dysfunction in Diabetes: from Molecular Mechanisms to Functional Significance and Therapeutic Opportunities. *Antioxid. Redox Signal.* 12 (4), 537–577. doi:10.1089/ars.2009.2531

Sohn, E. H., van Dijk, H. W., Jiao, C., Kok, P. H., Jeong, W., Demirkaya, N., et al. (2016). Retinal Neurodegeneration May Precede Microvascular Changes Characteristic of Diabetic Retinopathy in Diabetes Mellitus. *Proc. Natl. Acad. Sci. U S A.* 113 (19), E2655–E2664. doi:10.1073/pnas.1522014113

Solomon, S. D., Chew, E., Duh, E. J., Sobrin, L., Sun, J. K., VanderBeek, B. L., et al. (2017). Diabetic Retinopathy: A Position Statement by the American Diabetes Association. *Diabetes Care* 40 (3), 412–418. doi:10.2337/dc16-2641

Stitt, A. W. (2010). AGEs and Diabetic Retinopathy. *Invest. Ophthalmol. Vis. Sci.* 51 (10), 4867–4874. doi:10.1167/iovs.10-5881

Stitt, A. W., Curtis, T. M., Chen, M., Medina, R. J., McKay, G. J., Jenkins, A., et al. (2016). The Progress in Understanding and Treatment of Diabetic Retinopathy. *Prog. Retin. Eye Res.* 51, 156–186. doi:10.1016/j.preteyeres.2015.08.001

Sun, J. K., and Jampol, L. M. (2019). The Diabetic Retinopathy Clinical Research Network (DRCR.Net) and its Contributions to the Treatment of Diabetic Retinopathy. *Ophthalmic Res.* 62 (4), 225–230. doi:10.1159/000502779

Taki, K., Horie, T., Kida, T., Mimura, M., Ikeda, T., and Oku, H. (2020). Impairment of Autophagy Causes Superoxide Formation and Caspase Activation in 661 W Cells, a Cell Line for Cone Photoreceptors, under Hyperglycemic Conditions. *Int. J. Mol. Sci.* 21 (12). 4240. doi:10.3390/ijms21124240

Ting, D. S., Cheung, G. C., and Wong, T. Y. (2016). Diabetic Retinopathy: Global Prevalence, Major Risk Factors, Screening Practices and Public Health Challenges: a Review. *Clin. Exp. Ophthalmol.* 44 (4), 260–277. doi:10.1111/ceo.12696

Trento, M., Durando, O., Lavecchia, S., Charrier, L., Cavallo, F., Costa, M. A., et al. (2017). Vision Related Quality of Life in Patients with Type 2 Diabetes in the EUROCONDOR Trial. *Endocrine* 57 (1), 83–88. doi:10.1007/s12020-016-1097-0

Valente, E. M., Abou-Sleiman, P. M., Caputo, V., Muqit, M. M., Harvey, K., Gispert, S., et al. (2004). Hereditary Early-Onset Parkinson's Disease Caused by Mutations in PINK1. *Science* 304 (5674), 1158–1160. doi:10.1126/science.1096284

van Dijk, H. W., Verbraak, F. D., Kok, P. H., Garvin, M. K., Sonka, M., Lee, K., et al. (2010). Decreased Retinal Ganglion Cell Layer Thickness in Patients with Type 1 Diabetes. *Invest. Ophthalmol. Vis. Sci.* 51 (7), 3660–3665. doi:10.1167/iovs.09-5041

Wang, L., Sun, X., Zhu, M., Du, J., Xu, J., Qin, X., et al. (2019a). Epigallocatechin-3-gallate Stimulates Autophagy and Reduces Apoptosis Levels in Retinal Müller Cells under High-Glucose Conditions. *Exp. Cel Res* 380 (2), 149–158. doi:10.1016/j.yexcr.2019.04.014

Wang, S., Ji, L. Y., Li, L., and Li, J. M. (2019b). Oxidative Stress, Autophagy and Pyroptosis in the Neovascularization of Oxygen-Induced Retinopathy in Mice. *Mol. Med. Rep.* 19 (2), 927–934. doi:10.3892/mmr.2018.9759

Wang, W., and Lo, A. C. Y. (2018). Diabetic Retinopathy: Pathophysiology and Treatments. *Int. J. Mol. Sci.* 19 (6), 1816. doi:10.3390/ijms19061816

Wang, W., Wang, Q., Wan, D., Sun, Y., Wang, L., Chen, H., et al. (2017). Histone HIST1H1C/H1.2 Regulates Autophagy in the Development of Diabetic Retinopathy. *Autophagy* 13 (5), 941–954. doi:10.1080/15548627.2017.1293768

Wang, Y., Liu, X., Zhu, L., Li, W., Li, Z., Lu, X., et al. (2020). PG545 Alleviates Diabetic Retinopathy by Promoting Retinal Müller Cell Autophagy to Inhibit the Inflammatory Response. *Biochem. Biophys. Res. Commun.* 531 (4), 452–458. doi:10.1016/j.bbrc.2020.07.134

Wilkinson, C. P., Ferris, F. L., 3rd, Klein, R. E., Lee, P. P., Agardh, C. D., Davis, M., et al. (2003). Proposed International Clinical Diabetic Retinopathy and Diabetic Macular Edema Disease Severity Scales. *Ophthalmology* 110 (9), 1677–1682. doi:10.1016/s0161-6420(03)00475-5

Wolff, B. E., Bearse, M. A., Jr., Schneck, M. E., Dhamdhere, K., Harrison, W. W., Barez, S., et al. (2015). Color Vision and Neuroretinal Function in Diabetes. *Doc Ophthalmol.* 130 (2), 131–139. doi:10.1007/s10633-014-9476-4

Xie, Z., and Klionsky, D. J. (2007). Autophagosome Formation: Core Machinery and Adaptations. *Nat. Cel Biol* 9 (10), 1102–1109. doi:10.1038/ncb1007-1102

Yang, S., Zhang, J., and Chen, L. (2020). The Cells Involved in the Pathological Process of Diabetic Retinopathy. *Biomed. Pharmacother.* 132, 110818. doi:10.1016/j.biopha.2020.110818

Yang, Z., and Klionsky, D. J. (2009). An Overview of the Molecular Mechanism of Autophagy. *Curr. Top. Microbiol. Immunol.* 335, 1–32. doi:10.1007/978-3-642-00302-8_1

Yang, Z., and Klionsky, D. J. (2010). Mammalian Autophagy: Core Molecular Machinery and Signaling Regulation. *Curr. Opin. Cel Biol* 22 (2), 124–131. doi:10.1016/j.ceb.2009.11.014

Yao, J., Tao, Z. F., Li, C. P., Li, X. M., Cao, G. F., Jiang, Q., et al. (2014). Regulation of Autophagy by High Glucose in Human Retinal Pigment Epithelium. *Cell Physiol Biochem* 33 (1), 107–116. doi:10.1159/000356654

Yau, J. W., Rogers, S. L., Kawasaki, R., Lamoureux, E. L., Kowalski, J. W., Bek, T., et al. (2012). Global Prevalence and Major Risk Factors of Diabetic Retinopathy. *Diabetes Care* 35 (3), 556–564. doi:10.2337/dc11-1909

Yoshii, S. R., and Mizushima, N. (2017). Monitoring and Measuring Autophagy. *Int. J. Mol. Sci.* 18 (9). 1865. doi:10.3390/ijms18091865

Yu, J. Y., and Lyons, T. J. (2013). Modified Lipoproteins in Diabetic Retinopathy: A Local Action in the Retina. *J. Clin. Exp. Ophthalmol.* 4 (6). 314. doi:10.4172/2155-9570.1000314

Zhang, H., Chang, J. T., Guo, B., Hansen, M., Jia, K., Kovács, A. L., et al. (2015). Guidelines for Monitoring Autophagy in *Caenorhabditis elegans*. *Autophagy* 11 (1), 9–27. doi:10.1080/15548627.2014.1003478

Zhang, Y., Xi, X., Mei, Y., Zhao, X., Zhou, L., Ma, M., et al. (2019). High-glucose Induces Retinal Pigment Epithelium Mitochondrial Pathways of Apoptosis and Inhibits Mitophagy by Regulating ROS/PINK1/Parkin Signal Pathway. *Biomed. Pharmacother.* 111, 1315–1325. doi:10.1016/j.biopha.2019.01.034

Zhou, K. L., Zhou, Y. F., Wu, K., Tian, N. F., Wu, Y. S., Wang, Y. L., et al. (2015). Stimulation of Autophagy Promotes Functional Recovery in Diabetic Rats with Spinal Cord Injury. *Sci. Rep.* 5, 17130. doi:10.1038/srep17130

Zhou, P., Xie, W., Meng, X., Zhai, Y., Dong, X., Zhang, X., et al. (2019). Notoginsenoside R1 Ameliorates Diabetic Retinopathy through PINK1-dependent Activation of Mitophagy. *Cells* 8 (3), 213. doi:10.3390/cells8030213

Zhu, X. C., Yu, J. T., Jiang, T., and Tan, L. (2013). Autophagy Modulation for Alzheimer's Disease Therapy. *Mol. Neurobiol.* 48 (3), 702–714. doi:10.1007/s12035-013-8457-z

Conflict of Interest: The authors declare that the research was conducted in the absence of any commercial or financial relationships that could be construed as a potential conflict of interest.

frontiers in Pharmacology

ORIGINAL RESEARCH
published: 12 July 2021
doi: 10.3389/fphar.2021.696787

Safety and Efficacy of Intravitreal Chemotherapy (Melphalan) to Treat Vitreous Seeds in Retinoblastoma

Yacoub A. Yousef[1], Mays Al Jboor[2], Mona Mohammad[1], Mustafa Mehyar[1], Mario D. Toro[3,4]*, Rashed Nazzal[3], Qusai H. Alzureikat[2], Magdalena Rejdak[5], Mutasem Elfalah[6], Iyad Sultan[7], Robert Rejdak[3], Maysa Al-Hussaini[8] and Ibrahim Al-Nawaiseh[1]*

[1]Department of Surgery, Ophthalmology Division, King Hussein Cancer Center, Amman, Jordan, [2]The Eye Speciality Hospital, Amman, Jordan, [3]Chair and Department of General and Pediatric Ophthalmology, Medical University of Lublin, Lublin, Poland, [4]Department of Ophthalmology, University of Zurich, Zurich, Switzerland, [5]Medical Faculty of Warsaw, Warsaw, Poland, [6]Department of Special Surgery, Faculty of Medicine, The University of Jordan, Amman, Jordan, [7]Departments of Pediatrics Oncology, King Hussein Cancer Center, Amman, Jordan, [8]Departments of Pathology, King Hussein Cancer Center, Amman, Jordan

OPEN ACCESS

Edited by:
Ewa Teresa Marcinkowska, University of Wrocław, Poland

Reviewed by:
Hayyam Kiratli, Hacettepe University, Turkey
Ankit Tomar, The New York Eye Cancer Center, United States
Rodolfo Mastropasqua, University of Modena and Reggio Emilia, Italy

***Correspondence:**
Yacoub A. Yousef
yyousef@khcc.jo
Mario D. Toro
mario.toro@usz.ch

Specialty section:
This article was submitted to Experimental Pharmacology and Drug Discovery, a section of the journal Frontiers in Pharmacology

Received: *17 April 2021*
Accepted: *21 May 2021*
Published: *12 July 2021*

Citation:
Yousef YA, Al Jboor M, Mohammad M, Mehyar M, Toro MD, Nazzal R, Alzureikat QH, Rejdak M, Elfalah M, Sultan I, Rejdak R, Al-Hussaini M and Al-Nawaiseh I (2021) Safety and Efficacy of Intravitreal Chemotherapy (Melphalan) to Treat Vitreous Seeds in Retinoblastoma. Front. Pharmacol. 12:696787. doi: 10.3389/fphar.2021.696787

Background: Active vitreous seeds in eyes with retinoblastoma (Rb) adversely affects the treatment outcome. This study aimed to investigate the safety and efficacy of intravitreal melphalan chemotherapy (IViC) as a treatment for recurrent and refractory vitreous seeds in patients with Rb.

Methods: We used a retrospective non-comparative study of patients with intraocular Rb who had vitreous seeds and were treated by IViC (20–30 μg of melphalan) using the safety-enhanced anti-reflux technique. Tumor response, ocular toxicity, demographics, clinical features, and survival were analyzed.

Results: In total, 27 eyes were treated with 108 injections for recurrent (16 eyes) or refractory (11 eyes) vitreous seeds after failed systemic chemotherapy. A total of 15 (56%) were males, and 20 (74%) had bilateral disease. At diagnosis, the majority (n = 21) of the injected eyes were group D, and n = 6 were group C. Vitreous seeds showed complete regression in 21 (78%) eyes; 100% (n = 10) for eyes with focal seeds; 65% (n = 11/17 eyes) for eyes with diffuse seeds (p = 0.04); 7 (64%) eyes with refractory seeds; and 14 (87%) eyes with recurrent seeds showed complete response (p = 0.37). In total, 16 (59%) eyes developed side effects: retinal toxicity (48%), pupillary synechiae (15%), cataracts (30%), iris atrophy (7%), and retinal and optic atrophy (4%). Only one child was lost to follow-up whose family refused enucleation and none developed orbital tumor recurrence or distant metastasis.

Conclusion: IViC with melphalan is effective (more for focal than diffuse seeding) and a relatively safe treatment modality for Rb that can improve the outcomes of eye salvage procedures. However, unexpected toxicity can occur even with the standard dose of 20–30 μg.

Keywords: chemotherapy, melphalan, ocular toxicity, retinoblastoma, vitreous seeds

Abbreviations: Rb, retinoblastoma; KHCC, King Hussein Cancer Center; IViC, intravitreal chemotherapy; IIRC, international intraocular retinoblastoma classification; EBRT, external beam radiation therapy.

INTRODUCTION

Retinoblastoma is the most prevalent pediatric intraocular tumor (Kivela, 2009) for which enucleation is the ultimate treatment. Eye (globe) salvage can be achieved in many cases by employing a variety of management modalities, which includes systemic and/or regional chemotherapy and consolidation therapy (thermal and cryotherapy). However, managing recurrent or persistent vitreous seeding has been a major impediment that has reduced the apparent eye salvage rates in patients with advanced intraocular disease (Chan et al., 1995; Shields et al., 2002; Yousef et al., 2020c; Yousef et al., 2021).

Early studies have reported that the salvage rates for the groups A, B, and C retinoblastoma (classified using the International Intraocular Retinoblastoma Classification, IIRC) (Linnmurphree, 2005) were generally high (81–100%) compared to only about 50% for group D eyes (Shields et al., 2006; Yousef et al., 2021; Amine et al., 2021). This unfavorable outcome for in group D may be attributed to the presence of massive vitreous and/or subretinal seeds. Eventually, with the introduction of selective ophthalmic artery chemotherapy (IAC), the eye globe salvage rate for D eyes increased to 70%, while only 64% of D eyes with massive vitreous seeds could be managed with IAC (Munier et al., 2011; Abramson et al., 2012). Thus, radiotherapy (external beam radiation therapy, EBRT) continued to be used to treat the few cases of recurrent vitreous seeds to attain an improved tumor control rate of 46–91% (Shields et al., 2009; Yousef et al., 2020b) and avoid enucleation. Unfortunately, this was associated with a higher risk of secondary primary malignancies (Kleinerman et al., 2005).

Subsequently, intra-vitreal chemotherapy (IViC), specifically with melphalan, emerged in 2012 as a promising treatment technique for active recurrent or persistent vitreous seeds, improving the eye salvage rate to about 87% in an initial report (Munier et al., 2012a). The authors also reported an 81% tumor control in the eyes with active vitreous seeds that were initially planned for enucleation (Munier et al., 2012a). Most reports on the safety of intraocular melphalan have documented minimal ocular toxicity after an injected dose of 20–30 μg (calculated based on the patient's age) in the Caucasian populations of Europe and America (Munier, 2014; Shields et al., 2014; Francis et al., 2015). On the other hand, the reported toxicity was higher in Chinese retinoblastoma patients (Xue et al., 2019).

Therefore, the present study aimed to further investigate both the safety and toxicity of IViC with melphalan to treat eyes with intraocular Rb presenting with refractory vitreous seeds or recurrent seeds after failed systemic intravenous chemotherapy combined with focal consolidation in a lower-middle-income country in the Middle East (Jordan).

PATIENTS AND METHODS

This is a retrospective non-comparative analysis approved by the Institutional Review Board at the King Hussein Cancer Center (Amman, Jordan) (18KHCC27). The review board waived the need to obtain consent owing to the retrospective nature of the study. The study included 27 eyes with intraocular Rb (from 27 patients) with refractory or recurrent vitreous seeds who received the IViC treatment between January 2014 and June 2020. Eligibility criteria for administering IViC were (Munier et al., 2012b; Moulin et al., 2012):

(1) No tumor invasion of the anterior or posterior chamber.
(2) No associated retinal or anterior hyaloid detachment.
(3) Presence of an entry site for the injection that is free of active tumor or active vitreous seeds.

All group E and D eyes with massive vitreous seeds in all four quadrants of the eye where no clear safe quadrant for injection was available were not eligible to receive this treatment and were excluded. All eligible patients were examined by an ocular oncologist under anesthesia and fundus dilated to thoroughly examine the retina, and the retinal photos were documented using Retcam II (Clarity Medical Systems, CA, United States). Tumor location, seeds' features, and response to treatment were documented adequately. Informed consent for the treatment was obtained from the patients' parents, following which the procedures were performed under completely sterile conditions in the operating room.

Definitions

Vitreous seeding was classified into focal vitreous seeds (seeds limited to only one quadrant) and diffuse vitreous seeds (seeds that were extensive and detected in more than one quadrant of the eye globe). Based on the distance of the vitreous seeds from the retinal surface, they were grouped as either less than 3 mm or more than 3 mm from the surface of the retina.

Further, based on the pattern of vitreous seeding, three subtypes were defined: Type I (dust-like seeds), Type II (sphere-like seeds), and Type III (clouds-like seeds) (Susskind et al., 2016) (**Figure 1**). Response of vitreous seeds to the IViC was categorized into 3 patterns: Type 0 (complete disappearance of the vitreous seeds), Type I (calcific vitreous seeds), and Type II (amorphous vitreous seeds) (**Figure 2**).

Surgical Technique

First, the injection site was examined by indirect ophthalmoscopy followed by Ultrasound Bio-Microscopy (UBM) to confirm a clear site for injection (no tumors or retinal detachment). Ocular hypotony was induced by withdrawing 0.05–0.1 ml of aqueous fluid, which was sent for cytopathology screening. A 30-gauge sterile needle was used to inject the chemotherapy drug, melphalan, in the specified amount based on the patient's age. All patients received 20–30 μg of melphalan intravitreally by inserting the needle in pars plana 2.5–3.5 mm away from the limbus, perpendicular to the sclera toward the vitreous humor and away from the anatomical location of the lens.

Cryotherapy was applied (triple-freeze-thaw cryotherapy) at the injection site immediately afterward to sterilize the needle track from any possible active tumor cells. The eye was shaken manually after each injection to spread the chemotherapy in the vitreous. Each patient received a minimum of three injections and a maximum of eight injections 1–2 weeks apart.

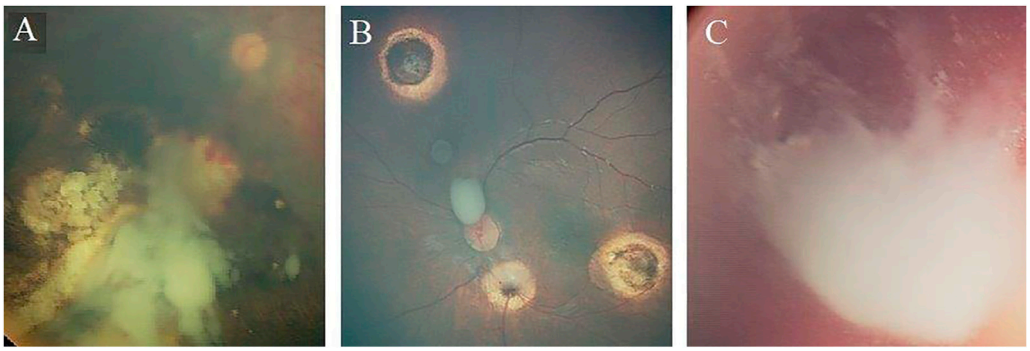

FIGURE 1 | Morphologic types of recurrent and refractory vitreous seeds in Rb patients. **(A)** Eye that harboures massive cloud (type III vitreous seeds). **(B)** Eye that harbours mixture of 2 types of vitreous seeds; sphere (type II vitreous seeds), and cloud (type III vitreous seeds). **(C)** Large cloud (type III vitreous seeds) associated with massive Dust (type I vitreous seeds)..

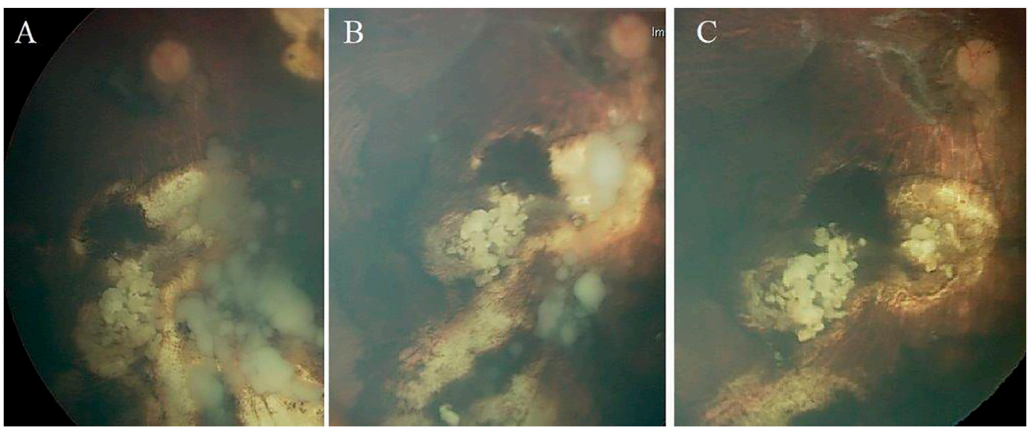

FIGURE 2 | Treatment response of vitreous seeding to intravitreal melphalan injection; **(A)** massive cloud of vitreous seeds that regressed partially after 3 injections **(B)** and totally disappeared after total of 6 injections **(C)**. This shows type 0 pattern of regression where vitreous seeds disappeared completely.

Drug Preparation

Commercially available 50 mg lyophilized powder of melphalan hydrochloride was reconstituted with 0.9% sodium chloride solution (preservative-free). Initially, a concentration of 5 mg/ml of melphalan was achieved by adding 10 ml of 0.9% normal saline followed by vigorous shaking of the drug till the solution becomes clear. A 0.2 mg/ml (200 μg/ml) sterile solution was obtained by mixing 1 ml of melphalan with 24 ml 0.9% sodium chloride. Then, the reconstituted drug (0.3 ml melphalan) was transferred to a 1 ml lock syringe through a 5 μ filter. The dosage is adjusted and customized accordingly; 20 μg/0.10 ml for 0–12 months of age, 25 μg/0.125 ml for 1–3 years of age, and 30 μg/0.15 ml for patients aging 3 years and above (Manjandavida and Shields, 2015). All associated active retinal tumors were treated by focal consolidation therapy (cryotherapy, transpupillary thermotherapy, or radioactive plaque therapy) as needed.

Outcome Measurement

Response to treatment was evaluated by examination under anesthesia after each injection and before the next injection. Successful therapy was defined by avoidance of enucleation or EBRT. Good tumor response was defined as a complete response (regression of all active seeds and no recurrence detected at 6 months after the last injection), while failed treatment was defined as residual active vitreous seeds and/or recurrent vitreous seeds within 6 months from the last injection.

Retinal toxicity was graded based on Munier's report (Munier, 2014) into five grades: Grade I: less than 2 clock hours of salt-and-pepper retinopathy in the peripheral retina and anterior to or at the equator; Grade II: greater than 2 clock hours of retinopathy that extends anteriorly or at the level of the equator; Grade III: retinopathy that extends posterior to the equator but not involving the macula; Grade IV: retinopathy involving the macula (maculopathy); and Grade V: extensive pan-retinopathy with concomitant optic disc atrophy.

TABLE 1 | Demographics, tumor characteristics, and management outcome.

Feature		No.	Complete response		Failure		*p* Value
Total	27 Patients	27	21	78%	6	22%	
Gender	Female	12	9	75%	3	25%	0.62
	Male	15	12	80%	3	20%	
Laterality	Unilateral	7	6	86%	1	14%	1.00
	Bilateral	20	15	75%	5	25%	
Vitreous seeds status	Persistent	11	7	64%	4	36%	0.37
	Recurrent	16	14	87%	2	13%	
IIRC	Group C	6	5	83%	1	17%	1.00
	Group D	21	16	76%	5	24%	
Associated subretinal seeds	With SRS	17	14	82%	3	18%	0.32
	Without SRS	10	7	70%	3	30%	
Tumor location	Macular	13	10	77%	3	33%	0.64
	Extramacular	14	11	79%	3	21%	
Type of vitreous seeds	Type I dust	8	6	75%	2	25%	0.61
	Type II sphere	3	3	100%	0	0%	
	Type III clouds	12	9	75%	3	25%	
	Mixed	4	3	75%	1	25%	
Distance from retina	<3 mm	7	6	86%	1	14%	1.00
	>3 mm	20	15	75%	5	25%	
Severity of vitreous seeds	Diffuse	17	11	65%	6	35%	0.04
	Focal	10	10	100%	0	0%	

Fisher's exact test was used to determine statistical significance and a p-value of <0.05 was considered statistically significant.

RESULTS

A total of 108 IViC injections were administered in 27 eyes from 27 patients with recurrent or refractory vitreous seeds (mean = median = 4 injections per eye; range = 3–8 injections). A standardized dose of 20–30 μg melphalan was given to all patients based on their age.

Demographics and Clinical Features

Of the 27 patients, 15 (56%) were boys, 12 (44%) were girls, and most of them (n = 20; 74%) had bilateral Rb. In total, 11 (41%) eyes had persistent refractory seeds, and 16 (59%) eyes had recurrent active seeds. Notably, only three eyes had recurrent seeds within 6 months after treatment with I-125 radioactive plaque therapy. At the time of diagnosis, the mean age was 17 months (median = 13, range = 4–50 months), and 6 eyes (22%) belonged to group C and 21 (78%) eyes to group D (**Table 1**). Other features of the treated vitreous seeds are summarized in **Table 1**.

Most of the eyes had diffuse vitreous seeds (n = 17, 63%), and n = 10 (37%) eyes had focal vitreous seeds. The distribution of the pattern of vitreous seeding in the treated eyes was: Type III clouds in 12 (44%) eyes, Type I dust in 8 (30%) eyes, Type II sphere in 3 (11%) eyes, and mixed in 4 (15%) eyes.

Previous Treatments

Primary systemic intravenous chemotherapy was given to all patients in this series (6–8 cycles of carboplatin + vincristine + etoposide; CVE). One patient received additional three cycles of topotecan systemic chemotherapy after the CVE.

The 6 group-C eyes and 13/21 group-D eyes received six cycles CVE, the 8 of group D eyes received eight cycles of CVE, and one of them received additional three cycles of systemic Topotecan. All affected eyes were also treated with focal consolidation therapy (transpupillary thermotherapy or cryotherapy as needed).

Three eyes were previously treated by radioactive Iodine-125 plaque therapy before receiving IViC. All these eyes had massive vitreous seeds more than 2 mm from the surface of the active tumor at time of radioactive plaque therapy. They showed initial regression or at least no progression immediately after the plaque therapy, and presented with vitreous seeds progression within 6 months from the date of radioactive plaque, while the main tumor was still inactive. Four eyes received periocular (sub-conjunctival) carboplatin injections 3 months before the IViC treatment. All the eyes that received radioactive plaque or subconjunctival carboplatin were group D eyes.

Response to Intravitreal Chemotherapy

Out of the 27 injected eyes, 21 (78%) eyes showed a complete response with no active vitreous seeds at the last day of follow-up (median number of injections = 4; range = 3–8). Complete suppression (type 0 response) was seen in n = 14 (52%) eyes, calcific seeds (type I response) in n = 8 (30%) eyes, and amorphous seeds (type II response) in n = 5 (19%) eyes. In total, five out of the 6 group-C eyes (83%) and 16 out of the 21 group-D eyes (76%) showed a complete response (p = 1.0). A complete response was noticed in 7 out of the 11 eyes with persistent vitreous seeds (64%) and in 14 out of 16 eyes with recurrent vitreous seeds (88%), which was not statistically significant (p = 0.37) (**Table 1**).

The treated vitreous seeds were successfully controlled by IViC in 14 (82%) eyes that had active sub-retinal seeds at the time of

TABLE 2 | Correlation between tumor characteristics and the number of injections.

Feature		No.	Complete response		Number of injections (Median)
Total	27 patients	27	21	78%	4
Number of injections	Total 108 injections (mean and median, 4 and 4 injections per eye; range, 3–8)				
Vitreous seeds status	Persistent	11	7	64%	5
	Recurrent	16	14	87%	3
Type of vitreous seeds	Type I dust	8	6	75%	3
	Type II sphere	3	3	100%	4
	Type III clouds	12	9	75%	5
	Mixed	4	3	75%	4
Severity of vitreous seeds	Diffuse	17	11	65%	5
	Focal	10	10	100%	3

injection and in 7 (70%) eyes that had no active or recurrent sub-retinal seeds (p = 0.32). Seeding in 6 (86%) of the treated eyes where the seeds were closer than 3 mm to the retina and 15 (75%) of the eyes where the seeds were more than 3 mm far from the retina was completely controlled by IViC (p = 1.00). On the other hand, all (100%) eyes with focal vitreous seeds were controlled by IViC, while only 11 (65%) of the eyes with diffuse vitreous seeds were controlled (p = 0.04). The number (median) of IViC injections mandated for treatment of the active seeds was three injections for eyes with dust-like seeds, four injections for eyes with sphere-like seeds and mixed seeds, and 5 for clouds vitreous seeds (**Table 2**).

Management Outcome and Complications

After a median follow-up of 42 months after the last IViC injection (range 9–72 months), 6 (22%) eyes failed the treatment and the patient had to undergo enucleation or EBRT.

Two eyes had massive recurrent vitreous seeds involving more than one quadrant (4 and 6 months after the last injection), one eye had ciliary body and anterior chamber invasion, and one eye had phthisis. Four of these were enucleated; one eye presented with massive recurrent vitreous seeds with concomitant active massive sub-retinal seeds 9 months after the IViC injections. The patient had a single eye, so he received three more cycles of systemic chemotherapy, and thereafter ended with EBRT. The sixth patient had a recurrent retinal tumor, sub-retinal seeds, and vitreous seeds associated with dense cataract, and a decision for enucleation was taken. The family refused this decision and decided not to treat. After getting lost in follow-up, they came back with a recurring orbital tumor. Even though parents refused further management and lost for follow-up again.

Out of 27 treated eyes, treatment side effects were seen in 16 (59%) eyes. In total, 13 (48%) eyes developed retinal toxicity: seven eyes had Grade I toxicity, three eyes had Grade II, two eyes had Grade III toxicity, no eye had Grade IV toxicity, and one eye developed Grade V toxicity (pan-retinopathy with optic atrophy). No patient developed endophthalmitis. Cataract was seen in eight (30%) eyes, five (19%) of them had a dense cataract that affected the fundus view, and, interestingly, three of them were previously treated by radioactive plaque therapy.

TABLE 3 | Side effects of intravitreal melphalan chemotherapy.

	Number of eyes	%
Median follow up (total 27 eyes)	42 months (range 6–72 months)	
Total number with eyes with side effects	16 eyes	59
Tumor recurrence[a]	6 eyes	22
Median time for recurrence	6 months (range 3–12 months)	
Retinal toxicity[b]	13 eyes	48
Pupillary synechia	4 eyes	15
Iris atrophy	2 eyes	7
Optic atrophy	1 eye	4
Cataract (Dense)[c]	8 (5) eyes	30 (19)
Hypotonia and phthisis bulbi	1 eye	4
Retinal hemorrhages	1 eye	4
Endophthalmitis	None	0
Orbital tumor recurrence	1[d]	4
Distant metastasis	None	0

[a]*Six eyes showed recurrent active tumor; three had massive recurrent vitreous seeds involving more than one quadrant (3, 4, and 6 months after the last injection), one eye had ciliary body and anterior chamber invasion, one eye had recurrent subretinal and vitreous seeds, and one eye had phthisis.*

[b]*In total, 13 (48%) eyes developed retinal toxicity; seven eyes had Grade I toxicity, three eyes had Grade II toxicity, two eyes had Grade III toxicity, none had Grade IV toxicity, and one eye had Grade V toxicity (pan-retinopathy with optic atrophy)*

[c]*Three of these eyes had radioactive plaque therapy.*

[d]*One of the patients had a recurrent retinal tumor, subretinal seeds, and vitreous seeds associated with dense cataract, and the decision was for enucleation. The family refused this decision and decided not to treat. After getting lost in follow-up, they came back with orbital tumor recurrence.*

All patients who developed significant cataracts (n = 5) had their cataract extracted surgically (with intraocular lens implantation without perforation of the posterior capsule) 12 months after the last injection, all of which were stable with no tumor or seeds recurrence after the surgery. Other complications included four (15%) eyes with pupillary synechia, two (7%) eyes with iris atrophy, 1 (4%) eye with optic atrophy, one (4%) eye with phthisis bulbi, and one (4%) eye with a retinal hemorrhage (**Table 3**).

All patients were alive by the last day of follow-up. Moreover, other than the child whose family refused enucleation and was lost in follow-up, no child in this study had a recurrence of orbital tumor, and none had metastasis to the CNS or the bone marrow. The eyes that had normal macula and optic disc had a median vision of 0.5 (range = 0.2–0.8).

DISCUSSION

In this study, 78% of the eyes with intraocular Rb that harbored active refractory or recurrent vitreous seeds benefitted from intravitreal melphalan chemotherapy and avoided enucleation and EBRT. However, 59% of the eyes showed some kind of complications ranging from mild retinal pigmentation to severe retinal toxicity and atrophy.

For decades, ophthalmologists have avoided inserting a needle inside an eye with active Rb (for both diagnosis and treatment) due to the potentially higher risk of tumor dissemination through the site of injection. Most of the published data about intravitreal chemotherapy for Rb belongs to developed countries where quality control is mandatory. This study was conducted in Jordan (a developing country) and we followed a strict safety-enhanced anti-reflux protocol (Munier et al., 2012a) to prevent tumor dissemination *via* the route of injection. This protocol included injection of the chemotherapeutic drug in the pars plana in the tumor-free quadrant, lowering the intraocular pressure, and freezing the needle track (triple-freeze-thaw) immediately after each injection. Because of this protocol, other than one child who refused treatment and was lost in follow-up, no child developed extraocular tumor dissemination or presented with tumor metastasis over the median 42 months (9–72 months) follow-up period. This safety data is supported by the data from the first report about the safety of anti-reflux technique for IViC by Munier et al. who were the first to elucidate this protocol in treating 23 eyes with Rb in Switzerland (Munier et al., 2012a), and they too did not report any case of metastasis (in a follow-up period of 22 months). Similarly, subsequent reports with a slightly longer follow up (not more than 66 months) that followed similar inclusion criteria and used the same injection protocol did not report any case of extraocular invasion or distant metastasis (Munier, 2014; Berry et al., 2017; Kiratli et al., 2017; Xue et al., 2019).

It is noteworthy that we followed our patients for a longer period, and no orbital recurrence or distant metastases were encountered. This indicates that IViC can be applied safely for Rb patients all around the world as long as the treating team followed a strict injection protocol. On the other hand, other studies about eyes that received intravitreal chemotherapy who have not mentioned clear selection criteria and did not strictly follow the anti-reflux measures reported a 0.4% chance of post-operative orbital tumor invasion and a 4.4% chance of brain metastasis, which is a significant risk for these children (Kaneko and Suzuki, 2003). This difference in the incidence of orbital recurrence and metastasis highlights the importance of following the eligibility criteria and strict anti-reflux injection technique to prevent metastasis. In our series, we saved 78% of the eyes with vitreous seeds that were otherwise planned to be enucleated, which is comparable to the previously reported data of 79–100% salvage rates with a dose of 20–30 μg, and 68–83% salvage with a dose of 8–20 μg (Ghassemi and Shields, 2012; Munier et al., 2012a; Shields et al., 2014; Xunda et al., 2016; Berry et al., 2017).

Earlier reports have shown melphalan to be the single most effective chemotherapy agent against Rb and being less toxic if used at specific doses (Inomata and Kaneko, 2004). This was based on previous *in vitro* studies by Inomata and Kaneko (1987), who found this drug to be the most efficient among the 12 tested. Preclinical studies in the rabbit have established that the vitreous concentration necessary (5.9 μg/ml) for tumor control can be achieved without retinal toxicity (Ueda et al., 1995). When extrapolated to the human vitreous volume, the injected dose corresponds to the injection of 20–30 μg. The possible side effects of IViC treatment include cataracts, uveitis, endophthalmitis, retinal toxicity, vitreous hemorrhage, optic atrophy, extraocular tumor extension, and metastasis. Most of the published data about local toxicity of IViC are from the Caucasian populations and very few for the Mediterranean and South-East Asia populations. Smith et al., 2013 presented a correlation between the dose of melphalan and the risk of ocular toxicity and showed that a 30 μg dose has fewer side effects than higher doses. Further, Francis reported a higher rate of ocular toxicity in more deeply pigmented dark eyes (Francis et al., 2014; Susskind et al., 2016; Francis et al., 2017) as the pigmentation may absorb higher levels of chemotherapy (like melphalan) leading to a higher retinal, RPE, and choroidal toxicity. Our Jordanian population falls in this group of pigmented eyes, so we expect higher rates of ocular toxicity than the Caucasian population.

Francis also reported anterior segment toxicity in 7% of eyes after IViC injections in the Caucasian population, while in China, 43% of patients developed pupillary synechiae, 40% had iris atrophy, and 27% developed cataracts (Francis et al., 2017; Xue et al., 2019). Chao et al. reported a case of diffuse chorioretinal atrophy after injecting a single dose of 8 μg melphalan (Chao et al., 2016). In our study, pupillary synechiae and iris atrophy occurred in 15% and 7% of patients, which is less than the reported value for China, but 30% of the patients developed cataracts, which is still higher than the Chinese numbers. Cataract in our patients could be attributed to the intravitreal melphalan injection, although three of these patients had previously undergone radioactive plaque therapy, while the other five eyes did not receive any form of radiation therapy. Overall, we are unable to conclude whether these anterior segment side effects are caused by IViC as almost all the eyes in our and other studies received more than two or three treatment modalities, including intravenous chemotherapy, IAC, cryotherapy, and laser therapy. Similarly, the high rate of cataract cannot be correlated to the close distance between the tip of the needle (and the injected melphalan) and the posterior surface of the lens, as all eyes received injections by the same technique, and all eyes were vigoureously shaked immediately after each injection. Strikingly, in Japan (Kaneko and Suzuki, 2003), the reported visual outcome for eyes that had extra macular tumors and were treated by 8–20 μg melphalan (lower dose than other studies) was ≥ 0.5 in 27% of the injected eyes, a result which is comparable to the visual outcome in our patients who were given a higher dose of 20–30 μg. This suggests that a dose of 20–30 μg melphalan given intravitreally is safe and effective for active vitreous seeds. Furthermore, it could be useful develop a biodegradable deliver system to inject melphalan in order to improve the pharmacology profile and the safety profile (Conti et al., 1997).

Because of emergence of cases that are resistant to melphalan alone, Ghassemi et al. (2014) reported a total of 17 combined

sessions of intravitreal injections using combined melphalan and topotecan, and they achieved complete response of vitreous seeds in 100% of eyes with minimal toxic effects, with a median of two injections (mean, 1.9). Similarly Kiratli et al. showed that the combined use of intravitreal melphalan and topotecan provide better results in terms of avoiding enucleation and vitreal and subretinal seed control, as the enucleation rate was 62% for eyes that received melphalan alone, while wnucleation rate was 11% in eyes that received combination of intravitreal melphalan and topotecan (Kiratli et al., 2020). In our study, all eyes received melphalane a lone, and the eye salvage rate was 78% that is notably less than for eyes received combined melphalan and topotecan, therefore administration of melphalan and topotecan combination may have favorable response over melphalan alone, and it mandates lower number of injections to control the seeds, but more studies with longer follow up are still needed to confirm the efficacy and safety of this combination.

Vitreous seeds have three different morphological types; dust seeds, spheres, and clouds. The time for regression of these different types of vitreous seeds was shown to be variable and dependent on the morphology of the seeds (Rishi et al., 2017). Dust seeds responded faster than spheres, while clouds mandate more injections to regress. Other reports have shown that dust seeds usually mandate three injections, spheres mandate six injections, while clouds mandate nine injections before complete seed regression (Francis et al., 2015; Xunda et al., 2016). Our results were similar to these data as the median number of injections mandated to get regression was three for dust seeds, four for spheres, and five for clouds. This is indicative of less volume of active cells in the dust seeds, while clouds harbor collections of aggregated active tumor cells, therefore the injected chemotherapy is unable to get in direct contact with the active tumor cells within the center of the cloud. Thus, more injections are needed to make the cloud fragment initially into dusts, and then these dusts have to be controlled by further injections. This said, although the morphology of seeds affects the number of injections needed to control the tumor, it has no impact on the chances of eye salvage.

Over decades, multiple treatment modalities were adopted to eradicate refractory active seeds before the era of IViC. Intra-arterial chemotherapy with melphalan could control two-thirds of the eyes with active vitreous seeds (Abramson et al., 2012) and this rate of vitreous seeds-control was higher than that with systemic chemotherapy, still, it is not as effective as intravitreal chemotherapy. Furthermore, EBRT was used successfully for control of only 22–64% of eyes with refractory vitreous seeds after the failure of systemic chemotherapy (Berry et al., 2013; Yousef et al., 2020a). Alternately, a combination of IAC and IViC salvaged 87% of the eyes with vitreous seeds (Lee et al., 2016); however, one-half of these eyes had dangerous sight-threatening side effects like hemorrhage, and one-third of them had significant retinal atrophy. We cannot say with full surety if these toxicities are secondary to the general total dose of melphalan that was injected or because of the technique of intra-arterial chemotherapy, which may obstruct the retinal circulation. Nevertheless, intravitreal chemotherapy is potentially more successful than intravenous chemotherapy, IAC, and EBRT for controlling active vitreous seeds in patients with Rb.

In conclusion, our results show that intravitreal melphalan chemotherapy is an effective and relatively safe treatment modality for retinoblastomas and has changed the outcome of eyes with vitreous seeds, significantly improving the ocular oncologists' capability to salvage eyes. However, there are side effects on both the anterior and posterior segments of the eye, and unanticipated serious toxicity may occur with the standard dose of 20–30 μg melphalan and more so in the eyes that have received multiple treatment modalities.

DATA AVAILABILITY STATEMENT

The original contributions presented in the study are included in the article/Supplementary Material, further inquiries can be directed to the corresponding authors.

ETHICS STATEMENT

The studies involving human participants were reviewed and approved by the IRB at King Hussein Cancer Center (code: 18KHCC27), approved this study, and waived the need for consent. Written informed consent for participation was not provided by the participants' legal guardians/next of kin because: retrospective study.

AUTHOR CONTRIBUTIONS

Conceptualization—YY, MA, and RN; methodology—YY and QA; software—I.S; validation—YY and MM; formal analysis—YY; investigation—MA; resources— MH, MS; data curation—MM and MR; writing—original draft preparation—YY and MA; writing—review and editing—YY, MH, and RN; supervision—IA-N; project administration—YY, MH and MT; funding acquisition—MT and RR. All authors contributed in writing, reviewing and editing the final manuscript. All authors agreed to publish the current version of this manuscript.

FUNDING

This research was supported in part by King Hussein Cancer Center and The Medical University of Lublin.

ACKNOWLEDGMENTS

We acknowledge Reem AlJabari (Department of Surgery), Ayat Al Rahamneh, Ayat Al Khuly, Adam Jarad, Sami AlTalla, and Moaath Aldhoon (Department of Nursing) (King Hussein Cancer Center, Amman, Jordan) for their assistance in recruiting patients for this study and collecting the RetCam Images.

REFERENCES

Abramson, D. H., Marr, B. P., Dunkel, I. J., Brodie, S., Zabor, E. C., Driscoll, S. J., et al. (2012). Intra-arterial Chemotherapy for Retinoblastoma in Eyes with Vitreous And/or Subretinal Seeding: 2-year Results. *Br. J. Ophthalmol.* 96, 499–502. doi:10.1136/bjophthalmol-2011-300498

Amin, S., AlJboor, M., Toro, M. D., Rejdak, R., Nowomiejska, K., Nazzal, R., et al. (2021). Management and Outcomes of Unilateral Group D Tumors in Retinoblastoma. *Clin. Ophthalmol.* 15, 65–72.

Berry, J. L., Bechtold, M., Shah, S., Zolfaghari, E., Reid, M., Jubran, R., et al. (2017). Not All Seeds Are Created Equal: Seed Classification Is Predictive of Outcomes in Retinoblastoma. *Ophthalmology* 124, 1817–1825. doi:10.1016/j.ophtha.2017.05.034

Berry, J. L., Jubran, R., Kim, J. W., Wong, K., Bababeygy, S. R., Almarzouki, H., et al. (2013). Long-term Outcomes of Group D Eyes in Bilateral Retinoblastoma Patients Treated with Chemoreduction and Low-Dose IMRT Salvage. *Pediatr. Blood Cancer* 60, 688–693. doi:10.1002/pbc.24303

Chan, H. S. L., Thorner, P. S., Haddad, G., and Gallie, B. L. (1995). Effect of Chemotherapy on Intraocular Retinoblastoma. *Int. J. Pediatr. Hematol. Oncol.*, 269–281.

Chao, A. N., Kao, L.-Y., Liu, L., and Wang, N.-K. (2016). Diffuse Chorioretinal Atrophy after a Single Standard Low- Dose Intravitreal Melphalan Injection in a Child with Retinoblastoma: a Case Report. *BMC Ophthalmol.* 16, 27. doi:10.1186/s12886-016-0204-6

Conti, B., Kao, L.-Y., Bucolo, C., Puglisi, C., Giunchedi, P., and Conte, U. (1997). Biodegradable Microspheres for the Intravitreal Administration of Acyclovir: In vitro/In Vivo Evaluation. *Eur. J. Pharmaceut. Sci.* 5 (5), 287–293. doi:10.1016/S0928-0987(97)00023-7

Francis, J. H., Abramson, D. H., Gaillard, M.-C., Marr, B. P., Beck-Popovic, M., and Munier, F. L. (2015). The Classification of Vitreous Seeds in Retinoblastoma and Response to Intravitreal Melphalan. *Ophthalmology* 122, 1173–1179. doi:10.1016/j.ophtha.2015.01.017

Francis, J. H., Brodie, S. E., Marr, B., Zabor, E. C., Mondesire-Crump, I., and Abramson, D. H. (2017). Efficacy and Toxicity of Intravitreous Chemotherapy for Retinoblastoma: Four-Year Experience. *Ophthalmology* 124, 488–495. doi:10.1016/j.ophtha.2016.12.015

Francis, J. H., Schaiquevich, P., Buitrago, E., Del Sole, M. J., Zapata, G., Croxatto, J. O., et al. (2014). Local and Systemic Toxicity of Intravitreal Melphalan for Vitreous Seeding in Retinoblastoma: a Preclinical and Clinical Study. *Ophthalmology* 121 (9), 1810–1817. doi:10.1016/j.ophtha.2014.03.028

Ghassemi, F., Shields, C. L., Ghadimi, H., Khodabandeh, A., and Roohipoor, R. (2014). Combined Intravitreal Melphalan and Topotecan for Refractory or Recurrent Vitreous Seeding from Retinoblastoma. *JAMA Ophthalmol.* 132 (8), 936–941. doi:10.1001/jamaophthalmol.2014.414

Ghassemi, F., and Shields, C. L. (2012). Intravitreal Melphalan for Refractory or Recurrent Vitreous Seeding from Retinoblastoma. *Arch. Ophthalmol.* 130 (1960), 1268–1271. doi:10.1001/archophthalmol.2012.1983

Inomata, M., and Kaneko, A. (1987). Chemosensitivity Profiles of Primary and Cultured Human Retinoblastoma Cells in a Human Tumor Clonogenic Assay. *Jpn. J. Cancer Res.* 78, 858–868.

Inomata, M., and Kaneko, A. (2004). *In Vitro* chemosensitivity Assays of Retinoblastoma Cells. *Int. J. Clin. Oncol.* 9, 31–35. doi:10.1007/s10147-003-0370-4

Kaneko, A., and Suzuki, S. (2003). Eye-preservation Treatment of Retinoblastoma with Vitreous Seeding. *Jpn. J. Clin. Oncol.* 33, 601–607. doi:10.1093/jjco/hyg113

Kiratli, H., Koç, I., Öztürk, E., Varan, A., and Akyüz, C. (2020). Comparison of Intravitreal Melphalan with and without Topotecan in the Management of Vitreous Disease in Retinoblastoma. *Jpn. J. Ophthalmol.* 64 (4), 351–358. doi:10.1007/s10384-020-00743-2

Kiratli, H., Koç, İ., Varan, A., and Akyüz, C. (2017). Intravitreal Chemotherapy in the Management of Vitreous Disease in Retinoblastoma. *Eur. J. Ophthalmol.* 27 (4), 423–427. doi:10.5301/ejo.5000921

Kivela, T. (2009). The Epidemiological challenge of the Most Frequent Eye Cancer: Retinoblastoma, an Issue of Birth and Death. *Br. J. Ophthalmol.* 93, 1129–1131. doi:10.1136/bjo.2008.150292

Kleinerman, R. A., Tucker, M. A., Tarone, R. E., Abramson, D. H., Seddon, J. M., Stovall, M., et al. (2005). Risk of New Cancers after Radiotherapy in Long-Term Survivors of Retinoblastoma: an Extended Follow-Up. *Jco* 23, 2272–2279. doi:10.1200/JCO.2005.05.054

Lee, J. H., Han, J. W., Hahn, S. M., Lyu, C. J., Kim, D. J., and Lee, S. C. (2016). Combined Intravitreal Melphalan and Intravenous/intra-Arterial Chemotherapy for Retinoblastoma with Vitreous Seeds. *Graefes Arch. Clin. Exp. Ophthalmol.* 254, 391–394. doi:10.1007/s00417-015-3202-0

Linnmurphree, A. (2005). Intraocular Retinoblastoma: the Case for a New Group Classification. *Ophthalmol. Clin. North America* 18, 41–53. doi:10.1016/j.ohc.2004.11.003

Manjandavida, F. P., and Shields, C. L. (2015). The Role of Intravitreal Chemotherapy for Retinoblastoma. *Indian J. Ophthalmol.* 63, 141–145. doi:10.4103/0301-4738.154390

Moulin, A. P., Gaillard, M.-C., Balmer, A., and Munier, F. L. (2012). Ultrasound Biomicroscopy Evaluation of Anterior Extension in Retinoblastoma: a Clinicopathological Study. *Br. J. Ophthalmol.* 96, 337–340. doi:10.1136/bjophthalmol-2011-300051

Munier, F. L., Beck-Popovic, M., Balmer, A., Gaillard, M.-C., Bovey, E., and Binaghi, S. (2011). Occurrence of Sectoral Choroidal Occlusive Vasculopathy and Retinal Arteriolar Embolization after Superselective Ophthalmic Artery Chemotherapy for Advanced Intraocular Retinoblastoma. *Retina* 31, 566–573. doi:10.1097/IAE.0b013e318203c101

Munier, F. L. (2014). Classification and Management of Seeds in Retinoblastoma Ellsworth Lecture Ghent August 24th 2013. *Ophthalmic Genet.* 35, 193–207. doi:10.3109/13816810.2014.973045

Munier, F. L., Gaillard, M.-C., Balmer, A., Soliman, S., Podilsky, G., Moulin, A. P., et al. (2012a). Intravitreal Chemotherapy for Vitreous Disease in Retinoblastoma Revisited: from Prohibition to Conditional Indications. *Br. J. Ophthalmol.* 96, 1078–1083. doi:10.1136/bjophthalmol-2011-301450

Munier, F. L., Soliman, S., Moulin, A. P., Gaillard, M.-C., Balmer, A., and Beck-Popovic, M. (2012b). Profiling Safety of Intravitreal Injections for Retinoblastoma Using an Anti-reflux Procedure and Sterilisation of the Needle Track. *Br. J. Ophthalmol.* 96, 1084–1087. doi:10.1136/bjophthalmol-2011-301016

Rishi, P., Sharma, T., Agarwal, V., Dhami, A., Maitray, A., Sharma, M., et al. (2017). Complications of Intravitreal Chemotherapy in Eyes with Retinoblastoma. *Ophthalmol. Retina* 1, 448–450. doi:10.1016/j.oret.2017.03.006

Shields, C. L., Honavar, S. G., Meadows, A. T., Shields, J. A., Demirci, H., Singh, A., et al. (2002). Chemoreduction Plus Focal Therapy for Retinoblastoma: Factors Predictive of Need for Treatment with External Beam Radiotherapy or enucleation11InternetAdvance Publication at ajo.Com April 8, 2002. *Am. J. Ophthalmol.* 133, 657–664. doi:10.1016/s0002-9394(02)01348-x

Shields, C. L., Manjandavida, F. P., Arepalli, S., Kaliki, S., Lally, S. E., and Shields, J. A. (2014). Intravitreal Melphalan for Persistent or Recurrent Retinoblastoma Vitreous Seeds. *JAMA Ophthalmol.* 132, 319–325. doi:10.1001/jamaophthalmol.2013.7666

Shields, C. L., Mashayekhi, A., Au, A. K., Czyz, C., Leahey, A., Meadows, A. T., et al. (2006). The International Classification of Retinoblastoma Predicts Chemoreduction success. *Ophthalmology* 113, 2276–2280. doi:10.1016/j.ophtha.2006.06.018

Shields, C. L., Ramasubramanian, A., Thangappan, A., Hartzell, K., Leahey, A., Meadows, A. T., et al. (2009). Chemoreduction for Group E Retinoblastoma: Comparison of Chemoreduction Alone versus Chemoreduction Plus Low-Dose External Radiotherapy in 76 Eyes. *Ophthalmology* 116, 544–551. e541. doi:10.1016/j.ophtha.2008.10.014

Smith, S. J., Smith, B. D., and Mohney, B. G. (2013). Ocular Side Effects Following Intravitreal Injection Therapy for Retinoblastoma: a Systematic Review. *Br. J. Ophthalmol.* 98, 292–297. doi:10.1136/bjophthalmol-2013-303885

Süsskind, D., Hagemann, U., Schrader, M., Januschowski, K., Schnichels, S., and Aisenbrey, S. (2016). Toxic Effects of Melphalan, Topotecan and Carboplatin on Retinal Pigment Epithelial Cells. *Acta Ophthalmol.* 94, 471–478. doi:10.1111/aos.12990

Ueda, M., Tanabe, J., Inomata, M., Kaneko, A., and Kimura, T. (1995). [Study on Conservative Treatment of Retinoblastoma-Eeffect of Intravitreal Injection of Melphalan on the Rabbit Retina]. *Nippon Ganka Gakkai Zasshi* 99 (11), 1230–1235.

Xue, K., Ren, H., Meng, F., Zhang, R., and Qian, J. (2019). Ocular Toxicity of Intravitreal Melphalan for Retinoblastoma in Chinese Patients. *BMC Ophthalmol.* 19, 61. doi:10.1186/s12886-019-1059-4

Xunda, J., Peiyan, H., Jing, L., Jiakai, L., Junyang, Z., and Peiquan, Z. (2016). Intravitreal Melphalan for Vitreous Seeds: Initial Experience in China. *J. Ophthalmol.* 2016, 4387286. doi:10.1155/2016/4387286

Yousef, Y. A., Mohammad, M., Jaradat, I., Shatnawi, R., Mehyar, M., and Al-Nawaiseh, I. (2020b). Prognostic Factors for Eye Globe Salvage by External Beam Radiation Therapy for Resistant Intraocular Retinoblastoma. *Oman J. Ophthalmol.* 13, 123–128. doi:10.4103/ojo.OJO_250_2019

Yousef, Y. A., Al-Nawaiseh, I., Mehyar, M., Sultan, I., Al-Hussaini, M., Jaradat, I., et al. (2021). How Telemedicine and Centralized Care Changed the Natural History of Retinoblastoma in a Developing Country. *Ophthalmology* 128, 130–137. doi:10.1016/j.ophtha.2020.07.026

Yousef, Y. A., Mohammad, M., Jaradat, I., Shatnawi, R., Banat, S., Mehyar, M., et al. (2020a). The Role of External Beam Radiation Therapy for Retinoblastoma after Failure of Combined Chemoreduction and Focal Consolidation Therapy. *Ophthalmic Genet.* 41, 20–25. doi:10.1080/13816810.2020.1719519

Yousef, Y. A., Noureldin, A. M., Sultan, I., Deebajah, R., Al-Hussaini, M., Shawagfeh, M., et al. (2020c). Intravitreal Melphalan Chemotherapy for Vitreous Seeds in Retinoblastoma. *J. Ophthalmol.* 2020, 1–7. doi:10.1155/2020/8628525

Conflict of Interest: The authors declare that the research was conducted in the absence of any commercial or financial relationships that could be construed as a potential conflict of interest.

frontiers in Pharmacology

ORIGINAL RESEARCH
published: 21 July 2021
doi: 10.3389/fphar.2021.705405

Brimonidine is Neuroprotective in Animal Paradigm of Retinal Ganglion Cell Damage

Federica Conti[1†], Giovanni Luca Romano[1†], Chiara Maria Eandi[2], Mario Damiano Toro[3,4], Robert Rejdak[4], Giulia Di Benedetto[1], Francesca Lazzara[1], Renato Bernardini[1], Filippo Drago[1], Giuseppina Cantarella[1‡] and Claudio Bucolo[1‡]*

[1]Department of Biomedical and Biotechnological Sciences, Section of Pharmacology, University of Catania, Catania, Italy, [2]Department of Ophthalmology, Jules Gonin Eye Hospital, Fondation Asile des Aveugles, University of Lausanne, Lausanne, Switzerland, [3]Department of Ophthalmology, University of Zurich, Zurich, Switzerland, [4]Chair and Department of General and Pediatric Ophthalmology, Medical University of Lublin, Lublin, Poland

OPEN ACCESS

Edited by:
Abdur Rauf,
University of Swabi, Pakistan

Reviewed by:
Jennifer Arcuri,
University of Miami Health System, United States
Philip Lazarovici,
Hebrew University of Jerusalem, Israel
M. S. Uddin,
Pharmakon Neuroscience Research Network (PNRN), Bangladesh

***Correspondence:**
Claudio Bucolo
claudio.bucolo@unict.it

[†]These authors have contributed equally to this work

[‡]These authors share last authorship

Specialty section:
This article was submitted to Experimental Pharmacology and Drug Discovery, a section of the journal Frontiers in Pharmacology

Received: *05 May 2021*
Accepted: *07 July 2021*
Published: *21 July 2021*

Citation:
Conti F, Romano GL, Eandi CM, Toro MD, Rejdak R, Di Benedetto G, Lazzara F, Bernardini R, Drago F, Cantarella G and Bucolo C (2021) Brimonidine is Neuroprotective in Animal Paradigm of Retinal Ganglion Cell Damage. Front. Pharmacol. 12:705405. doi: 10.3389/fphar.2021.705405

To investigate the neuroprotective effect of brimonidine after retinal ischemia damage on mouse eye. Glaucoma is an optic neuropathy characterized by retinal ganglion cells (RGCs) death, irreversible peripheral and central visual field loss, and high intraocular pressure. Ischemia reperfusion (I/R) injury model was used in C57BL/6J mice to mimic conditions of glaucomatous neurodegeneration. Mouse eyes were treated topically with brimonidine and pattern electroretinogram were used to assess the retinal ganglion cells (RGCs) function. A wide range of inflammatory markers, as well as anti-inflammatory and neurotrophic molecules, were investigated to figure out the potential protective effects of brimonidine in mouse retina. In particular, brain-derived neurotrophic factor (BDNF), IL-6, tumor necrosis factor-related apoptosis-inducing ligand (TRAIL) and its death receptor DR-5, TNF-α, GFAP, Iba-1, NOS, IL-1β and IL-10 were assessed in mouse retina that underwent to I/R insult with or without brimonidine treatment. Brimonidine provided remarkable RGCs protection in our paradigm. PERG amplitude values were significantly ($p < 0.05$) higher in brimonidine-treated eyes in comparison to I/R retinas. Retinal BDNF mRNA levels in the I/R group dropped significantly ($p < 0.05$) compared to the control group (normal mice); brimonidine treatment counteracted the downregulation of retinal BDNF mRNA in I/R eyes. Retinal inflammatory markers increased significantly ($p < 0.05$) in the I/R group and brimonidine treatment was able to revert that. The anti-inflammatory IL-10 decreased significantly ($p < 0.05$) after retinal I/R insult and increased significantly ($p < 0.05$) in the group treated with brimonidine. In conclusion, brimonidine was effective in preventing loss of function of RGCs and in regulating inflammatory biomarkers elicited by retinal I/R injury.

Keywords: neuroprotection, retinal ganglion cells, ischemia-reperfusion, brimonidine, PERG

INTRODUCTION

Glaucoma is an optic neuropathy characterized by retinal ganglion cells (RGCs) death, irreversible peripheral and central visual field loss and high IOP (Bucolo and Drago, 2011). Currently, six main classes of topical drugs are available; they include beta-blockers, carbonic anhydrase inhibitors, prostaglandin derivatives, sympathomimetics, miotics, and Rho-kinase inhibitors. For neovascular

glaucoma the therapeutic approach could be different, on this regards it is worth of note that anti-VEGF agents, used in clinical practice, such as ranibizumab, bevacizumab and aflibercept are considerably different in terms of molecular interactions when they bind with VEGF (Platania et al., 2015). Brimonidine is an $\alpha 2_A$-adrenergic receptor agonist, approved for lowering intraocular pressure (IOP) in patients with open-angle glaucoma. Although $\alpha 2_A$ receptors have been identified in the RGCs, the mechanisms by which $\alpha 2_A$ agonists exert neuroprotection are not well-established. There are many controversial studies on brimonidine and its effects to preserve retinal tissue. Some non-clinical findings have demonstrated that brimonidine possess retinal protective action (Lambert et al., 2011; Nizari et al., 2016; Marangoz et al., 2018). However, to date, clinical trials have failed to translate into similar efficacy in humans. Recently, a Cochrane systematic review (Sena and Lindsley, 2017) showed that although one clinical trial found less visual field loss in the brimonidine-treated group, the evidence was of such low certainty that it is not possible draw conclusions from this only finding. Incidentally, the authors concluded that further clinical research is needed to determine whether brimonidine may be beneficial for individuals with glaucoma. More recently, a systematic review and meta-analysis concluded that the clinical evidence of neuroprotective effect of brimonidine is inconclusive and needs stronger support maybe with large double-blind randomized clinical trials (Scuteri et al., 2020). To shed light on these controversial studies we aimed to investigate topical brimonidine on a well-known *in vivo* paradigm of retinal damage. The neurodegenerative process in several eye diseases is characterized by progressive death of RGCs, optic nerve degeneration, and sometime blindness (Chou et al., 2020). RGCs degeneration is often associated to ischemia in central retinal artery occlusion and ischemic optic neuropathies (Kunimi et al., 2019). Remarkable insights in therapy for retinal ischemia have arisen through the investigation of rodent models of ischemia-reperfusion. Retinal ischemia–reperfusion (I/R) is an experimental model that triggers an inflammatory process eliciting a large number of detrimental molecules such as TNF, tumor necrosis factor-related apoptosis-inducing ligand (TRAIL) and ILs (Osborne et al., 2004; Wei et al., 2011; Dibas et al., 2018).

Gliosis, another critical event contributing to glaucoma pathogenesis, is a hallmark of retinal degeneration. Retinal reactive glia cells increased glial fibrillary acidic protein (GFAP)-immunoreactivity and ionized calcium binding adaptor molecule 1 (Iba1). It is well known that injury-induced gliosis in the optic nerve head and retina promote the death of RGCs due to over-release of pro-inflammatory mediators (Ganesh and Chintala, 2011). TRAIL mediates different neuroinflammatory responses (Huang et al., 2011). TRAIL and its receptors were found up-regulated in brain ischemia-reperfusion (Cui et al., 2010). The unmet medical need in glaucoma is mainly related to disease progression (RGC death) despite IOP control. In fact, glaucoma progression could be related to neurotrophins deprivation; interestingly, low serum levels of BDNF and nerve growth factor (NGF) were associated to early moderate stages of glaucoma. It is worth of note that the potential therapeutic value of neurotrophins to manage glaucoma is important, however the main point that damper the development of these factors as eye drops is related to the drug delivery issues (Bucolo et al., 2018). On this regards it could be useful develop a biodegradable deliver system in order to sustain prolonged pharmacological levels of drug into the back of the eye (Conti et al., 1997) even though topical formulation is ideal. Aim of the present study was to investigate the neuroprotective effects of brimonidine eye drops in a mouse model of retinal I/R damage. Pattern electroretinogram (PERG) analysis, the most specific non-invasive technique for electrophysiological assessment of RGCs activity, was used to evaluate the *in vivo* protection of RCGs function. Further, the retinal inflammatory profile after I/R insult with or without brimonidine treatment was investigated.

MATERIALS AND METHODS

Animals

Male C57BL6/J mice (Charles River Laboratories, Italy) were housed in a temperature-controlled environment with free access to food and water during a 12-h light–dark cycle. All animals were treated according to the Principles for the Care and Use of Animals in Ophthalmic and Vision Research approved by the Association for Research in Vision and Ophthalmology. University of Catania (Italy) Ethics Committee approval #343.

Ischemic-Reperfusion Retina Damage

Retinal ischemia/reperfusion has been used as a model of retinal injury and has been described in many rodent species (Osborne et al., 2004; Gustavsson et al., 2008; Ulbrich et al., 2017; Stankowska et al., 2019). A validated modified I/R model (Hartsock et al., 2016) (Hartsock et al., 2016) was used in the present study. Mice were anesthetized by intraperitoneal injection with tiletamine + zolazepam (60 mg/kg) and medetomidine (40 μg/kg) plus a topical instillation of 0.4% oxybuprocaine (Novesina®, Laboratoires Thea, Clermont-Ferrand, France). The animals were placed on a heating pad to prevent hypothermia during the experiment. A 32-gauge needle, connected with a reservoir containing PBS, was introduced into the anterior chamber through the cornea to increase intraocular pressure (up to 90 mm Hg). Retinal ischemia was confirmed by an observation of blanching of the anterior segment and arteries in the eye. Following 60 min of ischemia, the needle was removed to allow rapid reperfusion. Ocular formulation of brimonidine tartrate (2 mg/ml) was instilled (10 μL) 60 min before I/R and after reperfusion, twice in 2 h. The effect of brimonidine was evaluated after 72 h from I/R insult. Mice were euthanized after 72 h from I/R insult, the eyes were enucleated, and the retinas collected.

Pattern Electroretinogram

As a sensitive measure of RGCs function we used the PERG (Chou et al., 2018). Anesthetized mice were transferred on a heating plate with the mouse superior incisor teeth hooked to a bite bar and the head gently restrained by two ear knobs. Body

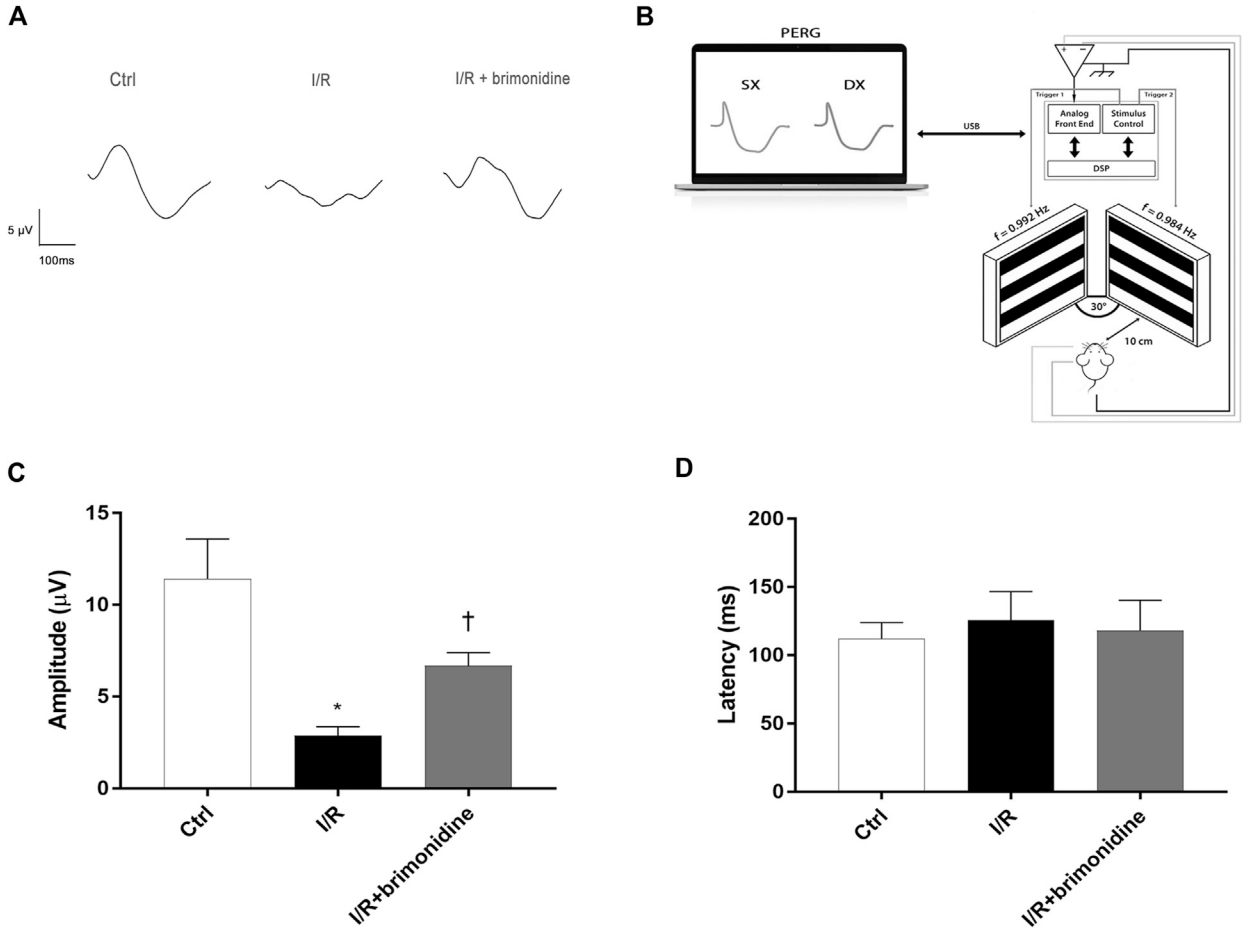

FIGURE 1 | RGCs function assessment. **(A)** Representative PERG waveforms in C57BL6/J mice control, I/R and I/R plus brimonidine. **(B)** Mouse PERG recording layout. **(C)** Comparison between PERG amplitude values (µV) and latency values **(D)** of control, I/R and brimonidine treated mice. Brimonidine significantly counteracted RCGs loss of function induced by I/R injury, after 72 h, in mice retina. In each panel, bars represent the mean values and corresponding standard errors (±SD). One-way ANOVA analysis was performed followed by the Tukey post-hoc test. *$p < 0.05$ *vs.* Ctrl; †$p < 0.05$ *vs.* I/R.

was kept at a constant temperature of 37°C using a feedback-controlled heating pad (TCAT-2LV, Physitemp Instruments, Inc., Clifton, NJ, United States). Two microliters of balanced salt solution (BSS) were topically applied to prevent corneal dryness. Simultaneous recordings of PERG response from both eyes were obtained using a common subcutaneous needle in the snout with a commercially available instrument (Jorvec Corp., Miami, FL, United States). **Figure 1**, panel B, shows the mouse PERG recording layout. Visual stimuli consisted of black-white horizontal bars generated on LED tablets and presented independently to each eye at 10 cm distance (56° vertical × 63° horizontal field; spatial frequency, 0.05 cycles/deg; 98% contrast; 800 cd/sqm mean luminance; left-eye reversal rate, 0.992 Hz; right-eye reversal rate, 0.984 Hz). Electrical signals recorded from the common snout electrode were averaged (>1,110 epochs), and PERG responses from each eye isolated by averaging at stimulus-specific synchrony. As previously described [17], PERG waveforms consisted of a positive wave (defined as P1) followed by a slower negative wave with a broad trough (defined as N2). Therefore, each waveform has been analyzed by measuring the peak-to-trough (P1-N2) amplitude defined as PERG amplitude and the time-to-peak of the P1 wave as PERG latency (Porciatti, 2015).

Ribonucleic Acid (RNA) Extraction and Complementary Deoxyribonucleic Acid (cDNA) Synthesis

Mice were sacrificed after 72 h from I/R and brimonidine treatment by cervical dislocation, eyes were enucleated, and retinas were isolated. The extraction of total RNA from mice retina samples was performed by using TRIzol Reagent (Invitrogen, Life Technologies, Carlsbad, CA) according to the manufacturer's protocol. The A260/A280 ratio of the optical density of RNA samples (measured with Nanodrop spectrophotometer ND-1000, Thermofisher) was 1.95–2.01. cDNA was synthesized from 500 ng of RNA with a reverse transcription kit (SuperScript™ II Reverse Transcriptase, Invitrogen, ThermoFisher Scientific, Carlsbad, CA, United States).

TABLE 1 | Primers used for RT-PCR.

Gene	Primer murine sequence/Catalogue number
18 s	Forward: 5′-GTTCCGACCATAAACGATGCC-3′ Reverse: 5′-TGGTGGTGCCCTTCCGTCAAT-3′
BDNF	Forward: 5′-GTTCGAGAGGTCTGACGACG-3′ Reverse: 5′-AGTCCGCGTCCTTATGGTTT-3′
IL-6	Cat. No. QT00098875

Quantitative Real-Time Polymerase Chain Reaction (RT-PCR)

RT-PCR was performed with the Rotor-Gene Q (Qiagen). The amplification reaction mix included Master Mix Qiagen (Qiagen QuantiNova SYBR Green Real Time-PCR Kit) and cDNA. For each sample, were made forty-five amplification cycles, in triplicate. Melting curve analysis confirmed the specificity of the amplified products. Results were analysed with the $2^{-\Delta\Delta Ct}$ method and expressed as fold change vs. control. Quantitative PCR experiments followed the MIQE guidelines. BDNF and IL-6 genes were analyzed by using specific primers purchased from Eurofin Genomics (Milan, Italy) and Qiagen (Milan, Italy) respectively. Gene expression levels were normalized with levels of a constitutively expressed gene (18S, Eurofin Genomics). Primer sequences are listed in **Table 1**.

Tissue Homogenization and Protein Extraction

Proteins were extracted from the retina samples with RIPA lysis buffer containing protease inhibitor cocktail, EDTA-free (Sigma, Inc.) by first sonicating for 20 s, and then centrifuging for 15 min at 14,000 rpm at 4°C. The supernatant was collected in new tubes and placed on ice. The protein concentration was measured using the Pierce™ Coomassie Protein Assay Kit (ThermoFisher, Monza, Italy).

Western Blot

Equal amounts of protein (30 μg) were resolved by 8–12% SDS-PAGE gels and transferred onto Hybond ECL nitrocellulose membranes (GE Healthcare, Little Chalfont, United Kingdom). Membranes were blocked for 1 h at room temperature with 5% nonfat dry milk in phosphate-buffered saline plus 0.1% Tween 20 (PBS-T) and were then probed overnight with the following appropriate primary antibodies: rabbit anti-TRAIL (1:200, ab2435; Abcam, Cambridge, United Kingdom); rabbit anti-DR5 (1:500, ab8416; Abcam Cambridge, United Kingdom); mouse anti-GFAP (1:500, ab3670; Cell Signaling Technology, Inc., Danvers, MA, United States); rabbit anti-Iba1 (1:1000, PA5-27436; Thermo Fisher Scientific Italy, Rodano, Milan, Italy); rabbit anti-TNF-α antibody (1:1000, NB600-587; Novus Biologicals, Milan, Italy); rabbit anti-IL10 antibody (1:500, 250,713; Abbiotec, San Diego, CA, United States); rabbit NOS2 (1:250, sc-651; Santa Cruz Biotechnology Inc., Santa Cruz, CA, United States); mouse anti-IL-1β (1:250, sc-52012; Santa Cruz Biotechnology Inc., Santa Cruz, CA, United States). Then, the membranes were washed with PBS-T, and probed with the appropriate horseradish peroxidase-conjugated anti-rabbit or anti-mouse IgG antibody (GENA934, GNENA931; Amersham Life Science, Buckinghamshire, United Kingdom) for 1 h at RT. Beta-Tubulin (1:500, sc5274; Santa Cruz Biotechnology Inc., Santa Cruz, CA, United States) was used as control to validate the amount of protein loaded in the gels. After washing with PBS-T, protein bands were visualized by enhanced chemiluminescence (Thermo Fisher Scientific, Milan, Italy) and scanned with the iBright FL1500 Imaging System (Thermo Fisher Scientific, Milan, Italy). Densitometric analysis of band intensity was done on immunoblots by using IMAGE J software (https://imagej.nih.gov/ij/).

Statistical Analysis

Statistical analysis was performed using GraphPad Prism Software, version 8 (GraphPad Software, Inc., San Diego, CA, United States). PERG amplitude and latency were analyzed for significance with one-way ANOVA followed by Tukey test for multiple comparisons. For single comparisons, Student's t test was applied. p values ≤ 0.05 were considered statistically significant. Data are plotted as mean ± SD.

RESULTS

Retinal Ganglion Cells Function was Ameliorated by Brimonidine TreatEment

Figure 1 shows that 72 h after I/R, RGCs function, measured with PERG, was reduced by more than 50%. This effect was significantly attenuated by brimonidine treatment. Representative PERG waveforms recorded from the eyes in each group are shown in **Figure 1A**. PERG amplitudes of control group, I/R group, and I/R plus brimonidine group were compared as shown in **Figure 1C**. The average value of control PERG amplitude was 13.8 μV in agreement with previous studies on wild type mice (Romano et al., 2020). No significant changes were observed in terms of latency in all groups (**Figure 1D**) as expected considering the short time after the injury, whereas the average PERG amplitude of I/R mice was significantly ($p < 0.05$) reduced compared to the control retina. Worth of note, the average value of PERG amplitude of I/R brimonidine–treated mice, was significantly ($p < 0.05$) higher when compared with I/R, suggesting a protection of RGC function.

Neuroprotective and Anti-inflammatory Effect of Brimonidine in I/R-Injured Mice

I/R injury significantly ($p < 0.05$) downregulated the mRNA expression of BDNF in mice retina, while treatment with brimonidine maintained BDNF mRNA levels close to the control group values, with a significant difference ($p < 0.05$) compared to I/R group (**Figure 2A**). Furthermore, I/R insult elicited significant ($p < 0.05$) increase of IL-6 mRNA levels, that was significantly ($p < 0.05$) reduced by brimonidine treatment (**Figure 2B**). To better investigate the anti-inflammatory effect of brimonidine treatment on mice retina, we analyzed different

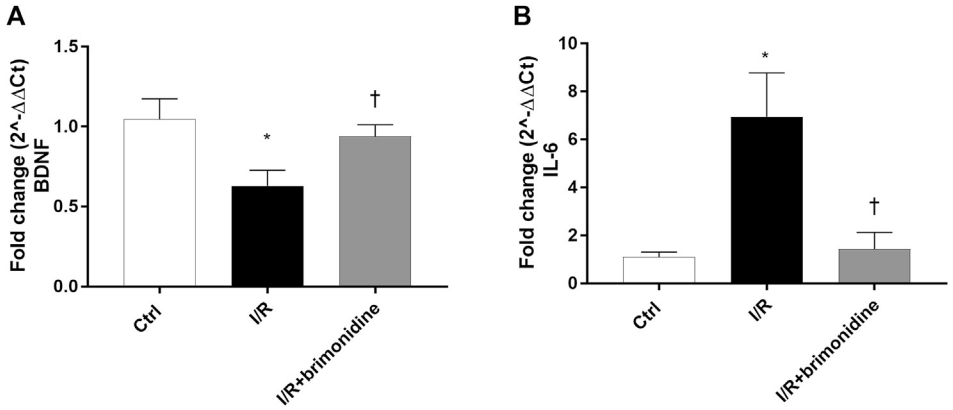

FIGURE 2 | BDNF and IL-6 mRNA expression in mice retina. Brimonidine treatment maintained BDNF **(A)** mRNA levels close to control group, in comparison to I/R injured mice. Furthermore, brimonidine reverted the up-regulation of IL-6 **(B)** elicited by I/R injury. The mRNA levels were evaluated by RT-PCR; values represent the mRNA fold changes relative to 18 S used as housekeeping gene. Values are reported as a mean ± SD ($n = 5$). One-way ANOVA analysis was performed followed by the Tukey post-hoc test. $^{*}p < 0.05$ *vs.* Ctrl; $^{\dagger}p < 0.05$ vs. I/R.

inflammatory mediators. In particular, we found that protein levels of TRAIL and its receptor DR-5, were significantly ($p < 0.05$) higher in I/R injured retina, while brimonidine treatment significantly ($p < 0.05$) reduced the expression of both proteins (**Figure 3A**). In consideration of the well-known involvement of retinal activated microglia, astrocytes and Muller glial cells in glaucoma, we assessed retinal Iba1 and GFAP expression, which were significantly ($p < 0.05$) increased after I/R injury (3-fold and 5-fold, respectively) compared to control (**Figure 3B**). The effect of brimonidine was demonstrated by the remarkable reduction of Iba1 and GFAP levels in the retinal tissue (**Figure 3B**). Furthermore, I/R insult significantly ($p < 0.05$) increased retinal levels of pro-inflammatory cytokines such as TNF-α, and reduced protein levels of IL-10, an anti-inflammatory molecule (**Figure 3B**). Protein levels of IL-1β and NOS2 were found significantly ($p < 0.05$) higher after I/R damage in comparison with control mice, and treatment with brimonidine significantly ($p < 0.05$) counteracted the expression of these proteins (**Figure 3C**).

DISCUSSION

Glaucoma is a progressive neurodegenerative disease, and the major unmet medical need in this condition is the protection of retinal ganglion cells. In fact, it is well known that pharmacological interventions intended to only lower IOP are not always effective in preventing visual field loss, even though IOP represents the major risk factor for glaucoma progression. Neuroprotective treatment for glaucoma endeavors to preserve vision by preventing the death of RGCs. Different experimental models of ocular hypertension and different electrophysiological measurements of RGCs function have shown that cell dysfunction occurs in the early phases preceding cell death (Chou et al., 2014; Porciatti, 2015). The time lag between RGC dysfunction and death may be related both on the magnitude of IOP elevation and the susceptibility to IOP stress.

In the present study we carried out retinal I/R in mouse eye, showing that ischemic insult elicited a significant impairment of RGCs function and a remarkable expression of several inflammatory markers, such as TNF and ILs, in the retina. We also found a significant glial cells activation as demonstrated by GFAP and Iba1 upregulation.

We showed that topical treatment with brimonidine preserved RGCs function and reverted the inflammatory profile elicited by I/R injury. Further, brimonidine was able to maintain physiological levels of BDNF in the retinal tissue of I/R mice group. Relevant non-clinical studies (Yoles et al., 1999) demonstrated that brimonidine has neuroprotective properties in optic nerve degeneration and retinal ischemia (Wheeler et al., 1999) even though the authors did not figure out the mechanism of that effect. It has been hypothesized that the neuroprotection of brimonidine is related to modulation of BDNF, this latter is a potent neurotrophic factor that prevent RGCs death after axotomy in the optic nerve (Mansour-Robaey et al., 1994). Gao et al. (2002) demonstrated that brimonidine was able to up-regulate the BDNF in retinal rat after 48 h from drug treatment. How the brimonidine up-regulate retinal BDNF remains to be elucidated, in fact the authors speculated that α2 receptor activation can result in the regulation of multiple signaling pathways directly or indirectly related with BDNF expression.

It has been also demonstrated that brimonidine was able to upregulate several growth factors such as BDNF, NT3 and CTNF in ischemic rat retina (Lonngren et al., 2006). Recently, it has been demonstrated (Ortin-Martinez et al., 2014) that topical brimonidine protects retinal tissue in a light-emitting diode-induced phototoxicity. More recently, Yukita et al. (2017) showed that brimonidine enhances the electrophysiological response of RGCs through the Trk-MAPK/ERK and PI3K pathways in axotomized rat eye, hypothesizing that these pathways regulate BDNF. Beside these important proofs, another inflammatory marker, called TRAIL, has been recently highlighted. TRAIL is a member of the TNF superfamily and it is constitutively

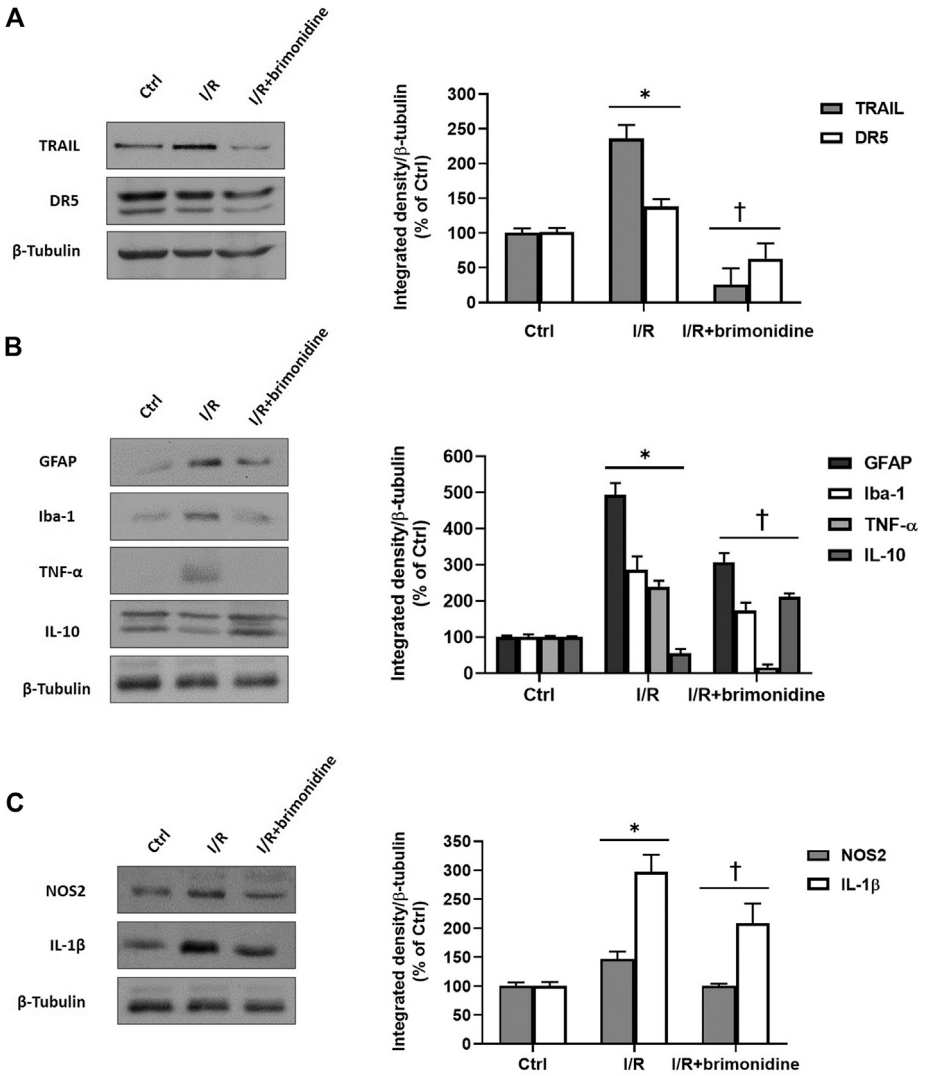

FIGURE 3 | Western Blot. **(A)** TRAIL and DR5 protein levels in control, I/R and brimonidine-treated mice retina; **(B)** GFAP, Iba-1, TNF-α and IL-10 proteins in mice retina w or w/o brimonidine; **(C)** NOS2 and IL-1β proteins in mice retina w or w/o brimonidine. Values represent protein expression relative to β-tubulin, used as housekeeping protein. Values are reported as mean ± SD ($n = 5$). One-way ANOVA analysis was performed followed by the Tukey post-hoc test. *$p < 0.05$ *vs.* Ctrl; †$p < 0.05$ vs. I/R.

expressed in retina (Lee et al., 2002). TRAIL acts mostly through the death receptor DR5, and it is a potent mediator of prominent neuronal loss induced in both chronic and acute neurodegenerative processes, including those related to brain ischemia (Martin-Villalba et al., 1999; Cantarella et al., 2014).

Upon injury, disease or inflammation, healthy neurons may get damaged eliciting an environment alteration that activate resting microglia with a release of pro-inflammatory molecules. In addition to its pro-inflammatory pattern, microglia can also stimulate an alternative activation pathway, associated with increased production of anti-inflammatory cytokines such as IL-10 and neurotrophic factors such as BDNF to promote neuronal recovery (Di Polo et al., 1998; Gallego et al., 2012; Gonzalez et al., 2014). Privation of oxygen and nutrients during ischemia, generates reactive oxygen species production leading to inflammation. I/R injury elevates the retinal expression of several inflammatory markers such as ILs, TNF-α, TRAIL and nitric oxide (NO) (Dreyer et al., 1996; Kawasaki et al., 2000; Tezel and Wax, 2000; Wang et al., 2005). These results are in accordance with the findings generated in the present study; moreover, we observed that RGCs damage elicited the upregulation of GFAP and Iba1, demonstrating glial cells activation (Mao and Yan, 2014).

In conclusion, the ocular topical brimonidine treatment showed retinal protection in an acute model of RCGs death, reducing the expression of inflammatory cytokines, enhancing the expression of BDNF, and preserving retinal function.

DATA AVAILABILITY STATEMENT

The raw data supporting the conclusion of this article will be made available by the authors, without undue reservation.

ETHICS STATEMENT

The animal study was reviewed and approved by the IACUC, University of Catania #343. All animals were treated according to the Principles for the Care and Use of Animals in Ophthalmic and Vision Research approved by the Association for Research in Vision and Ophthalmology.

AUTHOR CONTRIBUTIONS

CB, FC, GLR, and GC made substantial contributions to conception, design, and interpretation of data. FC, GLR, GD, FL, and MDT carried out formal analysis of data. CB, FL, GC, GD, CME, RR, RB, FD, and MDT wrote initial draft of the manuscript. CB, GC, CME, RR, RB, and FD reviewed the manuscript critically for important intellectual content and gave final approval of the version to be submitted.

FUNDING

GLR was supported by the PON AIM R&I 2014–2020—E66C18001260007.

REFERENCES

Bucolo, C., and Drago, F. (2011). Carbon Monoxide and the Eye: Implications for Glaucoma Therapy. *Pharmacol. Ther.* 130 (2), 191–201. doi:10.1016/j.pharmthera.2011.01.013

Bucolo, C., Platania, C. B. M., Drago, F., Bonfiglio, V., Reibaldi, M., Avitabile, T., et al. (2018). Novel Therapeutics in Glaucoma Management. *Cn.* 16 (7), 978–992. doi:10.2174/1570159X15666170915142727

Cantarella, G., Pignataro, G., Di Benedetto, G., Anzilotti, S., Vinciguerra, A., Cuomo, O., et al. (2014). Ischemic Tolerance Modulates TRAIL Expression and its Receptors and Generates a Neuroprotected Phenotype. *Cell Death Dis* 5, e1331. doi:10.1038/cddis.2014.286

Chou, T.-H., Romano, G. L., Amato, R., and Porciatti, V. (2020). Nicotinamide-Rich Diet in DBA/2J Mice Preserves Retinal Ganglion Cell Metabolic Function as Assessed by PERG Adaptation to Flicker. *Nutrients* 12 (7), 1910. doi:10.3390/nu12071910

Chou, T.-H., Tomarev, S., and Porciatti, V. (2014). Transgenic Mice Expressing Mutated Tyr437His Human Myocilin Develop Progressive Loss of Retinal Ganglion Cell Electrical Responsiveness and Axonopathy with normal Iop. *Invest. Ophthalmol. Vis. Sci.* 55 (9), 5602–5609. doi:10.1167/iovs.14-14793

Chou, T. H., Musada, G. R., Romano, G. L., Bolton, E., and Porciatti, V. (2018). Anesthetic Preconditioning as Endogenous Neuroprotection in Glaucoma. *Int. J. Mol. Sci.* 19 (1), 237. doi:10.3390/ijms19010237

Conti, B., Giannavola, C., Puglisi, G., and Giunchedi, P. (1997). Biodegradable Microspheres for the Intravitreal Administration of Acyclovir: *In Vitro*/*In Vivo* Evaluation. *Eur. J. Pharm. Sci.* 5 (Issue 5), 287–293. doi:10.1016/S0928-0987(97)00023-7

Cui, M., Wang, L., Liang, X., Ma, X., Liu, Y., Yang, M., et al. (2010). Blocking TRAIL-DR5 Signaling with Soluble DR5 Reduces Delayed Neuronal Damage after Transient Global Cerebral Ischemia. *Neurobiol. Dis.* 39 (2), 138–147. doi:10.1016/j.nbd.2010.03.018

Di Polo, A., Aigner, L. J., Dunn, R. J., Bray, G. M., and Aguayo, A. J. (1998). Prolonged Delivery of Brain-Derived Neurotrophic Factor by Adenovirus-Infected Muller Cells Temporarily Rescues Injured Retinal Ganglion Cells. *Proc. Natl. Acad. Sci.* 95 (7), 3978–3983. doi:10.1073/pnas.95.7.3978

Dibas, A., Millar, C., Al-Farra, A., and Yorio, T. (2018). Neuroprotective Effects of Psalmotoxin-1, an Acid-Sensing Ion Channel (ASIC) Inhibitor, in Ischemia Reperfusion in Mouse Eyes. *Curr. Eye Res.* 43 (7), 921–933. doi:10.1080/02713683.2018.1454478

Dreyer, E. B., Zurakowski, D., Schumer, R. A., Podos, S. M., and Lipton, S. A. (1996). Elevated Glutamate Levels in the Vitreous Body of Humans and Monkeys with Glaucoma. *Arch. Ophthalmol.* 114 (3), 299–305. doi:10.1001/archopht.1996.01100130295012

Gallego, B. I., Salazar, J. J., de Hoz, R., Rojas, B., Ramírez, A. I., Salinas-Navarro, M., et al. (2012). IOP Induces Upregulation of GFAP and MHC-II and Microglia Reactivity in Mice Retina Contralateral to Experimental Glaucoma. *J. Neuroinflammation* 9, 92. doi:10.1186/1742-2094-9-92

Ganesh, B. S., and Chintala, S. K. (2011). Inhibition of Reactive Gliosis Attenuates Excitotoxicity-Mediated Death of Retinal Ganglion Cells. *PLoS One* 6 (3), e18305. doi:10.1371/journal.pone.0018305

Gao, H., Qiao, X., Cantor, L. B., and WuDunn, D. (2002). Up-regulation of Brain-Derived Neurotrophic Factor Expression by Brimonidine in Rat Retinal Ganglion Cells. *Arch. Ophthalmol.* 120 (6), 797–803. doi:10.1001/archopht.120.6.797

González, H., Elgueta, D., Montoya, A., and Pacheco, R. (2014). Neuroimmune Regulation of Microglial Activity Involved in Neuroinflammation and Neurodegenerative Diseases. *J. Neuroimmunology* 274 (1-2), 1–13. doi:10.1016/j.jneuroim.2014.07.012

Gustavsson, C., Agardh, C.-D., Hagert, P., and Agardh, E. (2008). Inflammatory Markers in Nondiabetic and Diabetic Rat Retinas Exposed to Ischemia Followed by Reperfusion. *Retina* 28 (4), 645–652. doi:10.1097/IAE.0b013e31815ec32d

Hartsock, M. J., Cho, H., Wu, L., Chen, W.-J., Gong, J., and Duh, E. J. (2016). A Mouse Model of Retinal Ischemia-Reperfusion Injury through Elevation of Intraocular Pressure. *JoVE* 113, 54065. doi:10.3791/54065

Huang, Z., Song, L., Wang, C., Liu, J.-Q., and Chen, C. (2011). Hypoxia-ischemia Upregulates TRAIL and TRAIL Receptors in the Immature Rat Brain. *Dev. Neurosci.* 33 (6), 519–530. doi:10.1159/000334475

Kawasaki, A., Otori, Y., and Barnstable, C. J. (2000). Müller Cell protection of Rat Retinal Ganglion Cells from Glutamate and Nitric Oxide Neurotoxicity. *Invest. Ophthalmol. Vis. Sci.* 41 (11), 3444–3450. Retrieved from: https://www.ncbi.nlm.nih.gov/pubmed/11006237.

Kunimi, H., Miwa, Y., Katada, Y., Tsubota, K., and Kurihara, T. (2019). HIF Inhibitor Topotecan Has a Neuroprotective Effect in a Murine Retinal Ischemia-Reperfusion Model. *PeerJ* 7, e7849. doi:10.7717/peerj.7849

Lambert, W. S., Ruiz, L., Crish, S. D., Wheeler, L. A., and Calkins, D. J. (2011). Brimonidine Prevents Axonal and Somatic Degeneration of Retinal Ganglion Cell Neurons. *Mol. Neurodegeneration* 6 (1), 4. doi:10.1186/1750-1326-6-4

Lee, H.-o., Herndon, J. M., Barreiro, R., Griffith, T. S., and Ferguson, T. A. (2002). TRAIL: a Mechanism of Tumor Surveillance in an Immune Privileged Site. *J. Immunol.* 169 (9), 4739–4744. doi:10.4049/jimmunol.169.9.4739

Lönngren, U., Näpänkangas, U., Lafuente, M., Mayor, S., Lindqvist, N., Vidal-Sanz, M., et al. (2006). The Growth Factor Response in Ischemic Rat Retina and superior Colliculus after Brimonidine Pre-treatment. *Brain Res. Bull.* 71 (1-3), 208–218. doi:10.1016/j.brainresbull.2006.09.005

Mansour-Robaey, S., Clarke, D. B., Wang, Y. C., Bray, G. M., and Aguayo, A. J. (1994). Effects of Ocular Injury and Administration of Brain-Derived Neurotrophic Factor on Survival and Regrowth of Axotomized Retinal Ganglion Cells. *Proc. Natl. Acad. Sci.* 91 (5), 1632–1636. doi:10.1073/pnas.91.5.1632

Mao, C., and Yan, H. (2014). Roles of Elevated Intravitreal IL-1β and IL-10 Levels in Proliferative Diabetic Retinopathy. *Indian J. Ophthalmol.* 62 (6), 699–701. doi:10.4103/0301-4738.136220

Marangoz, D., Guzel, E., Eyuboglu, S., Gumusel, A., Seckin, I., Ciftci, F., et al. (2018). Comparison of the Neuroprotective Effects of Brimonidine Tartrate and Melatonin on Retinal Ganglion Cells. *Int. Ophthalmol.* 38 (6), 2553–2562. doi:10.1007/s10792-017-0768-z

Martin-Villalba, A., Herr, I., Jeremias, I., Hahne, M., Brandt, R., Vogel, J., et al. (1999). CD95 Ligand (Fas-L/apo-1l) and Tumor Necrosis Factor-Related Apoptosis-Inducing Ligand Mediate Ischemia-Induced Apoptosis in Neurons. *J. Neurosci.* 19 (10), 3809–3817Retrieved from: https://www.ncbi.nlm.nih.gov/pubmed/10234013. doi:10.1523/jneurosci.19-10-03809.1999

Nizari, S., Guo, L., Davis, B. M., Normando, E. M., Galvao, J., Turner, L. A., et al. (2016). Non-amyloidogenic Effects of α2 Adrenergic Agonists: Implications for Brimonidine-Mediated Neuroprotection. *Cel Death Dis* 7 (12), e2514. doi:10.1038/cddis.2016.397

Ortín-Martínez, A., Nadal-Nicolás, F. M., Jiménez-López, M., Alburquerque-Béjar, J. J., Nieto-López, L., García-Ayuso, D., et al. (2014). Number and Distribution of Mouse Retinal Cone Photoreceptors: Differences between an Albino (Swiss) and a Pigmented (C57/BL6) Strain. *PLoS One* 9 (7), e102392. doi:10.1371/journal.pone.0102392

Osborne, N. N., Casson, R. J., Wood, J. P. M., Chidlow, G., Graham, M., and Melena, J. (2004). Retinal Ischemia: Mechanisms of Damage and Potential Therapeutic Strategies. *Prog. Retin. Eye Res.* 23 (1), 91–147. doi:10.1016/j.preteyeres.2003.12.001

Platania, C. B. M., Di Paola, L., Leggio, G. M., Romano, G. L., Drago, F., Salomone, S., et al. (2015). Molecular Features of Interaction between VEGFA and Anti-angiogenic Drugs Used in Retinal Diseases: a Computational Approach. *Front. Pharmacol.* 6, 248. doi:10.3389/fphar.2015.00248

Porciatti, V. (2015). Electrophysiological Assessment of Retinal Ganglion Cell Function. *Exp. Eye Res.* 141, 164–170. doi:10.1016/j.exer.2015.05.008

Romano, G. L., Amato, R., Lazzara, F., Porciatti, V., Chou, T.-H., Drago, F., et al. (2020). P2X7 Receptor Antagonism Preserves Retinal Ganglion Cells in Glaucomatous Mice. *Biochem. Pharmacol.* 180, 114199. doi:10.1016/j.bcp.2020.114199

Scuteri, D., Bagetta, G., Nucci, C., Aiello, F., Cesareo, M., Tonin, P., et al. (2020). Evidence on the Neuroprotective Properties of Brimonidine in Glaucoma. *Prog. Brain Res.* 257, 155–166. doi:10.1016/bs.pbr.2020.07.008

Sena, D. F., and Lindsley, K. (2017). Neuroprotection for Treatment of Glaucoma in Adults. *Cochrane Database Syst. Rev.* 1, CD006539. doi:10.1002/14651858.CD006539.pub4

Stankowska, D. L., Dibas, A., Li, L., Zhang, W., Krishnamoorthy, V. R., Chavala, S. H., et al. (2019). Hybrid Compound SA-2 Is Neuroprotective in Animal Models of Retinal Ganglion Cell Death. *Invest. Ophthalmol. Vis. Sci.* 60 (8), 3064–3073. doi:10.1167/iovs.18-25999

Tezel, G., and Wax, M. B. (2000). Increased Production of Tumor Necrosis Factor-α by Glial Cells Exposed to Simulated Ischemia or Elevated Hydrostatic Pressure Induces Apoptosis in Cocultured Retinal Ganglion Cells. *J. Neurosci.* 20 (23), 8693–8700. Retrieved from: https://www.ncbi.nlm.nih.gov/pubmed/11102475. doi:10.1523/jneurosci.20-23-08693.2000

Ulbrich, F., Hagmann, C., Buerkle, H., Romao, C. C., Schallner, N., Goebel, U., et al. (2017). The Carbon Monoxide Releasing Molecule ALF-186 Mediates Anti-inflammatory and Neuroprotective Effects via the Soluble Guanylate Cyclase Ss1 in Rats' Retinal Ganglion Cells after Ischemia and Reperfusion Injury. *J. Neuroinflammation* 14 (1), 130. doi:10.1186/s12974-017-0905-7

Wang, X., Ng, Y.-K., and Tay, S. S.-W. (2005). Factors Contributing to Neuronal Degeneration in Retinas of Experimental Glaucomatous Rats. *J. Neurosci. Res.* 82 (5), 674–689. doi:10.1002/jnr.20679

Wei, Y., Gong, J., Yoshida, T., Eberhart, C. G., Xu, Z., Kombairaju, P., et al. (2011). Nrf2 Has a Protective Role against Neuronal and Capillary Degeneration in Retinal Ischemia-Reperfusion Injury. *Free Radic. Biol. Med.* 51 (1), 216–224. doi:10.1016/j.freeradbiomed.2011.04.026

Wheeler, L. A., Lai, R., and Woldemussie, E. (1999). From the Lab to the Clinic: Activation of an Alpha-2 Agonist Pathway Is Neuroprotective in Models of Retinal and Optic Nerve Injury. *Eur. J. Ophthalmol.* 9 (Suppl. 1), S17–S21. Retrieved from: https://www.ncbi.nlm.nih.gov/pubmed/10230601. doi:10.1177/112067219900901s09

Yoles, E., Wheeler, L. A., and Schwartz, M. (1999). Alpha2-adrenoreceptor Agonists Are Neuroprotective in a Rat Model of Optic Nerve Degeneration. *Invest. Ophthalmol. Vis. Sci.* 40 (1), 65–73. Retrieved from: https://www.ncbi.nlm.nih.gov/pubmed/9888428.

Yukita, M., Omodaka, K., Machida, S., Yasuda, M., Sato, K., Maruyama, K., et al. (2017). Brimonidine Enhances the Electrophysiological Response of Retinal Ganglion Cells through the Trk-MAPK/ERK and PI3K Pathways in Axotomized Eyes. *Curr. Eye Res.* 42 (1), 125–133. doi:10.3109/02713683.2016.1153112

Conflict of Interest: The authors declare that the research was conducted in the absence of any commercial or financial relationships that could be construed as a potential conflict of interest.

frontiers in Pharmacology

REVIEW
published: 21 July 2021
doi: 10.3389/fphar.2021.699623

Crosstalk Between Dysfunctional Mitochondria and Inflammation in Glaucomatous Neurodegeneration

Assraa Hassan Jassim[1], *Denise M. Inman*[2] *and Claire H. Mitchell*[1,3,4]*

[1]Department of Basic and Translational Science, University of Pennsylvania, Philadelphia, PA, United States, [2]Department of Pharmaceutical Sciences, North Texas Eye Research Institute, University of North Texas Health Science Center, Fort Worth, TX, United States, [3]Department of Ophthalmology, University of Pennsylvania, Philadelphia, PA, United States, [4]Department of Physiology, University of Pennsylvania, Philadelphia, PA, United States

Mitochondrial dysfunction and excessive inflammatory responses are both sufficient to induce pathology in age-dependent neurodegenerations. However, emerging evidence indicates crosstalk between damaged mitochondrial and inflammatory signaling can exacerbate issues in chronic neurodegenerations. This review discusses evidence for the interaction between mitochondrial damage and inflammation, with a focus on glaucomatous neurodegeneration, and proposes that positive feedback resulting from this crosstalk drives pathology. Mitochondrial dysfunction exacerbates inflammatory signaling in multiple ways. Damaged mitochondrial DNA is a damage-associated molecular pattern, which activates the NLRP3 inflammasome; priming and activation of the NLRP3 inflammasome, and the resulting liberation of IL-1β and IL-18 via the gasdermin D pore, is a major pathway to enhance inflammatory responses. The rise in reactive oxygen species induced by mitochondrial damage also activates inflammatory pathways, while blockage of Complex enzymes is sufficient to increase inflammatory signaling. Impaired mitophagy contributes to inflammation as the inability to turnover mitochondria in a timely manner increases levels of ROS and damaged mtDNA, with the latter likely to stimulate the cGAS-STING pathway to increase interferon signaling. Mitochondrial associated ER membrane contacts and the mitochondria-associated adaptor molecule MAVS can activate NLRP3 inflammasome signaling. In addition to dysfunctional mitochondria increasing inflammation, the corollary also occurs, with inflammation reducing mitochondrial function and ATP production; the resulting downward spiral accelerates degeneration. Evidence from several preclinical models including the DBA/2J mouse, microbead injection and transient elevation of IOP, in addition to patient data, implicates both mitochondrial damage and inflammation in glaucomatous neurodegeneration. The pressure-dependent hypoxia and the resulting metabolic vulnerability is associated with mitochondrial damage and IL-1β release. Links between mitochondrial dysfunction and inflammation can occur in retinal ganglion cells, microglia cells and astrocytes. In summary, crosstalk between damaged mitochondria and increased inflammatory signaling enhances pathology in glaucomatous neurodegeneration, with implications for other complex age-dependent neurodegenerations like Alzheimer's and Parkinson's disease.

Keywords: retinal ganglion cells, mitophagy, microglia, glaucoma, NLRP3 infammasome, astrocyte, metabolic vulnerability

OPEN ACCESS

Edited by:
Claudio Bucolo,
University of Catania, Italy

Reviewed by:
Chiara Bianca Maria Platania,
University of Catania, Italy
Julie Sanderson,
University of East Anglia,
United Kingdom

***Correspondence:**
Claire H. Mitchell
chm@upenn.edu

Specialty section:
This article was submitted to Experimental Pharmacology and Drug Discovery, a section of the journal Frontiers in Pharmacology

Received: *23 April 2021*
Accepted: *22 June 2021*
Published: *21 July 2021*

Citation:
Jassim AH, Inman DM and Mitchell CH (2021) Crosstalk Between Dysfunctional Mitochondria and Inflammation in Glaucomatous Neurodegeneration. Front. Pharmacol. 12:699623. doi: 10.3389/fphar.2021.699623

GLAUCOMATOUS NEURODEGENERATION

Glaucoma is a neurodegenerative disease that can ultimately lead to irreversible blindness (Tham et al., 2014). This etiologically complex optic neuropathy is characterized by progressive structural and functional loss of retinal ganglion cells (RGCs). Pathology is found in RGC compartments; the soma in the inner retina, the axons which form the core component of the optic nerve head (ONH) and the optic nerve (ON) relaying visual information to the brain. The retina, ONH, ON, and brain regions respond differently in glaucoma, giving rise to compartmentalized degeneration (Tamm et al., 2017). Accordingly, RGCs can execute autonomous degeneration to eliminate different parts of themselves upon insult, including the dendrites and soma within the retina itself, the axons passing through the ONH and ON, and the synapses within the brain (Whitmore et al., 2005).

Many forms of glaucoma are associated with elevated intraocular pressure (IOP). While lowering IOP is currently the primary therapy available to slow down glaucoma pathology, it does not necessarily prevent blindness, and glaucomatous neurodegeneration extends beyond IOP elevation into complex cellular pathologies. The moderate elevations in IOP associated with most common forms of glaucoma, with IOP values 21–30 mmHg, are largely asymptomatic, resulting in a delayed glaucoma diagnosis, which in turn defers therapy initiation until after RGC death has begun. Normal tension glaucoma (NTG) can occur in individuals with IOP in the normal range of 15–20 mmHg; however, patients still benefit from lowering IOP suggesting a differential pressure sensitivity to IOP among individuals (Josef et al., 2002; Whitmore et al., 2005; Calkins, 2012). Regardless of IOP levels, glaucomatous neurodegeneration involves a complex interaction between multiple factions including age, genetics, mechanical strain, hypoxia, neurochemical signaling, autophagy, cellular energetics and immune signals. In this review, we will discuss the crosstalk between mitochondrial dysfunction and inflammation during glaucoma.

MODELS OF GLAUCOMATOUS NEURODEGENERATION

Molecular mechanisms of glaucoma differ from person to person and across animal models (Fernandes et al., 2015; De Moraes et al., 2017; Pang and Clark, 2020). All models require certain compromises, there is no "perfect" model of glaucoma and thus comparing results from multiple models provides a better understanding of glaucoma pathology. As rodent models facilitate large-scale studies and genetic manipulations, they offer convenience as model systems.

The DBA/2J (D2) mouse is a well-established model of inherited glaucoma (Libby et al., 2005). IOP elevation is secondary to excessive iris pigment dispersion, which consequently blocks the trabecular meshwork and drives aqueous humor accumulation, thereby causing IOP elevation. This iris disease is linked to recessive mutations in tyrosinase-related protein 1 (Tyrp1) and glycoprotein nonmetastatic melanoma B (Gpnmb). These mutations induce melanogenesis toxicity and a subsequent inflammatory response directed at the iris, which forms structural melanosome abnormalities seen in both humans and D2 mice. IOP elevation in D2 mice is spontaneous and progressive, starting at 6 months (14–18 mmHg) and leveling off by 11 months at a value of about 28 mmHg (Mahesh et al., 2007).

Ocular hypertension (OHT) can also be induced in animal models through a variety of surgical interventions to impede aqueous outflow to some extent and hence elevate IOP. Transient IOP elevations are produced by cannulating the anterior chamber of the eye, while more sustained elevations in IOP can be produced following hypertonic saline injection into the episcleral vein, microbead injection into the anterior chamber of the eye, translimbal laser photocoagulation, or cauterization of episcleral veins. The microbead model offers advantages in the mouse given its flexibility and consistency that allows relative ease of use (Sappington et al., 2010; Samsel et al., 2011; Yang et al., 2012), although the best choice is based on the specific experimental questions being addressed. IOP can also be elevated following steroid application (Whitlock et al., 2010; Overby and Clark, 2015); systemic administration of dexamethasone has been used to demonstrate the role of dopamine and serotonin in IOP regulation (Bucolo et al., 2012; Platania et al., 2013), and has even been used to raise IOP in cows (Gerometta et al., 2004). The combined use of multiple models to confirm a specific outcome is preferable given the inherent compromises with each.

MITOCHONDRIAL DYSFUNCTION IN GLAUCOMA

Mitochondrial dysfunction has been strongly implicated in glaucomatous neurodegeneration in patients and multiple models of glaucoma (Kong et al., 2009; Munemasa et al., 2010; Lee et al., 2011; Kamel et al., 2017). Neurons are particularly sensitive to mitochondrial challenge as they require high levels of energy to maintain the electrochemical gradients necessary for optimal signal transmission, and ATP is the primary source of this energy. ATP is produced by mitochondria through oxidative phosphorylation of the electron transport chain and glycolysis (Frenzel et al., 2010). Neurons are particularly dependent on mitochondrial ATP as they have reduced levels of 6-phosphofructo-2-kinase/fructose-2, 6-bisphosphatase-3 activity (Pfkfb3), resulting in the shunting of glucose into the pentose-phosphate pathway at the expense of glycolysis (Herrero-Mendez et al., 2009; Bolanos et al., 2010). Levels of ATP were reduced in optic nerves of 6 month old D2 mice in proportion to IOP elevation, and the ability of the compound action potential to recover after oxygen-glucose deprivation was worse in mice with higher IOP levels, suggesting the rate of ATP generation was reduced in these mice to the level where it interfered with transmission of the visual signal along the optic nerve (Baltan

et al., 2010). This sensitivity occurred before changes in axon structure (Inman et al., 2006) or anterograde transport were detected (Dengler-Crish et al., 2014). Mitochondrial remodeling was found early in humans with glaucoma (Tribble et al., 2019) and the D2 glaucoma model (Cwerman-Thibault et al., 2017). Rat RGCs showed a sustained decrease in ATP production with IOP elevation that was maintained after IOP levels returned to baseline (Wu et al., 2015). These observations support the theory that mitochondrial dysfunction and ATP reduction are among the first changes that occur following IOP elevation and may be maintained.

In addition to reducing ATP levels, mitochondrial dysfunction also leads to increased generation of reactive oxygen species (ROS), and oxidative stress. Reduced cytochrome c oxidase (Complex IV) activity generates dysfunctional mitochondria, which in turn induces ROS production from the endoplasmic reticulum (ER) (Leadsham et al., 2013; Murphy, 2013). Consequently, the accumulation of dysfunctional mitochondria induces non-physiological ROS production, and the resulting oxidative stress can induce glaucomatous damage (Nita and Grzybowski, 2016). Mitochondrial dysfunction also drives the release of cytochrome c; while cytochrome c is normally involved in the electron transport chain, it can initiate a caspase protease cascade during apoptosis (Chandra et al., 2002; Calkins, 2012). Although apoptosis contributes to RGC degeneration in glaucoma, inhibition of apoptosis is not sufficient to prevent optic neuropathy (Libby et al., 2005). Overall, mitochondrial dysfunction contributes to glaucomatous neurodegeneration by decreasing levels of ATP, increasing ROS generation through reduced Complex IV generation, and defective pathogenesis.

HYPOXIA CONTRIBUTES TO MITOCHONDRIAL DYSFUNCTION

IOP elevation exerts a mechanical stretch injury and strain to the tissues of the ONH, pressing the central retinal artery as it passes through the ONH; the subsequent impairment of ocular blood flow reduces the oxygen supply to the retina and induces a localized hypoxia (Josef et al., 2002; Dai et al., 2012; Stowell et al., 2017). As oxidative phosphorylation is dependent on oxygen, prolonged hypoxia results in decreased mitochondrial ATP production. During intermittent hypoxia, the cell can switch from oxidative phosphorylation to glycolysis until oxygen level returns to normal; RGCs exposed to intermittent hypoxia are thus protected from degeneration in ischemic preconditioning (Gidday et al., 2015). In prolonged hypoxia, however, glycolysis is insufficient to meet the high energy demand of neurons. Hypoxia stimulates superoxide generation from Complex III of the electron transport chain. Superoxide is converted to H_2O_2 by superoxide dismutase, triggering hypoxia-inducible factor 1α (HIF-1α) stabilization and upregulation (Chandel et al., 1998; Chandel et al., 2000; Hamanaka and Chandel, 2009). Under physiological conditions, hypoxia is resolved by relief of oxidative stress, a metabolic switch to glycolysis, and removal of damaged mitochondria through mitophagy (Wu et al., 2016). However, prolonged hypoxia during glaucoma introduces dysfunctional feedback, impairing mitophagic induction and amplifying the accumulation of dysfunctional mitochondria that result in exacerbated oxidative stress and inflammation. Evidence exists for hypoxia at early stages of glaucoma in the D2 and microbead models (Jassim et al., 2021), and for oxidative stress (Jassim and Inman, 2019), mitochondrial dysfunction and limited mitophagy (Coughlin et al., 2015; Kleesattel et al., 2015) in glaucoma models.

Metabolic vulnerability also contributes to glaucomatous degeneration (Inman and Harun-or-Rashid, 2017; Williams et al., 2017; Harun-or-Rashid et al., 2018; Harun-or-Rashid et al., 2020). Axons rely primarily on glycolysis during glaucoma to compensate for mitochondrial dysfunction, though glycolysis is ultimately insufficient to rescue metabolic vulnerability associated with glaucoma (Jassim et al., 2021). Interestingly, the increased oxidative phosphorylation accompanying a ketogenic diet rescued RGC degeneration due, at least in part, to a reduction in inflammation (Harun-or-Rashid and Inman, 2018).

INFLAMMATION IN GLAUCOMA

Inflammation is now recognized as a key component of glaucoma neurodegeneration, and increased inflammatory signaling is one of the first changes detected in glaucoma. Activation of localized innate inflammatory signaling is of particular relevance in glaucoma, with involvement of cytokines and complement pathways clearly demonstrated at multiple stages of disease progression (Tezel, 2011; Rieck, 2013; Mac Nair and Nickells, 2015; Kamat et al., 2016; Russo et al., 2016; Bell et al., 2018). The elevated IOP in neovascular glaucoma is associated with high levels of vascular endothelial growth factor (VEGF), and anti-VEGF compounds are used for treatment (Platania et al., 2015; Slabaugh and Salim, 2017). Pro-inflammatory cytokine signaling is also evident in the models; for example, signs of inflammation are present throughout RGC compartments in D2 mice early, change with age, and drive glaucoma in the absence of elevated IOP (Wax et al., 2008; Bosco et al., 2011; Bosco et al., 2015; Wilson et al., 2015). Blocking inflammatory responses has shown promise in ameliorating glaucoma in models (Bosco et al., 2008; Howell et al., 2011; Bosco et al., 2012; Yang et al., 2016; Panchal et al., 2017; Harun-or-Rashid and Inman, 2018), emphasizing the negative impact of inflammation. Induced models of ocular hypertension and optic nerve crush models have also demonstrated inflammation (Morzaev et al., 2015), while inflammation was reported within 4–6 h in the retina after transient IOP elevation (Albalawi et al., 2017; Pronin et al., 2019). RGCs showed mechanosensitive release of multiple cytokines (Lim et al., 2016), while optic nerve head astrocytes showed rapid upregulation and release of IL-6 in response to IOP elevation (Lu et al., 2017). Glaucomatous human eyes and aqueous humor had increased markers for inflammatory cytokines and TNFα (Yang et al., 2011; Takai et al., 2012; Wang et al., 2018).

The NOD-, LRR- and pyrin domain-containing protein 3 (NLRP3) inflammasome is particularly important to

inflammatory signaling in glaucoma (Yerramothu et al., 2018). Inflammasomes are multiprotein complexes that can release pro-inflammatory cytokines and are members of Nod-Like Receptor (NLR) or pyrin and HIN domain-containing families (Guo et al., 2015). NLRs are encoded by 23 genes, but only NLRP1, NLRP2, NLRP3, NLRP6, NLRP12, and NLRC4 are capable of forming oligomeric complexes that can activate caspase-1 (CASP1) (Zheng et al., 2020). Inflammasome complexes are composed of cytosolic pattern recognition receptors (PRRs), CASP1, NLRP, and the adaptor protein apoptosis-associated speck-like protein containing a caspase activation and recruitment domain (ASP) (Swanson et al., 2019). The NLRP3 inflammasome is the most widely studied within a glaucoma context, and involvement involves both priming and activation steps. Inflammasome priming occurs through the activation of NFκB signaling (Jo et al., 2016); expression of inflammasome components is low under baseline conditions, and priming to increase expression is necessary for a response. The second step involving assembly and activation of the complex occurs in response to a stressful event; ASC fibrils are recruited and activate CASP1; the accumulation of detectable ASC clusters is a marker for inflammasome activation (Venegas et al., 2017). Activated CASP1 mediates the cleavage of IL-1β and IL-18 into releaseable forms that exit cells through gasdermin D (GSDMD), and in some cases triggering inflammatory cell death through pyroptosis (Liu et al., 2016).

Damage-associated molecular patterns (DAMPs) and pathogen-associated molecular patterns (PAMPs) are common triggers of inflammasome activation (Jo et al., 2016) and DAMPs, such as extracellular ATP and ROS can be released following cell damage (Yin et al., 2016). Extracellular ATP is a widespread mechanism to activate the NLRP3 inflammasome (Couillin et al., 2013), and ATP release is frequently triggered by mechanosensitive changes in tissues, thus providing a potential link between mechanical strain and inflammation (Ventura et al., 2019). This has particular relevance for glaucoma as ATP was elevated in the aqueous humor of humans with acute (Zhang et al., 2007) and chronic angle-closure glaucoma (Li et al., 2011). Increased levels of extracellular ATP accompanied the sustained elevation of IOP in rats following injection of hypertonic saline into episcleral veins, the Tg-MYOCY437H transgenic mouse model, and primates subjected to the laser photocoagulation of the trabecular meshwork (Lu et al., 2015). ATP release was induced from bovine retinal eyecups by elevated pressure (Reigada et al., 2008), and from ONH astrocytes subjected to moderate cyclic strain (Beckel et al., 2014). Under normal conditions, extracellular ATP is rapidly degraded by the ectonucleotidases (Reigada et al., 2005; Allard et al., 2017), but the involvement of ATP in glaucomatous RGC loss suggests that release levels can overwhelm this degradation in some cases (Sanderson et al., 2014).

A role for NLRP3 inflammasome involvement in the loss of RGCs associated with elevated IOP has been demonstrated by multiple groups. Intravitreal injection of ATP triggered significant IL-1β release and ASC speck induction in RGCs and astrocytes, supporting the detrimental effects of extracellular ATP in inflammasome activation (Pronin et al., 2019). Acute activation of NLRP1/NLRP3, CASP1, and IL-1β in mouse RGCs, astrocytes, and Müller glia was detected within 6 h of transient elevation IOP to 120 mmHg, with activation peaking after 12–24 h. Simultaneously, the pyroptotic pore was induced in the ganglion cell layer (GCL) and inner nuclear layer (INL) (Pronin et al., 2019). RGC degeneration was reduced in CASP1/CASP4 knockout (KO) and Panx1 KO mice, and by inhibition of pannexin, suggesting Panx1 activates the inflammasome following ATP release from ischemically or mechanically stressed cells. In a separate study, production of IL-1β following IOP elevation to 110 mmHg for 60 min was attributed to CASP 8 and the NLRP1/NLRP3 inflammasome (Chi et al., 2014). ASC, CASP1, and IL-1β rose in the retina following partial optic nerve crush, while RGC survival was greater when crush was performed in NLRP3 KO mice as compared to control (Puyang et al., 2016). ASC specks were increased in capillaries of contralateral normotensive eyes (Pronin et al., 2019) in addition to the hypertensive eyes; this may relate activated microglia in contralateral normotensive eyes (Rojas et al., 2014).

GLIA CONTRIBUTE TO INFLAMMATORY RESPONSES IN GLAUCOMA

Astrocytes, microglia, and Müller cells are the three major types of retinal glial cells, with the contribution by astrocytes and microglia particularly relevant to inflammation found with glaucoma (Wei et al., 2019; García-Bermúdez et al., 2021). Microglia are innate immune cells residing throughout the retina, ON, and brain. Microglia act as sensors and are one of the first responders following CNS injury, undergoing rapid morphologic and molecular changes as they become "activated" (Lannes et al., 2017). Some forms of activated microglia have beneficial actions, such as increased phagocytosis of toxic debris and release of anti-inflammatory signals (Chen and Trapp, 2016). However, microglia are a key source of inflammatory signals, with prolonged injury leading to excess production of pro-inflammatory cytokines and neurotoxic factors such as IL-6, Tumor necrotic factor-alpha (TNFα), NO, and superoxide (Rodríguez-Gómez et al., 2020). The microglia pro-inflammatory response is coupled with a decrease of the anti-inflammatory cytokine IL-10 during neurodegeneration that aggravates inflammation (Hickman et al., 2008; Heneka et al., 2013).

Reactive microglia have been localized to the retina and ON in multiple glaucoma models, and in human glaucoma (Yuan and Neufeld, 2001; Bosco et al., 2008). Microglial activation is detected in 3 month old D2 mice (Bosco et al., 2011; Bosco et al., 2012), and is predictive of subsequent neurodegeneration (Bosco et al., 2015). Early astrocyte reactivity and microglia activation were shown in the ON of D2 mice, and in rats with OHT following Translimbal Laser Photocoagulation (Son et al., 2010). Early microglial activation, NF-κB signaling, and neuroinflammation in the ONH were also reported in a cat genetic glaucoma model (Oikawa et al., 2020). Minocycline treatment and irradiation inhibited microglial activation and reduced RGC death in D2 mice (Bosco et al.,

2008; Bosco et al., 2012), supporting a negative impact of activated microglia on glaucoma progression. Recently, activated microglia were shown to induce reactive neurotoxic astrocytes by the release of interleukin-1 alpha (IL-1α), TNFα, and the classical complement component (C1q), and consequently drive RGC degeneration in the microbead glaucoma model (Liddelow et al., 2017; Guttenplan et al., 2020). Collectively, these studies provide strong evidence of the detrimental impact of activated microglia in glaucoma.

Glia-neuron interaction is emerging as a critical factor in neurodegeneration, and the pivotal role of ATP and purinergic signaling links cellular energetics to this interaction. Microglia constantly regulate and influence neurons via specialized somatic junctions (Madry et al., 2018; Cserep et al., 2020). ATP leakage from injured cells, through mechanosensitive channels, or from neuronal mitochondria through vesicular nucleotide transporter (vNUT) channels enriched at microglia-neuron contact sites is sensed by P2Y12 receptors on microglia, triggering process extension and migration toward the injured sites (Koizumi et al., 2013; Cserep et al., 2020). Whether P2Y12 receptors play a direct role in microglial surveillance, or potentiate the activity of THIK-1 potassium channels as recently suggested (Madry et al., 2018), P2Y12 receptor stimulation by ATP clearly contributes to surveillance. Stimulation of the P2X7 receptor has also been implicated in microglial phagocytosis and degradation (Campagno and Mitchell, 2021), an effect which may have particular impact in aging cells. Inhibition of the P2X7 receptor was shown to reduce microglia activation in D2 mice (Romano et al., 2020), suggesting a key role for the receptor in the inflammatory response in glaucoma. The P2X7 receptor also induces a rise in ROS (Bartlett et al., 2013; Munoz et al., 2017); whether this provides a pathway to link mitochondria with inflammation in glaucoma remains to be determined.

Optic nerve head astrocytes are also implicated in the link between mechanical strain and inflammation. Stretch and swelling of ONH astrocytes led to the release of ATP through pannexin hemichannels (Beckel et al., 2014). Stimulation of this released ATP through pannexins was implicated in the priming of the NLRP3 inflammasome, with increased expression of IL-1β, NLRP3 and caspase1 (Albalawi et al., 2017). Transient elevation of IOP led to a similar priming and release of IL-6 from optic nerve head astrocytes as well as ganglion cells (Lu et al., 2017).

Signaling from neurons back to glia also contributes to the link between mitochondrial dysfunction and inflammation in glaucoma. For example, fragmented and damaged mitochondria are found in activated microglia as a result of increased mitochondrial fission (Joshi et al., 2019). These damaged mitochondria are released into extracellular space, inducing an innate immune response by targeting adjacent astrocytes can also release dysfunctional mitochondria (Joshi et al., 2019). The resulting positive feedback can accelerate neuroinflammation. Inhibiting mitochondrial fission with heptapeptide P110, which inhibits binding of Drp1 to the mitochondrial receptor Fis1, reduced fragmentation and mitochondrial release from microglia, lessened astrocyte activation, and protected neurons from innate immune attack. Extracellular mitochondria can also signal between glia and neurons; functional mitochondria were found to be protective, while damaged mitochondria communicated pathology following stroke (Hayakawa et al., 2016). This suggests that the health of released mitochondrial may influence pathology in glaucoma.

Astrocytes are generally considered to protect neurons from oxidative stress, specifically via glutathione precursor synthesis, as they have strong antioxidant defenses regulated by the transcription factor Nrf2, a master regulator of redox homeostasis (Shih et al., 2003; Himori et al., 2013; Ghosh et al., 2020). However, reactive astrocytes contribute to neuronal degeneration in mice with sustained IOP elevation and reduction of their activated status rescued neuronal function (Guttenplan et al., 2020; Sterling et al., 2020). The decline in astrocytic antioxidant defense mechanisms and the increase in astrocytic reactivity during glaucoma occur simultaneously with mitochondria dysfunction, contributing to ROS accumulation and oxidative stress that enhance glaucoma progression (Tezel, 2006; Jassim and Inman, 2019). Intravitreal injection of neurotoxic astrocytes did not induce RGC neurodegeneration in the absence of neuronal injury, suggesting that injury and glial activation are required for neurodegeneration (Guttenplan et al., 2020).

CROSSTALK BETWEEN MITOCHONDRIAL DYSFUNCTION AND INFLAMMATION

Glaucoma is a complicated and progressive neurodegenerative disease where multiple pathways contribute to pathogenesis. Given that mitochondrial dysfunction and inflammation are two of the most potent influences, emerging evidence for interactions between these two factors has relevance for the etiology of glaucoma.

MITOCHONDRIAL DYSFUNCTION CONTRIBUTES TO INFLAMMATION

Mitochondrial dysfunction and inflammation are interdependent processes. Inhibition of Complex I by rotenone, or of Complex III by antimycin A, in bone marrow-derived macrophages and in primary mouse microglia (Ferger et al., 2010) induced oxidative stress, activated microglia, activated the NLRP3 inflammasome, and increased IL-1β production, resulting in pyroptosis (Zhou et al., 2011). Rotenone administration concomitant with inhibition of autophagy caused the accumulation of damaged mitochondria with downstream IL-1β production (Nakahira et al., 2011; Zhou et al., 2011). Furthermore, subcutaneous injections of rotenone in rats increased IL-1β within the hypothalamus, confirming that mitochondria may act upstream of inflammation (Yi et al., 2007). Antioxidant treatment using sulforaphane (SFN) significantly prevented RGC death and suppressed microglia and inflammasome activation in the transient IOP (110 mmHg for 1 h) model in

rats suggesting that ROS production is upstream of inflammation (Gong et al., 2019). Collectively, studies indicate that mitochondria play an important role in regulating inflammation and that mitochondrial dysfunction is upstream of inflammation (Misawa et al., 2013); this has yet to be determined in glaucoma, however.

Mitochondrial dysfunction may contribute to various forms of inflammatory signaling, with links to NLRP3 inflammasome signaling of particular relevance for neurodegeneration (Nakahira et al., 2011; Zhou et al., 2011; Gurung et al., 2015). Many of these pathological links are related to excess levels of ROS; while ROS are mainly generated as byproducts of oxidative phosphorylation, excess production or inadequate removal of ROS can result in oxidative stress. Accumulated ROS results in the opening of the mitochondrial permeability transition pores that facilitates release of ROS (Kozlov et al., 2017) and damaged mtDNA (Shimada et al., 2012) into the cytoplasm; both substances act as DAMPs to induce NLRP3 inflammasome activation and pyroptosis (Latz et al., 2013; Yin et al., 2016; Bai et al., 2018). As ROS are short-lived and act only across short distances (Veal et al., 2007), positional shifts that recruit NLRP3 towards mitochondria enhance the ability of ROS to increase NLRP3 activation. During activation of the NLRP3 inflammasome, NLRP3 redistributes from the ER to mitochondria-associated ER membranes (MAMSs), where NLRP3 connects to the ASC adaptor protein, localized on the mitochondria, enabling inflammasome assembly (Green et al., 2011; Misawa et al., 2013; Heid et al., 2013; Misawa et al., 2013). Although the approximation of NLRP3-ASC at MAMs is important for NLRP3 activation, other factors also contribute. For example, the mitochondria-associated adaptor molecule, MAVS, is required for NLRP3 inflammasome activity as it promotes the recruitment of NLRP3 to the mitochondria and the subsequent IL-1β production *in vivo* (Subramanian et al., 2013), however, this has yet to be shown in glaucoma.

Mitochondrial dysfunction can also lead to increased inflammatory signaling through the cyclic GMP–AMP synthase (cGAS)–stimulator of interferon genes (STING) pathway (West and Shadel, 2017). The enzyme cGAS detects cytoplasmic DNA, including mtDNA leaked from damaged mitochondria. The reaction product cGAMP activates STING (Gao et al., 2013), which in turn stimulates TANK-binding kinase 1 (TBK1), to promote homodimerization of interferon regulatory factor 3 (IRF3) (Tanaka and Chen, 2012). Nuclear translocation of this phosphorylated IRF3 enhances expression of interferons and an enlarged interferon response (Hopfner and Hornung, 2020). mtDNA released across the plasma membrane can activate cGAS- or TLR9-dependent interferon signaling, thus communicating the mitochondrial damage to neighboring cells (West and Shadel, 2017). Components of the cGAS-STING pathway have been identified in the murine retina (Tang et al., 2019). In retinal microvascular endothelial cells, mtDNA in the cytosol stimulated the cGAS-STING pathway and nuclear translocation of IRF3 (Guo et al., 2020). Mutations in optineurin (OPTN) associated with primary open angle glaucoma (E50K) reduced the phosphorylation of IRF3 and IFNα/β release assays in response to poly (I:C) stimulation of TLR3 (O'loughlin et al., 2020). Further investigations into the interactions between mtDNA releases as a result of mitochondrial dysfunction in glaucoma and the cGAS-STING-pathway promise to be informative.

Patients with glaucoma have an increased risk of developing Alzheimer's disease (Moon et al., 2018), and deposits of Alzheimer's disease marker amyloid beta (Aβ) accumulate in RGCs following IOP elevation (Guo et al., 2007), suggesting interactions between Aβ and mitochondria may contribute to the pathology. Aβ accumulation in mitochondrial cristae negatively impacted mitochondrial function. The translocase of the outer membrane (TOM) machinery moves Aβ across the membrane, allowing it to accumulate (Petersen et al., 2008). Human neuroblastoma cells also internalized extracellularly applied Aβ that colocalized with mitochondrial markers (Petersen et al., 2008). While Aβ accumulation has been shown in several glaucoma models (Mckinnon et al., 2002; Guo et al., 2007; Wilson et al., 2016), the accumulation of Aβ in neuronal and glial mitochondria has yet to be shown in glaucoma as it has in the brain.

Mitochondrial dysfunction drives metabolic vulnerability in the D2 mouse ON and retina, which in turn triggers AMP-activated protein kinase activation (AMPK), a cellular energy sensor, to activate NF-κB signaling and increase expression of inflammatory genes (Harun-or-Rashid and Inman, 2018). Treatment with a ketogenic diet reduces inflammation, possibly while inhibiting AMPK activation while also meeting the high neuronal energy demand. Expression of AMPK was upregulated in the RGC of mice with elevated IOP following injection of magnetic microbeads (Belforte et al., 2018). Additional exploration of the role of AMPK in connecting mitochondrial damage with inflammation in glaucoma is likely to be fruitful, given the role of AMPK in systemic disease, and the therapeutic potential of manipulating this pathway in ocular disease (Powell et al., 2020).

HYPOXIA CONTRIBUTES TO INFLAMMATION

The NLRP3 inflammasome can also link hypoxia to inflammation and suggests how hypoxia, and thus increased IOP in glaucoma, can contribute to inflammation. Chronic intermittent hypoxia increased levels of cytokines associated with M1-and M2-like microglial activation states (Snyder et al., 2017). In retinal pigmented epithelial cells, hypoxia induced expression of NLRP3 and IL-1β in a pathway dependent upon ATP release and the P2Y12 receptor, and inflammasome activation killed cells only under hypoxic conditions (Doktor et al., 2018). HIF-1α is implicated in hypoxia-mediated inflammasome priming as blockage of HIF-1α reduced expression of NLRP3, caspase 1 and IL-1β and of pyroptotic death in a stroke model (Jiang et al., 2020).

Similar connections between hypoxia and inflammation may occur in glaucoma. IOP elevation and hypoxia can induce pyroptosis by activating CASP8; CASP8 triggered NF-kB translocation to induce HIF-1α signaling, which in turn

facilitated NLRP12/NLRP3/NLRC4 assembly and activation *in vitro* and *in vivo* (Chen et al., 2020). Hypoxia also induces CASP1 release, NLRP3 inflammasome activation, IL-1β release, GSDMD cleavage, and pyroptosis (Watanabe et al., 2020). NLRP3 deficiency and CASP1 blockade significantly inhibited hypoxia-induced IL-1β release from macrophages. Indeed, genetic deletion of GSDMD, CASP8, or NLRP12 reduced RGC death after the transient IOP elevation model, where IOP was elevated to 110 mmHg for 90 min (Chen et al., 2020).

Given that oxidative phosphorylation in the mitochondria is dependent on oxygen and is the main source of cellular ATP in addition to glycolysis, hypoxia and glucose deprivation decrease ATP, facilitate K^+ efflux, and induce IL-1β release. Interestingly, these effects were reversible by K^+ efflux inhibition and K_{ATP} channel blockers in macrophages (Watanabe et al., 2020). The NLRP3 inflammasome acts as an intercellular sensor of ATP decrease induced by glucose and oxygen deprivation (Watanabe et al., 2020). Of relevance were studies showing that K_{ATP} channel opener KR-31378 protected RGCs from ischemic damage (Bucolo et al., 2018). In retinal vessels activation of the K_{ATP} channel dramatically increased the vasotoxicity of P2X7 receptor stimulation through elevation of calcium and increased oxidative stress (Shibata et al., 2018); such interactions may increase hypoxic challenge in glaucoma given the propensity of excess P2X7 receptor stimulation with elevated IOP (Mitchell et al., 2008). Further studies will be necessary to elucidate the precise link between the K_{ATP} channel, the P2X7 receptor, NLRP3 inflammasome activation and cellular metabolic crisis in glia vs. neurons during glaucoma.

There is also considerable evidence of a role for carbon monoxide in glaucoma (Bucolo and Drago, 2011). A carbon monoxide-releasing molecule, CORM-3, produced a dose-dependent reduction in IOP in the rabbit eye (Stagni et al., 2009). The precise mechanism remains to be determined, although action on KCa^{2+} channels in the outflow pathway has been suggested (Dong et al., 2007; Bucolo and Drago, 2011). Recent work in a model of hind limb ischemia suggests the stabilization of HIF-1α by hemeoxygenase 1 (Hmox1) is at least partially attributed to carbon monoxide, with carbon monoxide a by-product of the breakdown of heme by of Hmox1 (Dunn et al., 2021). In addition, carbon monoxide regulates mitochondrial biogenesis and gene expression, suggesting multiple protective sites in glaucoma are possible (Cherry and Piantadosi, 2015).

DYSFUNCTIONAL MITOPHAGY EXACERBATES INFLAMMATION

Mitophagy helps regulate mitochondria homeostasis by getting rid of dysfunctional mitochondria, and the inhibition of mitophagy results in the accumulation of damaged mitochondria and sometimes inflammasome activation. Mitophagy is driven by PTEN-induced putative kinase 1 (PINK1) and parkin (E3 ubiquitin ligase), where the cytoplasmic Parkin is recruited to the mitochondria to interact with PINK1 on the outer mitochondrial membrane and target dysfunctional mitochondria (Palikaras et al., 2018). Adaptor proteins such as p62 and OPTN join poly-ubiquitinated strands to light chain 3 (LC3), initiating autophagy. The mitochondrial accumulation of LC3 puncta after treatment with Complex I inhibitor rotenone indicate mitophagy is increased by mitochondrial stress (Zhou et al., 2011).

Impaired mitophagy has been implicated in glaucoma by multiple observations. Elevation of IOP in rats increased damaged mitochondria, parkin and optineurin levels in RGCs, while function was partially restored following overexpression of Parkin (Dai et al., 2018). Impaired mitophagy was also implicated in the myelinated ON axons of D2 mice by a rise in fragmented and damaged mitochondria without changes in PINK or parkin levels (Coughlin et al., 2015). These mice also displayed increased mitochondria within autophagosomes in distal and proximal axons (Kleesattel et al., 2015). An autosomal dominant form of normal tension glaucoma is linked to mutations in OPTN (Rezaie et al., 2002), and mice transgenic for E50K, the most common mutation in normal tension glaucoma, showed altered mitophagy and mitochondrial fission (Shim et al., 2016). Pink1 and Parkin KO mice both showed an increase in increased inflammation, but antioxidants abolished CASP1 activation, suggesting a role for ROS in the inflammation associated with impaired mitophagy (Sliter et al., 2018). These findings emphasize the importance of mitophagy in combating inflammation, and justify further examination in glaucoma.

NLRP3 inflammasome activation is negatively regulated by mitophagy (Latz et al., 2013; Lai et al., 2018). Autophagic proteins contribute to an anti-inflammatory response by regulating NLRP3 inflammation and mitochondrial integrity (Nakahira et al., 2011). Inflammasome activation recruits autophagy adaptor protein p62 to the mitochondria. Measuring LC3 and p62 puncta is a method of quantifying autophagy/mitophagy. LC3 and p62 enable mitophagy, thereby inhibiting NLRP3 inflammasome activation and preventing excessive IL-1β production by degrading damaged mitochondria in macrophages (Zhong et al., 2016). Depletion of genes for autophagic proteins (specifically LC3B and Beclin 1), and the use of mitophagy inhibitors (such as 3-methyladenine), promoted CASP1 activation, secretion of IL-1β and IL-18, and the accumulation of dysfunctional mitochondria in macrophages and *in vivo* (Nakahira et al., 2011). In addition, stimulation by lipopolysaccharide (LPS) or ATP led to the release of mtDNA and ROS into the cytosol and inflammasome-dependent secretion of IL-1β and IL-18 (Nakahira et al., 2011).

Mitophagy can limit apoptosis by reducing the accumulation of dysfunctional mitochondrial and oxidative stress, and facilitate the metabolic switch of the cell from oxidative phosphorylation to glycolysis to adapt to the hypoxia reported during glaucoma (Liu et al., 2012a; Jassim and Inman, 2019). Hypoxia-induced mitophagy occurs through the action of a mitochondrial associated membrane protein, FUNDC1, as reported *in vitro* (Liu et al., 2012a; Chen et al., 2016; Wu et al., 2016). During hypoxia, oxidative phosphorylation is expected to decline and glycolysis would become the primary ATP source in the

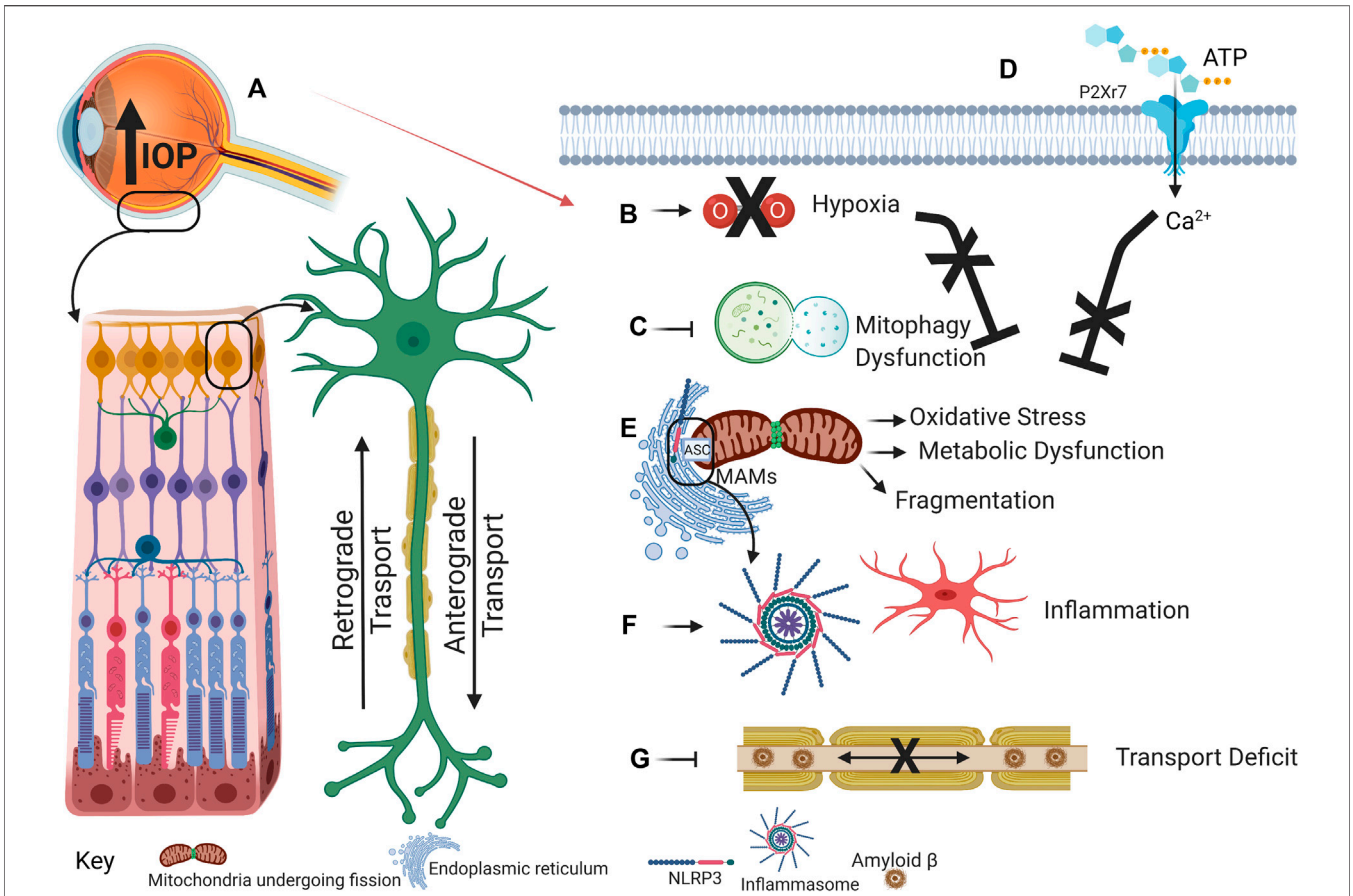

FIGURE 1 | This schematic illustrates the proposed cascade of events that link the increased intraocular pressure of glaucoma to mitochondrial dysfunction and the NLRP3 inflammasome. **(A)** Intraocular pressure increases as a result of perturbed aqueous humor outflow in the eye. **(B)** Intraocular pressure increase prevents efficient blood flow to the eye, resulting in hypoxia/ischemia. During physiological conditions, hypoxia induces mitophagy to eliminate dysfunctional mitochondrial accumulation. **(C)** However, during glaucoma, hypoxia-induced mitophagy may be inhibited. Concomitantly, external ATP binds to and opens the cation-selective P2X7R **(D)**. Ca^{2+} influx can stimulate mitochondrial dysfunction that will induce inflammation, activated microglia, and cytokine release. **(E)** Dysfunctional and fragmented mitochondria accumulate, thus promoting oxidative stress and metabolic vulnerability. Oxidative stress induces inflammasome assembly and activation as NLRP3, localized at the ER, comes into proximity to the ASC, localized at the mitochondria, on MAMs. **(F)** Inflammasome activation releases cytokines that establish a positive feedback loop to exacerbate further inflammatory response. **(G)** Aβ that has been demonstrated in mitochondria can also accumulate in axons, thereby inducing axon transport deficit that further contributes to glaucoma progression. Created with Biorender.com

TABLE 1 | Pharmacological targets to ameliorate mitochondrial dysfunction and inflammation.

Protein/ Gene	Biological target	Targeted pathway	Scientific evidence	References
HIF-1α	Nucleus	Hypoxic response	Hypoxia preconditioniong rescue RGC during glaucoma	Gidday et al. (2015)
K_{ATP} channel	Membrane	Metabolic function	K_{ATP} blockers reduced IL-1β release; K_{ATP} opener protected RGCs from ischemic damage	Watanabe et al. (2020)
HCAR1	Mitochondria	L-lactate receptor	Ketogenic diet stimulates HCAR1 to inhibit NLRP3 inflammasome in glaucoma	Harun-or-Rashid and Inman, (2018)
AMPK	Cytosol	Energy sensor protein kinase	Ketogenic diet reduced metabolic vulnerability and AMPK-induceds inflammation	Harun-or-Rashid and Inman, (2018)
cGAS	Interferon in cytosol	STING pathway	Detects leaked mtDNA	Sintim et al. (2019)
Aβ	Cytosol, mitochondria	Biomarker of neurodegeneration, impaired clearance	Accumulates in mitochondria cristae, blocks function; induces pro-inflamatory cytokines via P2X7R	Chiozzi et al., 2019, Petersen et al., 2008

cell. Although high reliance on glycolysis was recently shown in glaucomatous D2 ON (Jassim et al., 2021), degeneration proceeds, indicating that ATP produced from glycolysis is insufficient to meet the high energy demand of axons during glaucoma.

INFLAMMATION CAN INDUCE MITOCHONDRIAL DYSFUNCTION

While there is considerable evidence suggesting that dysfunctional mitochondria can trigger inflammation, the opposite is also true, with inflammation inducing mitochondrial dysfunction. Inflammasome assembly can impair organelle function and integrity; for example, activation of the NLRP3 inflammasome in macrophages reduced cytoplasmic levels of ATP and mitochondrial function (Heid et al., 2013). Inflammation in LPS-treated macrophages resulted in a metabolic shift from oxidative phosphorylation to glycolysis (Mills et al., 2016). Interestingly, Complex II and Complex I oxidation, and decreased NAD^+ were necessary for the pro-inflammatory response observed in these macrophages. TNFα induced a oxidative phosphorylation deficit in a mouse hippocampal cell line, suggesting a detrimental impact of inflammation on mitochondrial function (Doll et al., 2015). In optic nerve head astrocytes, stimulation of TLR3 led to a transfer of cellular ATP from cytoplasmic to extracellular compartments, suggesting inflammatory signaling can strain cellular energetics in relationship to glaucoma (Beckel et al., 2018).

Microglia metabolic reprogramming has been found in response to inflammation as cells switch between oxidative phosphorylation and glycolytic metabolism (Lauro and Limatola, 2020). Activated microglia have dysfunctional mitochondria and they switch to glycolysis to compensate for ATP loss. Stimulation of microglial cells with LPS reduced mitochondrial oxygen consumption, ATP production and oxidative phosphorylation, while increasing glycolysis (Volobouева et al., 2013). In addition, mitochondrial dysfunction in microglia propagates mitochondrial dysfunction in neurons and can block some of the alternative response triggered by IL-4 (Ferger et al., 2010). As this IL-4 response can reduce inflammation, mitochondrial dysfunction might contribute to the pathological changes found in activated microglia in glaucoma. Whether inflammatory stimuli lead microglia in the retina to switch from oxidative phosphorylation to glycolysis should be investigated given central role of microglia in glaucomatous pathogenesis.

DISCUSSION AND FUTURE DIRECTIONS

The strong support for mitochondrial dysfunction and inflammation in glaucoma outlined above, combined with growing evidence for crosstalk between mitochondrial dysfunction and inflammation in other neurodegenerations, suggests interaction between these processes contributes to the expanding pathogenesis in glaucoma patients. We propose that IOP elevation initiates hypoxia that contributes to mitochondrial dysfunction, oxidative stress, impaired mitophagy and inflammation and that these processes are exacerbated by interactions between inflammation and mitochondrial dysfunctional (**Figure 1**).

While expanding evidence for both inflammation and mitochondrial dysfunction supports crosstalk, the degree of interaction may be influenced by several key factors, and suggests several key targets for intervention (**Table 1**). For example, the microglial activation state is expected to have a considerable impact on waste accumulation and impaired mitophagy (Campagno and Mitchell, 2021). Investigations into compartmentalized interaction between ASC, NLRP3 and oxidative stress in soma, axon, and synapse has particular relevance for glaucoma given the ganglion cell architecture. The ability of inflammation to disrupt mitochondrial signaling remains largely undetermined in glaucoma. The development of *in vitro* models using neurons, astrocytes, and microglia, in addition to the use and development of mouse glaucoma models with knockout technologies, will enable us to resolve these questions.

AUTHOR CONTRIBUTIONS

CHM, DMI, and AHJ conceived, outlined, and wrote the review.

FUNDING

This work was supported by R01 EY013434 (CHM) R01 EY015537 (CHM) R01 EY026662 (DMI) and T32NS043126 (AHJ).

REFERENCES

Albalawi, F., Lu, W., Beckel, J. M., Lim, J. C., Mccaughey, S. A., and Mitchell, C. H. (2017). The P2X7 Receptor Primes IL-1β and the NLRP3 Inflammasome in Astrocytes Exposed to Mechanical Strain. *Front Cel Neurosci* 11, 227. doi:10.3389/fncel.2017.00227

Allard, B., Longhi, M. S., Robson, S. C., and Stagg, J. (2017). The Ectonucleotidases CD39 and CD73: Novel Checkpoint Inhibitor Targets. *Immunol. Rev.* 276, 121–144. doi:10.1111/imr.12528

Bai, H., Yang, B., Yu, W., Xiao, Y., Yu, D., and Zhang, Q. (2018). Cathepsin B Links Oxidative Stress to the Activation of NLRP3 Inflammasome. *Exp. Cel Res.* 362, 180–187. doi:10.1016/j.yexcr.2017.11.015

Baltan, S., Inman, D. M., Danilov, C. A., Morrison, R. S., Calkins, D. J., and Horner, P. J. (2010). Metabolic Vulnerability Disposes Retinal Ganglion Cell Axons to Dysfunction in a Model of Glaucomatous Degeneration. *J. Neurosci.* 30, 5644–5652. doi:10.1523/jneurosci.5956-09.2010

Bartlett, R., Yerbury, J. J., and Sluyter, R. (2013). P2X7 Receptor Activation Induces Reactive Oxygen Species Formation and Cell Death in Murine EOC13 Microglia. *Mediators Inflamm.* 2013, 271813. doi:10.1155/2013/271813

Beckel, J. M., Argall, A. J., Lim, J. C., Xia, J., Lu, W., Coffey, E. E., et al. (2014). Mechanosensitive Release of Adenosine 5′-triphosphate through Pannexin Channels and Mechanosensitive Upregulation of Pannexin Channels in Optic Nerve Head Astrocytes: A Mechanism for Purinergic Involvement in Chronic Strain. *Glia* 62, 1486–1501. doi:10.1002/glia.22695

Beckel, J. M., Gomez, N. M., Lu, W., Campagno, K. E., Nabet, B., Albalawi, F., et al. (2018). Stimulation of TLR3 Triggers Release of Lysosomal ATP in Astrocytes and Epithelial Cells that Requires TRPML1 Channels. *Sci. Rep.* 8, 5726. doi:10.1038/s41598-018-23877-3

Belforte, N., Vargas, J. L. C., and Polo, A. D. (2018). Metabolic Stress in Glaucoma Engages Early Activation of the Energy Biosensor Adenosine Monophosphate-Activated Protein Kinase Leading to Neuronal Dysfunction. *Ann. Eye Sci.* 3.AB015

Bell, K., Und Hohenstein-Blaul, N. V T., Teister, J., and Grus, F. (2018). Modulation of the Immune System for the Treatment of Glaucoma. *Cn* 16, 942–958. doi:10.2174/1570159x15666170720094529

Bolaños, J. P., Almeida, A., and Moncada, S. (2010). Glycolysis: a Bioenergetic or a Survival Pathway? *Trends Biochem. Sci.* 35, 145–149. doi:10.1016/j.tibs.2009.10.006

Bosco, A., Crish, S. D., Steele, M. R., Romero, C. O., Inman, D. M., Horner, P. J., et al. (2012). Early Reduction of Microglia Activation by Irradiation in a Model of Chronic Glaucoma. *PLoS One* 7. doi:10.1371/journal.pone.0043602

Bosco, A., Inman, D. M., Steele, M. R., Wu, G., Soto, I., Marsh-Armstrong, N., et al. (2008). Reduced Retina Microglial Activation and Improved Optic Nerve Integrity with Minocycline Treatment in the DBA/2J Mouse Model of Glaucoma. *Invest. Ophthalmol. Vis. Sci.* 49, 1437–1446. doi:10.1167/iovs.07-1337

Bosco, A., Romero, C. O., Breen, K. T., Chagovetz, A. A., Steele, M. R., Ambati, B. K., et al. (2015). Neurodegeneration Severity Can Be Predicted from Early Microglia Alterations Monitored *In Vivo* in a Mouse Model of Chronic Glaucoma. *Dis. Model. Mech.* 8, 443–455. doi:10.1242/dmm.018788

Bosco, A., Steele, M. R., and Vetter, M. L. (2011). Early Microglia Activation in a Mouse Model of Chronic Glaucoma. *J. Comp. Neurol.* 519, 599–620. doi:10.1002/cne.22516

Bucolo, C., and Drago, F. (2011). Carbon Monoxide and the Eye: Implications for Glaucoma Therapy. *Pharmacol. Ther.* 130, 191–201. doi:10.1016/j.pharmthera.2011.01.013

Bucolo, C., Leggio, G. M., Maltese, A., Castorina, A., D'Agata, V., Drago, F., et al. (2012). Dopamine-3 Receptor Modulates Intraocular Pressure: Implications for Glaucoma. *Biochem. Pharmacol.* 83, 680–686. doi:10.1016/j.bcp.2011.11.031

Bucolo, C., Platania, C. B. M., Drago, F., Bonfiglio, V., Reibaldi, M., Avitabile, T., et al. (2018). Novel Therapeutics in Glaucoma Management. *Cn* 16, 978–992. doi:10.2174/1570159x15666170915142727

Calkins, D. J. (2012). Critical Pathogenic Events Underlying Progression of Neurodegeneration in Glaucoma. *Prog. Retin. Eye Res.* 31, 702–719. doi:10.1016/j.preteyeres.2012.07.001

Campagno, K. E., and Mitchell, C. H. (2021). The P2X7 Receptor in Microglial Cells Modulates the Endolysosomal axis, Autophagy and Phagocytosis. *Front. Cell Neurosci.* 15, 66. doi:10.3389/fncel.2021.645244

Chandel, N. S., Maltepe, E., Goldwasser, E., Mathieu, C., Simon, M., and Schumacker, P. (1998). Mitochondrial Reactive Oxygen Species Trigger Hypoxia- Induced Transcription. *PNAS* 95.

Chandel, N. S., Mcclintock, D. S., Feliciano, C. E., Wood, T. M., Melendez, J. A., Rodriguez, A. M., et al. (2000). Reactive Oxygen Species Generated at Mitochondrial Complex III Stabilize Hypoxia-Inducible Factor-1α during Hypoxia. *J. Biol. Chem.* 275, 25130–25138. doi:10.1074/jbc.m001914200

Chandra, D., Liu, J.-W., and Tang, D. G. (2002). Early Mitochondrial Activation and Cytochrome C Up-Regulation during Apoptosis. *J. Biol. Chem.* 277, 50842–50854. doi:10.1074/jbc.m207622200

Chen, H., Deng, Y., Gan, X., Li, Y., Huang, W., Lu, L., et al. (2020). NLRP12 Collaborates with NLRP3 and NLRC4 to Promote Pyroptosis Inducing Ganglion Cell Death of Acute Glaucoma. *Mol. Neurodegener* 15, 26. doi:10.1186/s13024-020-00372-w

Chen, M., Chen, Z., Wang, Y., Tan, Z., Zhu, C., Li, Y., et al. (2016). Mitophagy Receptor FUNDC1 Regulates Mitochondrial Dynamics and Mitophagy. *Autophagy* 12, 689–702. doi:10.1080/15548627.2016.1151580

Chen, Z., and Trapp, B. D. (2016). Microglia and Neuroprotection. *J. Neurochem.* 136 (136 Suppl. l), 10–17. doi:10.1111/jnc.13062

Cherry, A. D., and Piantadosi, C. A. (2015). Regulation of Mitochondrial Biogenesis and its Intersection with Inflammatory Responses. *Antioxid. Redox Signaling* 22, 965–976. doi:10.1089/ars.2014.6200

Chi, W., Li, F., Chen, H., Wang, Y., Zhu, Y., Yang, X., et al. (2014). Caspase-8 Promotes NLRP1/NLRP3 Inflammasome Activation and IL-1 Production in Acute Glaucoma. *Proc. Natl. Acad. Sci.* 111, 11181–11186. doi:10.1073/pnas.1402819111

Chiozzi, P., Sarti, A. C., Sanz, J. M., Giuliani, A. L., Adinolfi, E., Vultaggio-Poma, V., et al. (2019). Amyloid β-dependent Mitochondrial Toxicity in Mouse Microglia Requires P2X7 Receptor Expression and Is Prevented by Nimodipine. *Scientific Rep.* 9, 6475. doi:10.1038/s41598-019-42931-2

Coughlin, L., Morrison, R. S., Horner, P. J., and Inman, D. M. (2015). Mitochondrial Morphology Differences and Mitophagy Deficit in Murine Glaucomatous Optic Nerve. *Invest. Ophthalmol. Vis. Sci.* 56, 1437–1446. doi:10.1167/iovs.14-16126

Cserép, C., Pósfai, B., Lénárt, N., Fekete, R., László, Z. I., Lele, Z., et al. (2020). Microglia Monitor and Protect Neuronal Function through Specialized Somatic Purinergic Junctions. *Science* 367, 528–537. doi:10.1126/science.aax6752

Cwerman-Thibault, H., Lechauve, C., Augustin, S., Roussel, D., Reboussin, É., Mohammad, A., et al. (2017). Neuroglobin Can Prevent or Reverse Glaucomatous Progression in DBA/2J Mice. *Mol. Ther. - Methods Clin. Development* 5, 200–220. doi:10.1016/j.omtm.2017.04.008

Dai, C., Khaw, P. T., Yin, Z. Q., Li, D., Raisman, G., and Li, Y. (2012). Structural Basis of Glaucoma: the Fortified Astrocytes of the Optic Nerve Head Are the Target of Raised Intraocular Pressure. *Glia* 60, 13–28. doi:10.1002/glia.21242

Dai, Y., Hu, X., and Sun, X. (2018). Overexpression of Parkin Protects Retinal Ganglion Cells in Experimental Glaucoma. *Cell Death Dis* 9, 88. doi:10.1038/s41419-017-0146-9

De Moraes, C. G., Liebmann, J. M., and Levin, L. A. (2017). Detection and Measurement of Clinically Meaningful Visual Field Progression in Clinical Trials for Glaucoma. *Prog. Retin. Eye Res.* 56, 107–147. doi:10.1016/j.preteyeres.2016.10.001

Dengler-Crish, C. M., Smith, M. A., Inman, D. M., Wilson, G. N., Young, J. W., and Crish, S. D. (2014). Anterograde Transport Blockade Precedes Deficits in Retrograde Transport in the Visual Projection of the DBA/2J Mouse Model of Glaucoma. *Front. Neurosci.* 8, 290. doi:10.3389/fnins.2014.00290

Doktor, F., Prager, P., Wiedemann, P., Kohen, L., Bringmann, A., and Hollborn, M. (2018). Hypoxic Expression of NLRP3 and VEGF in Cultured Retinal Pigment Epithelial Cells: Contribution of P2Y2 Receptor Signaling. *Purinergic Signal.* 14, 471–484. doi:10.1007/s11302-018-9631-6

Doll, D. N., Rellick, S. L., Barr, T. L., Ren, X., and Simpkins, J. W. (2015). Rapid Mitochondrial Dysfunction Mediates TNF-Alpha-Induced Neurotoxicity. *J. Neurochem.* 132, 443–451. doi:10.1111/jnc.13008

Dong, D.-L., Zhang, Y., Lin, D.-H., Chen, J., Patschan, S., Goligorsky, M. S., et al. (2007). Carbon Monoxide Stimulates the Ca2+-Activated Big Conductance K Channels in Cultured Human Endothelial Cells. *Hypertension* 50, 643–651. doi:10.1161/hypertensionaha.107.096057

Dunn, L. L., Kong, S. M. Y., Tumanov, S., Chen, W., Cantley, J., Ayer, A., et al. (2021). Hmox1 (Heme Oxygenase-1) Protects against Ischemia-Mediated Injury via Stabilization of HIF-1α (Hypoxia-Inducible Factor-1α). *Arteriosclerosis, Thromb. Vasc. Biol.* 41, 317–330.

Ferger, A. I., Campanelli, L., Reimer, V., Muth, K. N., Merdian, I., Ludolph, A. C., et al. (2010). Effects of Mitochondrial Dysfunction on the Immunological Properties of Microglia. *J. Neuroinflammation* 7, 45. doi:10.1186/1742-2094-7-45

Fernandes, K. A., Harder, J. M., Williams, P. A., Rausch, R. L., Kiernan, A. E., Nair, K. S., et al. (2015). Using Genetic Mouse Models to Gain Insight into Glaucoma: Past Results and Future Possibilities. *Exp. Eye Res.* 141, 42–56. doi:10.1016/j.exer.2015.06.019

Frenzel, M., Rommelspacher, H., Sugawa, M. D., and Dencher, N. A. (2010). Ageing Alters the Supramolecular Architecture of OxPhos Complexes in Rat Brain Cortex. *Exp. Gerontol.* 45, 563–572. doi:10.1016/j.exger.2010.02.003

Gao, D., Wu, J., Wu, Y.-T., Du, F., Aroh, C., Yan, N., et al. (2013). Cyclic GMP-AMP Synthase Is an Innate Immune Sensor of HIV and Other Retroviruses. *Science* 341, 903–906. doi:10.1126/science.1240933

García-Bermúdez, M. Y., Freude, K. K., Mouhammad, Z. A., Van Wijngaarden, P., Martin, K. K., and Kolko, M.. (2021). Glial Cells in Glaucoma: Friends, Foes, and Potential Therapeutic Targets. *Front. Neurol.* 12, 624983. doi:10.3389/fneur.2021.624983

Gerometta, R., Podos, S. M., Candia, O. A., Wu, B., Malgor, L. A., Mittag, T., et al. (2004). Steroid-induced Ocular Hypertension in normal Cattle. *Arch. Ophthalmol.* 122, 1492–1497. doi:10.1001/archopht.122.10.1492

Ghosh, A. K., Rao, V. R., Wisniewski, V. J., Zigrossi, A. D., Floss, J., Koulen, P., et al. (2020). Differential Activation of Glioprotective Intracellular Signaling Pathways in Primary Optic Nerve Head Astrocytes after Treatment with Different Classes of Antioxidants. *Antioxid. (Basel) 9*.

Gidday, J. M., Zhang, L., Chiang, C.-W., and Zhu, Y. (2015). Enhanced Retinal Ganglion Cell Survival in Glaucoma by Hypoxic Postconditioning after Disease Onset. *Neurotherapeutics* 12, 502–514. doi:10.1007/s13311-014-0330-x

Gombault, A., Baron, L., and Couillin, I. (2012). ATP Release and Purinergic Signaling in NLRP3 Inflammasome Activation. *Front. Immunol.* 3, 414. doi:10.3389/fimmu.2012.00414

Gong, Y., Cao, X., Gong, L., and Li, W. (2019). Sulforaphane Alleviates Retinal Ganglion Cell Death and Inflammation by Suppressing NLRP3 Inflammasome Activation in a Rat Model of Retinal Ischemia/reperfusion Injury. *Int. J. Immunopathol Pharmacol.* 33, 2058738419861777. doi:10.1177/2058738419861777

Green, D. R., Galluzzi, L., and Kroemer, G. (2011). Mitochondria and the Autophagy-Inflammation-Cell Death axis in Organismal Aging. *Science* 333, 1109–1112. doi:10.1126/science.1201940

Guo, H., Callaway, J. B., and Ting, J. P.-Y. (2015). Inflammasomes: Mechanism of Action, Role in Disease, and Therapeutics. *Nat. Med.* 21, 677–687. doi:10.1038/nm.3893

Guo, L., Salt, T. E., Luong, V., Wood, N., Cheung, W., Maass, A., et al. (2007). Targeting Amyloid-Beta in Glaucoma Treatment. *Proc. Natl. Acad. Sci.* 104, 13444–13449. doi:10.1073/pnas.0703707104

Guo, Y., Gu, R., Gan, D., Hu, F., Li, G., and Xu, G. (2020). Mitochondrial DNA Drives Noncanonical Inflammation Activation via cGAS–STING Signaling Pathway in Retinal Microvascular Endothelial Cells. *Cell Commun. Signaling* 18, 172. doi:10.1186/s12964-020-00637-3

Gurung, P., Lukens, J. R., and Kanneganti, T.-D. (2015). Mitochondria: Diversity in the Regulation of the NLRP3 Inflammasome. *Trends Mol. Med.* 21, 193–201. doi:10.1016/j.molmed.2014.11.008

Guttenplan, K. A., Stafford, B. K., El-Danaf, R. N., Adler, D. I., Münch, A. E., Weigel, M. K., et al. (2020). Neurotoxic Reactive Astrocytes Drive Neuronal Death after Retinal Injury. *Cel Rep.* 31, 107776. doi:10.1016/j.celrep.2020.107776

Hamanaka, R. B., and Chandel, N. S. (2009). Mitochondrial Reactive Oxygen Species Regulate Hypoxic Signaling. *Curr. Opin. Cel Biol.* 21, 894–899. doi:10.1016/j.ceb.2009.08.005

Harun-or-Rashid, M., Pappenhagen, N., Zubricky, R., Coughlin, L., Jassim, A. H., and Inman, D. M. (2020). MCT2 Overexpression Rescues Metabolic Vulnerability and Protects Retinal Ganglion Cells in Two Models of Glaucoma. *Neurobiol. Dis.*, 141, 104944. doi:10.1016/j.nbd.2020.104944

Harun-or-Rashid, M., and Inman, D. M. (2018). Reduced AMPK Activation and Increased HCAR Activation Drive Anti-inflammatory Response and Neuroprotection in Glaucoma. *J. Neuroinflammation* 15, 313. doi:10.1186/s12974-018-1346-7

Harun-or-Rashid, M., Pappenhagen, N., Palmer, P. G., Smith, M. A., Gevorgyan, V., Wilson, G. N., et al. (2018). Structural and Functional Rescue of Chronic Metabolically Stressed Optic Nerves through Respiration. *J. Neurosci.* 38, 5122–5139. doi:10.1523/jneurosci.3652-17.2018

Hayakawa, K., Esposito, E., Wang, X., Terasaki, Y., Liu, Y., Xing, C., et al. (2016). Transfer of Mitochondria from Astrocytes to Neurons after Stroke. *Nature* 535, 551–555. doi:10.1038/nature18928

Heid, M. E., Keyel, P. A., Kamga, C., Shiva, S., Watkins, S. C., and Salter, R. D. (2013). Mitochondrial Reactive Oxygen Species Induces NLRP3-dependent Lysosomal Damage and Inflammasome Activation. *J.I.* 191, 5230–5238. doi:10.4049/jimmunol.1301490

Heneka, M. T., Kummer, M. P., Stutz, A., Delekate, A., Schwartz, S., Vieira-Saecker, A., et al. (2013). NLRP3 Is Activated in Alzheimer's Disease and Contributes to Pathology in APP/PS1 Mice. *Nature* 493, 674–678. doi:10.1038/nature11729

Herrero-Mendez, A., Almeida, A., Fernández, E., Maestre, C., Moncada, S., and Bolaños, J. P. (2009). The Bioenergetic and Antioxidant Status of Neurons Is Controlled by Continuous Degradation of a Key Glycolytic Enzyme by APC/C-Cdh1. *Nat. Cel Biol* 11, 747–752. doi:10.1038/ncb1881

Hickman, S. E., Allison, E. K., and El Khoury, J. (2008). Microglial Dysfunction and Defective -Amyloid Clearance Pathways in Aging Alzheimer's Disease Mice. *J. Neurosci.* 28, 8354–8360. doi:10.1523/jneurosci.0616-08.2008

Himori, N., Yamamoto, K., Maruyama, K., Ryu, M., Taguchi, K., Yamamoto, M., et al. (2013). Critical Role of Nrf2 in Oxidative Stress-Induced Retinal Ganglion Cell Death. *J. Neurochem.* 127, 669–680. doi:10.1111/jnc.12325

Hopfner, K.-P., and Hornung, V. (2020). Molecular Mechanisms and Cellular Functions of cGAS-STING Signalling. *Nat. Rev. Mol. Cel Biol* 21, 501–521. doi:10.1038/s41580-020-0244-x

Howell, G. R., Macalinao, D. G., Sousa, G. L., Walden, M., Soto, I., Kneeland, S. C., et al. (2011). Molecular Clustering Identifies Complement and Endothelin Induction as Early Events in a Mouse Model of Glaucoma. *J. Clin. Invest.* 121, 1429–1444. doi:10.1172/jci44646

Inman, D. M., and Harun-or-Rashid, M. (2017). Metabolic Vulnerability in the Neurodegenerative Disease Glaucoma. *Front. Neurosci.* 11, 146. doi:10.3389/fnins.2017.00146

Inman, D. M., Sappington, R. M., Horner, P. J., and Calkins, D. J. (2006). Quantitative Correlation of Optic Nerve Pathology with Ocular Pressure and Corneal Thickness in the DBA/2 Mouse Model of Glaucoma. *Invest. Ophthalmol. Vis. Sci.* 47, 986–996. doi:10.1167/iovs.05-0925

Jassim, A. H. C. L., Coughlin, M., Kang, P. T., Chen, Y.-R., and Inman, D. M. (2019). Higher Reliance on Glycolysis Limits Glycolytic Responsiveness in Degenerating Glaucomatous Optic Nerve. *Mol. Neurobiol.* 56, 7097–7112. doi:10.1007/s12035-019-1576-4

Jassim, A. H., Fan, Y., Pappenhagen, N., Nsiah, N. Y., and Inman, D. M. (2021). Oxidative Stress and Hypoxia Modifies Mitochondrial Homeostasis during Glaucoma. *Antioxid. Redox Signal.* [Epub ahead of print]. doi:10.1089/ars.2020.8180

Jassim, and Inman (2019). Evidence of Hypoxic Glial Cells in a Model of Ocular Hypertension. *Invest. Ophthalmol. Vis. Sci.* 60, 1–15.

Jiang, Q., Geng, X., Warren, J., Eugene Paul Cosky, E., Kaura, S., Stone, C., et al. (2020). Hypoxia Inducible Factor-1α (HIF-1α) Mediates NLRP3 Inflammasome-Dependent-Pyroptotic and Apoptotic Cell Death Following Ischemic Stroke. *Neuroscience* 448, 126–139. doi:10.1016/j.neuroscience.2020.09.036

Jo, E.-K., Kim, J. K., Shin, D.-M., and Sasakawa, C. (2016). Molecular Mechanisms Regulating NLRP3 Inflammasome Activation. *Cell Mol Immunol* 13, 148–159. doi:10.1038/cmi.2015.95

Josef, F., Selim Orgul, V. P. C., Orzalesi, Nicola., GuNterKrieglstein, K., and Serra, Luis. Metzner. (2002). J.-P.R., Einar Stefa!NssonThe Impact of Ocular Blood Flow in Glaucoma. *Prog. Retin. Eye Res.* 21, 359–393.

Joshi, A. U., Minhas, P. S., Liddelow, S. A., Haileselassie, B., Andreasson, K. I., Dorn, G. W., 2nd, et al. (2019). Fragmented Mitochondria Released from Microglia Trigger A1 Astrocytic Response and Propagate Inflammatory Neurodegeneration. *Nat. Neurosci.* 22, 1635–1648. doi:10.1038/s41593-019-0486-0

Kamat, S. S., Gregory, M. S., and Pasquale, L. R. (2016). The Role of the Immune System in Glaucoma: Bridging the Divide between Immune Mechanisms in Experimental Glaucoma and the Human Disease. *Semin. Ophthalmol.* 31, 147–154. doi:10.3109/08820538.2015.1114858

Kamel, K., Farrell, M., and O'brien, C. (2017). Mitochondrial Dysfunction in Ocular Disease: Focus on Glaucoma. *Mitochondrion* 35, 44–53. doi:10.1016/j.mito.2017.05.004

Kleesattel, D., Crish, S. D., and Inman, D. M. (2015). Decreased Energy Capacity and Increased Autophagic Activity in Optic Nerve Axons with Defective Anterograde Transport. *Invest. Ophthalmol. Vis. Sci.* 56, 8215–8227. doi:10.1167/iovs.15-17885

Koizumi, S., Ohsawa, K., Inoue, K., and Kohsaka, S. (2013). Purinergic Receptors in Microglia: Functional Modal Shifts of Microglia Mediated by P2 and P1 Receptors. *Glia* 61, 47–54. doi:10.1002/glia.22358

Kong, G. Y. X., Van Bergen, N. J., Trounce, I. A., and Crowston, J. G. (2009). Mitochondrial Dysfunction and Glaucoma. *J. Glaucoma* 18, 93–100. doi:10.1097/ijg.0b013e318181284f

Kozlov, A. V., Lancaster, J. R., Jr., Meszaros, A. T., and Weidinger, A. (2017). Mitochondria-meditated Pathways of Organ Failure upon Inflammation. *Redox Biol.* 13, 170–181. doi:10.1016/j.redox.2017.05.017

Lai, M., Yao, H., Shah, S. Z. A., Wu, W., Wang, D., Zhao, Y., et al. (2018). The NLRP3-Caspase 1 Inflammasome Negatively Regulates Autophagy via TLR4-TRIF in Prion Peptide-Infected Microglia. *Front. Aging Neurosci.* 10, 116. doi:10.3389/fnagi.2018.00116

Lannes, N., Eppler, E., Etemad, S., Yotovski, P., and Filgueira, L. (2017). Microglia at center Stage: a Comprehensive Review about the Versatile and Unique Residential Macrophages of the central Nervous System. *Oncotarget* 8, 114393–114413. doi:10.18632/oncotarget.23106

Latz, E., Xiao, T. S., and Stutz, A. (2013). Activation and Regulation of the Inflammasomes. *Nat. Rev. Immunol.* 13, 397–411. doi:10.1038/nri3452

Lauro, C., and Limatola, C. (2020). Metabolic Reprograming of Microglia in the Regulation of the Innate Inflammatory Response. *Front. Immunol.* 11, 493. doi:10.3389/fimmu.2020.00493

Leadsham, J. E., Sanders, G., Giannaki, S., Bastow, E. L., Hutton, R., Naeimi, W. R., et al. (2013). Loss of Cytochrome C Oxidase Promotes RAS-dependent ROS Production from the ER Resident NADPH Oxidase, Yno1p, in Yeast. *Cel Metab.* 18, 279–286. doi:10.1016/j.cmet.2013.07.005

Lee, S., Van Bergen, N. J., Kong, G. Y., Chrysostomou, V., Waugh, H. S., O'Neill, E. C., et al. (2011). Mitochondrial Dysfunction in Glaucoma and Emerging Bioenergetic Therapies. *Exp. Eye Res.* 93, 204–212. doi:10.1016/j.exer.2010.07.015

Li, A., Zhang, X., Zheng, D., Ge, J., Laties, A. M., and Mitchell, C. H. (2011). Sustained Elevation of Extracellular ATP in Aqueous Humor from Humans with Primary Chronic Angle-Closure Glaucoma. *Exp. Eye Res.* 93, 528–533. doi:10.1016/j.exer.2011.06.020

Libby, R. T., Anderson, M. G., Pang, I.-H., Robinson, Z. H., Savinova, O. V., Cosma, I. M., et al. (2005). Inherited Glaucoma in DBA/2J Mice: Pertinent Disease Features for Studying the Neurodegeneration. *Vis. Neurosci.* 22, 637–648. doi:10.1017/s0952523805225130

Liddelow, S. A., Guttenplan, K. A., Clarke, L. E., Bennett, F. C., Bohlen, C. J., Schirmer, L., et al. (2017). Neurotoxic Reactive Astrocytes Are Induced by Activated Microglia. *Nature* 541, 481–487. doi:10.1038/nature21029

Lim, J. C., Lu, W., Beckel, J. M., and Mitchell, C. H. (2016). Neuronal Release of Cytokine IL-3 Triggered by Mechanosensitive Autostimulation of the P2X7 Receptor Is Neuroprotective. *Front. Cel Neurosci* 10, 270. doi:10.3389/fncel.2016.00270

Liu, L., Feng, D., Chen, G., Chen, M., Zheng, Q., Song, P., et al. (2012a). Mitochondrial Outer-Membrane Protein FUNDC1 Mediates Hypoxia-Induced Mitophagy in Mammalian Cells. *Nat. Cel Biol* 14, 177–185. doi:10.1038/ncb2422

Liu, X., Zhang, Z., Ruan, J., Pan, Y., Magupalli, V. G., Wu, H., et al. (2016). Inflammasome-activated Gasdermin D Causes Pyroptosis by Forming Membrane Pores. *Nature* 535, 153–158. doi:10.1038/nature18629

Lu, W., Albalawi, F., Beckel, J. M., Lim, J. C., Laties, A. M., and Mitchell, C. H. (2017). The P2X7 Receptor Links Mechanical Strain to Cytokine IL-6 Up-Regulation and Release in Neurons and Astrocytes. *J. Neurochem.* 141, 436–448. doi:10.1111/jnc.13998

Lu, W., Hu, H., Sévigny, J., Gabelt, B. A. T., Kaufman, P. L., Johnson, E. C., et al. (2015). Rat, Mouse, and Primate Models of Chronic Glaucoma Show Sustained Elevation of Extracellular ATP and Altered Purinergic Signaling in the Posterior Eye. *Invest. Ophthalmol. Vis. Sci.* 56, 3075–3083. doi:10.1167/iovs.14-15891

Mac Nair, C. E., and Nickells, R. W. (2015). Neuroinflammation in Glaucoma and Optic Nerve Damage. *Prog. Mol. Biol. Transl Sci.* 134, 343–363. doi:10.1016/bs.pmbts.2015.06.010

Madry, C., Kyrargyri, V., Arancibia-Cárcamo, I. L., Jolivet, R., Kohsaka, S., Bryan, R. M., et al. (2018). Microglial Ramification, Surveillance, and Interleukin-1β Release Are Regulated by the Two-Pore Domain K+ Channel THIK-1. *Neuron* 97, 299–312. doi:10.1016/j.neuron.2017.12.002

Mahesh, N., Maher, S., and Vittorio, P. (2007). IOP-dependent Retinal Ganglion Cell Dysfunction in Glaucomatous DBA/2J Mice. *Invest. Ophthalmol. Vis. Sci.* 48, 4573–4579.

Mckinnon, S. J., Lehman, D. M., Kerrigan-Baumrind, L. A., Merges, C. A., Pease, M. E., Kerrigan, D. F., et al. (2002). Caspase Activation and Amyloid Precursor Protein Cleavage in Rat Ocular Hypertension. *Invest. Ophthalmol. Vis. Sci.* 43, 1077–1087.

Mills, E. L., Kelly, B., Logan, A., Costa, A. S. H., Varma, M., Bryant, C. E., et al. (2016). Succinate Dehydrogenase Supports Metabolic Repurposing of Mitochondria to Drive Inflammatory Macrophages. *Cell* 167, 457–470. doi:10.1016/j.cell.2016.08.064

Misawa, T., Takahama, M., Kozaki, T., Lee, H., Zou, J., Saitoh, T., et al. (2013). Microtubule-driven Spatial Arrangement of Mitochondria Promotes Activation of the NLRP3 Inflammasome. *Nat. Immunol.* 14, 454–460. doi:10.1038/ni.2550

Mitchell, C. H., Lu, W., Hu, H., Zhang, X., Reigada, D., and Zhang, M. (2008). The P2X7 Receptor in Retinal Ganglion Cells: A Neuronal Model of Pressure-Induced Damage and protection by a Shifting Purinergic Balance. *Purinergic Signal.* 4, 313–321. doi:10.1007/s11302-008-9125-z

Moon, J. Y., Kim, H. J., Park, Y. H., Park, T. K., Park, E. C., Kim, C. Y., et al. (2018). Association between Open-Angle Glaucoma and the Risks of Alzheimer's and Parkinson's Diseases in South Korea: A 10-year Nationwide Cohort Study. *Sci. Rep.* 8, 11161. doi:10.1038/s41598-018-29557-6

Morzaev, D., Nicholson, J. D., Caspi, T., Weiss, S., Hochhauser, E., and Goldenberg-Cohen, N. (2015). Toll-like Receptor-4 Knockout Mice Are More Resistant to Optic Nerve Crush Damage Than Wild-type Mice. *Clin. Exp. Ophthalmol* 43, 655–665. doi:10.1111/ceo.12521

Munemasa, Y., Kitaoka, Y., Kuribayashi, J., and Ueno, S. (2010). Modulation of Mitochondria in the Axon and Soma of Retinal Ganglion Cells in a Rat Glaucoma Model. *J. Neurochem.* 115, 1508–1519. doi:10.1111/j.1471-4159.2010.07057.x

Munoz, F. M., Gao, R., Tian, Y., Henstenburg, B. A., Barrett, J. E., and Hu, H. (2017). Neuronal P2X7 Receptor-Induced Reactive Oxygen Species Production Contributes to Nociceptive Behavior in Mice. *Scientific Rep.* 7, 3539. doi:10.1038/s41598-017-03813-7

Murphy, M. P. (2013). Mitochondrial Dysfunction Indirectly Elevates ROS Production by the Endoplasmic Reticulum. *Cel Metab.* 18, 145–146. doi:10.1016/j.cmet.2013.07.006

Nakahira, K., Haspel, J. A., Rathinam, V. A. K., Lee, S.-J., Dolinay, T., Lam, H. C., et al. (2011). Autophagy Proteins Regulate Innate Immune Responses by Inhibiting the Release of Mitochondrial DNA Mediated by the NALP3 Inflammasome. *Nat. Immunol.* 12, 222–230. doi:10.1038/ni.1980

Nita, M., and Grzybowski, A. (2016). The Role of the Reactive Oxygen Species and Oxidative Stress in the Pathomechanism of the Age-Related Ocular Diseases and Other Pathologies of the Anterior and Posterior Eye Segments in Adults. *Oxidative Med. Cell. longevity* 2016, 3164734. doi:10.1155/2016/3164734

O'loughlin, T., Kruppa, A. J., Ribeiro, A. L. R., Edgar, J. R., Ghannam, A., Smith, A. M., et al. (2020). OPTN Recruitment to a Golgi-Proximal Compartment Regulates Immune Signalling and Cytokine Secretion. *J. Cel Sci.* 133. doi:10.1242/jcs.239822

Oikawa, K., Ver Hoeve, J. N., Teixeira, L. B. C., Snyder, K. C., Kiland, J. A., Ellinwood, N. M., et al. (2020). Sub-region-Specific Optic Nerve Head Glial Activation in Glaucoma. *Mol. Neurobiol.* 57, 2620–2638. doi:10.1007/s12035-020-01910-9

Overby, D. R., and Clark, A. F. (2015). Animal Models of Glucocorticoid-Induced Glaucoma. *Exp. Eye Res.* 141, 15–22. doi:10.1016/j.exer.2015.06.002

Palikaras, K., Lionaki, E., and Tavernarakis, N. (2018). Mechanisms of Mitophagy in Cellular Homeostasis, Physiology and Pathology. *Nat. Cel Biol* 20, 1013–1022. doi:10.1038/s41556-018-0176-2

Panchal, S. S., Patidar, R. K., Jha, A. B., Allam, A. A., Ajarem, J., and Butani, S. B. (2017). Anti-Inflammatory and Antioxidative Stress Effects of Oryzanol in Glaucomatous Rabbits. *J. Ophthalmol.* 2017, 1468716. doi:10.1155/2017/1468716

Pang, I.-H., and Clark, A. F. (2020). Inducible Rodent Models of Glaucoma. *Prog. Retin. Eye Res.* 75, 100799. doi:10.1016/j.preteyeres.2019.100799

Petersen, C. A. H., Alikhani, N., Behbahani, H., Wiehager, B., Pavlov, P. F., Alafuzoff, I., et al. (2008). The Amyloid Beta-Peptide Is Imported into Mitochondria via the TOM Import Machinery and Localized to Mitochondrial Cristae. *Proc. Natl. Acad. Sci. U S A.* 105, 13145–13150. doi:10.1073/pnas.0806192105

Platania, C. B., Di Paola, L., Leggio, G. M., Romano, G. L., Drago, F., Salomone, S., et al. (2015). Molecular Features of Interaction between VEGFA and Anti-angiogenic Drugs Used in Retinal Diseases: a Computational Approach. *Front. Pharmacol.* 6, 248. doi:10.3389/fphar.2015.00248

Platania, C. B. M., Leggio, G. M., Drago, F., Salomone, S., and Bucolo, C. (2013). Regulation of Intraocular Pressure in Mice: Structural Analysis of Dopaminergic and Serotonergic Systems in Response to Cabergoline. *Biochem. Pharmacol.* 86, 1347–1356. doi:10.1016/j.bcp.2013.08.010

Powell, S., Irnaten, M., and Brien, C. J.. (2020). A Review of Metabolic Sensors in Glaucoma. *Trends Ophthalmol.* 3.

Pronin, A., Pham, D., An, W., Dvoriantchikova, G., Reshetnikova, G., Qiao, J., et al. (2019). Inflammasome Activation Induces Pyroptosis in the Retina Exposed to Ocular Hypertension Injury. *Front. Mol. Neurosci.* 12, 36. doi:10.3389/fnmol.2019.00036

Puyang, Z., Feng, L., Chen, H., Liang, P., Troy, J. B., and Liu, X. (2016). Retinal Ganglion Cell Loss Is Delayed Following Optic Nerve Crush in NLRP3 Knockout Mice. *Sci. Rep.* 6, 20998. doi:10.1038/srep20998

Reigada, D., Lu, W., Zhang, M., and Mitchell, C. H. (2008). Elevated Pressure Triggers a Physiological Release of ATP from the Retina: Possible Role for Pannexin Hemichannels. *Neuroscience* 157, 396–404. doi:10.1016/j.neuroscience.2008.08.036

Reigada, D., Lu, W., Zhang, X., Friedman, C., Pendrak, K., Mcglinn, A., et al. (2005). Degradation of Extracellular ATP by the Retinal Pigment Epithelium. *Am. J. Physiology-Cell Physiol.* 289, C617–C624. doi:10.1152/ajpcell.00542.2004

Rezaie, T., Child, A., Hitchings, R., Brice, G., Miller, L., Coca-Prados, M., et al. (2002). Adult-onset Primary Open-Angle Glaucoma Caused by Mutations in Optineurin. *Science* 295, 1077–1079. doi:10.1126/science.1066901

Rieck, J. (2013). The Pathogenesis of Glaucoma in the Interplay with the Immune System. *Invest. Ophthalmol. Vis. Sci.* 54, 2393–2409. doi:10.1167/iovs.12-9781

Rodríguez-Gómez, J. A., Kavanagh, E., Engskog-Vlachos, P., Engskog, M. K. R., Herrera, A. J., Espinosa-Oliva, A. M., et al. (2020). Agents of the CNS Pro-inflammatory Response. *Cells* 9.

Rojas, B., Gallego, B. I., Ramírez, A. I., Salazar, J. J., De Hoz, R., Valiente-Soriano, F. J., et al. (2014). Microglia in Mouse Retina Contralateral to Experimental Glaucoma Exhibit Multiple Signs of Activation in All Retinal Layers. *J. neuroinflammation* 11, 133. doi:10.1186/1742-2094-11-133

Romano, G. L., Amato, R., Lazzara, F., Porciatti, V., Chou, T.-H., Drago, F., et al. (2020). P2X7 Receptor Antagonism Preserves Retinal Ganglion Cells in Glaucomatous Mice. *Biochem. Pharmacol.* 180, 114199. doi:10.1016/j.bcp.2020.114199

Russo, R., Varano, G. P., Adornetto, A., Nucci, C., Corasaniti, M. T., Bagetta, G., et al. (2016). Retinal Ganglion Cell Death in Glaucoma: Exploring the Role of Neuroinflammation. *Eur. J. Pharmacol.* 787, 134–142. doi:10.1016/j.ejphar.2016.03.064

Samsel, P. A., Kisiswa, L., Erichsen, J. T., Cross, S. D., and Morgan, J. E. (2011). A Novel Method for the Induction of Experimental Glaucoma Using Magnetic Microspheres. *Invest. Ophthalmol. Vis. Sci.* 52, 1671–1675. doi:10.1167/iovs.09-3921

Sanderson, J., Dartt, D. A., Trinkaus-Randall, V., Pintor, J., Civan, M. M., Delamere, N. A., et al. (2014). Purines in the Eye: Recent Evidence for the Physiological and Pathological Role of Purines in the RPE, Retinal Neurons, Astrocytes, Müller Cells, Lens, Trabecular Meshwork, Cornea and Lacrimal Gland. *Exp. Eye Res.* 127, 270–279. doi:10.1016/j.exer.2014.08.009

Sappington, R. M., Carlson, B. J., Crish, S. D., and Calkins, D. J. (2010). The Microbead Occlusion Model: a Paradigm for Induced Ocular Hypertension in Rats and Mice. *Invest. Ophthalmol. Vis. Sci.* 51, 207–216. doi:10.1167/iovs.09-3947

Shibata, M., Ishizaki, E., Zhang, T., Fukumoto, M., Barajas-Espinosa, A., Li, T., et al. (2018). Role of the Pore/Oxidant/K(ATP) Channel/Ca(2+) Pathway in P2X(7)-Induced Cell Death in Retinal Capillaries. *Vision (Basel)* 2.

Shih, A. Y., Johnson, D. A., Wong, G., Kraft, A. D., Jiang, L., Erb, H., et al. (2003). Coordinate Regulation of Glutathione Biosynthesis and Release by Nrf2-Expressing Glia Potently Protects Neurons from Oxidative Stress. *J. Neurosci.* 23, 3394–3406. doi:10.1523/jneurosci.23-08-03394.2003

Shim, M. S., Takihara, Y., Kim, K. Y., Iwata, T., Yue, B. Y., Inatani, M., et al. (2016). Mitochondrial Pathogenic Mechanism and Degradation in Optineurin E50K Mutation-Mediated Retinal Ganglion Cell Degeneration. *Sci. Rep.* 6, 33830. doi:10.1038/srep33830

Shimada, K., Crother, T. R., Karlin, J., Dagvadorj, J., Chiba, N., Chen, S., et al. (2012). Oxidized Mitochondrial DNA Activates the NLRP3 Inflammasome during Apoptosis. *Immunity* 36, 401–414. doi:10.1016/j.immuni.2012.01.009

Sintim, H. O., Mikek, C. G., Wang, M., and Sooreshjani, M. A. (2019). Interrupting Cyclic Dinucleotide-cGAS-STING axis with Small Molecules. *Med. Chem. Commun.* 10, 1999–2023. doi:10.1039/c8md00555a

Slabaugh, M., and Salim, S. (2017). Use of Anti-VEGF Agents in Glaucoma Surgery. *J. Ophthalmol.* 2017, 1645269. doi:10.1155/2017/1645269

Sliter, D. A., Martinez, J., Hao, L., Chen, X., Sun, N., Fischer, T. D., et al. (2018). Parkin and PINK1 Mitigate STING-Induced Inflammation. *Nature* 561, 258–262. doi:10.1038/s41586-018-0448-9

Snyder, B., Shell, B., Cunningham, J. T., and Cunningham, R. L. (2017). Chronic Intermittent Hypoxia Induces Oxidative Stress and Inflammation in Brain Regions Associated with Early-Stage Neurodegeneration. *Physiol. Rep.* 5, e13258. doi:10.14814/phy2.13258

Son, J. L., Soto, I., Oglesby, E., Lopez-Roca, T., Pease, M. E., Quigley, H. A., et al. (2010). Glaucomatous Optic Nerve Injury Involves Early Astrocyte Reactivity and Late Oligodendrocyte Loss. *Glia* 58, 780–789. doi:10.1002/glia.20962

Stagni, E., Privitera, M. G., Bucolo, C., Leggio, G. M., Motterlini, R., and Drago, F. (2009). A Water-Soluble Carbon Monoxide-Releasing Molecule (CORM-3) Lowers Intraocular Pressure in Rabbits. *Br. J. Ophthalmol.* 93, 254–257. doi:10.1136/bjo.2007.137034

Sterling, J. K., Adetunji, M. O., Guttha, S., Bargoud, A. R., Uyhazi, K. E., Ross, A. G., et al. (2020). GLP-1 Receptor Agonist NLY01 Reduces Retinal Inflammation and Neuron Death Secondary to Ocular Hypertension. *Cel Rep.* 33, 108271. doi:10.1016/j.celrep.2020.108271

Stowell, C., Burgoyne, C. F., Tamm, E. R., Ethier, C. R., Dowling, J. E., Downs, C., et al. (2017). Biomechanical Aspects of Axonal Damage in Glaucoma: A Brief Review. *Exp. Eye Res.* 157, 13–19. doi:10.1016/j.exer.2017.02.005

Subramanian, N., Natarajan, K., Clatworthy, M. R., Wang, Z., and Germain, R. N. (2013). The Adaptor MAVS Promotes NLRP3 Mitochondrial Localization and Inflammasome Activation. *Cell* 153, 348–361. doi:10.1016/j.cell.2013.02.054

Swanson, K. V., Deng, M., and Ting, J. P.-Y. (2019). The NLRP3 Inflammasome: Molecular Activation and Regulation to Therapeutics. *Nat. Rev. Immunol.* 19, 477–489. doi:10.1038/s41577-019-0165-0

Takai, Y., Tanito, M., and Ohira, A. (2012). Multiplex Cytokine Analysis of Aqueous Humor in Eyes with Primary Open-Angle Glaucoma, Exfoliation Glaucoma, and Cataract. *Invest. Ophthalmol. Vis. Sci.* 53, 241–247. doi:10.1167/iovs.11-8434

Tamm, E. R., Ethier, C. R., Dowling, J. E., Downs, C., Ellisman, M. H., Fisher, S., et al. (2017). Biological Aspects of Axonal Damage in Glaucoma: A Brief Review. *Exp. Eye Res.* 157, 5–12. doi:10.1016/j.exer.2017.02.006

Tanaka, Y., and Chen, Z. J. (2012). STING Specifies IRF3 Phosphorylation by TBK1 in the Cytosolic DNA Signaling Pathway. *Sci. Signal.* 5, ra20. doi:10.1126/scisignal.2002521

Tang, M., Pavlou, S., Chen, M., and Xu, H. (2019). cGAS-STING Pathway Activation in Murine Retina. *Acta Ophthalmologica* 97.

Tezel, G. (2006). Oxidative Stress in Glaucomatous Neurodegeneration: Mechanisms and Consequences. *Prog. Retin. Eye Res.* 25, 490–513. doi:10.1016/j.preteyeres.2006.07.003

Tezel, G. (2011). The Immune Response in Glaucoma: a Perspective on the Roles of Oxidative Stress. *Exp. Eye Res.* 93, 178–186. doi:10.1016/j.exer.2010.07.009

Tham, Y.-C., Li, X., Wong, T. Y., Quigley, H. A., Aung, T., and Cheng, C.-Y. (2014). Global Prevalence of Glaucoma and Projections of Glaucoma Burden through 2040. *Ophthalmology* 121, 2081–2090. doi:10.1016/j.ophtha.2014.05.013

Tribble, J. R., Vasalauskaite, A., Redmond, T., Young, R. D., Hassan, S., Fautsch, M. P., et al. (2019). Midget Retinal Ganglion Cell Dendritic and Mitochondrial Degeneration Is an Early Feature of Human Glaucoma. *Brain Commun.* 1, fcz035.

Veal, E. A., Day, A. M., and Morgan, B. A. (2007). Hydrogen Peroxide Sensing and Signaling. *Mol. Cel* 26, 1–14. doi:10.1016/j.molcel.2007.03.016

Venegas, C., Kumar, S., Franklin, B. S., Dierkes, T., Brinkschulte, R., Tejera, D., et al. (2017). Microglia-derived ASC Specks Cross-Seed Amyloid-β in Alzheimer's Disease. *Nature* 552, 355–361. doi:10.1038/nature25158

Ventura, A. L. M., Dos Santos-Rodrigues, A., Mitchell, C. H., and Faillace, M. P. (2019). Purinergic Signaling in the Retina: From Development to Disease. *Brain Res. Bull.* 151, 92–108. doi:10.1016/j.brainresbull.2018.10.016

Voloboueva, L. A., Emery, J. F., Sun, X., and Giffard, R. G. (2013). Inflammatory Response of Microglial BV-2 Cells Includes a Glycolytic Shift and Is Modulated by Mitochondrial Glucose-Regulated Protein 75/mortalin. *FEBS Lett.* 587, 756–762. doi:10.1016/j.febslet.2013.01.067

Wang, Y., Chen, S., Liu, Y., Huang, W., Li, X., and Zhang, X. (2018). Inflammatory Cytokine Profiles in Eyes with Primary Angle-Closure Glaucoma. *Biosci. Rep.* 38.

Watanabe, S., Usui-Kawanishi, F., Karasawa, T., Kimura, H., Kamata, R., Komada, T., et al. (2020). Glucose Regulates Hypoxia-Induced NLRP3 Inflammasome Activation in Macrophages. *J. Cel Physiol.*

Wax, M. B., Tezel, G., Yang, J., Peng, G., Patil, R. V., Agarwal, N., et al. (2008). Induced Autoimmunity to Heat Shock Proteins Elicits Glaucomatous Loss of Retinal Ganglion Cell Neurons via Activated T-Cell-Derived Fas-Ligand. *J. Neurosci.* 28, 12085–12096. doi:10.1523/jneurosci.3200-08.2008

Wei, X., Cho, K.-S., Thee, E. F., Jager, M. J., and Chen, D. F. (2019). Neuroinflammation and Microglia in Glaucoma: Time for a Paradigm Shift. *J. Neuro Res.* 97, 70–76. doi:10.1002/jnr.24256

West, A. P., and Shadel, G. S. (2017). Mitochondrial DNA in Innate Immune Responses and Inflammatory Pathology. *Nat. Rev. Immunol.* 17, 363–375. doi:10.1038/nri.2017.21

Whitlock, N. A., Mcknight, B., Corcoran, K. N., Rodriguez, L. A., and Rice, D. S. (2010). Increased Intraocular Pressure in Mice Treated with Dexamethasone. *Invest. Ophthalmol. Vis. Sci.* 51, 6496–6503. doi:10.1167/iovs.10-5430

Whitmore, A. V., Libby, R. T., and John, S. W. M. (2005). Glaucoma: Thinking in New Ways-A Rôle for Autonomous Axonal Self-Destruction and Other Compartmentalised Processes? *Prog. Retin. Eye Res.* 24, 639–662. doi:10.1016/j.preteyeres.2005.04.004

Williams, P. A., Harder, J. M., Foxworth, N. E., Cochran, K. E., Philip, V. M., Porciatti, V., et al. (2017). Vitamin B3modulates Mitochondrial Vulnerability and Prevents Glaucoma in Aged Mice. *Science* 355, 756–760. doi:10.1126/science.aal0092

Wilson, G. N., Inman, D. M., Dengler Crish, C. M., Smith, M. A., and Crish, S. D. (2015). Early Pro-inflammatory Cytokine Elevations in the DBA/2J Mouse Model of Glaucoma. *J. Neuroinflammation* 12, 176. doi:10.1186/s12974-015-0399-0

Wilson, G. N., Smith, M. A., Inman, D. M., Dengler-Crish, C. M., and Crish, S. D. (2016). Early Cytoskeletal Protein Modifications Precede Overt Structural Degeneration in the DBA/2J Mouse Model of Glaucoma. *Front. Neurosci.* 10, 494. doi:10.3389/fnins.2016.00494

Wu, J.-h., Zhang, S.-h., Nickerson, J. M., Gao, F.-j., Sun, Z., Chen, X.-y., et al. (2015). Cumulative mtDNA Damage and Mutations Contribute to the Progressive Loss of RGCs in a Rat Model of Glaucoma. *Neurobiol. Dis.* 74, 167–179. doi:10.1016/j.nbd.2014.11.014

Wu, W., Li, W., Chen, H., Jiang, L., Zhu, R., and Feng, D. (2016). FUNDC1 Is a Novel Mitochondrial-Associated-Membrane (MAM) Protein Required for Hypoxia-Induced Mitochondrial Fission and Mitophagy. *Autophagy* 12, 1675–1676. doi:10.1080/15548627.2016.1193656

Yang, Q., Cho, K.-S., Chen, H., Yu, D., Wang, W.-H., Luo, G., et al. (2012). Microbead-induced Ocular Hypertensive Mouse Model for Screening and Testing of Aqueous Production Suppressants for Glaucoma. *Invest. Ophthalmol. Vis. Sci.* 53, 3733–3741. doi:10.1167/iovs.12-9814

Yang, X., Hondur, G., and Tezel, G. (2016). Antioxidant Treatment Limits Neuroinflammation in Experimental Glaucoma. *Invest. Ophthalmol. Vis. Sci.* 57, 2344–2354. doi:10.1167/iovs.16-19153

Yang, X., Luo, C., Cai, J., Powell, D. W., Yu, D., Kuehn, M. H., et al. (2011). Neurodegenerative and Inflammatory Pathway Components Linked to TNF-A/tnfr1 Signaling in the Glaucomatous Human Retina. *Invest. Ophthalmol. Vis. Sci.* 52, 8442–8454. doi:10.1167/iovs.11-8152

Yerramothu, P., Vijay, A. K., and Willcox, M. D. P. (2018). Inflammasomes, the Eye and Anti-inflammasome Therapy. *Eye* 32, 491–505. doi:10.1038/eye.2017.241

Yi, P.-L., Tsai, C.-H., Lu, M.-K., Liu, H.-J., Chen, Y.-C., and Chang, F.-C. (2007). Interleukin-1β Mediates Sleep Alteration in Rats with Rotenone-Induced Parkinsonism. *Sleep* 30, 413–425. doi:10.1093/sleep/30.4.413

Yin, F., Sancheti, H., Patil, I., and Cadenas, E. (2016). Energy Metabolism and Inflammation in Brain Aging and Alzheimer's Disease. *Free Radic. Biol. Med.* 100, 108–122. doi:10.1016/j.freeradbiomed.2016.04.200

Yuan, L., and Neufeld, A. H. (2001). Activated Microglia in the Human Glaucomatous Optic Nerve Head. *J. Neurosci. Res.* 64, 523–532. doi:10.1002/jnr.1104

Zhang, X., Li, A., Ge, J., Reigada, D., Laties, A. M., and Mitchell, C. H. (2007). Acute Increase of Intraocular Pressure Releases ATP into the Anterior Chamber. *Exp. Eye Res.* 85, 637–643. doi:10.1016/j.exer.2007.07.016

Zheng, D., Liwinski, T., and Elinav, E. (2020). Inflammasome Activation and Regulation: toward a Better Understanding of Complex Mechanisms. *Cel Discov.* 6, 36. doi:10.1038/s41421-020-0167-x

Zhong, Z., Umemura, A., Sanchez-Lopez, E., Liang, S., Shalapour, S., Wong, J., et al. (2016). NF-κB Restricts Inflammasome Activation via Elimination of Damaged Mitochondria. *Cell* 164, 896–910. doi:10.1016/j.cell.2015.12.057

Zhou, R., Yazdi, A. S., Menu, P., and Tschopp, J. (2011). A Role for Mitochondria in NLRP3 Inflammasome Activation. *Nature* 469, 221–225. doi:10.1038/nature09663

Conflict of Interest: The authors declare that the research was conducted in the absence of any commercial or financial relationships that could be construed as a potential conflict of interest.

frontiers in Pharmacology

ORIGINAL RESEARCH
published: 26 July 2021
doi: 10.3389/fphar.2021.680734

Oral Aminoacids Supplementation Improves Corneal Reinnervation After Photorefractive Keratectomy: A Confocal-Based Investigation

Anna M Roszkowska[1], *Dario Rusciano*[2]*, *Leandro Inferrera*[1], *Alice Antonella Severo*[1] and *Pasquale Aragona*[1]

[1]Ophthalmology Clinic, Department of Biomedical Sciences, University of Messina, Messina, Italy, [2]Sooft Italia SpA Research Center, Catania, Italy

Aim of this retrospective study was to estimate the effect of oral supplementation with amino acids (AA) on corneal nerves regrowth after excimer laser refractive surgery with photorefractive keratectomy (PRK). Based on the pre and post-surgical treatment received, 40 patients with 12 months of follow-up were distributed in two groups: 20 patients had received oral AA supplementation 7 days before and 30 days after PRK, and 20 patients without AA supplementation, as untreated reference control. All patients followed the same standard post-operative topical therapy consisting of an association of antibiotic and steroid plus sodium hyaluronate during the first week, then steroid alone progressively decreasing during 30 days and sodium hyaluronate for the following 3 months. *In vivo* corneal confocal microscopy was used to evaluate the presence of sub-basal corneal nerve fibers during 12 months after PRK. Results have shown that sub-basal nerves regenerated significantly faster (p <0.05), and nerve fibers density was significantly higher (p <0.05) with a more regular pattern in the eyes of AA treated patients with respect to the untreated control group. Therefore, our data indicate that oral supplementation with AA improved significantly corneal nerve restoration after PRK and could thus be considered as an additional treatment during corneal surgical procedures.

Keywords: aminoacids, PRK, cornea, corneal nerves, nerve growth, confocal microscopy

OPEN ACCESS

Edited by:
Mario Damiano Toro,
Medical University of Lublin, Poland

Reviewed by:
Alessandro Arrigo,
San Raffaele Hospital (IRCCS), Italy
Federico Corvi,
Luigi Sacco Hospital, Italy
Edward Wylęgała,
Medical University of Silesia, Poland

***Correspondence:**
Dario Rusciano
dario.rusciano@sooft.it

Specialty section:
This article was submitted to Experimental Pharmacology and Drug Discovery, a section of the journal Frontiers in Pharmacology

Received: *15 March 2021*
Accepted: *15 July 2021*
Published: *26 July 2021*

Citation:
Roszkowska AM, Rusciano D, Inferrera L, Severo AA and Aragona P (2021) Oral Aminoacids Supplementation Improves Corneal Reinnervation After Photorefractive Keratectomy: A Confocal-Based Investigation. Front. Pharmacol. 12:680734. doi: 10.3389/fphar.2021.680734

INTRODUCTION

Photorefractive keratectomy (PRK) is a common excimer laser procedure still widely used to correct refractive errors. PRK is a surface ablation procedure, in which the corneal epithelium is removed to permit the laser to reshape the anterior corneal stroma. The depth of ablation varies in relation to the refractive error, therefore different amounts of the sub-basal nerve plexus (SBNP) fibers are injured in relation to the ablation zone (Erie, 2003; Tomás-Juan et al., 2015; Labetoulle et al., 2019). While the epithelium heals within 3–5 days (Erie, 2003), the complete regeneration of the SBNP nerves occurs during several months (Erie, 2003). The interruption of the nerve reflex between the cornea and the lacrimal glands interferes with normal lacrimation, so that the ocular surface may be altered by insufficient moistening, thus triggering eye dryness and patient's discomfort (Labetoulle et al., 2019). Additionally, the surgical procedure activates inflammation and keratocytes transformation to

fibroblasts and myofibroblasts that produce normally absent type IV collagen and disorganized extracellular matrix, that together to the abnormal arrangement pattern of collagen type I and III results clinically in corneal haze (Tomás-Juan et al., 2015). Therefore, it is critical that wound repair (involving epithelium, stroma and nerve fibers) occurs reasonably fast and definitely well, to reduce patient's discomfort and promote corneal healing thus allowing a fast and good recovery of vision.

Cell metabolism is tightly dependent on the availability of aminoacids (AA), which are necessary to build new macromolecules used in cell and extracellular matrix architecture. Moreover, AA may also have different functions, specifically linked to their molecular structure and interaction with cell regulatory mechanisms (Rusciano et al., 2016). The process of wound healing poses a serious challenge to cell metabolism, and in case of AA deficiency the whole process could be hampered, also impairing the immune defense, and finally exposing the tissue to an increased risk of infection (Herndon and Tompkins, 2004; Chandrasekaran et al., 2017). Some AAs are known to facilitate the process of wound healing (Stechmiller, 2010). Arginine triggers nitric oxide (NO) synthesis, thus stimulating collagen synthesis, antimicrobial activity, and blood flow (Alexander and Supp, 2014). Glutamine is an energy source and induces the expression of heat shock proteins, thus protecting the tissue from inflammation damage (Chow and Barbul, 2014). Leucine is normally metabolized into hydroxy-methylbutyrate (HMB), an active molecule blunting proteolysis, stimulating protein synthesis, decreasing apoptosis and increasing cell proliferation (Sipahi et al., 2013). An experimental model system evaluated wound healing in a skin full-thickness excisional model in rats receiving diets with a different content of essential AA. Results have shown that wound repair was accelerated, and inflammation reduced, in rats fed with an increased amount of essential AA (Corsetti et al., 2017). Oral AA supplementation has shown to help wound recovery in refractory patients after PRK (Vinciguerra et al., 2002) or cataract (Torres Munoz et al., 2003) surgery. Treatment with topical AA given as eye drops resulted in a better improvement of signs and symptoms in patients affected by dry eye (Sacchetti et al., 2012; Aragona et al., 2013).

Based on these premises, in this preliminary study we aimed to evaluate the regeneration of the sub-basal corneal nerve fibers in patients treated with standard post-surgical therapy who received an additional treatment with oral AA.

MATERIALS AND METHODS

This retrospective study included clinical and instrumental data from 40 eyes of 40 patients selected among those who were treated with PRK for myopia or composed myopic astigmatism and completed a follow-up of at least 12 months. Subjects were chosen from the database of the Cornea and Refractive Surgery section of Messina University Hospital Ophthalmology Unit. Inclusion criteria were: age between 20 and 40 years; spherical equivalent between −2.75 and −7 diopters with ablation depth between 45 and 100 microns; available follow up of 12 months. Among these subjects, all suitable for PRK, 20 were chosen who had received AA supplementation when the specific product was available, and 20 (as control reference group) who did not receive AA because treated in a previous period when the food supplement was not available.

TABLE 1 | L-aminoacid content per tablet (* denotes an essential AA).

Aminoacid	Amount (mg)
Leucine*	250
Lysine*	130
Isoleucine*	125
Valine*	125
Threonine*	70
Cystine	30
Histidine*	30
Phenylalanine*	20
Methionine*	10
Tyrosine	6
Tryptophan*	4

The PRK surgical procedure followed the same protocol for all patients. Oxybuprocaine hydrochloride anesthetic drops (Novesina, Thea Farma, Italy) were instilled before the surgical treatment, and the epithelium was removed with a blunt spatula in an area of 9 mm diameter, after 20% alcohol delamination for 20 s. PRK was performed with a Mel-70 G-Scan excimer laser (Carl Zeiss, Jena, Germany) provided with flying spot with gaussian profile with a diameter of 1.8 mm. The ablation zone was 7 mm with 1.8 mm of transition. After treatment, a soft therapeutic contact lens was applied for 5 days and removed when the epithelium healed.

All patients followed the same standard post-operative therapy used in our center, consisting for the first 5 days of eye drops with dexamethasone 0.1% and tobramycin 0.3% (Tobradex, Alcon, Italy) one drop four q.i.d. plus sodium hyaluronate (Blu Yal, Sooft Italia) one drop four q.i.d. for 6 days until healing of the epithelium; then fluorometholone 0.2% unit dose eye drops (Flumetol, Thea Farma, Italy) one drop for 4 times q.i.d. for 10 days, then 3 times daily for 20 days and twice daily for 10 days plus sodium hyaluronate (Blu Yal, Sooft Italia) one drop four q.i.d. for the following 2 months.

The oral supplementation treatment with AA consisted of one tablet containing an AA mix (Aminoftal® Sooft Italia SpA: **Table 1**) three times daily for 7 days before and 30 days after PRK surgery. The files of all subjects in the treatment group reported completion of the prescribed AA administration, with no one complaining of disturbs, intolerance or adverse effects related to the AA supplementation received.

To assess their eligibility for the PRK procedure all patients were subjected to a complete ophthalmological examination with visual acuity (VA) assessment, refraction, slit lamp evaluation, tonometry and fundus. The instrumental evaluation comprised corneal topography, tomography, corneal thickness, Schirmer test, TBUT and *in vivo* corneal confocal microscopy (IVCM). VA, refraction, corneal topography, pachymetry and IVCM were reassessed at 1–3–6 and 12 months after PRK.

IVCM was performed with the Confoscan 4 (Nidek Technologies, Vigonza, Italy), equipped with the Z-Ring to

TABLE 2 | Characteristics of enrolled patients.

Group	Males	Females	AGE (years) ± SD	Diopters ± SD	Ablation depth (mm) ± SD
AA	9	11	30.42 ± 4.45	-5.40 ± 2.2	68.71 ± 19.7
Control	8	12	31.08 ± 4.42	-5.92 ± 1.81	67.25 ± 21.5

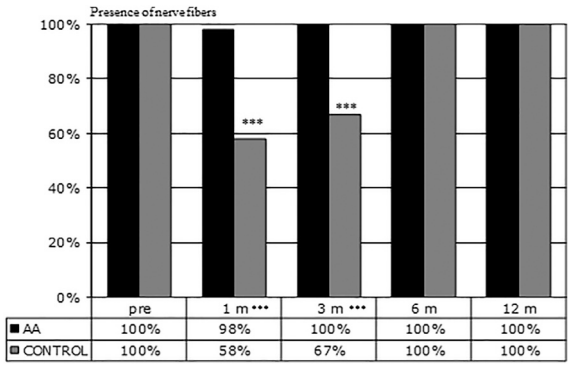

FIGURE 1 | Presence of nerve fibers during follow-up. Evaluation of the number of fields (3 fields/patient) presenting nerve fibers at the indicated time points. At 1 and 3 months corneal nerve regeneration resulted to be significantly faster in patients treated with AA than in the control group (***p < 0.001 by Fisher's exact test).

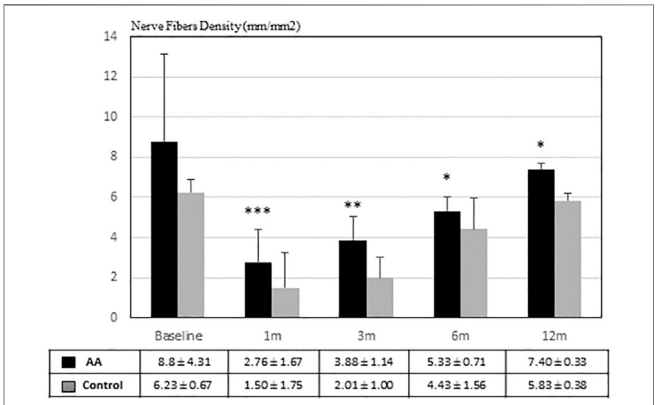

FIGURE 2 | Nerve Fibers Density (μm/mm^2) during follow-up. Nerve regeneration resulted to be significantly faster in patients treated with AA than in the control group (*p <0.05; **p <0.01; ***p < 0.001 by Student's t-test).

provide central image acquisition. The presence of nerve fibers of SBNP was detected at each time point and three fields for each eye were examined by the same experienced operator on 0.159 mm^2 frames. Sub-basal nerve plexus (SBNP) fibers were analyzed by the ImageJ/Neuron-J plug in (National Institute of Health, Bethesda, United States), a semiautomated software for nerve tracing and analysis showing a high interobserver repeatability (Cottrell et al., 2014; Dehghani et al., 2014).

The nerve fibers density (NFD) was calculated in μm/mm^2 and an average value was considered for calculations.

The number of subjects enrolled in the present study (n = 40: 20 controls and 20 AA-treated) was based on statistical power calculation made with G Power software version 3.1 setting the power to 0.80, α to 0.05 and considering a large effect size (on the basis of previous studies, showing how slow is nerve regeneration after PRK (Erie, 2003). Statistical analysis was performed with Graph Pad Prism (version 8). Fisher's exact test was used for non-parametric data (presence of nerve fibers), whereas unpaired Student's T-test was used to analyze the parametric data normally distributed (age, refractive error, ablation depth, NFD).

The study was approved by the Ethical Committee of the University Hospital of Messina (N. 65/18).

RESULTS

The demographic characteristics of patients included in this study are represented in **Table 2**. Both groups were homogeneous for sex, age, refractive error and depth of ablation (p > 0.05). Their spherical equivalent refraction was comprised between −5 and −6 diopters, and the mean ablation depth was 68.71 ± 19.7 mm in the AA group and 67.25 ± 21.5 mm in the control group (**Table 2**).

Figure 1 shows the percentage of eyes in which nerve fibers could be detected in selected confocal microscopy fields. After one-month, nerve fibers were present in 98% of eyes in the AA group and 58% in the control group (p <0.001). A significant difference in the amount of SBNP fibers was still present at 3 months (100 vs 67% p < 0.001), whereas at 6 and 12 months in all eyes SBNP fibers could be detected. These results indicate that corneal nerve regeneration is significantly faster in patients who received oral AA supplementation than in the control group not treated with AA.

Figure 2 shows SBNP nerve fibers density (NFD) calculated on confocal images in both groups during the follow-up between 1 month and 1 year. It is evident that NFD increased faster in patients treated with AA than in the control group. In fact, at each time point after PRK, the NFD was significantly higher in the eyes of AA treated patients than in control eyes (p < 0.001 at 1 month; p < 0.01 at 3 months; p < 0.05 at 6 and 12 months).

Figure 3 shows the evolution as seen at confocal microscopy of SBNP fibers repopulation in the subepithelial anterior corneal stroma after PRK at progressive times up until one year. **Figures 3A,B** illustrate the normal sub basal nerve fibers pattern with a regular almost parallel path at baseline evaluation, just before ablation. Pictures on the left column (**Figures 3C–E**) are representative of untreated control patients: Pictures on the right column (**Figures 3D–F**) are representative of AA-treated

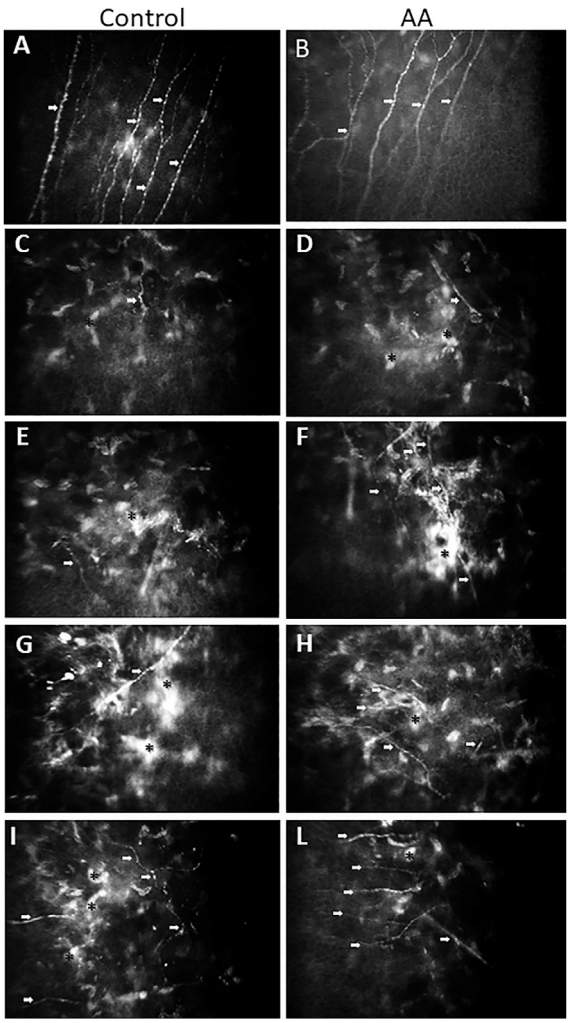

FIGURE 3 | Representative confocal images taken where the SBNP fibers best appear on focus. **(A)**: image taken from a control patient before PRK; **(B)**: image taken from an AA-treated patient before PRK. Both pictures show the normal path of SBNP fibers, which appear with a regular, almost parallel pattern. Representative confocal images of SBNP nerve fibers were taken at different times after PRK of the control patient (left column: treated for −3.50 D of SE with ablation of 67 microns) and of the AA-treated patient (right column: treated for −4.50 D of SE with ablation of 70 microns). After 1 month from PRK there is an initial presence of nerve fibers (among activated, hyper-reflective stromal cells) in the AA group **(D)**, while in the control group **(C)** no nerves or sporadic fibers could be detected. After 3 months from PRK an increased number of SBNP fibers is apparent in the AA group **(F)**, while in the control group **(E)** some nerve fibers start to be detectable. After 6 months from PRK all examined eyes exhibit SBNP fibers, but the density is significantly higher in the AA group **(H)** than in control eyes **(G)**. After 12 months from PRK the nerve fiber density is higher in the AA group, also showing a more regular linear pattern (L) than in control eyes of patients not treated with AA **(I)**. White arrows indicate growing fibers; asterisks indicate activated, hyper-reflective stromal cells.

patients. **Figures 3C,D** illustrates the appearance of subepithelial corneal stroma at 4 weeks after the intervention in subjects treated with oral aminoacids (D) or untreated controls (C). Some short and bundled nerve fibers start to be apparent in AA-treated patients among activated, hyper-reflective stromal cells, while no such evidence is present in control pictures, showing only the activated stromal cells. The situation at 3 months after PRK is shown in **Figures 3E,F**: an increasing number of sub-basal nerve plexus fibers is evident in AA-treated patients (F), while in controls nerve fibers start to make their appearance (E). At 6 months (**Figures 3G,H**) all eyes show the presence of growing nerve fibers, however with a higher density in the eyes of patients coming from AA (H) treatment group with respect to controls (G). A similar finding is still visible after 12 months from the intervention (**Figures 3I–L**), with confocal pictures of eyes of patients treated with AA (L) showing a higher density of nerve fibers, with a more regular pattern, while in control eyes nerve fibers continue to show an irregular pattern, among still highly hyperreflective stromal cells (I).

DISCUSSION

The results of this confocal-based retrospective study address for the first time the basic role of AA supplementation on corneal peripheral nerve regeneration after PRK. Our data show that a diet enriched in essential AA may enhance the regeneration of SBNP fibers lesioned by the PRK intervention, so that their density and pathway through the regenerating stroma is improved, and healing is achieved in shorter times with respect to patients in which the AA supplement was not given.

With 16,000 nerve terminations/mm^3, the cornea is the most densely innervated tissue of the human body (Guthoff et al., 2005). Therefore, PRK ablation, destroying SBNP fibers in the central cornea, makes the procedure very painful, since the remaining nerve endings after laser ablation are exposed at the surface until the epithelium regenerates and covers the surgical wound (Mohan et al., 2003). While epithelium regrowth occurs within few days (Olivieri et al., 2018), stromal remodeling and nerve regeneration are much slower events (Tomás-Juan et al., 2015). Even though new nerve fibers may appear from the ablation area within the first weeks, only half reinnervation is completed at 6 months, returning to pre-operative density only after 2 years (Erie et al., 2005). Such prolonged corneal nerve density reduction may lead to ocular surface discomfort and dry eye disease with different severity grade (Dohlman et al., 2016). Occasionally, more severe consequences may happen, such as hypoesthesia, neurotrophic ulcers, or chronic inflammation (Chao et al., 2014). Aberrant reinnervation may also occur and lead to allodynia or keratoneuralgia (Hamrah et al., 2017). Therefore, the timing and the quality of reinnervation after PRK are critical, so to rescue the correct corneal physiological behavior of the ocular surface functional unit (Stern et al., 2004). Keratocyte repopulation and healing of the ablated corneal stroma supply growth factors and biological cues guiding the correct regeneration of lesioned nerve endings. In fact, further to stromal ablation, the surviving keratocytes in corneal stroma are activated to stromal fibroblasts (SFs), which secrete neurotrophic and inflammatory factors regulating neurogenesis and wound healing (Yam et al., 2017). The regenerating corneal epithelium is

also a source of neurotrophic growth factors, such as NGF and GDNF, also contributing towards nerve regrowth (Di et al., 2017).

Several different topical treatments with eye drops have been tried to improve corneal nerve regeneration after keratectomy. Murine NGF purified from the submaxillary gland was used in a corneal flap rabbit model of LASIK and shown to accelerate the recovery of corneal sensitivity as measured by esthesiometry (Joo et al., 2004) and promote nerve regeneration as visualized by confocal microscopy (Ma et al., 2014). With the same rabbit model, a bioactive N-terminal peptide derived from the pituitary adenylate cyclase–activating polypeptide (PACAP27) has been shown to be able to promote neurite outgrowth as followed by histological analysis (Fukiage et al., 2007). Topical applications of PEDF in association with DHA also improved the recovery of sensitivity in rabbit corneas subjected to PRK (Cortina et al., 2012). In rodent models of corneal epithelial debridement, topical administration as eye drops of vitamin B12 and taurine, together with sodium hyaluronate, enhanced both re-epithelization and re-innervation (Romano et al., 2014). Finally, Ginkgo Biloba/hyaluronic acid (GB/HA) eye drops were given to a group of 15 patients (30 eyes) after PRK surgery and compared to hyaluronic acid alone. Confocal microscopy analysis performed at 1–3–6–9–12 months showed a clear advantage in both quantitative and qualitative effects in the GB/HA group (Bisantis, 2006). More recently, systemic administration of a secondary metabolite (epothilone B) produced by the *mycobacterium* Sorangium cellulosum, which is a microtubule stabilizing agent, has been found to lead to a favorable pharmacodynamics in the cornea and corneal nerves, and to speed up corneal reinnervation after epithelial debridement in mice (Wang et al., 2018).

However, whichever treatment is given to stimulate nerve regeneration, the necessary requirement in all instances is that enough "building" material is available to nerve cells and their neighboring cells to elongate their nerve endings in a permissive environment, in which stromal cells produce an extracellular matrix (ECM) favoring the whole process (Gonzalez-Perez et al., 2013). In fact, all these activities require new protein (structural and enzymatic) synthesis to allow and speed up the series of events leading to the restoration of the perturbed homeostasis of the tissue. This is also evident in our study, in which the relative amount of activated (hyper-reflective) stromal cells remains higher in control patients than in AA-treated patients (**Figure 3**), especially visible after 12 months (**Figures 3I–L**).

The availability of AA, and more specifically of the essential AA, those that must be taken through the diet, can be a limiting step in this process. Like what happens with muscle exercise, where mechanical stimulation results more effective in inducing growth of the muscle fibers in presence of an increased concentration of essential AA in blood (Church et al., 2020), also for nerve regeneration a similar situation may occur. This has been clearly shown in the goldfish model of retinal ganglion cells regeneration, in which transected ganglion cells demonstrate a marked increase in protein biosynthesis as their axons regrow into a primary target tissue (Giulian, 1984) and in which extracellular amino acids strongly contribute to the composition of the immediate precursor pool for protein synthesis in regenerating cells (Whitnall and Grafstein, 1981). A recent review on the effects of nutrition-related factors on peripheral nerve injuries highlighted the role of omega fatty acids, vitamins, antioxidants and proteins rich in essential AA in preserving nerve function and health, and in the recovery of injured tissue (Yildiran et al., 2020). In this respect, the bioavailability of free AA taken as food supplement is expected to be higher than that deriving from the metabolism of ingested food proteins, that require a complex enzymatic pathway and absorption process, and depends on the particular diet habits of the subject (Schmidt et al., 2016).

Moreover, AA may also have other functions beside the building of proteins, such as antioxidants or participate in the chain of neurotransmission. For instance, in a rat model of facial nerve crush injury systemic administration of n-acetylcysteine (a potent antioxidant) favored nerve recovery as shown by improved functional and electromyography outcomes (Rivera et al., 2017). AA can be utilized to synthesize both lipids and glucose. Increased intake of essential AA may increase laboratory animals' lifespan through the activation of Sirt-1 dependent mitochondrial biogenesis (D'Antona et al., 2010). Clinical studies in humans have addressed the role of essential AA in enhancing protein synthesis independently from age, and improving muscle catabolism in the elderly during prolonged bed rest (Cuthbertson et al., 2005; Ferrando et al., 2010). Finally, a metanalysis of clinical studies on patients with painful peripheral neuropathy showed that a food supplement of acetyl-L-carnitine (a precursor of neurotransmitters derived from the AA lysine and methionine) exerted several beneficial effects on nerve conduction parameters and nerve fiber regeneration, generally improving patients' condition (Di Stefano et al., 2019). All these effects may have both a direct and an indirect relevance because the healing of a tissue or an organ in the body depends on the state of the tissue or the organ by itself, but also from the general health condition of the body in which it resides. Therefore, since an adequate intake of essential AA can also improve the general health condition of the patient, this effect can reverberate on the healing properties of different organs, eye included (Pache and Flammer, 2006). Consistent with these premises, our results show that the intake of supplemental AA has a higher impact during the first 3 months, improving the initial stages of SBNP repopulation: in fact, a faster and wider repopulation of SBNP fibers is evident at 1 and 3 months in AA-treated subjects (**Figure 1**), while the statistical significance of NFD comparative data between treated and untreated patients becomes progressively lower at 6 and 12 months, however still pointing at some advantage for AA treated subjects (**Figure 2**). A similar treatment with the same AA food supplement was already reported in a previous study (Vinciguerra et al., 2002), in which patients with chronic epithelial defects, or with delayed re-epithelization times after PRK showed an improved healing response after oral AA treatment. Similarly, supplementation with the same AA mixture improved corneal stromal regeneration after cataract surgery (Torres Munoz et al., 2003). This finding is relevant also in our study, because keratocyte and stromal healing is critical for correct nerve growth (Gonzalez-Perez et al., 2013), thus suggesting that AA may contribute both a

direct (on nerve cells themselves) and an indirect (through keratocytes and the stroma) effect on SBNP restoration.

A limitation of these observations is the small number of patients under scrutiny; to be a retrospective study (therefore, no clinical data on eye dryness were available, and no pharmacokinetics could be programmed) conducted in a single center; and to be the first of its kind. Nonetheless, data obtained are very promising, and grant a prosecution of the study, in a prospective way and on a higher number of patients.

CONCLUSION

In this study we have clearly shown throughout 12 months of confocal microscopy observations that SBNP fibers lesioned during PRK grow faster and better when patients take a supplement of essential AA. Data presented in this study corroborate the function of exogenous AA in corneal nerve regeneration, in line with previous studies showing the role of supplemental AA given either as food supplement (Vinciguerra et al., 2002; Torres Munoz et al., 2003) or as topical eye drops (Sacchetti et al., 2012; Aragona et al., 2013) in the healing of the cornea and corneal nerves after surgical interventions or during the course of dry eye. It is likely that the effect of AA supplementation by improving both epithelial and stromal healing, and by providing a favorable growth milieu to regenerating nerve cells, finally results in a faster and better reinnervation of the lesioned cornea, most evident during the first 3 months post-surgery.

In conclusion, our results support the use of food supplements enriched with essential AA, or at least a diet rich in AA content, before and after PRK surgery, or in case of any surgical intervention that involves tissue and nerve regeneration.

DATA AVAILABILITY STATEMENT

The data analyzed in this study is subject to the following licenses/restrictions: Data on file at the Ophthalmology Dpt. Of the University of Messina (Italy). Requests to access these datasets should be directed to anna.roszkowska@unime.it

ETHICS STATEMENT

The studies involving human participants were reviewed and approved by the Ethical Committee of the University Hospital of Messina (N. 65/18). Written informed consent for participation was not required for this study in accordance with the national legislation and the institutional requirements.

AUTHOR CONTRIBUTIONS

Conceptualization, AR, PA.; methodology, AR, PA.; software, AR, LI, and AS; validation, AR, LI, AS, and PA; formal analysis, AR, LI; investigation, AR, LI, and AS; resources, AR, PA; data curation, AR; writing original draft preparation, AR, DR; writing review and editing, AR, DR; supervision, AR, PA.

REFERENCES

Alexander, J. W., and Supp, D. M. (2014). Role of Arginine and Omega-3 Fatty Acids in Wound Healing and Infection. *Adv. Wound Care* 3, 682–690. doi:10.1089/wound.2013.0469

Aragona, P., Rania, L., Roszkowska, A. M., Spinella, R., Postorino, E., Puzzolo, D., et al. (2013). Effects of Amino Acids Enriched Tears Substitutes on the Cornea of Patients with Dysfunctional Tear Syndrome. *Acta Ophthalmol.* 91 (6), e437–e444. doi:10.1111/aos.12134

Bisantis, F. (2006). *Effects of Ginkgo Biloba on Corneal Subepithelial Nerves Regeneration after PRK: A Confocal Microscopy Study. One-Year Results*. London: XXIX Congress of the ESCRS.

Chandrasekaran, P., Saravanan, N., Bethunaickan, R., and Tripathy, S. (2017). Malnutrition: Modulator of Immune Responses in Tuberculosis. *Front. Immunol.* 8. doi:10.3389/fimmu.2017.01316

Chao, C., Golebiowski, B., and Stapleton, F. (2014). The Role of Corneal Innervation in LASIK-Induced Neuropathic Dry Eye. *Ocul. Surf.* 12 (1), 32–45. doi:10.1016/j.jtos.2013.09.001

Chow, O., and Barbul, A. (2014). Immunonutrition: Role in Wound Healing and Tissue Regeneration. *Adv. Wound Care* 3, 46–53. doi:10.1089/wound.2012.0415

Church, D. D., Hirsch, K. R., Park, S., Kim, I.-Y., Gwin, J. A., Pasiakos, S. M., et al. (2020). Essential Amino Acids and Protein Synthesis: Insights into Maximizing the Muscle and Whole-Body Response to Feeding. *Nutrients* 12 (12), 3717. doi:10.3390/nu12123717

Corsetti, G., Romano, C., Pasini, E., Marzetti, E., Calvani, R., Picca, A., et al. (2017). Diet Enrichment with a Specific Essential Free Amino Acid Mixture Improves Healing of Undressed Wounds in Aged Rats. *Exp. Gerontol.* 96, 138–145. doi:10.1016/j.exger.2017.06.020

Cortina, M. S., He, J., Li, N., Bazan, N. G., and Bazan, H. E. P. (2012). Recovery of Corneal Sensitivity, Calcitonin Gene-Related Peptide-Positive Nerves, and Increased Wound Healing Induced by Pigment Epithelial-Derived Factor Plus Docosahexaenoic Acid after Experimental Surgery. *Arch. Ophthalmol.* 130 (1), 76–83. doi:10.1001/archophthalmol.2011.287

Cottrell, P., Ahmed, S., James, C., Hodson, J., McDonnell, P. J., Rauz, S., et al. (2014). Neuron J Is a Rapid and Reliable Open Source Tool for Evaluating Corneal Nerve Density in Herpes Simplex Keratitis. *Invest. Ophthalmol. Vis. Sci.* 55, 7312–7320. doi:10.1167/iovs.14-15140

Cuthbertson, D., Smith, K., Babraj, J., Leese, G., Waddell, T., Atherton, P., et al. (2005). Anabolic Signaling Deficits Underlie Amino Acid Resistance of Wasting, Aging Muscle. *FASEB j.* 19 (3), 1–22. doi:10.1096/fj.04-2640fje

D'Antona, G., Ragni, M., Cardile, A., Tedesco, L., Dossena, M., Bruttini, F., et al. (2010). Branched-chain Amino Acid Supplementation Promotes Survival and Supports Cardiac and Skeletal Muscle Mitochondrial Biogenesis in Middle-Aged Mice. *Cel Metab.* 12 (4), 362–372. doi:10.1016/j.cmet.2010.08.016

Dehghani, C., Pritchard, N., Edwards, K., Russell, A. W., Malik, R. A., and Efron, N. (2014). Fully Automated, Semiautomated, and Manual Morphometric Analysis of Corneal Subbasal Nerve Plexus in Individuals with and without Diabetes. *Cornea* 33 (7), 696–702. doi:10.1097/ico.0000000000000152

Di, G., Qi, X., Zhao, X., Zhang, S., Danielson, P., and Zhou, Q. (2017). Corneal Epithelium-Derived Neurotrophic Factors Promote Nerve Regeneration. *Invest. Ophthalmol. Vis. Sci.* 58 (11), 4695–4702. doi:10.1167/iovs.16-21372

Di Stefano, G., Di Lionardo, A., Galosi, E., Truini, A., and Cruccu, G. (2019). Acetyl-L-carnitine in Painful Peripheral Neuropathy: a Systematic Review. *Jpr* 12, 1341–1351. doi:10.2147/JPR.S190231

Dohlman, T. H., Lai, E. C., and Ciralsky, J. B. (2016). Dry Eye Disease after Refractive Surgery. *Int. Ophthalmol. Clin.* 56 (2), 101–110. doi:10.1097/IIO.0000000000000104

Erie, J. C. (2003). Corneal Wound Healing after Photorefractive Keratectomy: a 3-year Confocal Microscopy Study. *Trans. Am. Ophthalmol. Soc.* 101, 293–333.

Erie, J. C., McLaren, J. W., Hodge, D. O., and Bourne, W. M. (2005). Recovery of Corneal Subbasal Nerve Density after PRK and LASIK. *Am. J. Ophthalmol.* 140 (6), 1059–1064. doi:10.1016/j.ajo.2005.07.027

Ferrando, A. A., Paddon-Jones, D., Hays, N. P., Kortebein, P., Ronsen, O., Williams, R. H., et al. (2010). EAA Supplementation to Increase Nitrogen Intake Improves Muscle Function during Bed Rest in the Elderly. *Clin. Nutr.* 29 (1), 18–23. doi:10.1016/j.clnu.2009.03.009

Fukiage, C., Nakajima, T., Takayama, Y., Minagawa, Y., Shearer, T. R., and Azuma, M. (2007). PACAP Induces Neurite Outgrowth in Cultured Trigeminal Ganglion Cells and Recovery of Corneal Sensitivity after Flap Surgery in Rabbits. *Am. J. Ophthalmol.* 143 (2), 255–262. doi:10.1016/j.ajo.2006.10.034

Giulian, D. (1984). Target Regulation of Protein Biosynthesis in Retinal Ganglion Cells during Regeneration of the Goldfish Visual System. *Brain Res.* 296 (1), 198–201. doi:10.1016/0006-8993(84)90533-x

Gonzalez-Perez, F., Udina, E., and Navarro, X. (2013). Extracellular Matrix Components in Peripheral Nerve Regeneration. *Int. Rev. Neurobiol.* 108, 257–275. doi:10.1016/B978-0-12-410499-0.00010-1

Guthoff, R. F., Wienss, H., Hahnel, C., and Wree, A. (2005). Epithelial Innervation of Human Cornea. *Cornea* 24 (5), 608–613. doi:10.1097/01.ico.0000154384.05614.8f

Hamrah, P., Qazi, Y., Shahatit, B., Dastjerdi, M. H., Pavan-Langston, D., Jacobs, D. S., et al. (2017). Corneal Nerve and Epithelial Cell Alterations in Corneal Allodynia: An *In Vivo* Confocal Microscopy Case Series. *Ocul. Surf.* 15 (1), 139–151. doi:10.1016/j.jtos.2016.10.002

Herndon, D. N., and Tompkins, R. G. (2004). Support of the Metabolic Response to Burn Injury. *The Lancet* 363, 1895–1902. doi:10.1016/s0140-6736(04)16360-5

Joo, M.-J., Yuhan, K. R., Hyon, J. Y., Lai, H., Hose, S., Sinha, D., et al. (2004). The Effect of Nerve Growth Factor on Corneal Sensitivity after LaserIn Situ Keratomileusis. *Arch. Ophthalmol.* 122 (9), 1338–1341. doi:10.1001/archopht.122.9.1338

Labetoulle, M., Baudouin, C., Calonge, M., Merayo-Lloves, J., Boboridis, K. G., Akova, Y. A., et al. (2019). Role of Corneal Nerves in Ocular Surface Homeostasis and Disease. *Acta Ophthalmol.* 97, 137–145. doi:10.1111/aos.13844

Ma, K., Yan, N., Huang, Y., Cao, G., Deng, J., and Deng, Y. (2014). Effects of Nerve Growth Factor on Nerve Regeneration after Corneal Nerve Damage. *Int. J. Clin. Exp. Med.* 7 (11), 4584–4589.

Mohan, R. R., Hutcheon, A. E. K., Choi, R., Hong, J., Lee, J., Mohan, R. R., et al. (2003). Apoptosis, Necrosis, Proliferation, and Myofibroblast Generation in the Stroma Following LASIK and PRK. *Exp. Eye Res.* 76 (1), 71–87. doi:10.1016/s0014-4835(02)00251-8

Olivieri, M., Cristaldi, M., Pezzino, S., Lupo, G., Anfuso, C. D., Gagliano, C., et al. (2018). Experimental Evidence of the Healing Properties of Lactobionic Acid for Ocular Surface Disease. *Cornea* 37 (8), 1058–1063. doi:10.1097/ICO.0000000000001594

Pache, M., and Flammer, J. (2006). A Sick Eye in a Sick Body? Systemic Findings in Patients with Primary Open-Angle Glaucoma. *Surv. Ophthalmol.* 51 (3), 179–212. doi:10.1016/j.survophthal.2006.02.008

Rivera, A., Raymond, M., Grobman, A., Abouyared, M., and Angeli, S. I. (2017). The Effect of N-Acetyl-Cysteine on Recovery of the Facial Nerve after Crush Injury. *Laryngoscope Invest. Otolaryngol.* 2 (3), 109–112. doi:10.1002/lio2.68

Romano, M. R., Biagioni, F., Carrizzo, A., Lorusso, M., Spadaro, A., Micelli Ferrari, T., et al. (2014). Effects of Vitamin B12 on the Corneal Nerve Regeneration in Rats. *Exp. Eye Res.* 120, 109–117. doi:10.1016/j.exer.2014.01.017

Rusciano, D., Roszkowska, A. M., Gagliano, C., and Pezzino, S. (2016). Free Amino Acids: an Innovative Treatment for Ocular Surface Disease. *Eur. J. Pharmacol.* 787, 9–19. doi:10.1016/j.ejphar.2016.04.029

Sacchetti, M., Di Zazzo, A., and Bonini, S. (2012). Effetto degli aminoacidi somministrati per via topica in pazienti con secchezza oculare. *Ottica Fisiopat*, XVII.

Schmidt, J. A., Rinaldi, S., Scalbert, A., Ferrari, P., Achaintre, D., Gunter, M. J., et al. (2016). Plasma Concentrations and Intakes of Amino Acids in Male Meat-Eaters, Fish-Eaters, Vegetarians and Vegans: a Cross-Sectional Analysis in the EPIC-Oxford Cohort. *Eur. J. Clin. Nutr.* 70 (3), 306–312. doi:10.1038/ejcn.2015.144

Sipahi, S., Gungor, O., Gunduz, M., Clici, M., Demirci, M. C., and Tamer, A. (2013). The Effect of Oral Supplementation with a Combination of Beta-Hydroxy-Beta-Methylbutyrate, Arginine and Glutamine on Wound Healing: a Retrospective Analysis of Diabetic Haemodialysis Patients. *BMC Nephrol.* 14. doi:10.1186/1471-2369-14-8

Stechmiller, J. K. (2010). Understanding the Role of Nutrition and Wound Healing. *Nutr. Clin. Pract.* 25, 61–68. doi:10.1177/0884533609358997

Stern, M. E., Gao, J., Siemasko, K. F., Beuerman, R. W., and Pflugfelder, S. C. (2004). The Role of the Lacrimal Functional Unit in the Pathophysiology of Dry Eye. *Exp. Eye Res.* 78 (3), 409–416. doi:10.1016/j.exer.2003.09.003

Tomás-Juan, J., Murueta-Goyena Larrañaga, A., and Hanneken, L. (2015). Corneal Regeneration after Photorefractive Keratectomy: A Review. *J. Optom.* 8, 149–169. doi:10.1016/j.optom.2014.09.001

Torres Munoz, I., Grizzi, F., Russo, C., Camesasca, F. I., Dioguardi, N., and Vinciguerra, P. (2003). The Role of Amino Acids in Corneal Stromal Healing: a Method for Evaluating Cellular Density and Extracellular Matrix Distribution. *J. Refract Surg.* 19 (2 Suppl. l), S227–S230.

Vinciguerra, P., Camesasca, F. I., and Ponzin, D. (2002). Use of Amino Acids in Refractive Surgery. *J. Refract Surg.* 18 (3 Suppl. l), S374–S377. doi:10.3928/1081-597x-20020502-20

Wang, H., Xiao, C., Dong, D., Lin, C., Xue, Y., Liu, J., et al. (2018). Epothilone B Speeds Corneal Nerve Regrowth and Functional Recovery through Microtubule Stabilization and Increased Nerve Beading. *Sci. Rep.* 8 (1), 2647. doi:10.1038/s41598-018-20734-1

Whitnall, M. H., and Grafstein, B. (1981). The Relationship between Extracellular Amino Acids and Protein Synthesis Is Altered during Axonal Regeneration. *Brain Res.* 220 (2), 362–366. doi:10.1016/0006-8993(81)91226-9

Yam, G. H.-F., Williams, G. P., Setiawan, M., Yusoff, N. Z. B. M., Lee, X.-w., Htoon, H. M., et al. (2017). Nerve Regeneration by Human Corneal Stromal Keratocytes and Stromal Fibroblasts. *Sci. Rep.* 7, 45396. doi:10.1038/srep45396

Yildiran, H., Macit, M. S., and Özata Uyar, G. (2020). New Approach to Peripheral Nerve Injury: Nutritional Therapy. *Nutr. Neurosci.* 23 (10), 744–755. doi:10.1080/1028415X.2018.1554322

Conflict of Interest: DR is an employee of Sooft SpA, the pharmaceutical company selling the food supplement Aminoftal, used in this study.

The remaining authors declare that the research was conducted in the absence of any commercial or financial relationships that could be construed as a potential conflict of interest.

Publisher's Note: All claims expressed in this article are solely those of the authors and do not necessarily represent those of their affiliated organizations, or those of the publisher, the editors and the reviewers. Any product that may be evaluated in this article, or claim that may be made by its manufacturer, is not guaranteed or endorsed by the publisher.

frontiers in Pharmacology

ORIGINAL RESEARCH
published: 16 August 2021
doi: 10.3389/fphar.2021.707909

Short-and Long-Term Expression of Vegf: A Temporal Regulation of a Key Factor in Diabetic Retinopathy

Claudio Bucolo[1,2†], Annalisa Barbieri[3†], Ilaria Viganò[4], Nicoletta Marchesi[3], Francesco Bandello[5], Filippo Drago[1,2], Stefano Govoni[3], Gianpaolo Zerbini[4] and Alessia Pascale[3]*

[1]Department of Biomedical and Biotechnological Sciences, School of Medicine, University of Catania, Catania, Italy, [2]Center for Research in Ocular Pharmacology–CERFO, University of Catania, Catania, Italy, [3]Department of Drug Sciences, Pharmacology Section, University of Pavia, Pavia, Italy, [4]Complications of Diabetes Unit, Diabetes Research Institute, IRCCS Ospedale San Raffaele, Milan, Italy, [5]Department of Ophthalmology, IRCCS Ospedale San Raffaele, Vita-Salute University, Milan, Italy

To investigate the role of vascular endothelial growth factor (VEGF) at different phases of diabetic retinopathy (DR), we assessed the retinal protein expression of VEGF-A_{164} (corresponding to the $VEGF_{165}$ isoform present in humans, which is the predominant member implicated in vascular hyperpermeability and proliferation), HIF-1α and PKCβ/HuR pathway in *Ins2*^{Akita} (diabetic) mice at different ages. We used C57BL6J mice (WT) at different ages as control. Retina status, in terms of tissue morphology and neovascularization, was monitored *in vivo* at different time points by optical coherence tomography (OCT) and fluorescein angiography (FA), respectively. The results showed that VEGF-A_{164} protein expression increased along time to become significantly elevated ($p < 0.05$) at 9 and 46 weeks of age compared to WT mice. The HIF-1α protein level was significantly ($p < 0.05$) increased at 9 weeks of age, while PKCβII and HuR protein levels were increased at 46 weeks of age compared to WT mice. The thickness of retinal nerve fiber layer as measured by OCT was decreased in *Ins2*^{Akita} mice at 9 and 46 weeks of age, while no difference in the retinal vasculature were observed by FA. The present findings show that the retina of the diabetic *Ins2*^{Akita} mice, as expected for mice, does not develop proliferative retinopathy even after 46 weeks. However, diabetic *Ins2*^{Akita} mice recapitulate the same evolution of patients with DR in terms of both retinal neurodegeneration and pro-angiogenic shift, this latter indicated by the progressive protein expression of the pro-angiogenic isoform VEGF-A_{164}, which can be sustained by the PKCβII/HuR pathway acting at post-transcriptional level. In agreement with this last concept, this rise in VEGF-A_{164} protein is not paralleled by an increment of the corresponding transcript. Nevertheless, the observed increase in HIF-1α at 9 weeks indicates that this transcription factor may favor, in the early phase of the disease, the transcription of other isoforms, possibly neuroprotective, in the attempt to counteract the neurodegenerative effects of VEGF-A_{164}. The time-dependent VEGF-A_{164} expression in the retina of diabetic *Ins2*^{Akita} mice suggests that pharmacological intervention in DR might be chosen, among other reasons, on the basis of the specific stages of the pathology in order to pursue the best clinical outcome.

Keywords: VEGF, ELAV/HuR, retinopathy, diabetes, hyperglycemia, akita mouse

OPEN ACCESS

Edited by:
Valentina Vellecco, University of Naples Federico II, Italy

Reviewed by:
Shusheng Wang, Tulane University, United States
Sanjoy K. Bhattacharya, University of Miami, United States

****Correspondence:***
Gianpaolo Zerbini
zerbini.gianpaolo@hsr.it

†These authors have contributed equally to this work

Specialty section:
This article was submitted to Experimental Pharmacology and Drug Discovery, a section of the journal Frontiers in Pharmacology

Received: *10 May 2021*
Accepted: *06 August 2021*
Published: *16 August 2021*

Citation:
Bucolo C, Barbieri A, Viganò I, Marchesi N, Bandello F, Drago F, Govoni S, Zerbini G and Pascale A (2021) Short-and Long-Term Expression of Vegf: A Temporal Regulation of a Key Factor in Diabetic Retinopathy. Front. Pharmacol. 12:707909. doi: 10.3389/fphar.2021.707909

INTRODUCTION

Diabetic retinopathy (DR) is the major eye complication of diabetes mellitus and represents the leading cause of preventable blindness in the working age population, where roughly 90% of patients with type 1 diabetes and approximately 80% with type 2 diabetes for over 10 years will face the disease (Campbell and Doyle, 2019). Among common causes for blindness or severe vision impairment, DR takes the fifth place, and a recent meta-analysis underscores that, due to population growth together with a rise in the corresponding average age, the age-standardized prevalence of DR-related blindness will increase in the future (Leasher et al., 2016; Hammes 2018). The mechanisms involved in the progression of DR, characterized by an initial and prolonged ischemic phase followed by an aggressive vascular proliferation, are still argument of investigation. In particular, the role of VEGF (a factor involved in angiogenesis and cell permeability) on DR progression is still poorly understood. According to the level of microvascular- and ischemic-related damage, DR can be classified into two stages: an early non-proliferative stage (NPDR) and an advanced proliferative stage (PDR). The earliest sign of DR is the loss of pericytes contributing to inner blood-retinal barrier breakdown (Arboleda-Velasquez et al., 2015). Hallmarks of DR are also the increasing thickness of the basement membrane, the hyper-permeability, and the formation of microaneurysms. These functional alterations are followed by microvascular occlusions leading to a progressive retinal ischemia that induces the expression of the Vascular Endothelial Growth Factor-A (VEGF-A). VEGF-A, and especially the main pro-angiogenic isoform VEGF-A_{165}, has a primary role in promoting vascular hyperpermeability; indeed, *via* phosphorylation of endothelial tight junction proteins it modulates their degradation, finally leading to blood-retinal barrier disruption (Moran et al., 2016). Capillary leakage and subsequent retinal exudation and edema are typical features of the disease. Further, VEGF-A_{165} is a potent mitogen for endothelial cells triggering their proliferation, migration and tube formation resulting in the growth of new blood vessels along the inside surface of the retina and in the vitreous that, however, in the diabetic retina are fragile and may break (Antonetti et al., 2012). In turn, these events may entail vitreous hemorrhage, subsequent fibrosis, and tractional retinal detachment with risk of permanent vision loss in the affected eye (Dulull et al., 2019). Hence, due to this dual capability to promote both vascular permeability and pathologic angiogenic proliferation, VEGF-A constitutes a key player in DR and therefore a compelling druggable target (Amadio et al., 2016a; Zhao and Singh, 2018). Incidentally, analysis of VEGF-A interaction with binding domains of anti-angiogenic agents used in clinical practice is crucial in order to improve the design of new drugs (Platania et al., 2015).

VEGF-A expression can be regulated at both transcriptional, *via* hypoxia inducible factor-1α (HIF-1α), and post-transcriptional level through the PKCβ/HuR cascade (Amadio et al., 2008; Amadio et al., 2010; Amadio et al., 2012). Inside the retina the cells that may show an increased expression of VEGF in case of DR are retinal pigmented epithelial cells, pericytes, astrocytes, müller cells, glial cells, and endothelial cells (Antonetti et al., 2012).

The aim of the present study was to investigate the role of the PKCβII/HuR/VEGF-A pathway in the development of DR using the *Ins2^{Akita}* mouse animal model, which is characterized by a dominant mutation that induces the development of a spontaneous insulin-dependent diabetes with a rapid onset (Barber et al., 2005). Moreover, besides assessing the post-transcriptional involvement of the PKCβII/HuR cascade in regulating VEGF-A_{164} (corresponding to the $VEGF_{165}$ isoform present in humans) content, we also examined, in *Ins2^{Akita}* mice at different ages, the expression of HIF-1α to figure out the contribution of this specific transcriptional factor in the regulation of VEGF-A_{164} expression.

MATERIALS AND METHODS

Animals

The recent identification of *Ins2^{Akita}* mouse where diabetes, followed along time by the appearance of early signs of DR, develops as a consequence of a spontaneous mutation of the Insulin 2 gene makes it a unique model of "human diabetic complications" suitable for testing novel preventive approaches (Barber et al., 2005; Han et al., 2013).

Two groups of animals (5 per group), diabetic *Ins2^{Akita}* and normoglycemic (C57BL6) mice were followed for 46 weeks. Only males have been included in this study because disease progression in females is slower and less uniform (Han et al., 2013). *Ins2^{Akita}* female mice are resistant to develop diabetes and glycemia is often slightly, but not significantly increased when compared to controls (Al-Awar et al., 2016). Male C57BL6 and *Ins2^{Akita}* mice were housed in cages in a temperature-controlled room with a 12:12 light–dark cycle and free access to food and tap water. Body weight (g) and blood glucose concentrations (mg/dl) were measured weekly during the experimental period. The experimental study was approved by the Institutional Animal Care and Use Committee (IACUC) of the San Raffaele Scientific Institute in Milan, according to the National Legislation (D.L. 116/1992) and the European Directive (2010/63/EU) about the use of laboratory animals, and with the license of the Italian Board of Health.

Preparation of the Samples and Western Blotting

Retinae were homogenized, using a Teflon/glass homogenizer, in the following buffer: 20 mM Tris (pH 7.4), 2 mM EDTA, 0.5 mM EGTA, 50 mM β-mercaptoethanol, 0.32 mM sucrose and a protease inhibitor cocktail (Roche Molecular Biochemicals, Mannheim, Germany) at the dilution suggested by the manufacturer. Proteins were measured according to Bradford's method, using bovine albumin as internal standard. Then, the proteins were diluted in Sodium Dodecyl Sulphate (SDS) protein gel loading solution, boiled for 5 min, separated on SDS-PolyAcrylamide Gel Electrophoresis, and processed following

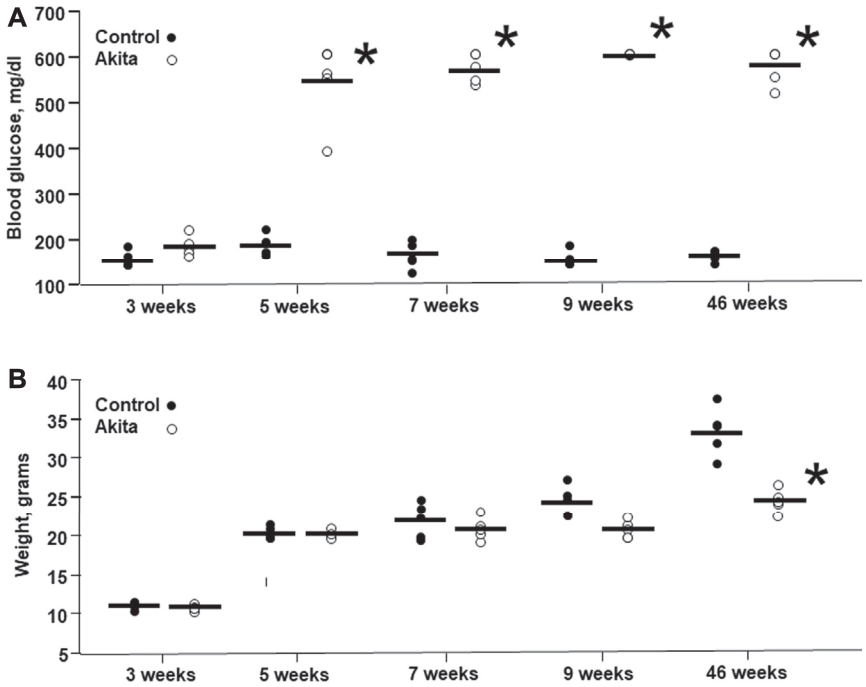

FIGURE 1 | Blood glucose levels and body weight in wild-type and *Ins2*^{Akita} mice animals at different ages. Blood glucose levels **(A)** are expressed in mg/dL, while body weight **(B)** is expressed in grams. The values are shown as filled dots for wild-type mice and open dots for *Ins2*^{Akita} animals *$p < 0.05$ student t-test, *vs* wild-type.

standard procedures. The mouse monoclonal anti-ELAV/HuR antibody (Santa Cruz Biotech. Inc., Dallas, TX, United States) was diluted at 1:1,000. The rabbit monoclonal antibodies anti-VEGF-A (Abcam, United Kingdom) and anti-HIF1α (Cell Signalling Technology, Netherlands) were diluted at 1:750 and 1:1,000, respectively. The rabbit polyclonal PKC βII (Santa Cruz Biotech. Inc.) was diluted at 1: 500, while the rat monoclonal antibody anti-α-tubulin (Thermo Fisher Scientific, Waltham, MA, United States) was diluted at 1:1,000. The specific antibodies were diluted in TBST buffer [10 mM Tris-HCl, 100 mM NaCl, 0.1% (v/v) Tween 20, pH 7.5] containing 6% milk. The nitrocellulose membrane signals were detected by chemiluminescence. Experiments were performed at least three times for each tissue preparation; the same membranes were reprobed with α-tubulin antibody to normalize the data. Statistical analysis of western blot data was performed on the densitometric values obtained with the ImageJ 1.50i software (downloadable at http://imagej.nih.image/ij).

Real Time RT-PCR

RNA was extracted from total homogenates by using RNeasy Mini Kit (Qiagen, Germany). The reverse transcription was performed following standard procedures. PCR amplifications were carried out using the Rotor-Gene Q instrument (Qiagen) in the presence of QuantiTect SYBR Green PCR mix (Qiagen) with the specific primers for $VEGF_{164}$ (provided by SIGMA). The GAPDH mRNA was chosen as the reference gene to normalize the data (the specific primers were provided by Qiagen).

Optical Coherence Tomography and Fluorescein Angiography

Optical coherence tomography (OCT) and fluorescein angiography (FA) were performed as previously described (Buccarello et al., 2017), taking advantage of the Micron IV instrument (Phoenix Research Laboratories, Pleasanton, CA, United States). Briefly, after anesthesia, mydriasis was induced by administering a drop of tropicamide 0.5% (Visumidriatic, Tibilux Pharma, Milan, Italy) in each eye. OCT images were acquired by performing a circular scan of 550 μm of diameter around the optic nerve head. Both eyes were examined, and the results were averaged. The segmentation of retinal layers was performed using Insight software (Phoenix Research Laboratories, Pleasanton, CA, United States), OCT was followed by the FA study. A solution of 1% fluorescein (5 ml/kg Monico S.p.A., Venezia, Italy) was administered by a single intraperitoneal injection (100 μL). For each animal, the images of central and peripheral retinal vasculature were acquired.

Statistical Analysis

For statistical analysis, the GraphPad Instat statistical package (version 3.05 GraphPad software, San Diego, CA, United States) was used. The data were analyzed by analysis of variance (ANOVA) followed, when significant, by an appropriate *post hoc* comparison test, as detailed in the legends. Differences were considered statistically significant when p values <0.05.

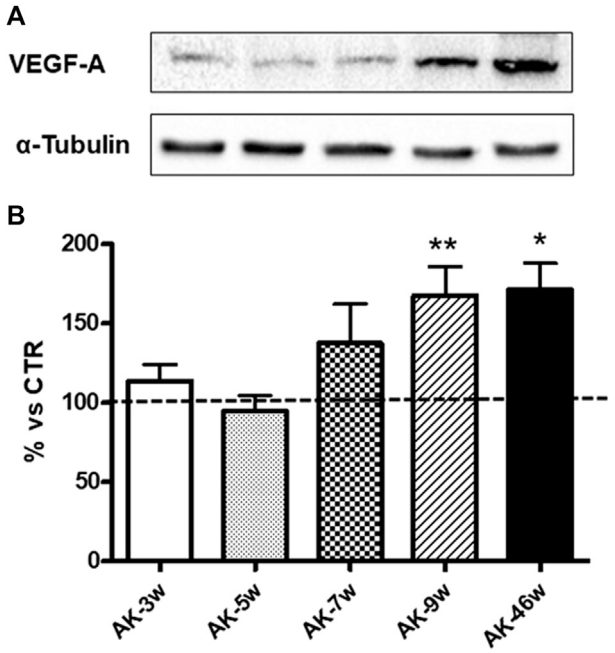

FIGURE 2 | VEGF-A protein levels in *Ins2*^{Akita} mice at different ages. **(A)**: Representative western blottings of VEGF-A_{164} and the respective α-tubulin, measured in the same samples, of total homogenates of retinae from *Ins2*^{Akita} (AK) mice at different ages (w = weeks). **(B)**: Densitometric analysis of VEGF-A_{164} immunoreactivities in the total homogenates of retinae from wild-type and AK mice at different ages. Alpha-tubulin was used as a loading control. Results are expressed as % (±S.E.M.) *vs* control wild-type (100%, dashed line). *$p < 0.05$, **$p < 0.01$ *vs* wild-type; Tukey's Multiple Comparison *post-hoc* test, n = 8–10.

RESULTS

Blood glucose levels, measured at 5, 7, 9, and 46 weeks of age, were significantly increased in *Ins2*^{Akita} mice in comparison with their relative wild-type littermates (**Figure 1A**). Conversely, body weight measured at 9 and 46 weeks of age was significantly reduced in *Ins2*^{Akita} mice, as a consequence of glycosuria, in comparison with their respective wild-type controls, reaching a statistical significance in 46 weeks old animals (**Figure 1B**).

VEGF protein is increased in *Ins2*^{Akita} mice: a time-dependent contribution of transcriptional and post-transcriptional mechanisms.

Given the key role of VEGF-A_{165} in DR development, we assessed its protein expression in wild-type and *Ins2*^{Akita} mice at different ages. As shown in **Figure 2**, in *Ins2*^{Akita} mice we found an increase in VEGF-A_{164} content (as previously mentioned, this isoform corresponds to the VEGF-A_{165} present in humans) already at 7 weeks (+38%), which reaches a statistical significance in 9 (+67%) and 46 (+71%) weeks old animals with respect to their relative wild-type littermates. No age-dependent changes in VEGF-A_{164} protein basal levels, measured in an independent set of experiments, were observed among wild-type mice (**Figure 3**).

We also measured VEGF-A_{164} mRNA levels *via* Real-time PCR. Preliminary results indicate a significant decrease in VEGF-A_{164} transcript content at 9 and 46 weeks (−78%, $p < 0.005$ and −63%, $p < 0.05$, respectively) compared to 3 weeks *Ins2*^{Akita} mice.

With the purpose of dissecting the implication of both transcriptional and post-transcriptional mechanisms in the regulation of VEGF-A_{164} protein expression, we measured, respectively, HIF-1α and PKCβII/HuR protein levels in the retina from wild-type and *Ins2*^{Akita} mice at different ages.

Concerning HIF-1α, as depicted in **Figure 4**, in *Ins2*^{Akita} mice we observed a progressive increase in its protein content starting from 3 weeks (+25%) to 7 weeks old animals (5 weeks: +41%; 7 weeks: +49%), reaching a statistically significant rise in 9 weeks old mice (+87%). Instead, a decrease was found in 46 weeks old *Ins2*^{Akita} mice (−33%), whose levels were significantly lower with respect to 9 weeks old *Ins2*^{Akita}animals. No age-dependent changes in HIF-1α protein basal levels, measured in an independent set of experiments, were observed among wild-type mice (**Figure 3**).

We then investigated the PKCβII/HuR pathway, since we previously demonstrated, in another animal model of DR, its key involvement in the post-transcriptional control of VEGF-A protein expression (Amadio et al., 2010). As shown in **Figure 5**, we observed a significant increase in both PKCβII (+29%) and HuR (+48%) protein levels only in 46 weeks old *Ins2*^{Akita} mice. No age-dependent changes in PKCβII and HuR protein basal levels, measured in an independent set of experiments, were observed among wild-type mice (**Figure 3**).

OCT and Fluorescein Angiography Evaluation

OCT and fluorescein angiography were performed during the entire study in wild-type and *Ins2*^{Akita} diabetic mice (**Figure 6**). The collected images did not highlight any retinal signs of vascular dysfunction in both groups of animals. Thickness of Retinal Nerve Fiber Layer (RNFL) was also examined. The results show a significant decrease in RNFL thickness in 9 weeks of age *Ins2*^{Akita} mice compared to wild-type littermates, which becomes even more pronounced in 46 weeks old animals (**Figure 7**).

DISCUSSION

Diabetic retinopathy is the primary cause of blindness in adults living in industrialized countries, being the global prevalence around 30–35% within the diabetic population. The loss of visual function is mainly associated with macular edema and the proliferative stage of the disease, with a dramatic impact in terms of countries health system costs. DR is triggered by the chronic hyperglycemia linked to the diabetic condition and by the following metabolic stress. This altered milieu induces changes at microvascular level that result in the inability of capillaries to guarantee to the retina the proper blood supply, thus entailing the formation of non-perfused areas and the development of a hypoxic environment that promotes the production of VEGF-A, a pivotal player in DR pathophysiology (Rigo et al., 2020).

VEGF-A belongs to a family that also includes VEGF-B, -C, -D, and placental growth factor (Amadio et al., 2016a; Ferrara

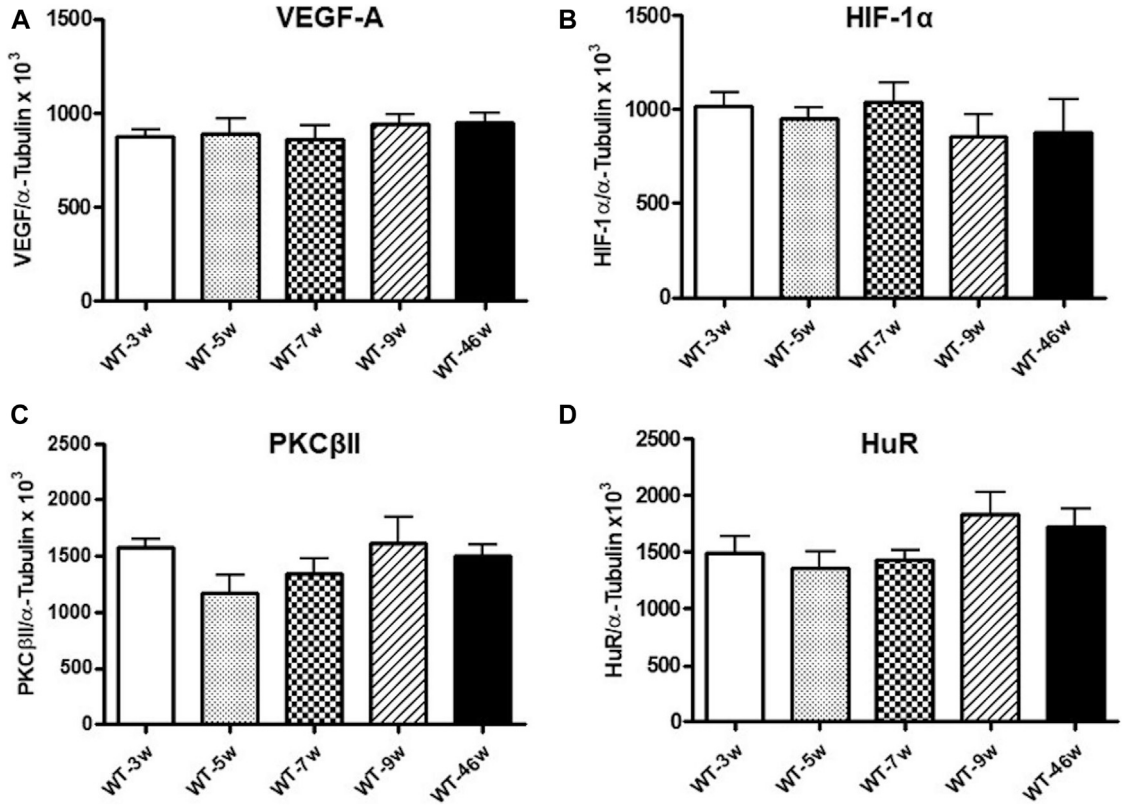

FIGURE 3 | VEGF-A, HIF-1α, PKCβII and HuR protein levels in wild-type mice at different ages. Densitometric analysis of VEGF-A_{164} **(A)**, HIF-1α **(B)**, PKCβII **(C)**, and HuR **(D)** immunoreactivities in the total homogenates of retinae from wild-type (WT) mice at different ages (w = weeks). Alpha-tubulin was used as a loading control. Results are expressed as mean grey levels ratios x 10^3 (mean ± S.E.M.) of VEGF-A_{164}/α-tubulin **(A)**, HIF-1α/α-tubulin **(B)**, PKCβII/α-tubulin **(C)** and HuR/α-tubulin **(D)** immunoreactivities measured by Western blotting, n = 5.

and Adamis, 2016). The human VEGF-A gene consists of eight exons separated by seven introns determining the generation of different isoforms, being the VEGF-A_{165} the predominant member and the main isoform implicated in vascular hyperpermeability and proliferation (Amadio et al., 2016a). In the diabetic retina, the expression of VEGF-A can be regulated by different pathways, including Protein Kinase C (PKC) (Clarke and Dodson, 2007; Yokota et al., 2007; Ye et al., 2010). PKC consists of at least 10 serine-threonine kinases ubiquitously expressed and involved in several cellular functions (Battaini and Mochly-Rosen, 2007; Govoni et al., 2010). It is worth of note, that the diabetes-related hyperglycemia induces a rise in the amount of diacylglycerol, the physiological activator of PKC. Among the various isoforms, the PKCβ seems to be the isoenzyme primarily activated in the retina, although other PKCs can be also implicated (Aiello, 2002; Kim et al., 2010).

In the present study, we used the *Ins2*^{Akita} mouse as an animal model of type 1 diabetes, which is endowed with a dominant mutation that induces the development of a spontaneous insulin-dependent diabetes with a rapid onset (Barber et al., 2005). Notably, the mutation in the Insulin 2 gene elicits a conformational change in the insulin protein and its consequent accumulation in pancreatic β cells, leading to β-cells death (Olivares et al., 2017). As supported by literature data, the *Ins2*^{Akita} mouse is an excellent model to explore the molecular mechanisms implicated in the initiation and early progression of DR. The development, in the *Ins2*^{Akita} mouse of the late, neovascular stages of DR remains presently unclear (Han et al., 2013; McLenachan et al., 2013). Indeed, we showed that by 5 weeks of age the animals present already significantly elevated levels of blood glucose compared to wild-type littermates, while a decrease in the body weight, due to glycosuria, is evident starting from 9 weeks of age. We also observed a time-dependent increase in VEGF-A_{164} (this isoform corresponds to the VEGF-A_{165} present in humans) content at retinal level, starting from 7 weeks of age and becoming gradually more pronounced. This rise in VEGF-A_{164} protein is not paralleled by an increment of the corresponding transcript, strongly suggesting that it can be sustained by the PKCβII/HuR pathway acting at post-transcriptional level. Nevertheless, the observed increase in HIF-1α at 9 weeks indicates that this transcription factor may favor, in the early phase of the disease, the transcription of other isoforms, possibly neuroprotective, in the attempt to counteract

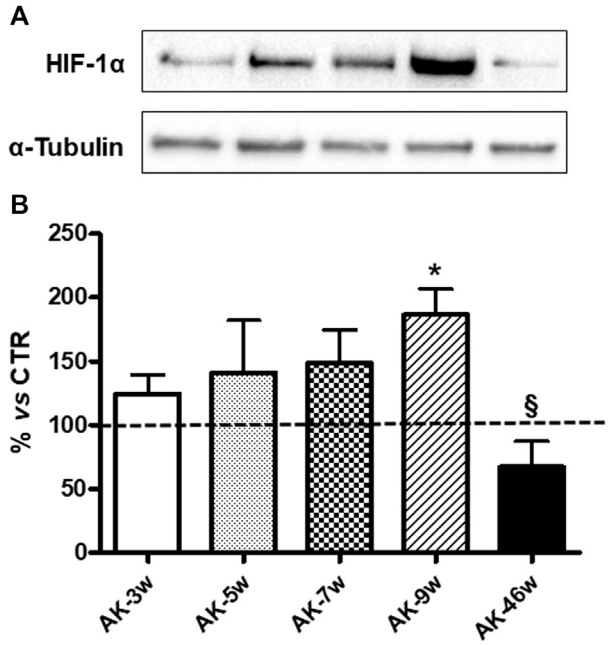

FIGURE 4 | HIF-1α protein levels in *Ins2*^{Akita} mice at different ages. **(A)**: Representative western blottings of HIF-1α and the respective α-tubulin, measured in the same samples, of total homogenates of retinae from *Ins2*^{Akita} (AK) mice at different ages (w = weeks). **(B)**: Densitometric analysis of HIF-1α immunoreactivities in the total homogenates of retinae from wild-type and AK mice at different ages. Alpha-tubulin was used as a loading control. Results are expressed as % (±S.E.M.) *vs* control wild-type (100%, dashed line). $^{*}p < 0.05$ *vs* wild-type and $^{§}p < 0.05$ *vs* AK-9w; Tukey's Multiple Comparison *post-hoc* test, n = 8–10.

the neurodegenerative effects of VEGF-A_{164}. It is worth of note, that our data show a distinct temporal regulation of VEGF-A expression, implicating two different molecular processes: transcriptional and post-transcriptional. In fact, the transcription factor HIF-1α seems to contribute to the earlier increase in VEGF-A protein content, possibly trying to counteract the neurodegenerative effects of DR through the promotion of neuroprotective VEGF-A isoforms, such as $VEGF_{120/121}$. The late rise in VEGF-A seems, instead, to rely upon the PKCβII/HuR cascade acting at post-transcriptional level, which favors the expression of $VEGF_{164}$, the member primary implicated in vascular hyperpermeability and proliferation. To this last regard, these results confirm our previous findings showing, both *in vitro* (Amadio et al., 2008; Amadio et al., 2012; Marchesi et al., 2020; Platania et al., 2020) and *in vivo* (Amadio et al., 2010), a post-transcriptional control of VEGF-A expression mediated by the RNA binding protein (RBP) ELAV/HuR.

In mammals, ELAV proteins are a small family of evolutionarily conserved RBPs, orthologues of the elav gene discovered in the fruit fly Drosophila melanogaster. The family includes the ubiquitously expressed HuR and three neuron-specific members (nELAV), namely HuB, HuC, and HuD. The four ELAV proteins can virtually influence any aspect of the post-synthesis fate of the targeted mRNAs, being stability and translation the most relevant and studied mechanisms. Indeed, following intra- and extracellular inputs, ELAV mainly determine an increase in the cytoplasmic stability and/or rate of translation of the target transcripts, by preferentially binding to ARE (adenine-uracil-rich elements) *cis-acting* elements present within their sequence, although other

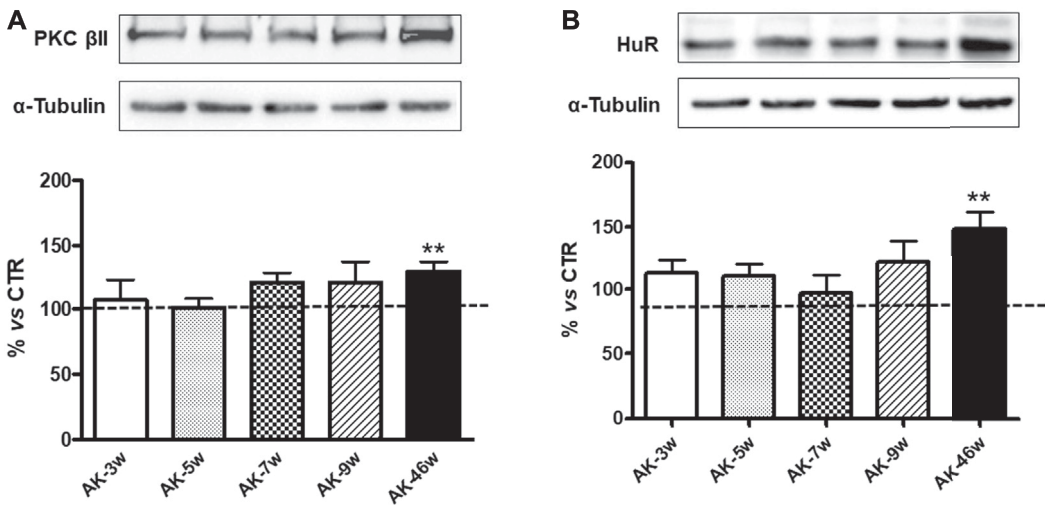

FIGURE 5 | PKCβII and HuR protein levels in *Ins2*^{Akita} mice at different ages. Upper panels: Representative western blottings of PKCβII **(A)**, HuR **(B)** and the respective α-tubulin, measured in the same samples, of total homogenates of retinae from *Ins2*^{Akita} (AK) mice at different ages (w = weeks). Lower panels: Densitometric analysis of PKCβII **(A)** and HuR **(B)** immunoreactivities in the total homogenates of retinae from wild-type and AK mice at different ages. Alpha-tubulin was used as a loading control. Results are expressed as % (±S.E.M.) *vs* control wild-type (100%, dashed line). $^{**}p < 0.01$ *vs* wild-type; unpaired *t*-test, n = 8–10.

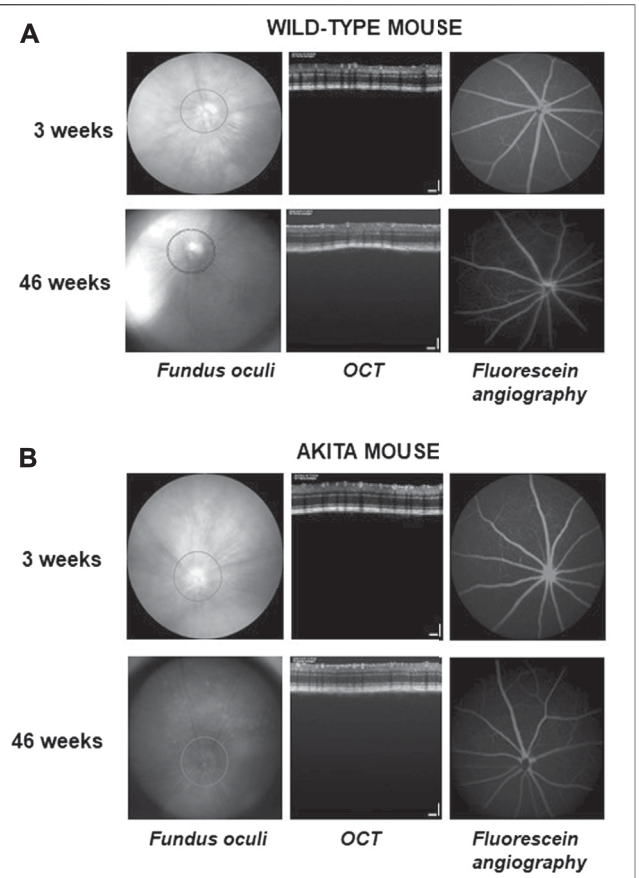

FIGURE 6 | Fundus oculi **(left)**, optical coherence tomography (OCT; center) and fluorescein angiography **(right)** performed during the study in wild-type and *Ins2*^{Akita} animals. The shown images were taken in the left eye of a representative wild-type **(A)** or *Ins2*^{Akita} **(B)** mice at 3 and 46 weeks of age.

intravenous injection of streptozotocin (STZ), we previously demonstrated that, following a PKC β-mediated phosphorylation, the ELAV/HuR binds to VEGF-A mRNA and positively affects its expression in the retina, thus contributing to abnormally enhanced VEGF-A content in the retinal tissue (Amadio et al., 2010). Notably, STZ-induced diabetic rats show the same features of the NPDR observed in humans, including blood vessels dilation and increased vascular permeability. Further, we also reported that nano-systems loaded with a commercially available siRNA, which specifically switches off the ELAV/HuR expression when injected into the eye of diabetic rats, was able to attenuate the increase in VEGF-A content without suppressing its basal levels (Amadio et al., 2016b). These findings, together with the present data underline the key role of the PKCβ/HuR cascade in regulating the pathologic overexpression of VEGF. Incidentally, the use of nano- or micro-systems could be useful to ameliorate the intra-ocular delivery of pharmacological agents (Conti et al., 1997).

The results obtained by OCT, a non-invasive imaging technique that allows collecting information on the retina morphology, indicate that the retinal nerve fiber layer (RNFL) thickness is dramatically reduced in 46 weeks of age *Ins2*^{Akita} mice, and strongly suggest that this neurodegenerative event may be sustained by the increased VEGF-A_{164} levels. Within this general context, it should be taken into consideration that the VEGF-A gene is alternatively spliced to generate VEGF-A_{xxxa} and VEGF-A_{xxxb} isoforms, being the last ones potentially endowed with anti-angiogenic and anti-permeability properties (Qiu et al., 2009). Of interest, it has been reported that DR is associated with a switch in splicing from anti-towards pro-angiogenic isoforms (Perrin et al., 2005). Although the antibody used in the study allowed us to primarily detect VEGF-A_{164a}, it is tempting to speculate that the observed increase in this isoform goes to the

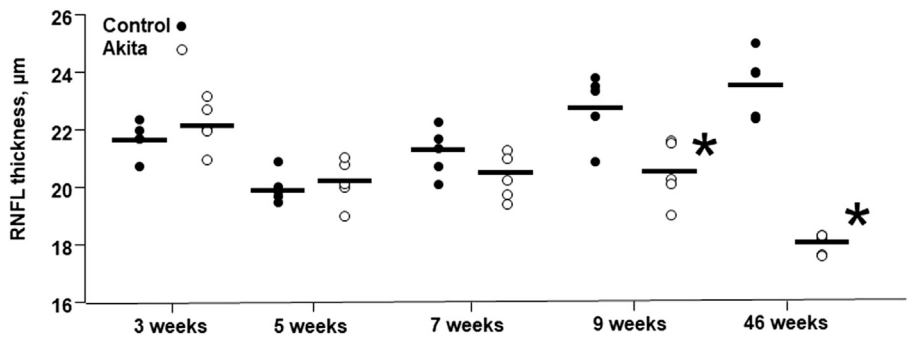

FIGURE 7 | Retinal nerve fiber layer thickness in wild-type and *Ins2*^{Akita} animals. Retinal nerve fiber layer (RNFL) thickness is expressed in µm and the values are shown as filled dots for wild-type mice and open dots for *Ins2*^{Akita} animals. *$p < 0.05$, student *t*-test *vs* control wild-type.

consensus elements may be implicated (Pascale and Govoni, 2012).

Within this context, in another model of experimental diabetes induced in rodents, namely rats exposed to a single

detriment of the corresponding VEGF-A_{164b}, which has a critical role in cell protection and survival (Peiris-Pagès 2012). Therefore, this switch in isoforms production might promote a degenerative process in the retina leading to a decrease in RNFL thickness, as

we detected in the present work. Nevertheless, it should be also underlined that the literature data regarding VEGF-A_{xxxb} isoforms are conflicting, and some authors even question the existence of VEGF-A_{xxxb} isoforms themselves (Harris et al., 2012; Bridgett et al., 2017).

In conclusion, these data seem to suggest that pharmacological intervention in clinical practice might be chosen, among other reasons, based on the specific stages of the diabetic retinopathy to pursue the best clinical outcome. Clinical studies to evaluate this possibility may be warranted.

DATA AVAILABILITY STATEMENT

The raw data supporting the conclusions of this article will be made available by the authors, without undue reservation.

ETHICS STATEMENT

The animal study was reviewed and approved by Institutional Animal Care and Use Committee (IACUC) of the San Raffaele Scientific Institute in Milan.

AUTHOR CONTRIBUTIONS

CB, GZ, and AP made substantial contributions to conception, design, and interpretation of data. AB, NM, GZ, AP, and IV carried out experiments. AB, NM, GZ, AP, and IV carried out formal analysis of data. CB, GZ, and AP wrote initial draft of the manuscript. CB, AB, GZ, AP, FD, SG, and FB reviewed the manuscript critically for important intellectual content and gave final approval of the version to be submitted.

FUNDING

This work was supported by National Grant PRIN 2015JXE7E8 from the Italian Ministry of Education, University and Research (MIUR).

SUPPLEMENTARY MATERIAL

The Supplementary Material for this article can be found online at: https://www.frontiersin.org/articles/10.3389/fphar.2021.707909/full#supplementary-material

REFERENCES

Aiello, L. P. (2002). The Potential Role of PKC Beta in Diabetic Retinopathy and Macular Edema. *Surv. Ophthalmol.* 47, S263–S269. doi:10.1016/s0039-6257(02)00391-0

Al-Awar, A., Kupai, K., Veszelka, M., Szűcs, G., Attieh, Z., Murlasits, Z., et al. (2016). Experimental Diabetes Mellitus in Different Animal Models. *J. Diabetes Res.* 2016, 9051426. doi:10.1155/2016/9051426

Amadio, M., Bucolo, C., Leggio, G. M., Drago, F., Govoni, S., and Pascale, A. (2010). The PKCbeta/HuR/VEGF Pathway in Diabetic Retinopathy. *Biochem. Pharmacol.* 80 (8), 1230–1237. doi:10.1016/j.bcp.2010.06.033

Amadio, M., Govoni, S., and Pascale, A. (2016a). Targeting VEGF in Eye Neovascularization: What's New?: A Comprehensive Review on Current Therapies and Oligonucleotide-Based Interventions under Development. *Pharmacol. Res.* 103, 253–269. doi:10.1016/j.phrs.2015.11.027

Amadio, M., Osera, C., Lupo, G., Motta, C., Drago, F., Govoni, S., et al. (2012). Protein Kinase C Activation Affects, via the mRNA-Binding Hu-Antigen R/ELAV Protein, Vascular Endothelial Growth Factor Expression in a Pericytic/endothelial Coculture Model. *Mol. Vis.* 18, 2153–2164.

Amadio, M., Pascale, A., Cupri, S., Pignatello, R., Osera, C., D Agata, V. V., et al. (2016b). Nanosystems Based on siRNA Silencing HuR Expression Counteract Diabetic Retinopathy in Rat. *Pharmacol. Res.* 111, 713–720. doi:10.1016/j.phrs.2016.07.042

Amadio, M., Scapagnini, G., Lupo, G., Drago, F., Govoni, S., and Pascale, A. (2008). PKCbetaII/HuR/VEGF: A New Molecular cascade in Retinal Pericytes for the Regulation of VEGF Gene Expression. *Pharmacol. Res.* 57 (1), 60–66. doi:10.1016/j.phrs.2007.11.006

Antonetti, D. A., Klein, R., and Gardner, T. W. (2012). Diabetic Retinopathy. *N. Engl. J. Med.* 366 (13), 1227–1239. doi:10.1056/NEJMra1005073

Arboleda-Velasquez, J. F., Valdez, C. N., Marko, C. K., and D'Amore, P. A. (2015). From Pathobiology to the Targeting of Pericytes for the Treatment of Diabetic Retinopathy. *Curr. Diab. Rep.* 15 (2), 573–592. doi:10.1007/s11892-014-0573-2

Barber, A. J., Antonetti, D. A., Kern, T. S., Reiter, C. E., Soans, R. S., Krady, J. K., et al. (2005). The Ins2Akita Mouse as a Model of Early Retinal Complications in Diabetes. *Invest. Ophthalmol. Vis. Sci.* 46 (6), 2210–2218. doi:10.1167/iovs.04-1340

Battaini, F., and Mochly-Rosen, D. (2007). Happy Birthday Protein Kinase C: Past, Present and Future of a Superfamily. *Pharmacol. Res.* 55 (6), 461–466. doi:10.1016/j.phrs.2007.05.005

Bridgett, S., Dellett, M., and Simpson, D. A. (2017). RNA-sequencing Data Supports the Existence of Novel VEGFA Splicing Events but Not of VEGFAxxxb Isoforms. *Sci. Rep.* 7 (1), 58. doi:10.1038/s41598-017-00100-3

Buccarello, L., Sclip, A., Sacchi, M., Castaldo, A. M., Bertani, I., ReCecconi, A., et al. (2017). The C-Jun N-Terminal Kinase Plays a Key Role in Ocular Degenerative Changes in a Mouse Model of Alzheimer Disease Suggesting a Correlation between Ocular and Brain Pathologies. *Oncotarget* 8 (47), 83038–83051. doi:10.18632/oncotarget.19886

Campbell, M., and Doyle, S. L. (2019). Current Perspectives on Established and Novel Therapies for Pathological Neovascularization in Retinal Disease. *Biochem. Pharmacol.* 164, 321–325. doi:10.1016/j.bcp.2019.04.029

Clarke, M., and Dodson, P. M. (2007). PKC Inhibition and Diabetic Microvascular Complications. *Best Pract. Res. Clin. Endocrinol. Metab.* 21, 573–586. doi:10.1016/j.beem.2007.09.007

Conti, B., Bucolo, C., Giannavola, C., Puglisi, G., Giunchedi, P., and Conte, U. (1997). Biodegradable Microspheres for the Intravitreal Administration of Acyclovir: *In Vitro*/*In Vivo* Evaluation. *Eur. J. Pharm. Sci.* 5 (5), 287–293. doi:10.1016/S0928-0987(97)00023-7

Dulull, N., Kwa, F., Osman, N., Rai, U., Shaikh, B., and Thrimawithana, T. R. (2019). Recent Advances in the Management of Diabetic Retinopathy. *Drug Discov. Today* 24 (8), 1499–1509. doi:10.1016/j.drudis.2019.03.028

Ferrara, N., and Adamis, A. P. (2016). Ten Years of Anti-vascular Endothelial Growth Factor Therapy. *Nat. Rev. Drug Discov.* 15 (6), 385–403. doi:10.1038/nrd.2015.17

Govoni, S., Amadio, M., Battaini, F., and Pascale, A. (2010). Senescence of the Brain: Focus on Cognitive Kinases. *Curr. Pharm. Des.* 16 (6), 660–671. doi:10.2174/138161210790883732

Hammes, H. P. (2018). Diabetic Retinopathy: Hyperglycaemia, Oxidative Stress and beyond. *Diabetologia* 61 (1), 29–38. doi:10.1007/s00125-017-4435-8

Han, Z., Guo, J., Conley, S. M., and Naash, M. I. (2013). Retinal Angiogenesis in the Ins2(Akita) Mouse Model of Diabetic Retinopathy. *Invest. Ophthalmol. Vis. Sci.* 54, 574–584. doi:10.1167/iovs.12-10959

Harris, S., Craze, M., Newton, J., Fisher, M., Shima, D. T., Tozer, G. M., et al. (2012). Do anti-angiogenic VEGF (VEGFxxxb) Isoforms Exist? A Cautionary Tale. *PLoS One* 7 (5), e35231. doi:10.1371/journal.pone.0035231

Kim, J. H., Kim, J. H., Jun, H. O., Yu, Y. S., and Kim, K. W. (2010). Inhibition of Protein Kinase C delta Attenuates Blood-Retinal Barrier Breakdown in Diabetic Retinopathy. *Am. J. Pathol.* 176, 1517–1524. doi:10.2353/ajpath.2010.090398

Leasher, J. L., Bourne, R. R. A., Flaxman, S. R., Jonas, J. B., Keeffe, J., Naidoo, K., et al. (2016). Global Estimates on the Number of People Blind or Visually Impaired by Diabetic Retinopathy: A Meta-Analysis from 1990 to 2010. *Dia Care* 39 (9), 1643–1649. doi:10.2337/dc15-2171

Marchesi, N., Barbieri, A., Fahmideh, F., Govoni, S., Ghidoni, A., Parati, G., et al. (2020). Use of Dual-Flow Bioreactor to Develop a Simplified Model of Nervous-Cardiovascular Systems Crosstalk: A Preliminary Assessment. *PLoS One* 15 (11), e0242627. doi:10.1371/journal.pone.0242627

McLenachan, S., Chen, X., McMenamin, P. G., and Rakoczy, E. P. (2013). Absence of Clinical Correlates of Diabetic Retinopathy in the Ins2Akita Retina. *Clin. Exp. Ophthalmol.* 41 (6), 582–592. doi:10.1111/ceo.12084

Moran, E. P., Wang, Z., Chen, J., Sapieha, P., Smith, L. E., and Ma, J. X. (2016). Neurovascular Cross Talk in Diabetic Retinopathy: Pathophysiological Roles and Therapeutic Implications. *Am. J. Physiol. Heart Circ. Physiol.* 311 (3), H738–H749. doi:10.1152/ajpheart.00005.2016

Olivares, A. M., Althoff, K., Chen, G. F., Wu, S., Morrisson, M. A., DeAngelis, M. M., et al. (2017). Animal Models of Diabetic Retinopathy. *Curr. Diab. Rep.* 17 (10), 93–100. doi:10.1007/s11892-017-0913-0

Pascale, A., and Govoni, S. (2012). The Complex World of post-transcriptional Mechanisms: Is Their Deregulation a Common Link for Diseases? Focus on ELAV-like RNA-Binding Proteins. *Cell. Mol. Life Sci.* 69 (4), 501–517. doi:10.1007/s00018-011-0810-7

Peiris-Pagès, M. (2012). The Role of VEGF 165b in Pathophysiology. *Cell. Adh. Migr.* 6 (6), 561–568. doi:10.4161/cam.22439

Perrin, R. M., Konopatskaya, O., Qiu, Y., Harper, S., Bates, D. O., and Churchill, A. J. (2005). Diabetic Retinopathy Is Associated with a Switch in Splicing from Anti- to Pro-angiogenic Isoforms of Vascular Endothelial Growth Factor. *Diabetologia* 48 (11), 2422–2427. doi:10.1007/s00125-005-1951-8

Platania, C. B., Di Paola, L., Leggio, G. M., Romano, G. L., Drago, F., Salomone, S., et al. (2015). Molecular Features of Interaction between VEGFA and Anti-angiogenic Drugs Used in Retinal Diseases: a Computational Approach. *Front. Pharmacol.* 6, 248–261. doi:10.3389/fphar.2015.00248

Platania, C. B. M., Pittalà, V., Pascale, A., Marchesi, N., Anfuso, C. D., Lupo, G., et al. (2020). Novel Indole Derivatives Targeting HuR-mRNA Complex to Counteract High Glucose Damage in Retinal Endothelial Cells. *Biochem. Pharmacol.* 175, 113908. doi:10.1016/j.bcp.2020.113908

Qiu, Y., Hoareau-Aveilla, C., Oltean, S., Harper, S. J., and Bates, D. O. (2009). The Anti-angiogenic Isoforms of VEGF in Health and Disease. *Biochem. Soc. Trans.* 37 (Pt 6), 1207–1213. doi:10.1042/BST0371207

Rigo, S., Duchâteau, E., and Rakic, J. M. (2020). [What's New in Diabetic Retinopathy ?]. *Rev. Med. Liege.* 75 (5-6), 432–439.

Ye, X., Xu, G., Chang, Q., Fan, J., Sun, Z., Qin, Y., et al. (2010). ERK1/2 Signaling Pathways Involved in VEGF Release in Diabetic Rat Retina. *Inves.t Ophthalmol. Vis. Sci.* 51 (10), 5226–5233. doi:10.1167/iovs.09-4899

Yokota, T., Utsunomiya, K., Taniguchi, K., Gojo, A., Kurata, H., and Tajima, N. (2007). Involvement of the Rho/Rho Kinase Signaling Pathway in Platelet-Derived Growth Factor BB-Induced Vascular Endothelial Growth Factor Expression in Diabetic Rat Retina. *Jpn. J. Ophthalmol.* 51, 424–430. doi:10.1007/s10384-007-0471-0

Zhao, Y., and Singh, R. P. (2018). The Role of Anti-vascular Endothelial Growth Factor (Anti-VEGF) in the Management of Proliferative Diabetic Retinopathy. *Drugs Context* 7, 212532. doi:10.7573/dic.212532

Conflict of Interest: The authors declare that the research was conducted in the absence of any commercial or financial relationships that could be construed as a potential conflict of interest.

Publisher's Note: All claims expressed in this article are solely those of the authors and do not necessarily represent those of their affiliated organizations, or those of the publisher, the editors and the reviewers. Any product that may be evaluated in this article, or claim that may be made by its manufacturer, is not guaranteed or endorsed by the publisher.

frontiers in Pharmacology

ORIGINAL RESEARCH
published: 20 October 2021
doi: 10.3389/fphar.2021.732833

Cytoprotective Effects of Water Soluble Dihydropyrimidinthione Derivative Against UV-B Induced Human Corneal Epithelial Cell Photodamage

Enming Du[1], Guojuan Pu[1], Siyu He[1], Fangyuan Qin[1], Yange Wang[1], Gang Wang[1], Zongming Song[1], Junjie Zhang[1]* and Ye Tao[1,2]**

[1]Henan Eye Institute, Henan Eye Hospital, People's Hospital of Zhengzhou University, Henan University School of Medicine, Henan Provincial People's Hospital, Zhengzhou, China, [2]Lab of Visual Cell Differentiation and Modulation, Basic Medical College, Zhengzhou University, Zhengzhou, China

OPEN ACCESS

Edited by:
Mario Damiano Toro,
Medical University of Lublin, Poland

Reviewed by:
Rodrigo Franco,
University of Nebraska-Lincoln, United States
Surya Pratap Singh,
Banaras Hindu University, India

***Correspondence:**
Ye Tao
toy1011@163.com
Junjie Zhang
zhangjj66@126.com
Zongming Song
szmeyes@126.com

Specialty section:
This article was submitted to Experimental Pharmacology and Drug Discovery, a section of the journal Frontiers in Pharmacology

Received: 29 June 2021
Accepted: 29 September 2021
Published: 20 October 2021

Citation:
Du E, Pu G, He S, Qin F, Wang Y, Wang G, Song Z, Zhang J and Tao Y (2021) Cytoprotective Effects of Water Soluble Dihydropyrimidinthione Derivative Against UV-B Induced Human Corneal Epithelial Cell Photodamage. Front. Pharmacol. 12:732833. doi: 10.3389/fphar.2021.732833

Excessive UV-B exposure is well known to be a risk factor for corneal phototoxicity including direct DNA damage and disturbances in the antioxidant balance. Here, we showed a successful synthesis of a water-soluble and biocompatible small molecule **DHPM 1** with dihydropyrimidinthione skeleton, which could effectively protect human corneal epithelial (HCE-2) cells from UV-B damage. In separate experiments, **DHPM 1** absorbed UV-B rays and exhibited scavenging activity against intracellular ROS induced by UV-B radiation, thereby reducing the levels of DNA fragmentation. Additionally, UV-B exposure increased the expression of cleaved caspase-3, as well as the ratio of Bax/Bcl-2 at protein levels, while pretreatment with **DHPM 1** significantly reversed these changes. To the best of our knowledge, this is the first report of a study based on dihydropyrimidinthione derivatives to develop a promising eye drops, which may well find extensive applications in UV-B caused corneal damage.

Keywords: dihydropyrimidinthione, UV-B, human corneal epithelial cell, photodamage, cytoprotective effects

INTRODUCTION

Ultraviolet radiation (UV), an important risk factor for ocular diseases, is further categorised as: UV-C (200–280 nm), UV-B (280–320 nm) and UV-A (320–400 nm). Sunshine is a natural source of environment UV. As the shorter wavelengths of UV-C radiation are almost exclusively filtered by ozone in the stratosphere, the terrestrial environment is mainly exposed to UV-B (3%) and UV-A (97%) radiation (Ibrahim et al., 2012). Although it accounts for only ~3% of terrestrial light, UV-B with a highly energetic wavelength is more biologically effective at damaging ocular tissue than UV-A. In addition, the human cornea absorbs ~90% of UV-B radiation, in contrast to only ~30% in the UV-A region (Young, 2006). Therefore, the eye (especially cornea) is the most susceptible organ to UV-B induced damage aside from skin (Kolozsvari et al., 2002). Under physiological conditions, the cornea is a transparent avascular tissue, which protects the lens and retina in the eyes against UV-B induced damaging effects by absorbing the majority of UV-B radiation. The typical UV-B induced corneal disorders contain photokeratitis, pterygium, climatic droplet keratopathy, damage to the epithelium, edema and apoptosis of corneal cells. At the cellular level, UV-B induced corneal phototoxicity could be caused by direct DNA damage, as well as by the generation of reactive oxygen

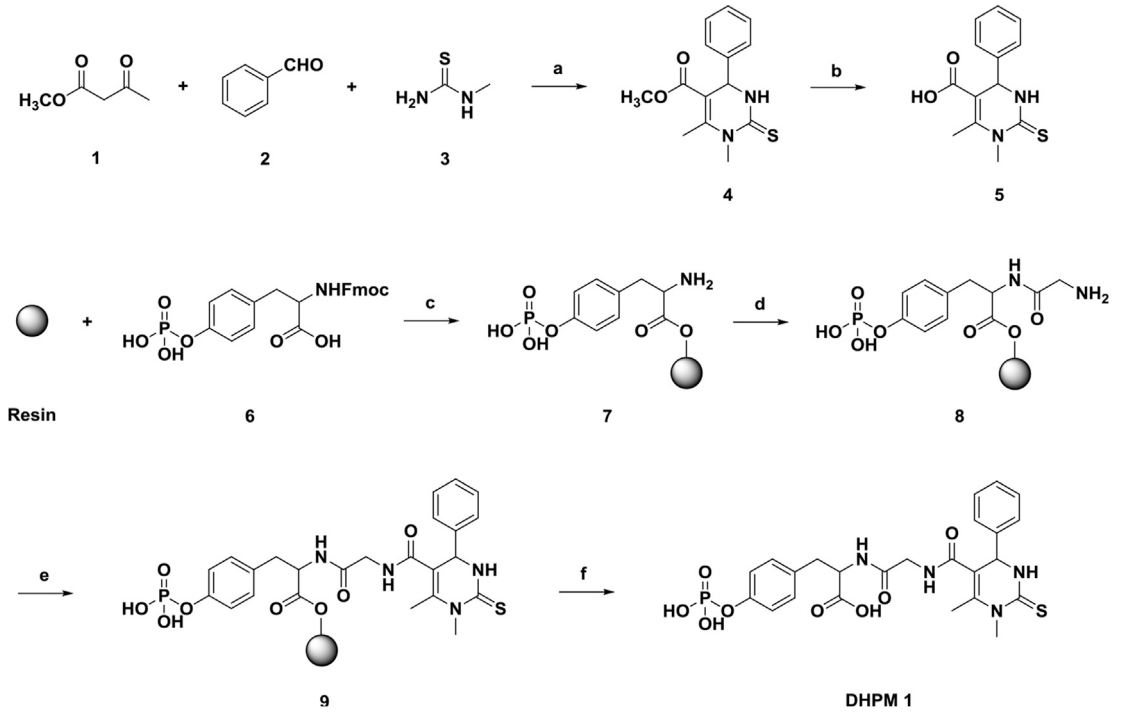

SCHEME 1 | Reagents and conditions: **(a)** 20 mol% $MgCl_2$, AcOH, 100°C; **(b)** NaOH; **(c)** 1) DIEA, DMF; 2) DCM/MeOH/DIEA (80:15:5); 3) 20% piperidine in DMF; **(d)** 1) Glycine, HBTU, DIEA, DMF; 2) 20% piperidine in DMF; **(e)** 7, HBTU, DIEA, DMF; **(f)** 95% TFA in CH_2Cl_2.

species (ROS) and inflammatory cytokines (Tsai et al., 2012; Bigagli et al., 2017). ROS overproduction can elicit DNA mutations, lipid peroxidation and protein denaturation and induce pro-inflammatory cytokines, which plays an important role in promoting corneal inflammation (Bigagli et al., 2017). Meanwhile, UV-B by itself can also trigger the activation of NLRP3 inflammasomes and the secretion of IL-1β and/or IL-18 in human corneal epithelial (HCE) cells (Korhonen et al., 2020).

3,4-Dihydropyrimidine-2(*1H*)-ones and thiones (**DHPMs**) are a class of heterocyclic compounds, which have been intensively investigated mainly due to their diverse pharmacological properties, including calcium antagonists, α_{1a} adrenoreceptor antagonists, anticarcinogens, antibacterial, antiviral, antioxidants, etc. (Kappe, 2000; Pineiro et al., 2013) Recently, Tao et al. have prepared a series of polymers with **DHPMs** side chains. The optimized polymer **P (1)(4)-co-P(PEGMA)** with attractive antioxidant profiles showed much better UV-C resistant capability than superoxide dismutase (SOD). ~100% L929 cells remained viable with 10 mg/ml of **P (1)(4)-co-P(PEGMA)**, suggesting its excellent cellular safety. After UV-C radiation (254 nm, 0.27 J/cm^2), **P (1)(4)-co-P(PEGMA)** could protect cells from UV-C damage in a dose-dependent manner, especially almost 100% protection was achieved at 5 mg/ml (Mao et al., 2018). In order to further improve the UV protective abilities, three fluorescent polymers were prepared by introducing conjugated moieties into the original polymer structures and they were superior to the original polymer in effectively preventing UV-C induced DNA damage (Mao et al., 2021).

Encouraged by its excellent free-radical scavenging and UV resistant activities of **DHPMs**, we therefore explored designing a phosphotyrosine-containing small molecule of DHPMs as an alternative approach to achieve the excellent protection in the UV-B irradiated HCE-2 cell line. Phosphotyrosine [H-Try (H_2PO_3)-OH] with highly aqueous solubility at neutral pH can significantly improve the biocompatibility of **DHPMs** (Shy et al., 2020), which still require further refinement to achieve the applications in medicine. We have also explored the therapeutic potential of the new designed small molecule by investigating whether it can alleviate DNA damage and reduce ROS overproduction when administered before UV-B exposure.

MATERIALS AND METHODS

Materials

Unless otherwise noted, solvents and reagents were obtained from commercial sources and used without further purification. Dulbecco's modified eagle's medium (DMEM, Gibco), phosphate buffered saline (PBS, Gibco), fetal bovine serum (FBS, Gibco), trypsin-EDTA (0.25%, Gibco), Alexa Fluor® 488-conjugated rabbit anti-phospho-histone H2A.X (Ser139) (20E3) mAb (Cell Signaling Technology, United States), Casepase 3 (active) rabbit monoclonal antibody (Beyotime Biotech, China), Bax rabbit monoclonal antibody

(Beyotime Biotech, China), Bcl-2 rabbit monoclonal antibody (Sino Biological, China), β-actin rabbit monoclonal antibody (Beyotime Biotech, China), Calcein-AM/PI Double Stain Kit (Beyotime Biotech, China), Reactive Oxygen Species Assay Kit (Beyotime Biotech, China), Cell Counting Kit-8 (APExBIO Technology LLC, United States) were used as purchased.

Instruments

High-resolution mass spectra (HRMS) were obtained on a Thermo Exactive Plus spectrometer. NMR spectra were recorded on Varian Mercury 400 MHz spectrometers. The purity of final products was determined by high-performance liquid chromatography (HPLC). The UV-B light source (NanJing Nationol Electronic Co. Ltd., China) was a large area irradiation ultraviolet lamp that emitted 106 μW/cm^2 at the distance of 10 cm. The wavelength range of UV-B was 280–320 nm, with an average of 302 nm. UV absorption spectra were recorded on a UV-VIS spectrophotometer (UV 1800 SPC, Macy, China) using quartz cuvettes of 1 cm path length. The flow cytometry analyses were performed on a BD FACSCanto^{TM} flow cytometer (λex 488 nm and λem 500–600 nm for phospho-histone H2A.X (Ser139) (20E3) rabbit mAb). Confocal microscopic images were obtained on a Zeiss 780 using the following filters: λex 488 nm and λem 500–600 nm for DCF; λex 488 nm and λem 500–530 nm for Calcein AM; λex 561 nm and λem 600–700 nm for PI. The blots were visualized with Clarity Western ECL Substrate (Applygen, China) on Chemiluminescence imaging system (Tanon-5200 Multi, China).

METHODS

Chemicals

Synthesis of compound **4**. Benzaldehyde (530 mg, 5.0 mmol), methyl acetoacetate (580 mg, 5.0 mmol), *N*-methylthiourea (675 mg, 7.5 mmol), acetic acid (5.0 ml) and magnesium chloride (95 mg, 1.0 mmol) were successively added to a 100 ml centrifuge tube. The tube was sealed and stirred for 2 h at 100°C. After completion, the reaction mixture was cooled and poured into crushed ice with vigorous stirring. The obtained crude was filtered, washed with cold water and diethyl ether to afford a white powder (1.2 g, 87%). HRMS calcd for $C_{14}H_{17}N_2O_2S$ $[M + H]^+$ 277.1005, found 277.1011; ^{1}H NMR (400 MHz, DMSO-d_6): δ 9.87 (d, J = 4.8 Hz, 1H), 7.36–7.18 (m, 5H), 5.21 (d, J = 4.8 Hz, 1H), 3.64 (s, 3H), 3.48 (s, 3H), 2.53 (s, 3H); ^{13}C NMR (100 MHz, DMSO-d_6): δ 150.4, 140.5, 126.5, 121.5, 110.8 (2C), 110.0, 108.7 (2C), 92.0, 49.6, 49.1, 36.8, 20.9.

Synthesis of compound **5**. To a solution of methanol (5 ml) and 1 N NaOH solution (aq., 10 ml) was added compound **4** (552 mg, 2.0 mmol) and then refluxed for 1 h. After cooled to room temperature, the reaction mixture was poured onto crushed ice, acidified with 1 N HCl (aq.). The crude product was filtered and dried to afford compound **5** (430 mg, 82%). HRMS calcd for $C_{14}H_{17}N_2O_2S$ $[M + H]^+$ 263.0849, found 263.0850; ^{1}H NMR (400 MHz, DMSO-d_6): δ 12.56 (s, 1H), 9.78 (d, J = 3.6 Hz, 1H), 7.36–7.31 (m, 2H), 7.28–7.20 (m, 3H), 5.21 (d, J = 3.6 Hz, 1H), 3.47 (s, 3H), 2.52 (s, 3H); ^{13}C NMR (100 MHz, DMSO-d_6): δ 178.1, 167.1, 147.4, 142.2, 128.6 (2C), 127.6, 126.0 (2C), 106.2, 52.3, 36.1, 16.2.

DHPM 1 was synthesized by solid phase peptide synthesis (SPPS). 2-Chlorotrityl chloride resin (1.0 g, 1 mmol) was swelled in anhydrous dichloromethane for 20 min. Fmoc-L-Tyr (H_2PO_3)-OH (1.45 g, 3 mmol), DIEA (825 μL, 5 mmol) was dissolved in anhydrous DMF and then conjugated to swelled resin for 2 h. Subsequently washing with anhydrous DMF for three times, blocking unreacted sites of resin with DCM/MeOH/DIEA (80:15:5) for 20 min and re-washing with anhydrous DMF for five times. 20% Piperidine in DMF was used to remove the Fmoc group for 30 min and then washed successively with anhydrous DMF, methanol, cyclohexane and dichloromethane. Fmoc-Gly-OH (890 mg, 3 mmol) was activated with HBTU/DIEA in anhydrous DMF and then conjugated to above-mentioned resin for 2 h. 20% Piperidine in DMF was used to remove the Fmoc group for 30 min. Subsequently washing successively with anhydrous DMF, methanol, cyclohexane and dichloromethane. Then, compound **5** (780 mg, 3 mmol) was activated with HBTU/DIEA and conjugated to the resin for 2 h. Subsequently washing successively with anhydrous DMF, methanol, cyclohexane and dichloromethane. **DHPM 1** was cleaved off the resin with TFA for 2 h. After removing the solvent, anhydrous ether was added under sonication to afford the crude product, which was further purified by reversed-phase HPLC (420 mg, 75%). HRMS for $C_{24}H_{28}N_4O_8PS$ $[M + H]^+$: 563.1366; found 563.1357; ^{1}H NMR (400 MHz, DMSO-d_6): δ 9.48 (d, J = 4.8 Hz, 1H), 8.23 (dt, J = 5.6, 2.4 Hz, 1H), 8.19 (t, J = 7.2 Hz, 1H), 7.35–7.02 (m, 9H), 5.13 (d, J = 4.0 Hz, 1H), 4.45–4.37 (m, 1H), 3.92–3.75 (m, 1H), 3.73–3.56 (m, 1H), 3.41 (s, 3H), 2.22 (s, 3H), 3.05–2.95 (m, 1H), 2.90–2.78 (m, 1H); ^{13}C NMR (100 MHz, DMSO-d_6): δ 177.8, 172.7, 168.8, 166.8, 150.1, 142.1, 137.3, 132.8, 130.1 (2C), 128.5 (2C), 127.4, 126.0 (2C), 119.8, 119.7, 112.1, 53.6, 53.1, 41.8, 36.0, 35.8, 16.6.

UV Absorption Spectroscopy

UV spectrum of **DHPM 1** (20 μg/ml) was performed with a UV-VIS spectrophotometer. The path length of the cuvette was 1 cm. The detection range was set to 200–400 nm and the spectral resolution to 1.0 nm.

Cell Viability Assay

The human corneal epithelial cell line (HCE-2) was purchased from the American Type Culture Collection (ATCC, United States) and cultured in DMEM containing 10% FBS, 100 U/ml penicillin and 100 μg/ml streptomycin. Incubation was carried out at 37°C with a humidified atmosphere of 5% CO_2. Cells in exponential growth phase were seeded in a 96 well plate at a concentration of 10^4 cells/well and allowed to attach to the wells for 12 h. The culture medium was removed followed by addition of 100 μl culture medium containing different concentrations of **DHPM 1**. Parallel cultures of HCE-2 cells were irradiated with a UV-B lamp at the indicated dosages and then post-incubated for 24 h. Then, cell viability was detected by CCK-8 assay. All experiments were conducted

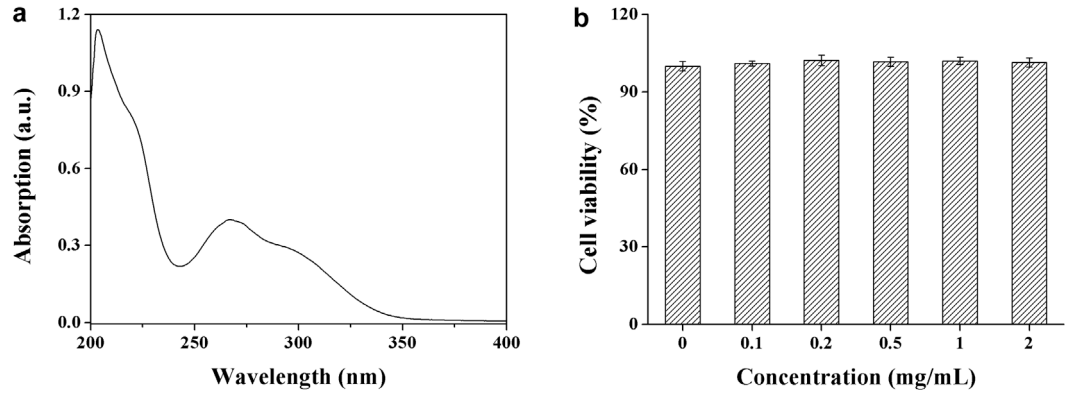

FIGURE 1 | The UV absorption spectrum **(a)** and biocompatibility **(b)** of **DHPM 1**.

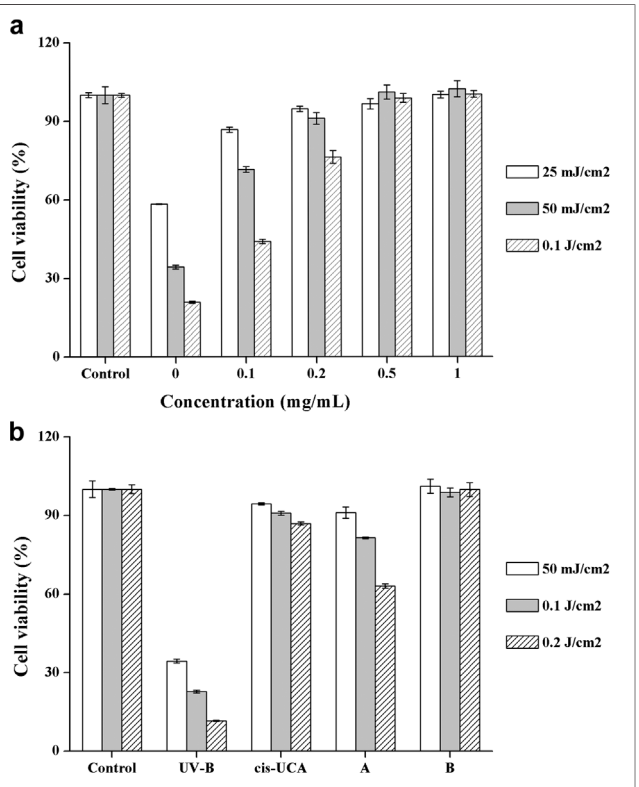

FIGURE 2 | (a) Cell viability with **DHPM 1** at different concentrations after exposure to UV-B radiation (302 nm); **(b)** Cell viability with ***cis*-UCA** (0.1 mg/ml) and **DHPM 1** at different concentrations (A: 0.2 mg/ml; B: 0.5 mg/ml) after exposure to UV-B radiation (302 nm); non-irradiated cultures served as controls. The data were presented as means ± SD, $n = 3$.

triplicate. The results were calculated as means ± SD, which are expressed as cell viability (%).

Cell Viability Imaging Assay

HCE-2 cells in exponential growth phase were seeded in a 35 mm glass-bottom dish (5×10^4 cells) and allowed to attach to the dish for 12 h. The culture medium was removed followed by addition of 2.0 ml culture medium containing different concentrations of **DHPM 1**. Parallel cultures of HCE-2 cells were irradiated with a UV-B lamp at the indicated dosages and then post-incubated for 24 h. After washing with PBS, cells were further stained with commercial Calcein AM (2 μM) and PI (4.5 μM) at 37°C for 7 min in the dark. Cells were then washed twice with fresh live cell imaging solution and visualized by laser confocal microscopy (LSM 780, Carl Zeiss) immediately (λex: 488 nm for Calcein AM, 561 nm for PI; λem: 500–530 nm for Calcein AM, 600–700 nm for PI). The percentages of live/dead cells analysis was quantified with the fluorescence intensities of Calcein AM and PI, respectively.

Intracellular ROS Assay

The cell samples were prepared as cell viability imaging assay and a fluorescence microscopic image analysis was performed using the ROS sensitive probe DCFH-DA as a tool for direct visualization of intracellular ROS generation in the HCE-2 cells. Briefly, **DHPM 1** (0 or 0.5 mg/ml) was added to the cells, which was irradiated or not irradiated with UV-B at 0.1 J/cm^2. After incubation for 7 h, cells were washed with live cell imaging solution for three times, and further stained with commercial DCFH-DA (10 μM) at 37°C for 20 min in the dark. Cells were then washed two times with fresh live cell imaging solution and visualized by laser confocal microscopy (LSM 780, Carl Zeiss) immediately (λex: 488 nm, λem: 500–650 nm for DCF). The fluorescence intensity of DCF showing the generation of intracellular ROS level was analyzed by flow cytometer.

DNA Damage Assay

HCE-2 cells in exponential growth phase were seeded in a 6 well plate at a concentration of 5×10^5 cells/well and allowed to attach to the wells for 12 h. The culture medium was removed followed by addition of 2.0 ml culture medium containing different concentrations of **DHPM 1** (0 or 0.5 mg/ml). Parallel cultures of HCE-2 cells were irradiated or not irradiated with UV-B at 0.1 J/cm^2. After incubation for 4 h, cells were harvested and then

immobilized with 4% paraformaldehyde solution for 15 min followed by 90% methanol permeabilization for 10 min. The cells were washed with PBS and then kept in the Alexa Fluor 488-conjugated rabbit anti-phospho-histone H2A.X (Ser139) (20E3) mAb (1:50 dilution) solution for 1 h. Cells were washed with PBS and then analyzed by flow cytometer (λex: 488 nm, λem: 500–560 nm).

Western Blot Analysis

HCE-2 cells in exponential growth phase were seeded in a 6 well plate at a concentration of 8×10^5 cells/well and allowed to attach to the wells for 12 h. The culture medium was removed followed by addition of 2.0 ml culture medium containing different concentrations of **DHPM 1** (0 or 0.5 mg/ml). Parallel cultures of HCE-2 cells were irradiated or not irradiated with UV-B at 0.1 J/cm^2. After incubation for 6 h, cultured cells were harvested and lysed in an RIPA buffer that contained an EDTA-free protease inhibitor cocktail. After centrifugation, the supernatants were retrieved and protein concentrations were measured with a BCA kit. Protein samples were separated by SDS-PAGE and transferred to PVDF membranes. After blocking with 5% skimmed milk, the membranes were incubated with various primary antibodies overnight at 4°C then incubated with secondary antibodies at room temperature for 1 h. The protein bands were detected with an enhanced chemiluminescence plus kit.

Statistical Analysis

Statistical analysis was performed using GraphPad Prism Version 8.0 software. All the data are presented as the mean ± SD. Statistical difference was analyzed by One-Way ANOVA and $p < 0.05$ was considered statistically significant.

RESULTS

Synthesis

We began our exploration of water-soluble **DHPM 1** by applying tricomponent Biginelli reaction and solid phase peptide synthesis (SPPS). As shown in **Scheme 1**, methyl acetoacetate (**1**), benzaldehyde (**2**) and *N*-methylthiourea (**3**) were added to a tube. $MgCl_2$ and acetic acid were used as the catalyst and solvent, respectively. The tube was sealed and then kept in a shaker at 100°C for 2 h. After completion, compound **4** was easily purified in 87% yield after simple washing with water and diethyl ether. Demethylation of **4** with 1 N NaOH (aq.) solution followed by acidification with diluted HCl afforded the desired compound **5** in high yield (82%). Subsequent transformation of **5** to the target **DHPM 1** was achieved employing Fmoc SPPS technique. Purification using preparative high-pressure liquid chromatography (HPLC) provided an 75% isolated yield of **DHPM 1** with a 98% purity. With the desired **DHPM 1** in hand, the water solubility was determined to be ~2.5 mg/ml in PBS (pH 7.4).

UV Absorption

To test the cytoprotective ability of **DHPM 1** against the UV photodamage, we first checked the UV absorption spectrum ranging from 200 to 400 nm. As shown in **Figure 1a**, **DHPM 1** exhibited the strongest absorption at 206 nm, while there is no obvious absorption in the 350–400 nm region. In addition, **DHPM 1** showed an absorptive capacity for UV-B (280–320 nm) and the peak wavelength of absorption occurred at ~300 nm. Thus, the UV (especially UV-B) absorbing properties of **DHPM 1** might be closely associated with its cytoprotective effect against UV-B radiation.

Biocompatibility

Analysis of cell viability by CCK-8 assay revealed that there was no significant effect in response to 2 mg/ml **DHPM 1** in the non-irradiated cells during the 24 h incubation (**Figure 1b**), which indicated that **DHPM 1** possessed high biocompatibility with no observable *in vitro* toxicity and showed great promise for intracellular bio-applications.

Cell Viability With UV-B Exposure

To verify the cytoprotective effect of **DHPM 1** in UV-B irradiated HCE-2 cells, we examined its influence on cell survival. As shown in **Figure 2a**, cell viability in untreated control cells was 100%, whereas exposure of the HCE-2 cells to UV-B radiation induced a significant loss of viability in a dose-dependent manner, which were reduced to 58, 34 and 21%, respectively. On the contrary, 87, 72 and 44% cells remained viable with 0.1 mg/ml of **DHPM 1** and the cell viability was increased by 20–40% compared with corresponding UV-B radiation group in the absence of **DHPM 1**. Interestingly, **DHPM 1** at concentrations of 0.5 mg/ml and above could restore the metabolic activity of the UV-B irradiated cells to the level of the non-irradiated cells even at the high UV-B doses (0.1 J/cm^2). These results suggested that **DHPM 1** could protect HCE-2 cells against UV-B radiation.

The most promising molecule reported in the literature so far is ***cis*-UCA** and 0.1 mg/ml ***cis*-UCA** was optimally anti-inflammatory and cytoprotective treatment option against UV-B induced inflammation and cellular damage in human corneal cells (Viiri et al., 2009; Korhonen et al., 2020). A head-to-head comparison of ***cis*-UCA** and **DHPM 1** demonstrated that cytoprotective effect of 0.2 mg/ml **DHPM 1** was equivalent to that of 0.1 mg/ml ***cis*-UCA** after UV-B exposure at an energy of 50 mJ/cm^2. 0.2 mg/ml **DHPM 1** exhibited an accelerated reduction in cell viability by increasing doses of UV-B, 63% (**DHPM 1**) vs 87% (***cis*-UCA**) at 0.2 J/cm^2 UV-B radiation. Encouragingly, 0.5 mg/ml **DHPM 1** could keep cell viability ~100% even at the highest dose of UV-B radiation, which was better than that of 0.1 mg/ml ***cis*-UCA**. The molar concentrations of 0.5 mg/ml **DHPM 1** and 0.1 mg/ml ***cis*-UCA** are 890 and 724 μM, respectively, suggesting they have similar UV-B resistance capacities (**Figure 2b**).

The Calcein AM/PI assay is a rapid and simple approach to simultaneously observe living and dead cells (Calcein AM can enter and only accumulate in living cells, while PI only stains the nucleus of dead cells). We also used Calcein AM/PI double staining to qualitatively evaluate cell viability after UV-B radiation. After adding fresh culture medium containing **DHPM 1** (0 or 0.5 mg/ml), HCE-2 cells were exposed to UV-B radiation at the dose of 0.1 J/cm^2 and then post-incubated for 24 h prior to further analysis. In the presence of **DHPM 1** (0 or

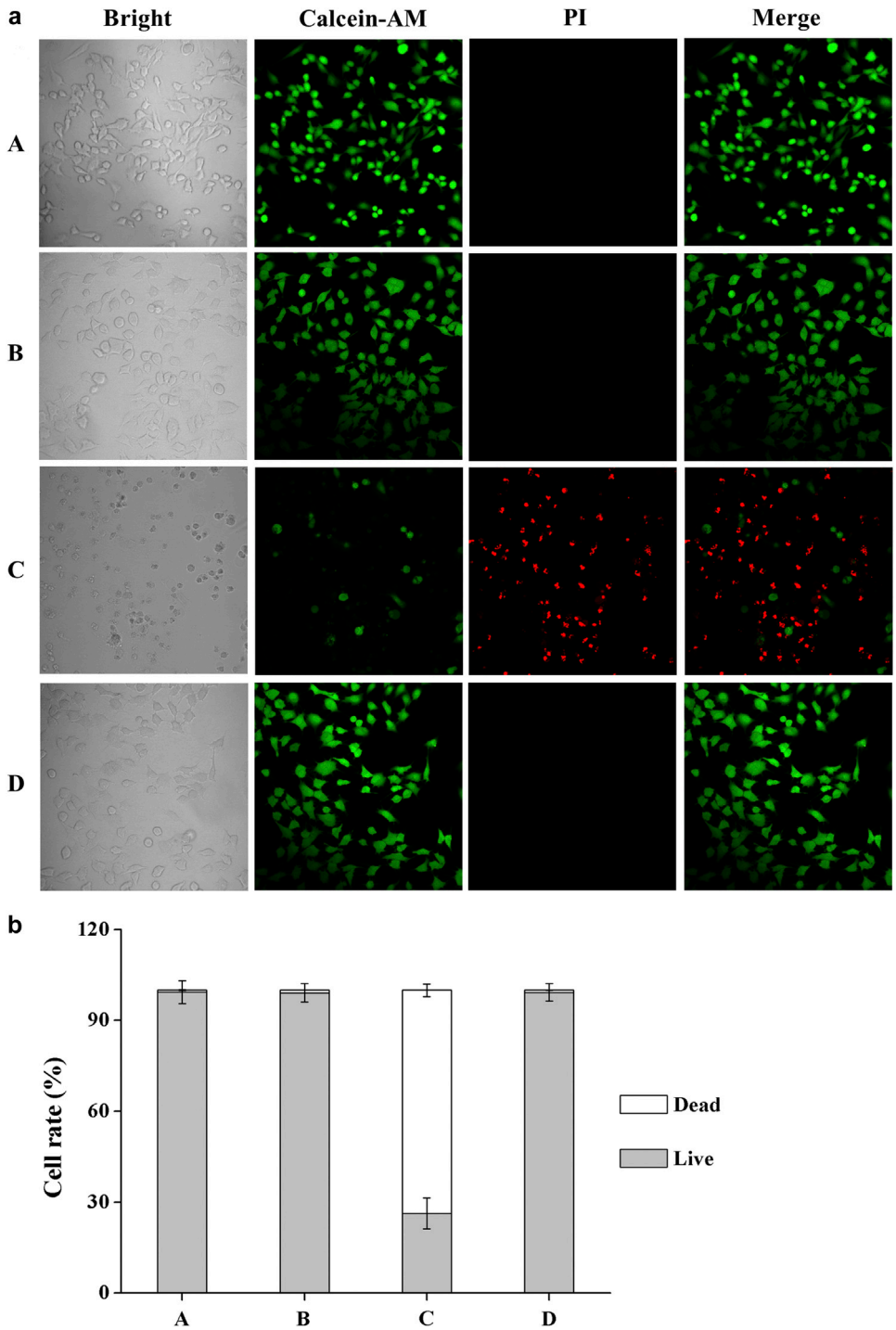

FIGURE 3 | (a) Calcein AM/PI double staining of HCE-2 cells without UV-B radiation in the presence of **DHPM 1** at 0 **(A)** or 0.5 mg/ml **(B)**; with UV-B radiation in the presence of **DHPM 1** at 0 **(C)** or 0.5 mg/ml **(D)**; **(b)** The percentages of live/dead cells analysis in the groups **(A–D)** (n = 3).

0.5 mg/ml), HCE-2 cells without UV radiation were tested as the control. Calcein AM/PI double staining revealed that most HCE-2 cells cultured without **DHPM 1** became shriveled and rounded, which were stained by PI as red spots after exposure to UV-B radiation. However, cells cultured with **DHPM 1** (0.5 mg/ml) survived the same process with viability similar to that of the control (**Figure 3**). These results agreed well with the quantitative data obtained by a CCK-8 assay (**Figure 2**), confirming that **DHPM 1** is a novel drug candidate to protect HCE-2 cells from fatal UV-B damage.

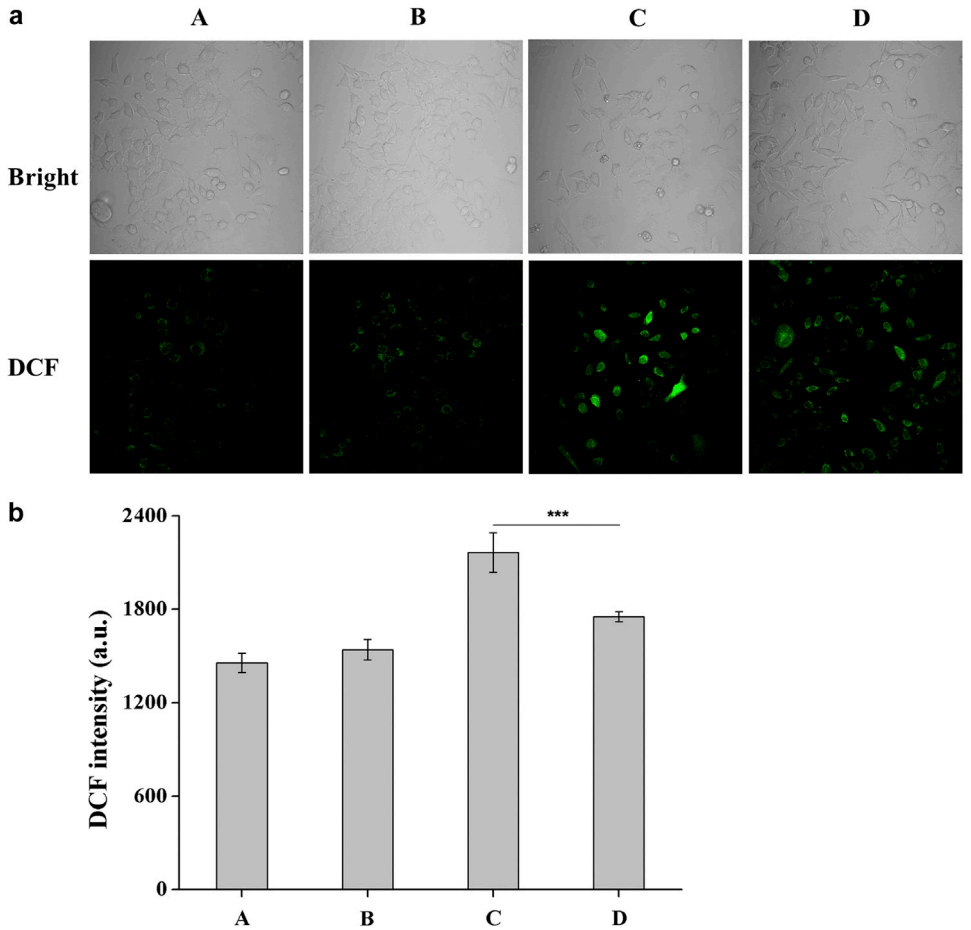

FIGURE 4 | (a) Fluorescent images of DCFH-DA staining of HCE-2 cells without UV-B radiation in the presence of **DHPM 1** at 0 **(A)** or 0.5 mg/ml **(B)**; with UV-B radiation in the presence of **DHPM 1** at 0 **(C)** or 0.5 mg/ml **(D)**; **(b)** The DCF intensity analysis in the groups **(A–D)** (n = 3, ***p < 0.001).

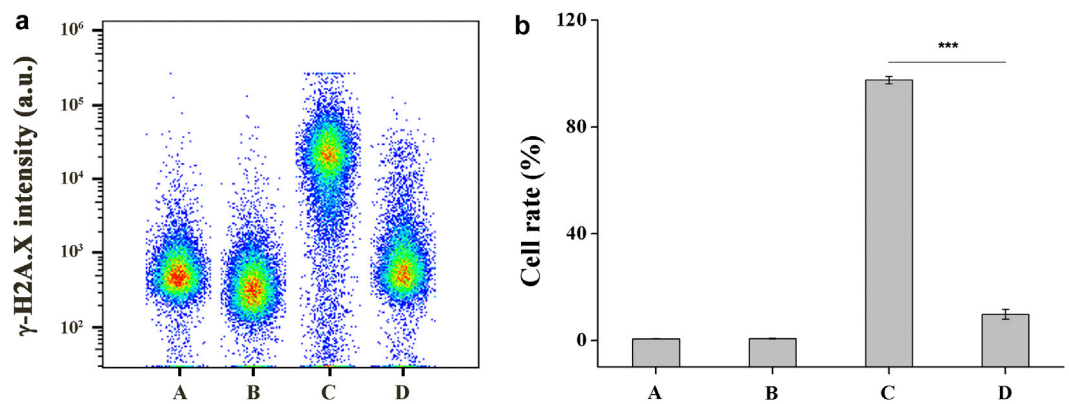

FIGURE 5 | (a) Flow cytometry analysis of damaged DNA in HCE-2 cells without UV-B radiation in the presence of **DHPM 1** at 0 (A) or 0.5 mg/ml (B); with UV-B radiation in the presence of **DHPM 1** at 0 (C) or 0.5 mg/ml (D); **(b)** The percentages of DNA damaged cells analysis in the groups A–D (n = 3, ***p < 0.001).

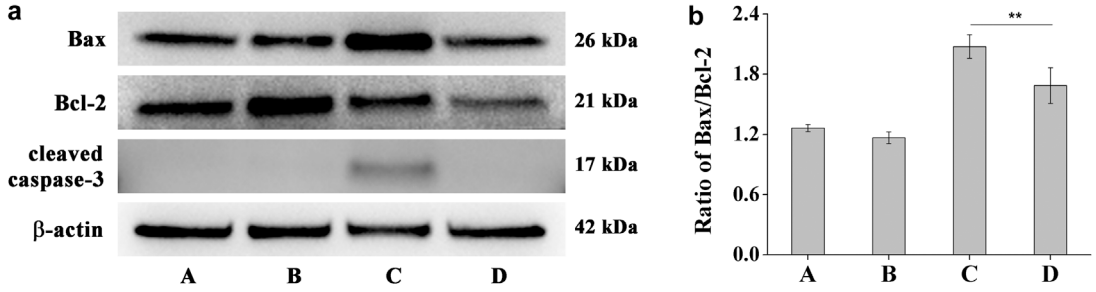

FIGURE 6 | (a) Bax, Bcl-2 and cleaved Caspase-3 protein expression alterations in HCE-2 cells without UV-B radiation in the presence of **DHPM 1** at 0 (A) or 0.5 mg/ml (B); with UV-B radiation in the presence of **DHPM 1** at 0 (C) or 0.5 mg/ml (D); **(b)** The ratio of Bax/Bcl-2 protein expression in the groups A–D ($n = 3$, $^{**}p < 0.01$).

ROS Generation

DCFH-DA is an oxidation-sensitive fluorescent probe and can be oxidized to a highly fluorescent DCF (2′,7′-dichlorofluorescein), which corresponded to the increased ROS level in the HCE-2 cells. Combination with confocal microscope gives this method more simplicity and sensitivity for the observation of ROS generation. The microscopic images of DCF fluorescence showing the generation of intracellular ROS level were presented in **Figure 4**. The results obtained after 7 h of post-incubation revealed that UV-B exposure induced an obvious increase in the ROS level while a significant reduction in the DCF fluorescence was observed when **DHPM 1** (0.5 mg/ml) was applied, which indicated the intracellular ROS scavenging activities of **DHPM 1**.

DNA Damage

UV-induced DNA damage can cause H2A.X to be rapidly phosphorylated by PI3K-like kinase at Ser139 site, which is a biomarker for evaluating DNA double-strand breaks (Paull et al., 2000). A flow cytometry-based quantification of phosphorylated H2A.X (γ-H2A.X) with Alexa Fluor 488 conjugated phospho-histone H2A.X (Ser139) (20E3) rabbit mAb was used to study the UV-B protection mechanism of **DHPM 1**. Flow cytometry analysis data indicated damaged DNA in 0.6 and 97.6% of cells before and after UV-B radiation, respectively. In contrast, the damaged DNA significantly decreased as the concentration of the **DHPM 1** increases from 0.1 to 0.5 mg/ml and reached up to 9.8% of cells cultured with 0.5 mg/ml of **DHPM 1** was detected after UV-B exposure, verifying that **DHPM 1** played an important role in protecting the UV-B induced DNA damage (**Figure 5**).

Bax, Bcl-2 and cleaved Caspase-3 Expressions

The Bcl-2 and caspase families of proteins are related to the modulation of apoptosis process (Elmore, 2007). In order to better understand the protective mechanisms against UV-B induced apoptosis in HCE-2 cells, we analyzed the effect of **DHPM 1** on the expression of Bax, Bcl-2 and cleaved Caspase-3. Before exposure to UV-B irradiation, HCE-2 cells were pretreated with 0.5 mg/ml **DHPM 1**. The western blot results illustrated in **Figure 6** showed that UV-B exposure significantly augmented the ratio of Bax/Bcl-2 at protein levels, which was restored by **DHPM 1**. Specifically, levels that were almost 1.6-fold and 1.3-fold higher than the control level were observed, respectively. In addition, UV-B exposure also stimulated the expression of cleaved Caspase-3, which was fully reversed in the presence of **DHPM 1**. Consistent with previous research, UV-B induced cell apoptosis through initiating the caspase-3 signaling pathway activation, which could be inhibited by **DHPM 1** to prevent the apoptosis of HCE-2 cells.

DISCUSSION

Skin and cornea are the two surfaces exposed to environmental UV radiation. Although human cornea shares many similarities with skin, there is a clear difference between corneal epithelial cells and keratinocytes. With uniquely specialized tissues, the cornea lacks features skin possesses, such as a thicker epithelial layer, stratum corneum and melanocytes, which help to resist UV damage. Therefore, the cornea on the anterior surface of the eye is particularly susceptible to the damage from excessive UV exposure, especially UV-B radiation (Roberts, 2001; Bashir et al., 2017). Clinically, acute UV-B exposure can cause photokeratitis, producing damage to the corneal epithelium, stroma and endothelium, and then develop into haze, edema and opacification. The sources of UV-B radiation include the well-known sunlight reflected off snow or off water and various high-intensity lamps. Photokeratitis is an inflammatory response and its clinical condition is generally reversible in most cases and largely self-resolving without any specific medical intervention. However, if the dose of UV-B exposure is substantial, inner corneal endothelial cells will be damaged and chronic UV-B exposure can also lead to climatic droplet keratopathy (CDK) and endothelial dysfunction. For humans, these damages would be expected to be irreversible (Doughty, 2019).

In the present work, we designed and synthesized a new dihydropyrimidinthione derivative (**DHPM 1**) with highly

aqueous solubility and biocompatibility to ameliorate UV-B radiation mediated HCE-2 cell damage. Under different intensities of UV-B radiation (25–100 mJ/cm^2), 0.1 mg/ml **DHPM 1** could increase the viabilities by 20–40%. More importantly, the viability of the HCE-2 cells was almost unaffected by 0.5 mg/ml **DHPM 1** treatment and its UV-B resistance capacity was equally to that of ***cis*-UCA**, a promising treatment option to suppress UV-B induced cellular damage in human corneal and conjunctival epithelial cells (**Figures 2**, **3**).

UV-B can be directly absorbed by DNA, resulting in the formation of cyclobutane pyrimidine dimers (CPD) as well as pyrimidine 6-4 pyrimidone photoproducts (6-4 PP) followed by DNA damage or cell death (Bashir et al., 2017). In this work, **DHPM 1** can absorb UV-B energy and effectively inhibit HCE-2 cells damage. The absorption spectrum of **DHPM 1** overlapped with the UV-B spectrum (280–320 nm), suggesting that UV-B absorption effect of **DHPM 1** acts as a cytoprotective mechanism against UV-B induced cell damage (Tanito et al., 2003; Hyun et al., 2012). Additionally, an excessive UV-B exposure induces the production of ROS, such as hydrogen peroxide, singlet oxygen, hydroxyl radicals and superoxide anions, which can react with lipids, proteins and DNA, leading to the lipid peroxidation and, finally, cell death (Bashir et al., 2017). Indeed, several antioxidant agents, such as ascorbic acid, Fucoxanthin, Dacriovis™, EGCG, *Dunaliella salina* (*D. salina*), Rebamipide and Carteolol hydrochloride, have been reported to ameliorate UV-B induced corneal damage by reducing or preventing oxidative stress (Tanito et al., 2003; Suh et al., 2008; Chen et al., 2011; Tsai et al., 2012; Chen et al., 2014; Chen et al., 2016; Bigagli et al., 2017). As a kind of important antioxidant, **DHPMs** have also been intensively investigated as ROS scavenger (Pineiro et al., 2013). In the present study, we found that UV-B mediated oxidative damage caused an increase of intracellular ROS levels as compared to the normal control group, while treatment with **DHPM 1** significantly reversed these changes (**Figure 4**). Moreover, UV-B exposure can induce an inflammatory response in the cornea and inhibition of inflammatory factors has been considered as another treatment option for UVB-induced phototoxic status (Teng et al., 2018; Chen et al., 2020). In previous studies, ***cis*-UCA** was reported to be a promising anti-inflammatory compound, which could prevent the IL-1β and IL-18 secretion and therapeutically reduce the levels of IL-6, IL-8, and LDH in UV-B exposed HCE cells *in vitro* (Korhonen et al., 2020; Viiri et al., 2009; Jauhonen et al., 2011). This could serve as another way to investigate the protective mechanism of **DHPM 1** in UV-B mediated corneal damage.

The mechanisms of apoptosis are highly complex and sophisticated. There are two main apoptotic pathways: the extrinsic and intrinsic pathways. They converge on the same terminal, or execution pathway, which is initiated by the cleavage of caspase-3 and results in DNA fragmentation, etc. (Elmore, 2007) Previous studies have demonstrated that the intrinsic pathway is more important in UV-B induced apoptosis of corneal epithelial cells (Ubels et al., 2016; Du et al., 2017; Zhao et al., 2020; Maugeri et al., 2020). In our present study, UV-B induced an increase in the Bax/Bcl-2 ratio and the activation of caspase-3 in HCE-2 cells, which were prevented by **DHPM 1** to different extents (**Figure 6**). Thus, attenuating the intrinsic apoptosis pathway is the major mechanism underlying the protective effects of **DHPM 1** against UV-B induced HCE-2 cell damage.

CONCLUSION

Although the antioxidant properties of **DHPMs** are well described in previous studies, this is the first work demonstrating that DHPMs prevents UVB-induced corneal damage *in vitro*. In the present work, we reported a new water-soluble dihydropyrimidinthione derivative **DHPM 1** with excellent cytoprotective properties against UV-B caused corneal damage. Our results demonstrated that the protective effects of **DHPM 1** likely derived from its ability to not only reduce the number of cell-damaging UV photons by the absorption spectrum but possibly attenuate ROS generation. **DHPM 1** also decreased the ratio of Bax/Bcl-2 and inhibited the activation of caspase 3, which subsequently prevented apoptosis via caspase 3 pathway. Topical **DHPM 1** eye drops may provide a safe and effective protective treatment option for UV-B induced damage on ocular surface. Therefore, further *in vivo* studies are required.

DATA AVAILABILITY STATEMENT

The original contributions presented in the study are included in the article/**Supplementary Material**, further inquiries can be directed to the corresponding authors.

AUTHOR CONTRIBUTIONS

ED, YT, JZ, and ZS conceived and designed the experiments. ED, GP, SH, FQ, YW, and GW performed the experiments and analysed the statistical data. YT, JZ, and ZS wrote the drafted the manuscript. All authors commented and approved the submitted manuscript.

FUNDING

This work was supported by grants from the National Natural Science Foundation of China (No. 82003294 and U1904166), Natural Science Foundation of Henan Province (No. 202300410537), Henan Provincial Medical Science and Technology Program (No. LHGJ20190823) and Basic Research Project of Henan Eye Institute (No. 21JCZD002).

SUPPLEMENTARY MATERIAL

The Supplementary Material for this article can be found online at: https://www.frontiersin.org/articles/10.3389/fphar.2021.732833/full#supplementary-material

REFERENCES

Bashir, H., Seykora, J. T., and Lee, V. (2017). Invisible Shield: Review of the Corneal Epithelium as a Barrier to UV Radiation, Pathogens, and Other Environmental Stimuli. *J. Ophthalmic Vis. Res.* 12, 305–311. doi:10.4103/jovr.jovr_114_17

Bigagli, E., Cinci, L., D'Ambrosio, M., and Luceri, C. (2017). Pharmacological Activities of an Eye Drop Containing Matricaria Chamomilla and Euphrasia Officinalis Extracts in UVB-Induced Oxidative Stress and Inflammation of Human Corneal Cells. *J. Photochem. Photobiol. B* 173, 618–625. doi:10.1016/j.jphotobiol.2017.06.031

Chen, B. Y., Lin, D. P., Su, K. C., Chen, Y. L., Wu, C. Y., Teng, M. C., et al. (2011). Dietary Zerumbone Prevents against Ultraviolet B-Induced Cataractogenesis in the Mouse. *Mol. Vis.* 17, 723–730.

Chen, M. H., Tsai, C. F., Hsu, Y. W., and Lu, F. J. (2014). Epigallocatechin Gallate Eye Drops Protect against Ultraviolet B-Induced Corneal Oxidative Damage in Mice. *Mol. Vis.* 20, 153–162.

Chen, S. J., Lee, C. J., Lin, T. B., Liu, H. J., Huang, S. Y., Chen, J. Z., et al. (2016). Inhibition of Ultraviolet B-Induced Expression of the Proinflammatory Cytokines TNF-α and VEGF in the Cornea by Fucoxanthin Treatment in a Rat Model. *Mar. Drugs* 14, 13. doi:10.3390/md14010013

Chen, W., Guo, J., Guo, H., Kong, X., Bai, J., and Long, P. (2020). Protective Effect of Vitamin C against Infancy Rat Corneal Injury Caused by Acute UVB Irradiation. *Biomed. Res. Int.* 2020, 8089273. doi:10.1155/2020/8089273

Doughty, M. J. (2019). Methods of Assessment of the Corneas of the Eyes Laboratory Rabbits Exposed to Solar Ultraviolet-B Radiation. *Photochem. Photobiol.* 95, 467–479. doi:10.1111/php.13031

Du, S., Han, B., Li, K., Zhang, X., Sha, X., and Gao, L. (2017). *Lycium Barbarum* Polysaccharides Protect Rat Corneal Epithelial Cells against Ultraviolet B-Induced Apoptosis by Attenuating the Mitochondrial Pathway and Inhibiting JNK Phosphorylation. *Biomed. Res. Int.* 2017, 5806832. doi:10.1155/2017/5806832

Elmore, S. (2007). Apoptosis: a Review of Programmed Cell Death. *Toxicol. Pathol.* 35, 495–516. doi:10.1080/01926230701320337

Hyun, Y. J., Piao, M. J., Zhang, R., Choi, Y. H., Chae, S., and Hyun, J. W. (2012). Photo-protection by 3-bromo-4, 5-dihydroxybenzaldehyde against Ultraviolet B-Induced Oxidative Stress in Human Keratinocytes. *Ecotoxicol Environ. Saf.* 83, 71–78. doi:10.1016/j.ecoenv.2012.06.010

Ibrahim, O. M., Kojima, T., Wakamatsu, T. H., Dogru, M., Matsumoto, Y., Ogawa, Y., et al. (2012). Corneal and Retinal Effects of Ultraviolet-B Exposure in a Soft Contact Lens Mouse Model. *Invest. Ophthalmol. Vis. Sci.* 53, 2403–2413. doi:10.1167/iovs.11-6863

Jauhonen, H. M., Kauppinen, A., Paimela, T., Laihia, J. K., Leino, L., Salminen, A., et al. (2011). *Cis*-urocanic Acid Inhibits SAPK/JNK Signaling Pathway in UV-B Exposed Human Corneal Epithelial Cells *In Vitro*. *Mol. Vis.* 17, 2311–2317.

Kappe, C. O. (2000). Biologically Active Dihydropyrimidones of the Biginelli-Type-Aa Literature Survey. *Eur. J. Med. Chem.* 35, 1043–1052. doi:10.1016/S0223-5234(00)01189-2

Kolozsvári, L., Nógrádi, A., Hopp, B., and Bor, Z. (2002). UV Absorbance of the Human Cornea in the 240- to 400-nm Range. *Invest. Ophthalmol. Vis. Sci.* 43, 2165–2168.

Korhonen, E., Bisevac, J., Hyttinen, J. M. T., Piippo, N., Hytti, M., Kaarniranta, K., et al. (2020). UV-B-induced Inflammasome Activation Can Be Prevented by *Cis*-Urocanic Acid in Human Corneal Epithelial Cells. *Invest. Ophthalmol. Vis. Sci.* 61, 7. doi:10.1167/iovs.61.4.7

Mao, T., Liu, G., Wu, H., Wei, Y., Gou, Y., Wang, J., et al. (2018). High Throughput Preparation of UV-Protective Polymers from Essential Oil Extracts via the Biginelli Reaction. *J. Am. Chem. Soc.* 140, 6865–6872. doi:10.1021/jacs.8b01576

Mao, T., He, X., Liu, G., Wei, Y., Gou, Y., Zhou, X., et al. (2021). Fluorescent Polymers via post-polymerization Modification of Biginelli-type Polymers for Cellular protection against UV Damage. *Polym. Chem.* 12, 852–857. doi:10.1039/D0PY00503G

Maugeri, G., D'Amico, A. G., Amenta, A., Saccone, S., Federico, C., Reibaldi, M., et al. (2020). Protective Effect of PACAP against Ultraviolet B Radiation-Induced Human Corneal Endothelial Cell Injury. *Neuropeptides* 79, 101978. doi:10.1016/j.npep.2019.101978

Paull, T. T., Rogakou, E. P., Yamazaki, V., Kirchgessner, C. U., Gellert, M., and Bonner, W. M. (2000). A Critical Role for Histone H2AX in Recruitment of Repair Factors to Nuclear Foci after DNA Damage. *Curr. Biol.* 10, 886–895. doi:10.1016/S0960-9822(00)00610-2

Pineiro, M., Nascimento, B. F. O., and Rocha Gonsalves, A. Md. A. (2013). *Dihydropyrimidinone Derivatives: Redox Reactivity, Pharmacological Relevance and Medicinal applicationsIn: Quinones Occurrence, Medicinal and Physiological Importance*. Editors E. R. Price and S. C. Johnson (New York: Nova Science Publishers. Inc.), 1–44.

Roberts, J. E. (2001). Ocular Phototoxicity. *J. Photochem. Photobiol. B* 64, 136–143. doi:10.1016/S1011-1344(01)00196-8

Shy, A. N., Li, J., Shi, J., Zhou, N., and Xu, B. (2020). Enzyme-instructed Self-Assembly of the Stereoisomers of Pentapeptides to Form Biocompatible Supramolecular Hydrogels. *J. Drug Target.* 28, 760–765. doi:10.1080/1061186X.2020.1797048

Suh, M. H., Kwon, J. W., Wee, W. R., Han, Y. K., Kim, J. H., and Lee, J. H. (2008). Protective Effect of Ascorbic Acid against Corneal Damage by Ultraviolet B Irradiation: a Pilot Study. *Cornea* 27, 916–922. doi:10.1097/ICO.0b013e31816f7068

Tanito, M., Takanashi, T., Kaidzu, S., Yoshida, Y., and Ohira, A. (2003). Cytoprotective Effects of Rebamipide and Carteolol Hydrochloride against Ultraviolet B-Induced Corneal Damage in Mice. *Invest. Ophthalmol. Vis. Sci.* 44, 2980–2985. doi:10.1167/iovs.02-1043

Teng, M. C., Wu, P. C., Lin, S. P., Wu, C. Y., Wang, P. H., Chen, C. T., et al. (2018). Danshensu Decreases UVB-Induced Corneal Inflammation in an Experimental Mouse Model via Oral Administration. *Curr. Eye Res.* 43, 27–34. doi:10.1080/02713683.2017.1379543

Tsai, C. F., Lu, F. J., and Hsu, Y. W. (2012). Protective Effects of Dunaliella salina - a Carotenoids-Rich Alga - against Ultraviolet B-Induced Corneal Oxidative Damage in Mice. *Mol. Vis.* 18, 1540–1547.

Ubels, J. L., Glupker, C. D., Schotanus, M. P., and Haarsma, L. D. (2016). Involvement of the Extrinsic and Intrinsic Pathways in Ultraviolet B-Induced Apoptosis of Corneal Epithelial Cells. *Exp. Eye Res.* 145, 26–35. doi:10.1016/j.exer.2015.11.003

Viiri, J., Jauhonen, H. M., Kauppinen, A., Ryhänen, T., Paimela, T., Hyttinen, J., et al. (2009). Cis-urocanic Acid Suppresses UV-B-Induced Interleukin-6 and -8 Secretion and Cytotoxicity in Human Corneal and Conjunctival Epithelial Cells *In Vitro*. *Mol. Vis.* 15, 1799–1805.

Young, A. R. (2006). Acute Effects of UVR on Human Eyes and Skin. *Prog. Biophys. Mol. Biol.* 92, 80–85. doi:10.1016/j.pbiomolbio.2006.02.005

Zhao, C., Li, W., Duan, H., Li, Z., Jia, Y., Zhang, S., et al. (2020). NAD+ Precursors Protect Corneal Endothelial Cells from UVB-Induced Apoptosis. *Am. J. Physiol. Cel Physiol.* 318, C796–C805. doi:10.1152/ajpcell.00445.2019

Conflict of Interest: The authors declare that the research was conducted in the absence of any commercial or financial relationships that could be construed as a potential conflict of interest.

frontiers in Pharmacology

ORIGINAL RESEARCH
published: 04 November 2021
doi: 10.3389/fphar.2021.720345

Short-Term Efficacy and Safety Outcomes of Brolucizumab in the Real-Life Clinical Practice

Andrea Montesel[1†], *Claudio Bucolo*[2†], *Ferenc B. Sallo*[1†] *and Chiara M. Eandi*[1*†]

[1]Department of Ophthalmology, University of Lausanne, Fondation Asile des Aveugles, Jules Gonin Eye Hospital, Lausanne, Switzerland, [2]Department of Biomedical and Biotechnological Sciences, School of Medicine, University of Catania, Catania, Italy

OPEN ACCESS

Edited by:
Maria Grazia Morgese,
University of Foggia, Italy

Reviewed by:
Vincenza Maria Elena Bonfiglio,
University of Catania, Italy
Ahmad M Mansour,
American University of Beirut, Lebanon
Dinah Zur,
Tel Aviv Sourasky Medical Center, Israel

***Correspondence:**
Chiara M. Eandi
chiara.eandi@unito.it

†ORCID:
Andrea Montesel
orcid.org/0000-0002-1910-9976
Claudio Bucolo
orcid.org/0000-0002-4879-4140
Ferenc B. Sallo
orcid.org/0000-0003-4313-3965
Chiara M. Eandi
orcid.org/0000-0003-3656-1689

Specialty section:
This article was submitted to Experimental Pharmacology and Drug Discovery, a section of the journal Frontiers in Pharmacology

Received: 04 June 2021
Accepted: 22 October 2021
Published: 04 November 2021

Citation:
Montesel A, Bucolo C, Sallo FB and Eandi CM (2021) Short-Term Efficacy and Safety Outcomes of Brolucizumab in the Real-Life Clinical Practice. Front. Pharmacol. 12:720345. doi: 10.3389/fphar.2021.720345

To report the early efficacy and safety outcomes of treatment with intravitreal injections of brolucizumab (IVT-B) in patients presenting neovascular age-related macular degeneration (nAMD) in a tertiary clinical setting. A retrospective case series of patients that received IVT-B with a minimum of two injections performed and at least 4 weeks of follow-up after last injection. Nineteen eyes of 19 patients were included. The number of IVT-B performed for the whole cohort was 58 injections; the mean number of IVT-B per patient was 3.0 ± 1.0 (range 2–6); the mean follow-up time was 14.4 ± 9.0 weeks. Mean baseline best-corrected visual acuity was 0.4 ± 0.4 logMAR and at the last follow-up was 0.4 ± 0.6 logMAR (p = 0.778). All eyes showed a reduction in retinal thickness, with the central macular thickness being 470 ± 151 µm at baseline and 360 ± 144 µm at the last follow-up (p = 0.001). Intra-retinal fluid was present at baseline in 12 eyes (63%) and in three eyes (16%) at the last follow-up (p = 0.065). Sub-retinal fluid was present at baseline in 17 eyes (89%) and at the last follow-up in three eyes (16%, p = 0.011). Pigment epithelium detachment was apparent in the 16 eyes (84%) at baseline and was still present in 14 eyes (73%, p = 0.811). One adverse event of intraocular inflammation was reported. In conclusion, our short-term experience showed that brolucizumab was highly effective in restoring the anatomy and in stabilizing the visual acuity of eyes with nAMD. Its safety profile should be evaluated carefully and needs further investigations.

Keywords: brolucizumab, anti-vascular endothelial growth factor, intravitreal route, neovascular age-related macular degeneration, retina, choroid

HIGHLIGHTS

Brolucizumab, the newest agent approved in clinical use for the treatment of neovascular age-related macular degeneration, was designed by grafting the complementarity-determining regions of a novel anti-VEGF-A antibody onto a human single-chain antibody fragment. Lately, the American Society of Retinal Specialists highlighted some Adverse Drug Reactions in patients receiving brolucizumab. The present study reported short-term effective anatomical and functional outcomes of brolucizumab in a real-world practice, which confirm results from randomized clinical trials. These data are important for the ophthalmic community and the pharmacovigilance system, particularly for the safety profile. The safety profile of brolucizumab needs further investigations and signs of intraocular inflammation should be evaluated with careful patient monitoring.

INTRODUCTION

Age-related macular degeneration (AMD) is the most common cause of irreversible vision loss in people aged 55 years and older in western industrialized countries (Reibaldi et al., 2016). Neovascular AMD (nAMD) accounts for most cases of AMD-related severe vision loss (Solomon et al., 2019). Intravitreal (IVT) injections of anti-vascular endothelial growth factor (VEGF) agents are currently the gold standard treatment of nAMD (Li et al., 2020). In general, the goals of anti-VEGF therapy in neovascular AMD are to achieve excellent functional visual acuity and maintain a dry macula on clinical and OCT examination. The duration of VEGF suppression appears to vary between drugs as well as with individualized patient responses. On this regard, new effective drugs or innovative intravitreal nano-systems represent two strategies to reduce the injection burden (Conti et al., 1997). Brolucizumab is a newly available anti-VEGF agent that has recently been approved for intraocular use by the United States Food and Drug Administration (FDA) and the European Medicines Agency (EMA), based primarily on the results of two large phase three, multicenter, active-controlled, randomized, double-masked trials, HAWK and HARRIER (Dugel et al., 2020). Brolucizumab (Beovu®, Novartis Pharma AG, Basel, Switzerland) is a low molecular weight (26 kDa versus 48 kDa of ranibizumab and 115 kDa of aflibercept), single-chain antibody fragment that targets all forms of VEGF-A with high affinity (Ricci et al., 2020). The results of the registration trials of brolucizumab were promising, showing gains in visual acuity that were non-inferior to aflibercept and better anatomical outcomes than aflibercept, with a similar safety profile (Sharma et al., 2020). Brolucizumab showed a potential extension of the dosing regimen to 12 weeks intervals, reducing the burden of the treatment, on both patients and physicians. Nevertheless, an increasing number of unforeseen post-marketing adverse events (AEs) following brolucizumab treatment have been reported as intraocular inflammation (IOI), retinal vasculitis and/or retinal artery occlusion associated with severe vision loss (Monés et al., 2020); so there is a rising concern about its clinical use in the ophthalmology community (Rosenfeld et al., 2020). Clinical data regarding the use of intravitreal injections of brolucizumab (IVT-B) outside the above-mentioned clinical trials are still limited. To our knowledge, there are only a few brief reports that investigated the real-world efficacy and safety of brolucizumab (Avayon et al., 2020; Bulirsch et al., 2021; Maruko et al., 2021; Sharma et al., 2021), thus our investigation aims to report our real-life experience with this new anti-VEGF agent in a cohort of nAMD patients.

MATERIALS AND METHODS

Study Population

This is a retrospective, observational, monocentric study at the Jules Gonin Eye Hospital. Clinical records of nAMD patients treated with IVT-B in routine clinical practice at our Institution from March to December 2020 were reviewed. Inclusion criteria were a diagnosis of nAMD with any type of choroidal neovascularization involving the foveal region, a minimum of two injections, including the loading dose, and 4-weeks follow-up following the last IVT-B. Exclusion criteria were the presence of macular diseases other than nAMD, and a history of intraocular inflammation. Treatment-naïve nAMD eyes as well as eyes already under treatment with anti-VEGF intravitreal injection for active choroidal neovascularization (CNV) secondary to nAMD were enrolled. For treatment-naïve eyes, the decision of treatment with IVT-B was proposed to the patient following an extensive discussion of the risks and benefits involved. For patients already receiving IVT injections, the decision of switching to brolucizumab was proposed by the retina specialist based on active exudation persisting after at least three IVTs of other anti-VEGF agents (ranibizumab or aflibercept). The first IVT-B was performed 1 month after the last ranibizumab and 2 months after the last aflibercept. The presence of refractory active exudation was assessed by a senior retina specialist (C.M.E) on the basis of OCT qualitative features suggestive of exudative disease activity following previously published guidelines (Schmidt-Erfurth et al., 2014; Spaide et al., 2020). All patients provided written informed consent before the IVT-B, as usual procedure in clinical care.

Prior to the first IVT-B, all patients underwent best-corrected visual acuity (BCVA) measurement using an Early Treatment Diabetic Retinopathy Study (ETDRS) chart, intraocular pressure (IOP) measurement, a complete slit lamp biomicroscopy examination, fundus ophthalmoscopy following pupil dilation with 1% tropicamide eye drops, and optical coherence tomography (OCT) (Heidelberg Spectralis, Heidelberg Industries, Heidelberg, Germany) imaging.

In the case of treatment-naïve nAMD eyes, fluorescein (FA) and indocyanine green (ICGA) angiography were also performed (Heidelberg Spectralis, Heidelberg Industries, Heidelberg, Germany). Follow-up visits were monthly for the first 3 months, and bimonthly (q8) or every 3 months (q12) subsequently, accordingly to the treatment interval. At each follow-up visit, patients underwent BCVA and IOP measurements, slit-lamp anterior segment and fundus biomicroscopic examinations and OCT imaging.

Treatment Protocol and IVT Injections

IVT-B treatment was scheduled according to the label registered with SwissMedic, the Swiss Agency for Therapeutic Products Brolucizumab (Beovu®, 2020) (https://www.swissmedic.ch/swissmedic/en/home/about-us/publications/public-summary-swiss-par/public-summary-swisspar-beovu.html. Accessed 30 Nov 2020). An initial loading dose of three monthly IVT-B injections was scheduled. Safety evaluations were conducted at every visit, with special regard to signs of IOI. The symptoms of IOI were explained to each patient and they were advised to contact the clinic immediately, should any of these symptoms (such as floaters, blurred vision, metamorphopsia, scotoma, visual field defects) appear during follow-up. Treatment intervals following the loading dose were determined by a

TABLE 1 | Characteristics of the Study Population.

Gender (n)	74% female (14), 26% male (5)
Mean age ± SD (Range)	78.0 ± 8.4 (63–92) Years
Naïve/Previously treated Eyes (n)	79% Eyes previously treated with IVT injections (15), 21% Treatment naïve eyes (4)
Previous IVT injections, Mean ± SD (Range) (Naïve patient excluded, n = 15)	47.2 ± 43.8 (4–139)
	14 eyes ranibizumab 25.0 ± 29.5 (3–98)
	9 eyes aflibercept 39.7 ± 32.5 (2–90)
Mean N° of IVT-B ± SD (Range)	3.0 ± 1.0 (2–6)
Mean follow-up time ± SD (Range)	14.4 ± 9.0 (4.0–35.8) Weeks

[SD, standard deviation; IVT, intravitreal; IVT-B intravitreal injection of brolucizumab].

senior retinal specialist (CME) based on clinical evaluation of the anatomical and functional response to the first three doses and a q8 or a q12 interval was adopted as necessary, in accordance with the registration trials (Dugel et al., 2020).

IOI and uveitis reaction were graded according to the Standardization of Uveitis Nomenclature (SUN) Working Group guidelines (Nussenblatt et al., 1985; Jabs et al., 2005).

Data Collection and Analysis

Collected data included the demographic characteristics and ophthalmic history of the patients, the number of previous intravitreal injections, functional (BCVA) and anatomical parameters, and postoperative complications. For non-treatment-naïve eyes, data just prior to the first IVT-B was considered the baseline, and the subsequent data after brolucizumab injections were included in the analysis. Therefore, in this study we analyzed BCVA at baseline before the IVT-B and at the last follow-up. Central macular thickness (CMT) was measured in OCT volume scans in the central subfield of an Early Treatment of Diabetic Retinopathy Study grid, centered on the fovea. Centering to the fovea and retinal layer segmentation during OCT examination were manually controlled and adjusted if needed for fixation or segmentation misalignments. The presence of intra-retinal fluid (IRF), sub-retinal fluid (SRF), and pigment epithelial detachment (PED) were recorded in OCT B-scans at baseline and at the last follow-up visit by two independent retinal specialists (CME and AM). A qualitative grading as resolution, reduction or increase of IRF, SRF, and PED from baseline to last follow-up was also performed based on the OCT B-scans by two independent retinal specialists (CME and AM). In case of disagreement, a third retina specialist (FS) graded the scans.

Statistical analysis was performed using SPSS software (Version 25.0, SPSS Inc., Chicago, United States). Data were analyzed with frequency and descriptive statistics for qualitative variables. The normality of data samples was assessed with the Kolmogorov–Smirnov test. Statistical comparison between baseline and the last follow-up data for continuous variables was performed using Student's paired *t*-test with a 95% CI. Correlation for multiple testing was performed using the Bonferroni test. A two-tailed Fisher's exact test was used to analyze the association between categorical variables with results statistically significant when associated with a p-value ≤ 0.05.

RESULTS

Characteristic of the Study Population

Nineteen eyes of 19 patients met the inclusion criteria and were included in the analysis. The baseline characteristics of the study population are summarized in **Table 1**. Fourteen patients were female (74%) and five males (26%), with a mean age of 78 ± 8.4 years. Four eyes (21%) were treatment naïve, while 15 eyes (79%) had been previously treated using other available anti-VEGF agents. In particular, 14 eyes received a total of 350 IVT injections of ranibizumab (mean 25.0 ± 29.5, range 3–98), and nine eyes received a total of 358 IVT injections of aflibercept (mean 39.7 ± 32.5, range 3–90). Over the study time, the total number of IVT-B injections performed was 58, with a mean of 3.0 ± 1.0 (range 2–6) injections per eye, and an average follow-up time of 14.4 ± 9.0 (range 4.0–35.8) weeks (**Table 1**). At anterior segment and fundus biomicroscopic examination, the study population presented several factors limiting the potential for visual recovery. In particular, four eyes (21%) presented geographic atrophy and/or retinal fibrosis affecting the central foveal area, three eyes (16%) presented a clinically relevant cataract, one eye (5%) was amblyopic and one eye (5%) presented an epiretinal membrane (**Figure 1**). Seven eyes (37%) were pseudophakic and one eye (5%) had received verteporfin photodynamic therapy (PDT) for nAMD 1 year prior to baseline. No other ocular comorbidity was reported and no topical treatment was used apart from lubricants. None of the patients had a previous history of intraocular inflammation.

Functional and Anatomic Outcomes

The complete functional and anatomical parameters are summarized in **Tables 2**, **3**.

Mean BCVA at baseline was 0.4 ± 0.4 [range from −0.1 to 1.3] logMAR [Snellen equivalent 20/50 (20/16—20/400)], and at the last follow-up was 0.4 ± 0.6 [range from −0.1 to 2] logMAR (20/50 [20/16—20/2000], $p = 0.778$, 95% CI = −0.15 to 0.11, post-hoc statistical power analysis 7.2%). Seven eyes (37%) gained at least one line of vision, nine eyes (47%) remained stable, and three eyes (16%) lost one line of vision.

Concerning the anatomical outcomes, we observed an overall reduction of macular thickness from baseline in all 19 eyes. In particular, the CMT was 470 ± 151 μm (range 235–802) at

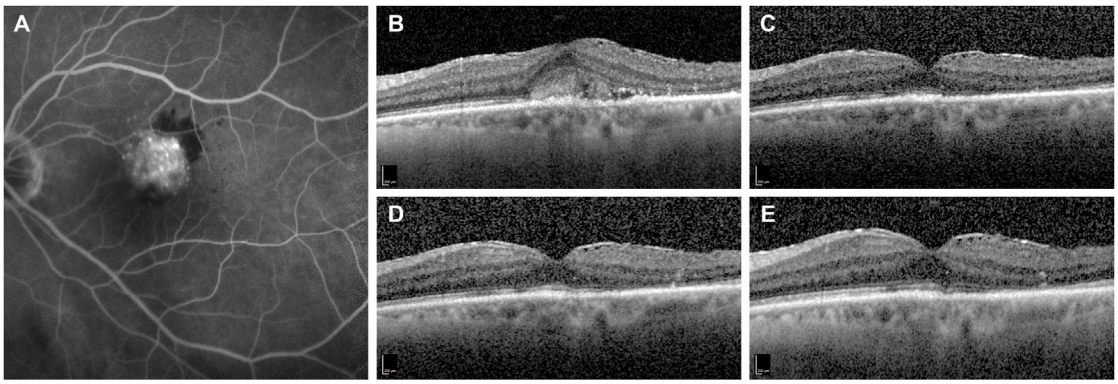

FIGURE 1 | Representative case of a naïve patient presenting with choroidal neovascularization secondary to neovascular age-related macular degeneration treated with monthly intravitreal brolucizumab (IVT-B). **(A)** Baseline fluorescein angiography demonstrates the presence of a subfoveal type 2 choroidal neovascularization with adjacent subretinal hemorrhage. **(B)** Optical coherence tomography (OCT) B-scan at baseline reveals the presence of mild subretinal fluid (SRF) and subretinal hyperreflective material (SHRM) in the foveal area. An epiretinal membrane is also visible. **(C)** OCT B-scan 1 month after the first IVT-B shows the resolution of the SRF and the SHRM with reduction of the central subfield thickness from 375 to 295 μm. **(D)** OCT B-scans at 2-month and **(E)** at 3-month visit demonstrate the absence of recurrences and a dry macula after the loading dose. Best-corrected visual acuity improved from 20/100 to 20/50.

TABLE 2 | Functional and Anatomical Outcomes.

Outcome	Baseline	Last follow-up	*p*
Mean BCVA (logMAR) ± SD (Range)	0.4 ± 0.4 (–0.1–1.3)	0.4 ± 0.6 (–0.1–2)	0.778[a]
Mean CMT (μm) ± SD (Range)	470 ± 151 (235–802)	360 ± 144 (203–728)	0.001*[a]
Presence of IRF (n)	63% (12)	16% (3)	0.065[b]
Presence of SRF (n)	89% (17)	16% (3)	0.011*[b]
Presence of PED (n)	84% (16)	73% (14)	0.811[b]

[p, p-value; BCVA, best corrected visual acuity; LogMAR, logarithm of the minimum angle of resolution; CMT, central macular thickness; IRF, intra-retinal fluid; SRF, sub-retinal fluid; PED, pigment epithelial detachment].
**statistically significant.*
[a]Student paired t-test.
[b]Two-tailed Fisher's exact test.

TABLE 3 | Analysis of the OCT parameters of exudation.

Baseline	Resolved	Reduced	Stable	Increased
IRF (n = 12)	75% (n = 9)	25% (n = 3)	0% (n = 0)	0% (n = 0)
SRF (n = 17)	82% (n = 14)	18% (n = 3)	0% (n = 0)	0% (n = 0)
PED (n = 16)	13% (n = 2)	31% (n = 5)	56% (n = 9)	0% (n = 0)

[OCT, optical coherence tomography; IRF, intra-retinal fluid; SRF, sub-retinal fluid; PED, pigment epithelial detachment].

baseline and 360 ± 144 μm (range 203–728) at last the follow-up (p = 0.001, 95% CI = 51.95–168.98, post-hoc statistical power analysis 94.8%). IRF was present in 12 eyes (63%) at baseline and in three eyes (16%) at the last follow-up. This change was not statistically significant (p = 0.065). SRF was present in 17 eyes (89%) at baseline and in three eyes (16%) at the last follow-up visit. This difference was statistically significant (p = 0.011). The OCT B-scan revealed the presence of a PED in 16 eyes (84%) at baseline and in 14 eyes (73%) at the last follow-up, with no statistical difference between the two time points (p = 0.811) (**Table 2**). At the last follow-up visit, we found a resolution or decrease of all types of fluid in the majority of eyes. In particular, IRF completely resolved in nine (75%) and reduced in three (25%) of the 12 eyes; SRF completely resolved in 14 (82%) and reduced in three (18%) of the 17 eyes (**Figures 1**, **2**); PED completely resolved in two (13%) and reduced in five (31%) of the 16 eyes, while remained stable in nine eyes (56%; **Table 3**). Differences between treatment-naïve and previously treated eyes were not analyzed as the two groups presented a high discrepancy in sample size (four vs 15 eyes).

Safety

In our sample, we found one ocular adverse event. An 85-year-old female who had previously received 82 injections of aflibercept and 12 injections of ranibizumab was switched to brolucizumab due to refractory SRF. The last ranibizumab injection was delivered 4 weeks prior to the first brolucizumab injection, and she received a total of two injections of brolucizumab. Three days after the second IVT-B, she presented with a mild decrease in visual acuity (from 20/50 right before the IVT-B to 20/63), anterior chamber inflammation and an intermediate uveitis classified as mild

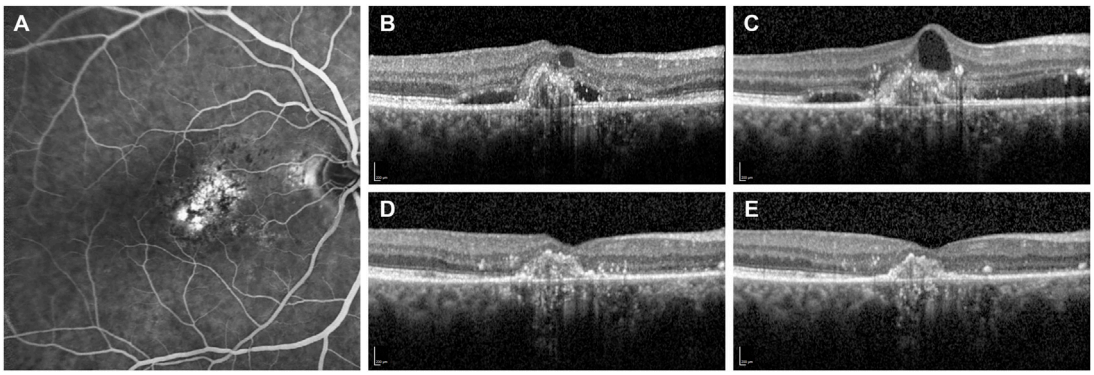

FIGURE 2 | Fluorescein angiography and optical coherence tomography (OCT) B-scans of a patient with subfoveal choroidal neovascularization secondary to neovascular age-related macular degeneration. **(A)** Baseline fluorescein angiography demonstrates the presence of a subfoveal type 1 choroidal neovascularization. **(B)** OCT B-scan at the diagnosis shows a hypereflective subfoveal lesion with intra- and sub-retinal accumulation of fluid (IRF and SRF). **(C)** OCT B-scan at 13-month follow-up after a total of eight IVT injections of ranibizumab demonstrates the persistence of IRF and SRF. Therefore, the patient was switched to monthly intravitreal brolucizumab (IVT-B). **(D)** OCT B-scan 1-month visit after the first IVT-B reveals the complete resolution of IRF and SRF with a reduction of the central subfield thickness from 354 to 233 µm. **(E)** OCT B-scan at 3-month visit after the third IVT-B shows a dry retina and no recurrences are observed. Furthermore, the visual acuity improved from 20/125 to 20/80.

vitreitis following the Standardization of Uveitis Nomenclature (SUN) Working Group criteria (vitreous haze on dilated fundus microscopy with the details of the posterior pole slightly hazy).(Nussenblatt et al., 1985; Jabs et al., 2005). FA and ICGA were performed excluding retinal vasculitis with or without retinal vascular occlusions and a diagnosis of intraocular inflammation was made. Treatment with prednisolone 1% eyedrops six times daily and 50 mg of oral prednisolone daily was started. After 1 week, the vision remained stable at 20/50 and the symptomatology gradually improved. Steroid treatment was then tapered over a period of 30 days, the inflammatory signs completely resolved without any residual vision loss and the patient was switched back to ranibizumab injections with no further adverse events. An individual case safety report (ICSR) was submitted to the Swiss regulatory authority (SwissMedic). We did not find any other previously described systemic or ocular adverse event.

DISCUSSION

In the present study, we reported our short-term real-life clinical experience with using intravitreal brolucizumab for the treatment of nAMD patients. At last follow-up, all eyes in this cohort showed a decrease of the CMT with mostly a complete resolution of IRF and SRF and a stabilization of the BCVA. In the registration trials HAWK and HARRIER, brolucizumab showed a greater fluid resolution and a non-inferior visual function in comparison to aflibercept, which were maintained until week 96 (Dugel et al., 2020; Dugel et al., 2021). The results of the present study confirm the high efficacy of brolucizumab in achieving improved anatomical outcomes in nAMD patients, especially in reducing the fluids in the different retinal compartments (SRF, IRF, PED), and consequently, macular thickness. This is remarkable if we consider that the majority (79%) of our patients presented nAMD refractory to other anti-VEGF agents (**Figure 2**). In particular, fluid reduction was particularly remarkable in the SRF compartment, which reached a statistical significance (p = 0.011) at the last visit compared to baseline. The reduction magnitude of IRF and PED size was overall positive even though it did not reach statistical significance (p = 0.065 and p = 0.811, respectively). None of the eyes showed a deterioration of their anatomical condition at baseline in terms of any of the study parameters.

Visual acuity remained stable despite the anatomical improvement, and the change in BCVA pre-IVT-B and at the last follow-up was not statistically significant (p = 0.778).This may be attributed to the fact that most of the eyes in our cohort presented a longstanding history of nAMD with chronic intra- and sub-retinal fluid accumulation that might limit the potential for visual recovery. Moreover, the mean number of previous anti-VEGF injections in the majority of the enrolled eyes was 32, with only four treatment-naïve eyes, while the HAWK and HARRIER trials included selected treatment-naïve eyes only, with a relatively good visual acuity (mean baseline BCVA of Snellen 20/63) (Dugel et al., 2021). Eyes with a baseline BCVA lower than Snellen 20/400, or with fibrosis and/or GA present affecting the central subfield were also excluded from these trials (Dugel et al., 2020). In addition, the follow-up period of our study was too short to reveal an effective improvement in the visual function of our patients and also the post-hoc power analysis (7.2%) revealed a scarce sample size. Nevertheless, our results are comparable to those of the BREW study (Sharma et al., 2021), which was also conducted over a short follow-up period, and included a previously treated patient sample. Also in this study, change in visual acuity following brolucizumab treatment, even if it showed some improvement, did not reach statistical significance (Sharma et al., 2021).

The presence of fluid is a hallmark of disease activity and therefore retinal fluid control is the aim of nAMD management. So far, brolucizumab has shown encouraging results in reducing the presence or amount of fluids in the different retinal compartments (Enríquez et al., 2021). In this context, early real-life experiences with brolucizumab are in accordance with our results showing improvement of anatomical characteristics visible on OCT. In particular, Bulirsch et al. (2021) and Avaylon et al. (2020) showed beneficial OCT outcomes at the one-month visit after the first brolucizumab injection in a cohort of 63 eyes and six patients respectively. Recently, Haensli et al. (2021) reported functional and anatomical improvement at 6-month follow up in seven eyes insufficiently responding to previous anti-VEGF agents. However, it is reasonable to question the impact of retinal fluids on the visual acuity of the patients. This aspect still presents controversy. In fact, according to the current paradigm, the goal of anti-VEGF treatments is to keep the retina as dry as possible, with a zero-tolerance approach to retina fluids (Schmidt-Erfurth et al., 2014), and retreatment strategies such as the treat and extend approach aim to prevent recurrences (Rufai et al., 2017; Silva et al., 2018). Some recent findings, however, paradoxically correlated the presence of SRF with better visual acuity as compared to a dry macula, hypothesizing a protective effect of SRF to vision-threatening macular atrophy (Guymer et al., 2019; Jaffe et al., 2019; Siedlecki et al., 2020). Moreover, the complete resolution of retinal fluids could also increase the long-term incidence of geographic atrophy (Grunwald et al., 2014; Grunwald et al., 2017; Sadda et al., 2018). On the other hand, the results of the HAWK and HARRIER trials highlighted also the importance of fluctuations in the amount of fluids (Sharma et al., 2020a). In these trials, higher central subfield thickness variability, as an indicator of higher fluid fluctuation, was associated with lower BCVA gains up until 96 weeks, while a more stable CMT was associated with both better visual outcomes and a fluid-free retina (Dugel et al., 2021). A recent post-hoc analysis confirmed the importance of fluid control by reducing retinal thickness fluctuations. In particular, eyes treated in the CATT and IVAN studies that presented greater fluctuation in retinal thickness were associated with lower BCVA and a higher risk of developing GA and fibrosis compared to eyes that had less fluctuation (Evans et al., 2020). In this respect, brolucizumab seems promising, but further long-term studies are needed to completely assess its impact on visual function.

In our cohort, one patient developed vitritis 3 days after the second IVT-B. The IOI was diagnosed promptly and managed using high-dose topical and oral corticosteroid therapy with complete resolution without vision loss. Overall, the safety profile of IVT-B in our cohort is in accordance with the post-hoc analysis of the study HAWK and HARRIER, where in eyes treated with 6 mg brolucizumab, the incidence of IOI reported by the investigators was at least 4.6%, with the 48% of the IOI occurring within the first 3 months (Monés et al., 2020). Several case reports described intraocular inflammation (IOI), retinal vasculitis and/or retinal artery occlusion associate with severe visual acuity loss within the first 3 months after IVT-B (Baumal et al., 2020; Kondapalli et al., 2020; Sharma et al., 2020b; Maruko et al., 2021). Therefore, the ophthalmic community is aware of these potential severe adverse events and a post-marketing reporting system actively collects the AEs and will help to determine the figures of this concern in real-life clinical practice (www.brolucizumab.info). Although the pathogenesis of these AEs has not been established with sureness and is currently under investigation (Sharma et al., 2020c; Kondapalli et al., 2020), current recommendations include active surveillance of brolucizumab patients, prompt investigation of every patient experiencing floaters or ocular discomfort persisting for more than 2 days after IVT-B and also of patients presenting with vision loss or light sensitivity at any time following brolucizumab injection (Baumal et al., 2020a). Routine monitoring should be more comprehensive than in standard clinical practice, with special attention to detecting the clinical findings of IOI, retinal arteritis and retinal occlusive events. Wide-field imaging of the retinal periphery is advised to detect any form of inflammation, leakage and/or ischemia (Baumal et al., 2020a).

Our study presents limitations and strengths. First, the small sample size, the short follow-up period, and its retrospective design limit the outcomes of our study. The aim or our investigation was to report the early outcomes of the clinical use of the new drug brolucizumab, hence it was conducted over a relatively small cohort of patient with a short follow-up period, limiting the power and quality of our outcomes. The differences between treatment-naïve and previously treated eyes were not analyzed as presented a high discrepancy in sample size. The eyes included in this study represented the first patients treated at our center with this new molecule starting on March 2020. Therefore in the switch group, we recruited mostly eyes refractory to other anti-VEGF treatments with persistence of retinal fluid despite the regular and 4–6 weeks interval intravitreal treatments, as shown by the high number of previous injections. Moreover, 9 out of 19 included eyes (47%) presented baseline low vision and in 5 (26%) of them the presence of atrophic and/or fibrotic changes or amblyopia limited the potential for visual recovery. However, even in these eyes with chronic lesions, refractory to other anti-VEGF drugs, the good anatomical response to IV-B with complete resolution of fluid resulted in a stabilization of visual acuity and a subjective improvement.

On the other side, we believe that these results represent indeed a strength of this study. In fact, the heterogeneous population enrolled, characterized by a wide spectrum of baseline clinical features and duration of the disease, represents a real-life situation that differs from the selected patients in clinical trials and therefore, it reflects the treatment outcomes of a real clinical practice. To our knowledge, this is one of only a few reports so far on real-life outcomes of intravitreal brolucizumab for the treatment of nAMD. For this reason, we believe that it is of interest to the ophthalmic community and the pharmacovigilance system. Of course, reports on larger cohorts and longer follow up are needed to support the preliminary real-life experiences of this treatment.

In conclusion, in our early real-life experience, brolucizumab resulted highly effective in restoring the anatomy of eyes affected by nAMD and in stabilizing the visual acuity of both treatment-naïve eyes and of eyes refractory to other anti-VEGF intravitreal agents. Nevertheless, the safety profile of this new anti-VEGF treatment should be evaluated carefully and needs further investigations.

DATA AVAILABILITY STATEMENT

The raw data supporting the conclusion of this article will be made available by the authors, without undue reservation.

ETHICS STATEMENT

The studies involving human participants were reviewed and approved by Commission Cantonal d'Ethique de la Recherche (CER-VD). The patients/participants provided their written informed consent to participate in this study.

AUTHOR CONTRIBUTIONS

Conceptualization AM, CE; methodology, analysis, investigation AM, CE; writing, review and editing AM, FS, CB, CE; supervision, CE; funding acquisition, CE.

REFERENCES

Avaylon, J., Lee, S., and Gallemore, R. P. (2020). Case Series on Initial Responses to Intravitreal Brolucizumab in Patients with Recalcitrant Chronic Wet Age-Related Macular Degeneration. *Int. Med. Case Rep. J.* 13, 145–152. doi:10.2147/IMCRJ.S252260

Baumal, C. R., Bodaghi, B., Singer, M., Tanzer, D. J., Seres, A., Joshi, M. R., et al. (2020a). Expert Opinion on Management of Intraocular Inflammation, Retinal Vasculitis, And/or Vascular Occlusion after Brolucizumab Treatment. *Ophthalmol. Retina* 5, S2468–S6530. doi:10.1016/j.oret.2020.09.020

Baumal, C. R., Spaide, R. F., Vajzovic, L., Freund, K. B., Walter, S. D., John, V., et al. (2020). Retinal Vasculitis and Intraocular Inflammation after Intravitreal Injection of Brolucizumab. *Ophthalmology* 127, 1345–1359. doi:10.1016/j.ophtha.2020.04.017

Beovu® (active substance: brolucizumab) (2020).). https://www.swissmedic.ch/swissmedic/en/home/about-us/publications/public-summary-swiss-par/public-summary-swiss-par-beovu.html (Accessed Nov 30, 2020).

Bulirsch, L. M., Saßmannshausen, M., Nadal, J., Liegl, R., Thiele, S., and Holz, F. G. (2021). Short-Term Real-World Outcomes Following Intravitreal Brolucizumab for Neovascular AMD: SHIFT Study. *Br. J. Ophthalmol* 0, 1–7. doi:10.1136/bjophthalmol-2020-318672

Conti, B., Bucolo, C., Giannavola, C., Puglisi, G., Giunchedi, P., and Conte, U. (1997). Biodegradable Microspheres for the Intravitreal Administration of Acyclovir: *In Vitro*/*In Vivo* Evaluation. *Eur. J. Pharm. Sci.* 5, 287–293. doi:10.1016/S0928-0987(97)00023-7

Dugel, P. U., Koh, A., Ogura, Y., Jaffe, G. J., Schmidt-Erfurth, U., Brown, D. M., et al. (2020). HAWK and HARRIER: Phase 3, Multicenter, Randomized, Double-Masked Trials of Brolucizumab for Neovascular Age-Related Macular Degeneration. *Ophthalmology* 127, 72–84. doi:10.1016/j.ophtha.2019.04.017

Dugel, P. U., Singh, R. P., Koh, A., Ogura, Y., Weissgerber, G., Gedif, K., et al. (2021). HAWK and HARRIER: Ninety-Six-Week Outcomes from the Phase 3 Trials of Brolucizumab for Neovascular Age-Related Macular Degeneration. *Ophthalmology* 128 (1), 89–99. doi:10.1016/j.ophtha.2020.06.028

Enríquez, A. B., Baumal, C. R., Crane, A. M., Witkin, A. J., Lally, D. R., Liang, M. C., et al. (2021). Early Experience with Brolucizumab Treatment of Neovascular Age-Related Macular Degeneration. *JAMA Ophthalmol.* 139, 441–448. doi:10.1001/jamaophthalmol.2020.7085

Evans, R. N., Reeves, B. C., Maguire, M. G., Martin, D. F., Muldrew, A., Peto, T., et al. (2020). Associations of Variation in Retinal Thickness with Visual Acuity and Anatomic Outcomes in Eyes with Neovascular Age-Related Macular Degeneration Lesions Treated with Anti-Vascular Endothelial Growth Factor Agents. *JAMA Ophthalmol.* 138, 1043–1051. doi:10.1001/jamaophthalmol.2020.3001

Grunwald, J. E., Daniel, E., Huang, J., Ying, G. S., Maguire, M. G., Toth, C. A., et al. (2014). Risk of Geographic Atrophy in the Comparison of Age-Related Macular Degeneration Treatments Trials. *Ophthalmology* 121, 150–161. doi:10.1016/j.ophtha.2013.08.015

Grunwald, J. E., Pistilli, M., Daniel, E., Ying, G. S., Pan, W., Jaffe, G. J., et al. (2017). Incidence and Growth of Geographic Atrophy during 5 Years of Comparison of Age-Related Macular Degeneration Treatments Trials. *Ophthalmology* 124, 97–104. doi:10.1016/j.ophtha.2016.09.012

Guymer, R. H., Markey, C. M., McAllister, I. L., Gillies, M. C., Hunyor, A. P., and Arnold, J. J. (2019). Tolerating Subretinal Fluid in Neovascular Age-Related Macular Degeneration Treated with Ranibizumab Using a Treat-And-Extend Regimen: FLUID Study 24-Month Results. *Ophthalmology* 126, 723–734. doi:10.1016/j.ophtha.2018.11.025

Haensli, C., Pfister, I. B., and Garweg, J. G. (2021). Switching to Brolucizumab in Neovascular Age-Related Macular Degeneration Incompletely Responsive to Ranibizumab or Aflibercept: Real-Life 6 Month Outcomes. *J. Clin. Med.* 10, 2666. doi:10.3390/jcm10122666

Jabs, D. A., Nussenblatt, R. B., and Rosenbaum, J. T. (2005). Standardization of Uveitis Nomenclature for Reporting Clinical Data. Results of the First International Workshop. *Am. J. Ophthalmol.* 140 (3), 509–516. doi:10.1016/j.ajo.2005.03.057

Jaffe, G. J., Ying, G. S., Toth, C. A., Daniel, E., Grunwald, J. E., Martin, D. F., et al. (2019). Macular Morphology and Visual Acuity in Year Five of the Comparison of Age-Related Macular Degeneration Treatments Trials. *Ophthalmology* 126, 252–260. doi:10.1016/j.ophtha.2018.08.035

Kondapalli, S. S. A. (2020). Retinal Vasculitis after Administration of Brolucizumab Resulting in Severe Loss of Visual Acuity. *JAMA Ophthalmol.* 138, 1103–1104. doi:10.1001/jamaophthalmol.2020.2810

Li, E., Donati, S., Lindsley, K. B., Krzystolik, M. G., and Virgili, G. (2020). Treatment Regimens for Administration of Anti-Vascular Endothelial Growth Factor Agents for Neovascular Age-Related Macular Degeneration. *Cochrane Database Syst. Rev.* 5, CD012208. doi:10.1002/14651858.CD012208.pub2

Maruko, I., Okada, A. A., Iida, T., Hasegawa, T., Izumi, T., Kawai, M., et al. (2021). Brolucizumab-Related Intraocular Inflammation in Japanese Patients with Age-Related Macular Degeneration: A Short-Term Multicenter Study. *Graefes Arch. Clin. Exp. Ophthalmol.* 259, 2857–2859. doi:10.1007/s00417-021-05136-w

Monés, J., Srivastava, S. K., Jaffe, G. J., Tadayoni, R., Albini, T. A., Kaiser, P. K., et al. (2021). Risk of Inflammation, Retinal Vasculitis, and Retinal Occlusion-Related Events with Brolucizumab. *Ophthalmology* 128, 1050–1059. doi:10.1016/j.ophtha.2020.11.011

Nussenblatt, R. B., Palestine, A. G., Chan, C. C., and Roberge, F. (1985). Standardization of Vitreal Inflammatory Activity in Intermediate and Posterior Uveitis. *Ophthalmology* 92, 467–471. doi:10.1016/s0161-6420(85)34001-0

Reibaldi, M., Longo, A., Pulvirenti, A., Avitabile, T., Russo, A., Cillino, S., et al. (2016). Geo Epidemiology of Age-Related Macular Degeneration: New Clues into the Pathogenesis. *Am. J. Ophthalmol.* 161, 72–78. doi:10.1016/j.ajo.2015.09.031

Ricci, F., Bandello, F., Navarra, P., Staurenghi, G., Stumpp, M., and Zarbin, M. (2020). Neovascular Age-Related Macular Degeneration: Therapeutic Management and New-Upcoming Approaches. *Int. J. Mol. Sci.* 21, 8242. doi:10.3390/ijms21218242

Rosenfeld, P. J., and Browning, D. J. (2020). Reply to Letter from Novartis on "Is This a 737 Max Moment for Brolucizumab?". *Am. J. Ophthalmol.* 216, A7–A8. doi:10.1016/j.ajo.2020.06.034

Rufai, S. R., Almuhtaseb, H., Paul, R. M., Stuart, B. L., Kendrick, T., Lee, H., et al. (2017). A Systematic Review to Assess the 'Treat-And-Extend' Dosing Regimen for Neovascular Age-Related Macular Degeneration Using Ranibizumab. *Eye (Lond)* 31, 1337–1344. doi:10.1038/eye.2017.67

Sadda, S. R., Tuomi, L. L., Ding, B., Fung, A. E., and Hopkins, J. J. (2018). Macular Atrophy in the HARBOR Study for Neovascular Age-Related Macular Degeneration. *Ophthalmology* 125, 878–886. doi:10.1016/j.ophtha.2017.12.026

Schmidt-Erfurth, U., Chong, V., Loewenstein, A., Larsen, M., Souied, E., Schlingemann, R., et al. (2014). Guidelines for the Management of Neovascular Age-Related Macular Degeneration by the European Society of Retina Specialists (EURETINA). *Br. J. Ophthalmol.* 98, 1144–1167. doi:10.1136/bjophthalmol-2014-305702

Sharma, A., Kumar, N., Bandello, F., Kuppermann, B. D., Loewenstein, A., and Regillo, C. D. (2020b). Brolucizumab: The Road Ahead. *Br. J. Ophthalmol.* 104, 1631–1632. doi:10.1136/bjophthalmol-2020-317528

Sharma, A., Kumar, N., Parachuri, N., Sadda, S. R., Corradetti, G., Heier, J., et al. (2021). Brolucizumab-Early Real-World Experience: BREW Study. *Eye (Lond)* 35, 1045–1047. doi:10.1038/s41433-020-1111-x

Sharma, A., Kumar, N., Parachuri, N., Sharma, R., Bandello, F., Kuppermann, B. D., et al. (2020c). Brolucizumab and Immunogenicity. *Eye (Lond)* 34, 1726–1728. doi:10.1038/s41433-020-0853-9

Sharma, A., Kumar, N., Parachuri, N., Sharma, R., Bandello, F., Kuppermann, B. D., et al. (2020a). Brolucizumab and Fluid in Neovascular Age-Related Macular Degeneration (N-AMD). *Eye (Lond)* 34, 1310–1312. doi:10.1038/s41433-020-0831-2

Sharma, A., Parachuri, N., Kumar, N., Sharma, R., Bandello, F., Kuppermann, B. D., et al. (2020). Brolucizumab-Key Learnings from HAWK and HARRIER. *Eye (Lond)* 34, 1318–1320. doi:10.1038/s41433-020-0842-z

Siedlecki, J., Fischer, C., Schworm, B., Kreutzer, T. C., Luft, N., Kortuem, K. U., et al. (2020). Impact of Sub-Retinal Fluid on the Long-Term Incidence of Macular Atrophy in Neovascular Age-Related Macular Degeneration under Treat & Extend Anti-Vascular Endothelial Growth Factor Inhibitors. *Sci. Rep.* 10, 8036. doi:10.1038/s41598-020-64901-9

Silva, R., Berta, A., Larsen, M., Macfadden, W., Feller, C., and Monés, J. (2018). Treat-and-Extend versus Monthly Regimen in Neovascular Age-Related Macular Degeneration: Results with Ranibizumab from the TREND Study. *Ophthalmology* 125, 57–65. doi:10.1016/j.ophtha.2017.07.014

Solomon, S. D., Lindsley, K., Vedula, S. S., Krzystolik, M. G., and Hawkins, B. S. (2019). Anti-Vascular Endothelial Growth Factor for Neovascular Age-Related Macular Degeneration. *Cochrane Database Syst. Rev.* 3, CD005139. doi:10.1002/14651858.CD005139.pub4

Spaide, R. F., Jaffe, G. J., Sarraf, D., Freund, K. B., Sadda, S. R., Staurenghi, G., et al. (2020). Consensus Nomenclature for Reporting Neovascular Age-Related Macular Degeneration Data Consensus on Neovascular Age-Related Macular Degeneration Nomenclature Study Group. *Ophthalmology* 127, 616–636. doi:10.1016/j.ophtha.2019.11.004

Conflict of Interest: The authors declare that the research was conducted in the absence of any commercial or financial relationships that could be construed as a potential conflict of interest.

The reviewer VMEB declared a shared affiliation, with no collaboration, with one of the authors CB to the handling Editor.

Publisher's Note: All claims expressed in this article are solely those of the authors and do not necessarily represent those of their affiliated organizations, or those of the publisher, the editors and the reviewers. Any product that may be evaluated in this article, or claim that may be made by its manufacturer, is not guaranteed or endorsed by the publisher.

frontiers in Pharmacology

ORIGINAL RESEARCH
published: 05 November 2021
doi: 10.3389/fphar.2021.778165

Effects of Vitamin D_3 and Meso-Zeaxanthin on Human Retinal Pigmented Epithelial Cells in Three Integrated *in vitro* Paradigms of Age-Related Macular Degeneration

Francesca Lazzara[1], *Federica Conti*[1], *Chiara Bianca Maria Platania*[1], *Chiara M. Eandi*[2,3], *Filippo Drago*[1,4] *and Claudio Bucolo*[1,4]*

[1]Department of Biomedical and Biotechnological Sciences, School of Medicine, University of Catania, Catania, Italy, [2]Department of Ophthalmology, Fondation Asile des Aveugles, Jules Gonin Eye Hospital, University of Lausanne, Lausanne, Switzerland, [3]Department of Surgical Sciences, University of Torino, Torino, Italy, [4]Center for Research in Ocular Pharmacology–CERFO, University of Catania, Catania, Italy

OPEN ACCESS

Edited by:
Cesare Mancuso, Catholic University of the Sacred Heart, Italy

Reviewed by:
Enza Palazzo, Università della Campania Luigi Vanvitelli, Italy
Moreno Paolini, University of Bologna, Italy

***Correspondence:**
Claudio Bucolo
bucocla@unict.it

Specialty section:
This article was submitted to Experimental Pharmacology and Drug Discovery, a section of the journal Frontiers in Pharmacology

Received: *16 September 2021*
Accepted: *30 September 2021*
Published: *05 November 2021*

Citation:
Lazzara F, Conti F, Platania CBM, Eandi CM, Drago F and Bucolo C (2021) Effects of Vitamin D_3 and Meso-Zeaxanthin on Human Retinal Pigmented Epithelial Cells in Three Integrated in vitro *Paradigms of Age-Related Macular Degeneration. Front. Pharmacol. 12:778165. doi: 10.3389/fphar.2021.778165*

Age-related macular degeneration (AMD) is a degenerative retinal disease and one of major causes of irreversible vision loss. AMD has been linked to several pathological factors, such as oxidative stress and inflammation. Moreover, Aβ (1–42) oligomers have been found in drusen, the extracellular deposits that accumulate beneath the retinal pigmented epithelium in AMD patients. Hereby, we investigated the hypothesis that treatment with 1,25(OH) $_2D_3$ (vitamin D_3) and meso-zeaxanthin, physiologically present in the eye, would counteract the toxic effects of three different insults on immortalized human retinal pigmented epithelial cells (ARPE-19). Specifically, ARPE-19 cells have been challenged with Aβ (1–42) oligomers, H_2O_2, LPS, and TNF-α, respectively. In the present study, we demonstrated that the combination of $1,25(OH)_2D_3$ and meso-zeaxanthin significantly counteracted the cell damage induced by the three insults, at least in these *in vitro* integrated paradigms of AMD. These results suggest that combination of $1,25(OH)_2D_3$ and meso-zeaxanthin could be a useful approach to contrast pathological features of AMD, such as retinal inflammation and oxidative stress.

Keywords: $1,25(OH)_2D_3$, meso-zeaxanthin, amyloid beta, inflammation, oxidative stress, cytokines

INTRODUCTION

Age-related macular degeneration (AMD) is a progressive neurodegenerative and multifactorial disease that if not treated or managed can impair irreversibly the visual function (Cascella et al., 2014; Pennington and DeAngelis, 2016) in the elderly population (usually older than 60 years) (Nowak, 2006). AMD affects the macula, that is, the central portion of the retina, which is highly sensitive to visual stimuli due to the high density of retinal photoreceptors. In the macula of AMD patients, between the retinal pigment epithelium (RPE) and Bruch's membrane, lesions named *drusen* have been found. These lesions are characterized by accumulation of extracellular material, lipid, and protein aggregates. Moreover, the number and size of drusen, along with the presence of choroidal neovascularization, have been found to correlate with the stage of AMD (early, intermediate, or advanced) (Zajaç-Pytrus et al., 2015). Generally, AMD is classified into atrophic (dry or

non-exudative form) and neovascular or exudative forms (wet form). Wet AMD is characterized by overexpression of the vascular endothelial growth factor (VEGF-A), which leads to the breakdown of the blood–retinal barrier and choroidal neovascularization (Kauppinen et al., 2016). Retinal degeneration in wet AMD is tightly linked to choroidal neovascularization (CNV) and growth of leaky blood vessels under the macula, due to overproduction of pro-angiogenic factors (VEGF family) and inflammatory cytokines. Dry AMD can progress to the severe stage, wet AMD, which if not managed can lead to macular edema, retinal detachment, and then to irreversible blindness. Actually, only patients with the wet form (neovascular AMD) can be benefitted from pharmacological therapy, specifically the intravitreal administration of anti-vascular endothelial growth factors (anti-VEGF) (Holekamp, 2019), although anti-VEGF agents, used in clinical practice, such as ranibizumab, bevacizumab, and aflibercept, are considerably different in terms of molecular interactions when they bind with VEGF (Giurdanella et al., 2015; Platania et al., 2015). Currently, one of the main unmet medical needs in AMD management is the lack of effective pharmacological treatment for the dry AMD, which represents the 90% of AMD cases (Buschini et al., 2015). Moreover, the pathophysiology of the AMD is only partially understood, considering that it is the result of the interaction between environmental, metabolic, and genetic factors. Main hallmarks of AMD are represented by tissue dysfunctions (RPE, Bruch's membrane, and choriocapillaris), associated to chronic oxidative stress, autophagy decline, inflammation (Levy et al., 2015; Eandi et al., 2016; Guillonneau et al., 2017), and angiogenesis (Kauppinen et al., 2016; Layana et al., 2017). Several studies highlighted that inflammation is one of the main driving factors of AMD pathogenesis. In fact, drusen deposits contain numerous inflammation-related factors, along with lipids, amyloid-β (Aβ) aggregates, and oxidation by-products (Bucolo et al., 1999; Wang et al., 2009; Krohne et al., 2010). Furthermore, it has been demonstrated that the formation of drusen is induced by chronic low-level inflammation and complement activation, as a result of the activation of inflammatory pathways, such as NFκB (Hageman et al., 2001; D.H. et al., 2002; Johnson et al., 2011). Moreover, the activation of the inflammasome, by amyloid-β, was reported to contribute to RPE dysfunction during AMD (Anderson et al., 2013; Liu et al., 2013). Macrophages, attracted by drusen to the sub-RPE space, release tumor necrosis factor α (TNF-α) that binds tumor necrosis factor receptor 1 (TNFR1), and then stimulate RPE cells' inflammatory response. AMD is also known as the "dementia of the eye," due to the age-dependent accumulation of amyloid beta oligomers in drusen deposits. Several studies demonstrated that Aβ-related damage is common to both the retina and brain, as well as the disruption of the tight junctions in the blood–brain barrier (BRB) and the blood–retinal barrier (BRB) (Parks et al., 2004; Bruban et al., 2009; Biron et al., 2011). Together with inflammation and Aβ-related damage, reactive oxygen species (ROS) have a central role in AMD (Kohen and Nyska, 2002). The altered cellular homeostasis in RPE cells, related to ROS overproduction, can be induced by several factors, such as, aging process, light exposure, diet, and cigarette smoking.

Indeed, because of the multifactorial pathophysiology of both dry and wet AMD, we designed an integrated *in vitro* model of AMD, stimulating RPE cells with three different challenges: Aβ oligomers, hydrogen peroxide (H_2O_2), and inflammatory stimuli (LPS and TNF-α), and testing the effects of *in vitro* treatment with anti-inflammatory, anti-angiogenic, and antioxidant molecules: $1,25(OH)_2D_3$ (vitamin D_3), meso-zeaxanthin (MZ), and their combination. Specifically, vitamin D_3 is a secosteroid able to modulate cell differentiation, homeostasis, and apoptosis through direct and indirect mechanisms of action. The first one is activated by the binding of the active form of vitamin D_3 to its receptor (VDR), a transcriptional factor. VDR is expressed in most human cells, supporting the hypothesis that vitamin D_3 has a pleiotropic effect. Moreover, anti-inflammatory and anti-angiogenic effects of vitamin D_3 have been widely elucidated both in *in vitro* and *in vivo* studies (Majewski et al., 1996; Albert et al., 2007; Maj et al., 2018; Almeida Moreira Leal et al., 2020). Interestingly, the vitamin D_3 receptor is expressed in the RPE layer, which along with enzymes is able to convert the inactive form into the active form. The rationale of this *in vitro* study came from previous reports that have shown a tight link between vitamin D_3 serum levels and AMD progression. In fact, it has been found that a low vitamin D_3 level in serum can be a risk factor for the progression of AMD (Parekh et al., 2007; Millen et al., 2011; Annweiler et al., 2016; Merle et al., 2017; Kan et al., 2020). These findings could be linked to the activation of macrophages phagocytosis of Aβ deposits, along with anti-inflammatory and antioxidant action exerted by vitamin D_3 (Lee et al., 2012).

Meso-zeaxanthin [(3R, 30S)-b, b-carotene-3, 30-diol, MZ] is one of the three xanthophyll carotenoids localized in the *macula lutea*. Carotenoids are lipid-soluble yellow–orange–red pigments with antioxidant and immunomodulatory activity; reduction in carotenoid levels has been linked to increased risk of cardiovascular disease, diabetes, and cancer (Sesso et al., 2004; Hozawa et al., 2006; Eliassen et al., 2015). In particular, MZ is one of the powerful antioxidant carotenoids found in the RPE cell layer. Basically, the source of meso-zeaxanthin in the eye is represented by the endogenous conversion of lutein in the retinal pigment epithelium (Shyam et al., 2017; Green-Gomez et al., 2020). A specific carotenoid-binding protein (Z-binding protein) regulates the retinal uptake from blood of lutein, which can be converted into meso-zeaxanthin (Thurnham et al., 2008; Nolan et al., 2013).

Given these premises on vitamin D_3 and meso-zeaxanthin activities, we tested the efficacy of these two compounds and their combination in three different *in vitro* models of AMD. We found that their combination significantly counteracted the damage induced by Aβ-amyloid oligomers, H_2O_2, and inflammatory stimuli in immortalized human RPE (ARPE-19) cells. Moreover, a bioinformatic analysis evidenced that the combination of these compounds effectively covers the pathways associated with the three stimuli, resembling the AMD multifactorial pathology.

METHODS

Human retinal pigment epithelial cells (ARPE-19) were purchased from ATCC® (Manassas, Virginia, USA). Cells were cultured at 37 °C (humidified atmosphere with 5% CO2) in ATCC-formulated DMEM:F12 medium (ATCC number 30–2006) with 100 U/ml penicillin, 100 µg/ml streptomycin, and 10% fetal bovine serum (FBS). After reaching confluence (70%), ARPE-19 cells were pretreated for 24 h with 50 nM of $1,25(OH)_2D_3$ (Sigma Aldrich, D1530-1mg, St. Louis, MO), 0.1 µM of meso-zeaxanthin (MZ) (Sigma Aldrich, USP reference standard #1733119, St. Louis, MO), and the combination (combo) of $1,25(OH)_2D_3$ (50 nM) and meso-zeaxanthin (MZ, 0.1 µM). Both pretreatment and treatment were performed in medium supplemented with 5% FBS to starve cells. After pretreatment, ARPE-19 cells were challenged with four different stimuli: amyloid-β oligomers (1 and 2.5 µM; amyloid β-protein 1–42 HFIP-treated, Bachem H-7442.0100) (Calafiore et al., 2012; Caruso et al., 2021), hydrogen peroxide (400 µM H_2O_2), LPS (150 ng/ml and 10 µg/ml, Enzo ALX-581–010-L001, Farmingdale, NY), and tumor necrosis-alpha (TNF-α) (10 ng/ml, Thermo Fisher Scientific, Carlsbad, CA), in order to simulate retinal degeneration, retinal oxidative stress, and early and late inflammation, respectively. $1,25(OH)_2D_3$, MZ, and the combo were also added to the medium containing negative stimuli.

Cell Viability

The 3-[4,5-dimethylthiazol-2-yl]-2,5-diphenyl tetrasodium bromide (MTT; Chemicon, Temecula, CA) was used to assess cell viability after Aβ (1–42) and H_2O_2 challenge. Optimal cell density was obtained by seeding 3×10^4 cells/well in 96-well plates (Costar, Corning, NY, United States). After pretreatment, ARPE-19 cells were subjected to co-treatment in a fresh medium for 48 h with Aβ (1–42) (1 µM) and for 6 and 24 h with H_2O_2 (400 µM). At the end of the treatment, ARPE-19 cells were incubated at 37°C with MTT (0.5 mg/ml) for 3 h; then DMSO was added, and absorbance was measured at 570 nm in a plate reader (VariosKan, Thermo Fisher Scientific, Waltham, MA, United States). Graphs were built converting absorbance (abs) to viability (=% of control) using the following equation $(absx \div absctrl-) \times 100$, where absx is absorbance in the x well, and absctrl− is the average absorbance of negative control cells (untreated cells).

Lactate Dehydrogenase Cell Release

Lactate dehydrogenase (LDH) cell release was measured using the Cytotoxicity Detection KitPLUS (LDH) (ROCHE, Mannheim, Germany). ARPE-19 cells were seeded at 2×10^4 cells/well in 96-well plates (Costar, Corning, NY, United States). After pretreatment, cells were co-treated for 48 h with Aβ (1–42) (1 µM) and for 6 and 24 h in the oxidative stress model (H_2O_2 400 µM). In control groups, only fresh medium was added. After these time points, according to manufacturer's protocol, lysis solution was added to positive control wells (non-treated cells) for 15 min. After transferring 100 µl of medium in a new multi-well plate, 100 µl of working solution was added. After 10–15 min at room temperature, at last, 50 µl of stop solution was added. The absorbance values were measured at 490 nm using a plate reader (VarioSkan, Thermo Fisher Scientific, Waltham, MA, United States). LDH release is reported as LDH (% control) $(absx \div absctrl+) \times 100$. In the equation, abs_x is absorbance in the x well and abs_{ctrl+} is the average absorbance of positive control cells (untreated lysed cells). Absorbance values were corrected by subtracting medium absorbance.

Reactive Oxygen Species Production

ROS were measured by a 2′,7′-dichlorofluoresceindiacetate (DCFDA)–Cellular Reactive Oxygen Species Detection Assay Kit (Abcam, Cambridge, United Kingdom). DCFDA, a cell permeable fluorogenic dye, is deacetylated by cellular esterases to a non-fluorescent compound and later oxidized by ROS to highly fluorescent 2′,7′-dichlorofluorescein (DCF); fluorescence intensity is proportional to cell ROS concentration. Optimal cell density was obtained by seeding 20×10^3 cells/well in 96-well plates (Costar, Corning, NY, United States). After reaching confluence (70%), ARPE-19 cells were pretreated with $1,25(OH)_2D_3$, mesozeaxanthin, and the combo for 24 h. Subsequently, cells were submitted to co-treatment for 48 h in amyloid-β challenge (1 µM). After treatment, media were aspirated and cells were washed by adding 100 µl/well of 1X buffer, according to manufacturer's protocol; after washing, ARPE-19 cells were stained by adding 100 µl/well of the diluted DCDFA solution (25 µM). Cells were also incubated with this solution for 45 min at 37°C in the dark. After removing DCDFA solution, 100 µl/well of 1X buffer was added, and ROS concentration was measured immediately by detection of DCF fluorescence (λ_{ex} = 495 nm, λ_{em} = 529 nm) with a Varioskan™ Flash Multimode Reader. According to manufacturer's protocol, for treatment lower than or equal to 6 h, it is possible to treat cells after adding DCDFA solution. Thus, after 24 h of pretreatment with drug formulations, ARPE-19 cells were washed and stained with DCDFA for 45 min. After removing DCDFA solution and washing again, ARPE-19 cells underwent co-treatment for 6 h in H_2O_2 challenge (400 µM). At the end of time point, ROS concentration was measured immediately without washing. Results were reported as percentage of control after background subtraction; to determine total ROS formation, the fluorescence was normalized to the fluorescent intensity of control cells (untreated cells).

Extraction of Total Ribonucleic Acid and cDNA Synthesis

Extraction of total RNA, from ARPE-19 cells, was performed with a TRIzol Reagent (Invitrogen, Life Technologies, Carlsbad, CA, United States). The A_{260}/A_{280} ratio of optical density of RNA samples (measured with Multimode Reader Flash di Varioskan™) was 1.95–2.01; this RNA purity was confirmed with the electrophoresis in non-denaturing 1% agarose gel (in TAE). cDNA was synthesized from 2 µg RNA with a reverse transcription kit (SuperScript™ II Reverse transcriptase,

Invitrogen, Thermo Fisher Scientific, Carlsbad, CA, United States).

Real-Time Reverse Transcriptase–Polymerase Chain Reaction

Real-time PCR was carried out with the Rotor-Gene Q (Qiagen). The amplification reaction mix included the Master Mix Qiagen (10 µl) (Qiagen QuantiNova SYBR Green Real-Time PCR Kit) and cDNA (1 µL, 100 ng). Forty-five amplification cycles were carried out for each sample. Results were analyzed with the $2^{-\Delta\Delta}$Ct method. Quantitative PCR experiments followed the MIQE guidelines. Gene expression levels were normalized with levels of two housekeeping genes (18S and GAPDH). Primers were purchased from Eurofins Genomics (Milan, Italy) and Qiagen (Milan, Italy). Forward and reverse primer sequences (for human genes) and the catalog number are herein listed: human IL-1β (forward: 5′-AGCTACGAATCTCCGACCAC-3'; reverse: 5′-CGTTATCCCATGTGTCGAAGAA-3′), human IL-6 (Catalog Number QT00083720), human TNF-α (forward 5′-AGCCCATGTTGTAGCAAACC-3'; reverse 5′-TGAGGTACA GGCCCTCTGAT-3′), human MMP-9 (forward 5′-CTTTGA GTCCGGTGGACGAT-3'; reverse 5′-TCGCCAGTACTTCCC ATCCT-3′), human VEGF-A (forward 5′-AGGGCAGAATCA TCACGAAG-3'; reverse 5′-ATCCGCATAATCTGCATGGT-3′), human 18S (forward 5′-AGTCCCTGCCCTTTG-3'; reverse 5′-GATCCGAGGGCCTCACTAAAC-3′), and human GAPDH (forward 5′-CTGCACCACCAACTGCTTAG-3'; reverse 5′-AGGTCCACCACTGACACGTT-3′).

Western Blot

ARPE-19 cells were cultured in 60-mm petri dishes at a density of 1.3×10^6. After 24 h of pretreatment with drugs and co-treatment with different stimuli (400 µM of H_2O_2 for 4 h, 10 µg/ml of LPS for 2 h, amyloid-β oligomers 2.5 µM for 48 h, and TNF-α 10 ng/ml for 2 h), cytoplasmic and nuclear proteins were extracted by using the CER/NER kit (NE-PER, Invitrogen, Life Technologies, Carlsbad, USA), according to the manufacturer's protocol. The protein content was determined by the BCA Assay Kit (Pierce™ BCA Protein Assay Kit, Invitrogen, Life Technologies, Carlsbad, United States). Extracted proteins (20 µg) were loaded on a NuPAGE ™ 10% Bis-Tris mini protein gel (Invitrogen, Life Technologies, Carlsbad, CA, United States). After electrophoresis, proteins were transferred to a nitrocellulose membrane (Invitrogen, Life Technologies, Carlsbad, CA, United States). Membranes were blocked with milk, 5% Tris-buffered saline, and 0.2% Tween 20 (TBST) for 1 h at room temperature. Membranes were incubated overnight (4°C) with appropriate primary phospho-NFκB p65 (Ser536; mouse mAb #3036 Cell Signaling Technology, MA, United States, 1:500 dilution), anti-GAPDH (Rabbit mAb #2118 Cell Signaling Technology, MA, United States; 1:1,000 dilution), and anti-lamin B (Mouse monoclonal IgG_{2b}, sc-365214 Santa Cruz Biotechnology; 1:1,000 dilution) antibodies. After overnight incubation, the membranes were then incubated with secondary chemiluminscent antibodies (ECL anti-mouse, NA931 and ECL anti-rabbit, NA934, 1:2000 dilution) for 1 h at room temperature. After secondary antibody, the membranes were incubated with ECL (SuperSignal™ West Pico PLUS Chemiluminescent Substrate, Thermo Fisher Scientific, Carlsbad, CA, United States) and were detected through I-Bright™ 1500 (Invitrogen, Life Technologies, Carlsbad, CA, United States) by using chemiluminescence. Densitometry analyses of blots were performed at non-saturating exposures and analyzed using ImageJ software (NIH, Bethesda, MD). Values were normalized to GAPDH and lamin B, which were used as housekeeping control for cytoplasmic and nuclear fraction, respectively.

Bioinformatics

The STITCH compound app of Cytoscape v. 3.7.0 was used to build an integrated network resembling all the experimental results obtained with our integrated *in vitro* model. Inputs were (i.e., query terms) β amyloid, LPS, TNF-α, H_2O_2, meso-zeaxanthin, vitamin D_3, IL-6, Il-1β, VEGF-A, and MMP-9. The number of interactors was limited to 15, and the default confidence score was set to 0.40. Enrichment of information was included in the analysis. A centrality metrics analysis was carried out treating the network as an indirect graph (Platania et al., 2015, 2018). Functional clusters were identified with Cytoscape using specific terms: β amyloid, H_2O_2, LPS, TNF-α, vitamin D_3, and meso-zeaxanthin.

Statistical Analysis

Statistical analysis was performed with GraphPad Prism 7 (GraphPad software, La Jolla, California). All experiments were repeated five times ($n = 5$), and the data are reported as mean ± SD. One-way analysis of variance (ANOVA) was carried out, and Tukey's post hoc test was used for multiple comparisons. Differences between groups were considered statistically significant for p-values < 0.05.

RESULTS

Aβ-Oligomers Damage

In this study, we tested the protective effect of $1,25(OH)_2D_3$, meso-zeaxanthin (MZ), and their combination against Aβ (1–42) oligomer-induced cytotoxicity, through measurement of ARPE-19 cell viability, after challenge with Aβ (**Figure 1**). Preliminary studies were carried out with the MTT assay to evaluate Aβ-oligomer toxicity on ARPE-19 cells, and we found that 1 µM Aβ-oligomers for 48 h induced roughly 17% cell death. Indeed, 1 µM Aβ-oligomers concentration was used also for LDH and ROS assays. In preliminary studies, ARPE-19 cells were pretreated with different concentrations of $1,25(OH)_2D_3$, MZ, and their combination for 24 h. Therefore, cells were incubated with 1 µM Aβ for 48 h, the most effective compound concentrations were 50 nM and 0.1 µM for $1,25(OH)_2D_3$ and MZ, respectively; indeed we used these concentrations also in the combination of the two compounds [combo: $1,25(OH)_2D_3$ 50 nM + MZ 0.1 µM]. $1,25(OH)_2D_3$ and the combo pretreament significantly ($p < 0.05$) counteracted cell toxicity induced by challenge with Aβ (MTT assay, **Figure 1A**). Moreover, LDH

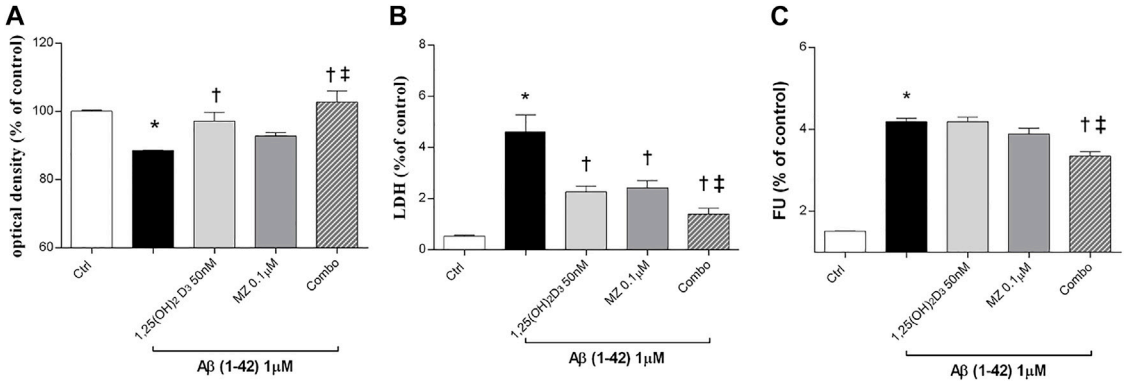

FIGURE 1 | 1,25$(OH)_2D_3$, meso-zeaxanthin (MZ), and their combination show protective effect in ARPE-19 cells treated with Aβ (1–42). Cells were pretreated for 24 h with tested compounds and for 48 h with Aβ insult. At the end of treatment were carried out MTT **(A)**, LDH **(B)**, and the ROS assay **(C)**. Values are reported as mean ± SD ($n = 5$). Data were analyzed by one-way ANOVA and Tukey's post hoc test for multiple comparisons. *p < 0.05 vs. control; †p < 0.05 vs. Aβ, ‡p < 0.05 vs. 50 nM 1,25$(OH)_2D_3$ or 0.1 μM MZ.

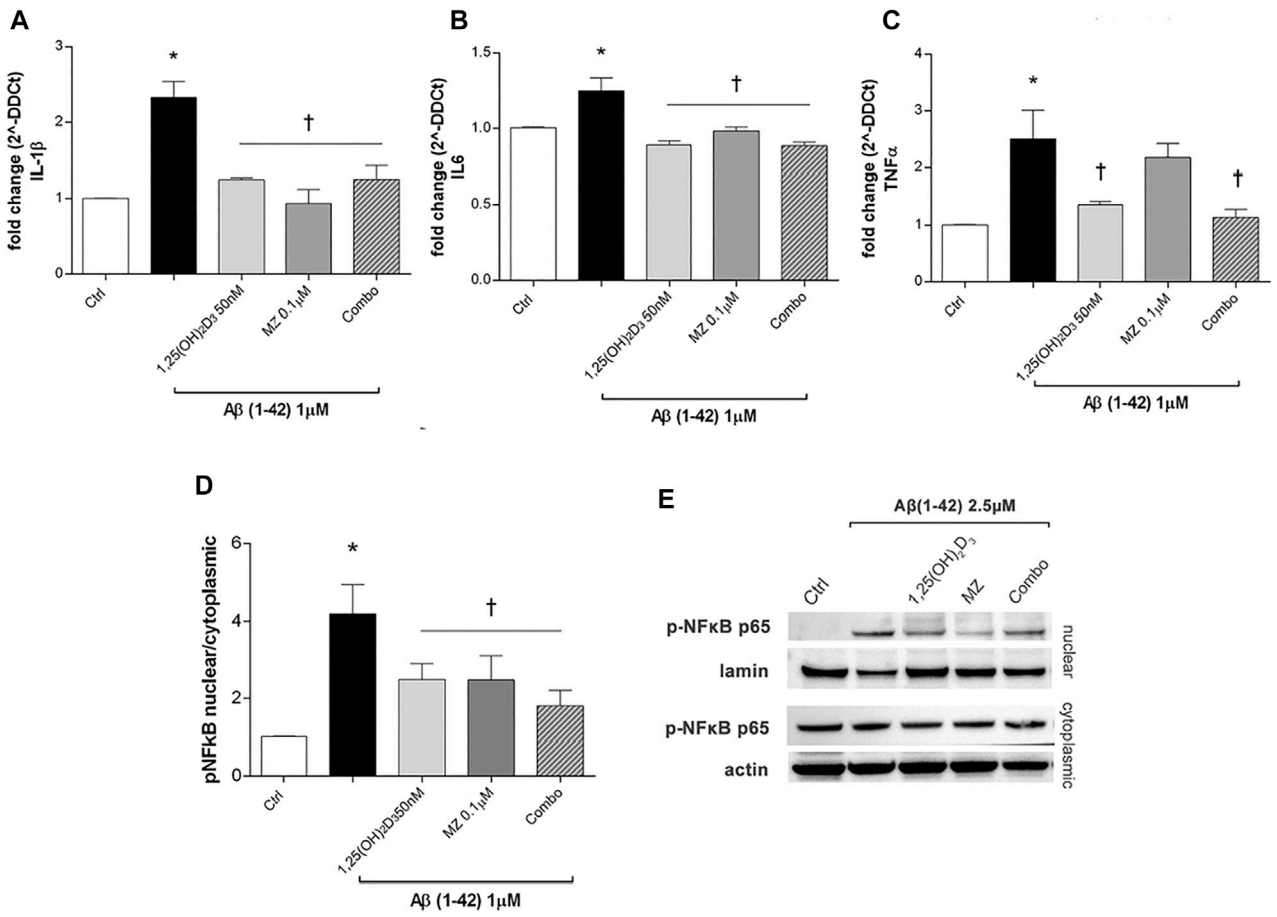

FIGURE 2 | Treatment of ARPE-19 cells with 1,25$(OH)_2D_3$, meso-zeaxanthin (MZ), and their combination (combo) counteract inflammation after Aβ (1–42) exposure. The treatment with 1,25$(OH)_2D_3$, MZ, and their combo reduced IL-1β **(A)**, IL-6 **(B)**, and TNF-α **(C)** mRNA expression. The mRNA levels were evaluated by qPCR. **(D)** Western blot analysis. Densitometry analysis of each band (ratio of nuclear *p*-NFκB p-65/lamin B and cytoplasmic *p*-NFκB p-65/actin) was carried out with the ImageJ program. **(E)** Representative blots of nuclear and cytoplasmic extracted proteins from control and treated cells. Each bar represents the mean value ±SD ($n = 5$; each run in triplicate). One-way ANOVA and Tukey's post hoc test for multiple comparisons were carried out. *$p < 0.05$ vs. control; †$p < 0.05$ vs. Aβ.

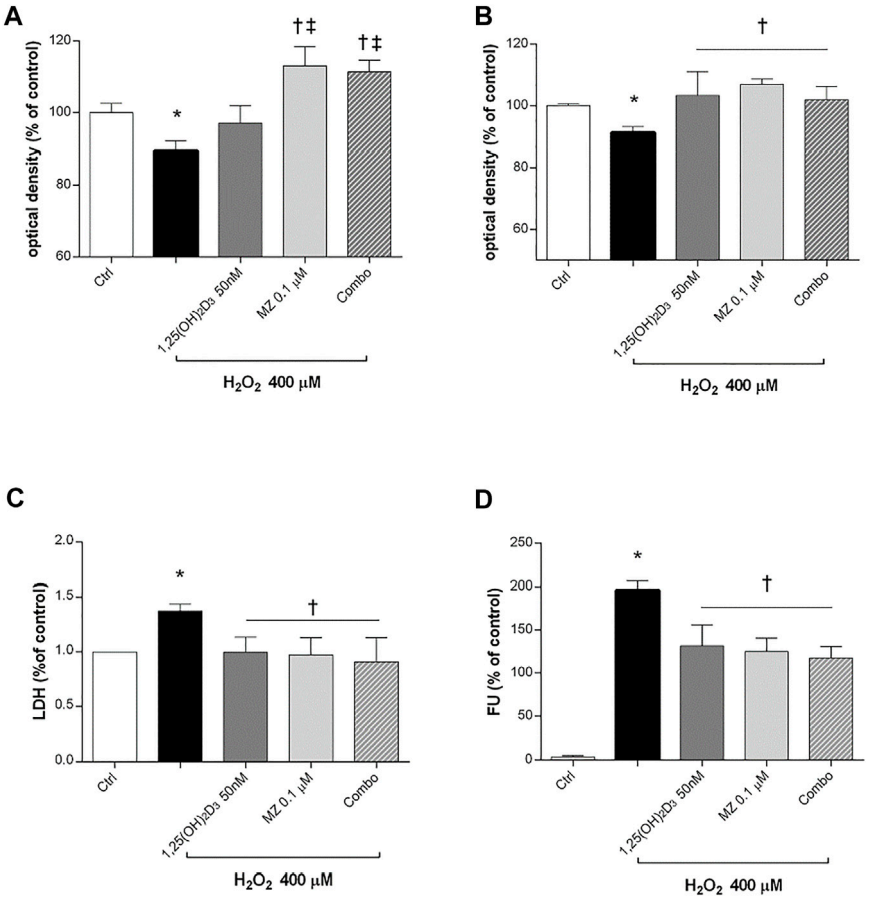

FIGURE 3 | 1,25$(OH)_2D_3$, meso-zeaxanthin (MZ), and their combination protect ARPE-19 cells from oxidative damage. ARPE-19 cells were pretreated for 24 h with 1,25$(OH)_2D_3$ (50 nM), MZ (0.1 μM), and their combo (1,25$(OH)_2D_3$ 50 nM, MZ 0.1 μM), and then treated with H_2O_2 (400 μM) for the MTT assay at 6 **(A)** and 24 h **(B). (C)** LDH release of ARPE-19 cells treated for 24 h with H_2O_2 (400 μM). **(D)** Pretreatment with 1,25$(OH)_2D_3$ (50 nM), MZ (0.1 μM), and their combination decreased ROS (fluorescent units, FU) production in ARPE-19 cells, challenged for 6 h with 400 μM H_2O_2. The results are expressed as mean ± SD (n = 5; each run in triplicate). Data were analyzed by one-way ANOVA and Tukey's post hoc test for multiple comparisons. *$p < 0.05$ vs. ctrl; †$p < 0.05$ vs. H_2O_2; ‡$p < 0.05$ vs. 1,25$(OH)_2D_3$.

release was significantly increased ($p < 0.05$) after treatment with Aβ; the tested compounds 1,25$(OH)_2D_3$ and MZ, and their combination (combo), induced a significant ($p < 0.05$) reduction of cell damage after 48 h (**Figure 1B**). Finally, we analyzed the antioxidant activity of tested compounds. After 48 h of exposure, Aβ-oligomer insult significantly increased ($p < 0.05$) ROS release in ARPE-19 cells. Only the combination of 1,25$(OH)_2D_3$ and MZ was able to significantly reduce the amount of ROS after 48 h ($p < 0.05$) (**Figure 1C**), compared to Aβ-positive control cells.

After 24h, Aβ oligomers exposure (1 μM) significantly ($p < 0.05$) increased mRNA expression of IL-1β, IL-6, and TNF-α (**Figures 2A–C**) in ARPE-19 cells. The treatment with 1,25$(OH)_2D_3$, meso-zeaxanthin (MZ), and their combination significantly decreased IL-1β (**Figure 2A**) and IL-6 (**Figure 2B**), while only 1,25$(OH)_2D_3$ and the combo significantly reduced TNF-α mRNA expression (**Figure 2C**). Furthermore, Aβ treatment significantly ($p < 0.05$) increased nuclear translocation of p-NFκB p65 after 48 h of insult (**Figure 2D**). On the other hand, pretreatment for 24 h with 1,25$(OH)_2D_3$, MZ, and combo significantly ($p < 0.05$) reduced the translocation *p*-NFκB p65, confirming the anti-inflammatory effect of these two compounds and their combination, in retinal pigmented epithelial cells, challenged with Aβ oligomers (**Figures 2D,E**).

Oxidative Stress

Preliminary studies on ARPE-19 cells were carried out to assess the best H_2O_2 concentration and time of exposure to oxidative stress able to elicit roughly 15% cell death. Therefore, human retinal pigmented epithelial cells were pretreated for 24 h with 1,25$(OH)_2D_3$ (50 nM), meso-zeaxanthin (MZ) (0.1 μM), and combo (1,25$(OH)_2D_3$ 50 nM, MZ 0.1 μM), and then cells were incubated in 400 μM H_2O_2 for 6 h (**Figure 3A**) and 24 h (**Figure 3B**). After 6 h of challenge, 1,25$(OH)_2D_3$ was not able to counteract H_2O_2-induced cell damage, instead after 24 h both compounds and their combination significantly restored cell viability. Moreover, H_2O_2 significantly ($p < 0.05$) increased LDH levels in ARPE-19 cells, and the pretreatment with tested compounds induced a significant

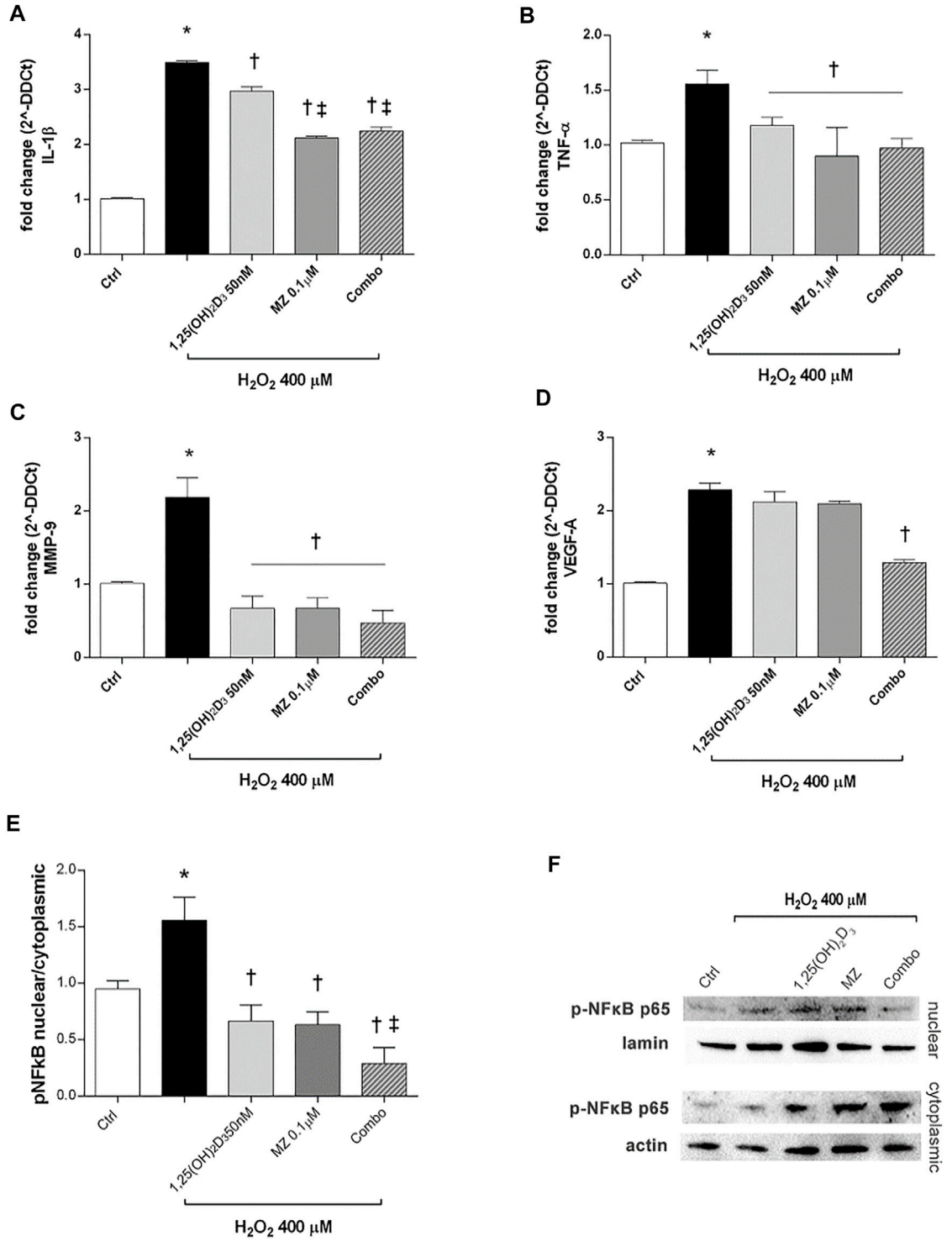

FIGURE 4 | 1,25$(OH)_2D_3$, MZ, and their combination attenuate H_2O_2-induced inflammation. 1,25$(OH)_2D_3$, MZ, and the combination reduced IL-1β **(A)**, TNF-α **(B)**, and MMP-9 **(C)** mRNA expression. The combo decreased VEGF-A mRNA expression induced after 6 h of H_2O_2 treatment **(D)**. ARPE-19 cells were pretreated for 24 h with 1,25$(OH)_2D_3$ (50 nM), MZ (0.1 μM), and their combo (1,25$(OH)_2D_3$ 50 nM + meso-zeaxanthin 0.1 μM), and then challenged with H_2O_2 (400 μM) for 6 h. The mRNA levels were evaluated by qPCR. **(E)** Western blot analysis. Densitometry analysis of each band (ratio of nuclear *p*-NFκB p-65/lamin B and cytoplasmic *p*-NFκB p-65/actin) was carried out with ImageJ program. **(F)** Representative blots of nuclear and cytoplasmic proteins. Each bar represents mean value ±SD (n = 5; each run in triplicate). Data were analyzed by one-way ANOVA and Tukey's post hoc test for multiple comparisons. *$p < 0.05$ vs. control; †$p < 0.05$ vs. H_2O_2; ‡$p < 0.05$ vs. 1,25$(OH)_2D_3$ and MZ.

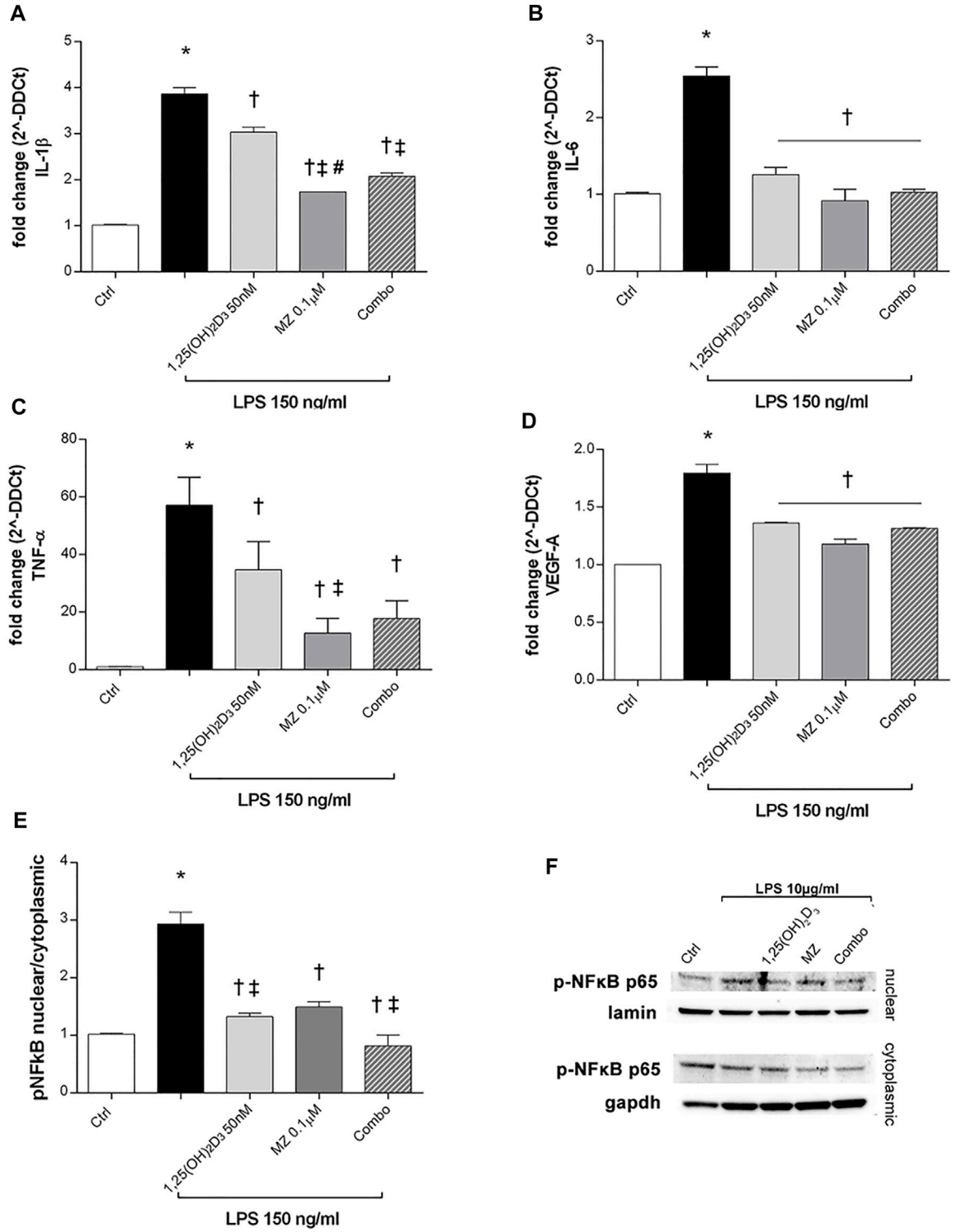

FIGURE 5 | 1,25$(OH)_2D_3$, meso-zeaxanthin (MZ), and their combination protect ARPE-19 cells from LPS-induced damage. 1,25$(OH)_2D_3$, meso-zeaxanthin (MZ), and their combo reduced IL-1β **(A)**, IL-6 **(B)**, TNF-α **(C)**, and VEGF-A **(D)** mRNA expression. ARPE-19 cells were pretreated for 24 h with 1,25$(OH)_2D_3$ (50 nM), MZ (0.1 μM), and their combo (1,25$(OH)_2D_3$ 50 nM + MZ 0.1 μM), and then challenged with LPS (150 ng/ml) for 2 h. The mRNA levels were evaluated by qPCR. **(E)** Densitometry of *p*-NFκB p65 nuclear translocation in treated cells. ARPE-19 cells were pretreated for 24 h with 1,25$(OH)_2D_3$ (50 nM), MZ (0.1 μM), and their combo (1,25$(OH)_2D_3$ 50 nM + MZ 0.1 μM), and then challenged with LPS (10 μg/ml) for 2 h. **(F)** Representative images of blots of nuclear and cytoplasmic protein. Each bar represents the mean value ±SD ($n = 5$; each run in triplicate). Data were analyzed by one-way ANOVA and Tukey's post hoc test for multiple comparisons. *$p < 0.05$ vs. control; †$p < 0.05$ vs. LPS; ‡$p < 0.05$ vs. 1,25$(OH)_2D_3$ and MZ; #$p < 0.05$ vs. combo.

reduction of cell damage (**Figure 3C**). Furthermore, we evaluated the effect of the tested compounds and their combination in terms of ROS production on ARPE-19 cells after H_2O_2 exposure. After 6h, H_2O_2 significantly increased ($p < 0.05$) ROS in ARPE-19 cells, compared to control cells (**Figure 3D**). Pretreatment with $1,25(OH)_2D_3$, MZ, and their combination significantly ($p < 0.05$) counteracted oxidative stress in retinal cells, reducing ROS release.

Furthermore, we analyzed IL-1β and TNF-α mRNA levels to assess the effect of $1,25(OH)_2D_3$ and meso-zeaxanthin (MZ) in modulation of inflammatory response, in ARPE-19 cells challenged with H_2O_2 (400 μM) for 6 h. H_2O_2 challenge led to significant ($p < 0.05$) increase in IL-1β and TNF-α mRNA expression (**Figures 4A,B**). Treatment with $1,25(OH)_2D_3$ (50 nM), MZ (0.1 μM), and their combination reverted the effect of H_2O_2 (**Figures 4A,B**). Furthermore, we assessed effects of those compounds in reducing MMP-9 and VEGF-A mRNA levels, both involved in retinal angiogenesis and neovascularization. H_2O_2 treatment induced a significant ($p < 0.05$) upregulation of both factors (**Figures 4C,D**). The MMP-9 mRNA levels were significantly ($p < 0.05$) reduced by $1,25(OH)_2D_3$, MZ, and their combination, compared to H_2O_2-treated cells (**Figure 4C**). Only the combination of $1,25(OH)_2D_3$ and MZ significantly reduced VEGF-A mRNA levels, in comparison to cells exposed to H_2O_2 ($p < 0.05$) (**Figure 4D**). Furthermore, we assessed the effect of tested compounds in terms of p65-NFκB nuclear translocation. H_2O_2 challenge led to a higher ($p < 0.05$) p-p65 nuclear translocation after 4 h. This process was significantly ($p < 0.05$) counteracted by pretreatment with $1,25(OH)_2D_3$ (50 nM), MZ (0.1 μM), and their combination. Particularly, the combo significantly inhibited p65-NFκB translocation, compared to tested compounds and H_2O_2-exposed cells (**Figures 4E,F**).

LPS Insult

ARPE-19 cells were pretreated with $1,25(OH)_2D_3$ (50 nM), meso-zeaxanthin (MZ, 0.1 μM), and their combination (combo: $1,25(OH)_2D_3$ 50 nM + MZ 0.1 μM) for 24h, and then exposed to LPS (150 ng/ml) for 2 h. IL-1β, IL-6, and TNF-α mRNA levels were significantly increased in the LPS-stimulated cells, compared to control cells ($p < 0.05$). Both compounds and their combination ($p < 0.05$) significantly reduced cytokine mRNA levels (**Figures 5A–C**). MZ significantly reduced TNF-α mRNA expression, compared to 50 nM $1,25(OH)_2D_3$ and the combo (50 nM $1,25(OH)_2D_3$ + 0.1 μM MZ). Furthermore, LPS treatment significantly induced the upregulation of VEGF-A mRNA ($p < 0.05$) (**Figure 5D**), and the treatment with $1,25(OH)_2D_3$, MZ, and their combo significantly reduced the expression of the latter ($p < 0.05$). After 2 h exposure, LPS (10 μg/ml) led to a significant increase of *p*-NFκB p65 nuclear translocation, in comparison to control cells ($p < 0.05$) (**Figures 5E,F**). The treatment with $1,25(OH)_2D_3$, MZ, and their combo significantly inhibited this translocation, leading to a reduction in p-p65 nuclear protein amount ($p < 0.05$) (**Figures 5E,F**).

TNF-α Insult

To evaluate ARPE-19 cells response to TNF-α challenge (10 μg/ml), we analyzed TNF-α, IL-6, and IL-1β mRNA levels. After 2 h, those cytokines were significantly increased by TNF-α treatment (10 ng/ml) ($p < 0.05$) and were strongly downregulated by $1,25(OH)_2D_3$, meso-zeaxanthin (MZ), and the combo pretreatments ($p < 0.05$) (**Figures 6A–C**). We confirmed the anti-inflammatory effects of tested compounds against TNF-α exposure also through evaluation of the *p*-NFκB p65 nuclear translocation (**Figures 6D,E**). TNF-α challenge significantly increased the nuclear translocation of p-NFκB p65 ($p < 0.05$). Only the combination of $1,25(OH)_2D_3$ and MZ significantly reduced the amount of nuclear *p*-NFκB p65 ($p < 0.05$) (**Figures 6D,E**).

Bioinformatic Analysis

We built the protein–compound interaction network that resembled our integrated *in vitro* model of AMD through the STITCH compound app of Cytoscape v. 3.7.0, according to the approach described in the Methods section. The network was characterized by 136 nodes and 463 edges; a centrality metrics analysis was carried out treating the network as an indirect graph. Nodes with highest betweenness centrality have represented using a color scale (blue < red) (**Figure 7**), and the following nodes were characterized by the highest betweenness centrality and the average shortest path: APP > TLR4> IL6> TNF-α> PSEN1> H_2O_2> CAT > IL-1β, VEGF-A. We identified in this network functional clusters associated to the *in vitro* models used in our study: amyloid β (**Supplementary Figure S1**), H_2O_2 (**Supplementary Figure S2**), and inflammation, that is, LPS (**Supplementary Figure S3**) and TNF-α challenge (**Supplementary Figure S4**).

The cluster related to vitamin D_3 covered most of the network (**Figure 8**), but meso-zeaxanthin was linked only to RPE65 and VEGF-A. This last result would be linked to lack of literature data on meso-zeaxanthin, beyond compound antioxidant properties, and the documented RPE65 "lutein to meso-zeaxanthin" isomerase activity (Shyam et al., 2017).

DISCUSSION

Although several pathogenic mechanisms have been linked to onset and progression of AMD, management, and treatment of AMD is still affected by several unmet medical needs. Specifically, only wet AMD could be therapeutically managed through costly and invasive treatments, such as the anti-VEGF intravitreal injections, which can be ineffective in about 15% of patients (Krebs et al., 2013). Non-responders to intravitreal anti-VEGF treatments can encounter to irreversible vision loss, leading to burden of care linked to direct and indirect costs of blindness. Moreover, no therapy has been already approved for treatment of dry AMD, or for treatment of early phases of the disease.

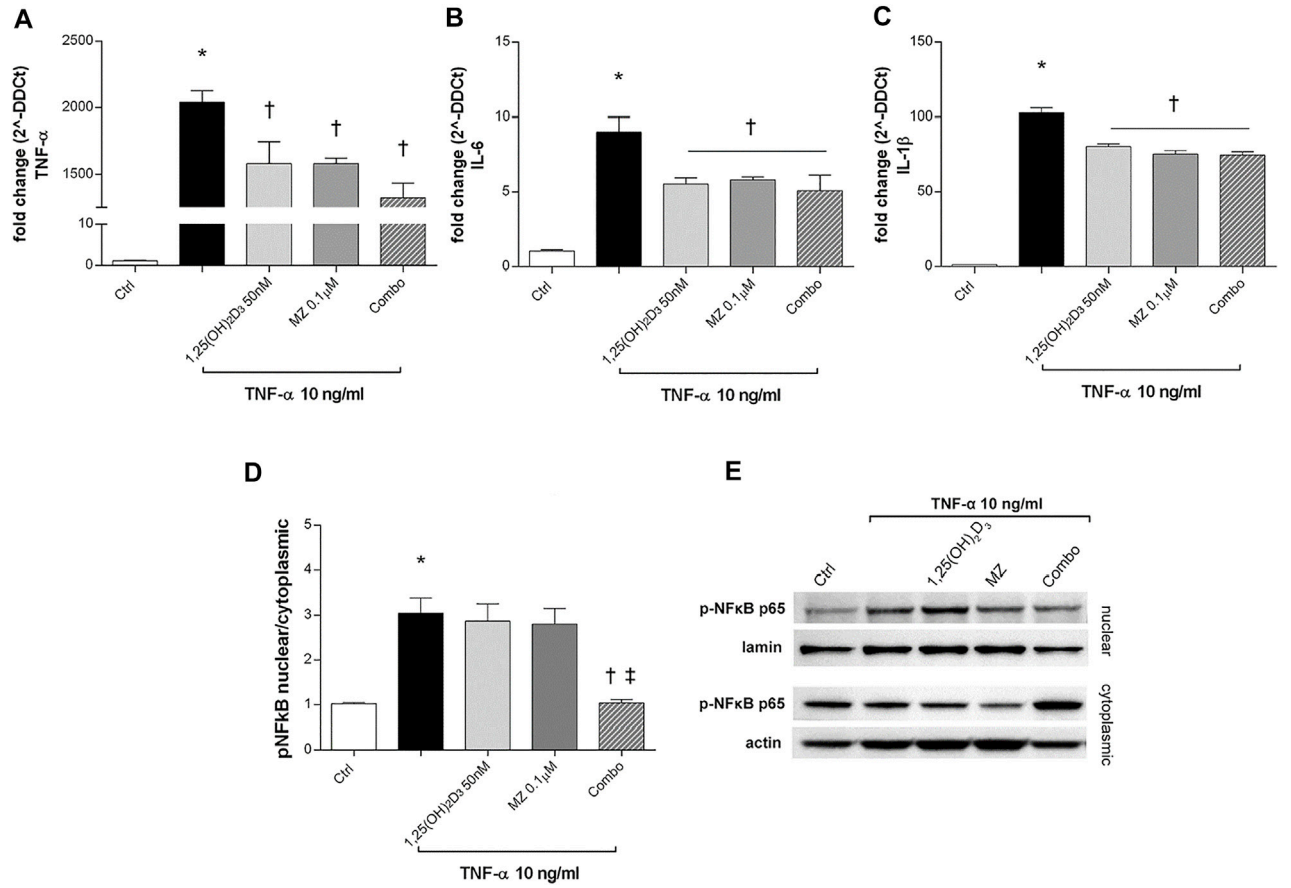

FIGURE 6 | 1,25$(OH)_2D_3$, meso-zeaxanthin (MZ), and the combination inhibit LPS-induced inflammation. 1,25$(OH)_2D_3$, meso-zeaxanthin (MZ), and their combo reduced TNF-α **(A)**, IL-6 **(B)**, and IL-1β **(C)** mRNA expression. ARPE-19 cells were pretreated for 24 h with 1,25$(OH)_2D_3$ (50 nM), MZ (0.1 μM), and their combo (1,25$(OH)_2D_3$ 50 nM + MZ 0.1 μM), and then challenged with TNF-α (10 ng/ml) for 2h, both for mRNA and protein analyses. The mRNA levels were evaluated by qPCR. **(D)** Densitometric analysis of each band (ratio of nuclear *p*-NFκB p65/lamin B and cytoplasmic *p*-NFκB p65/actin) was carried out with the ImageJ program. **(E)** Representative images of nuclear and cytoplasmic proteins. Each bar represents the mean value ±SD ($n = 5$; each run in triplicate). Data were analyzed by one-way ANOVA and Tukey's post hoc test for multiple comparisons. *$p < 0.05$ vs. control; †$p < 0.05$ vs. TNF-α; ‡$p < 0.05$ vs. 1,25$(OH)_2D_3$ and MZ.

Multivitamins and mineral supplementation are largely marketed for AMD patients, and clinical trials were carried out regarding specific formulations; the first was the Age-Related Eye Disease Study (2001) formulation, containing vitamins C and E, beta-carotene, and zinc with copper (Age-Related Eye Disease Study Research Group 2001; Kassoff et al., 2001; Chew et al., 2013a, 2014). A second trial "The Age-Related Eye Disease Study 2" (AREDS2) evidenced that substitution of β-carotene with lutein/zeaxanthin was safer for smokers and former smokers. In this AREDS2 study, lutein or zeaxanthin was compared with placebo. The authors found that there was a modest or no effect on AMD progression, but this was not statistically significant since all participants took the AREDS formula, and there was no proper control group (Chew et al., 2013b). On this regard, a systematic review with a meta-analysis evidenced that lutein and zeaxanthin supplements have little or no effect in AMD progression (Evans and Lawrenson, 2017), although this conclusion had a low level of certainty. In the same systematic review, authors evidenced that AMD subjects taking antioxidants multivitamin supplementation, including vitamin D_3, were at lower risk of AMD progression, but no evidence on visual acuity was found by meta-analysis. Since, there is no intervention to slow down the progression of the disease, depending on the AMD stage, correct supplementation of antioxidants and vitamins would be of benefit, but up to now, current supplement formulation trials did not provide evidence-based efficacy.

Therefore, in search of an improved formulation of supplements, we hereby explored for the first time, in an integrated *in vitro* model of AMD, the effects of 1,25$(OH)_2D_3$ (vitamin D_3) and meso-zeaxanthin combination on several endpoints related to inflammation, oxidative stress, and cellular damage: amyloid β, H_2O_2, and inflammatory insults, that is, LPS and TNFα. The rationale of these integrated *in vitro* models of AMD is behind its multifactorial pathogenic etiology (Bucolo et al., 2006; Di Filippo et al., 2014; Fisichella et al., 2016; Platania et al., 2017, 2019; Romano et al., 2017;

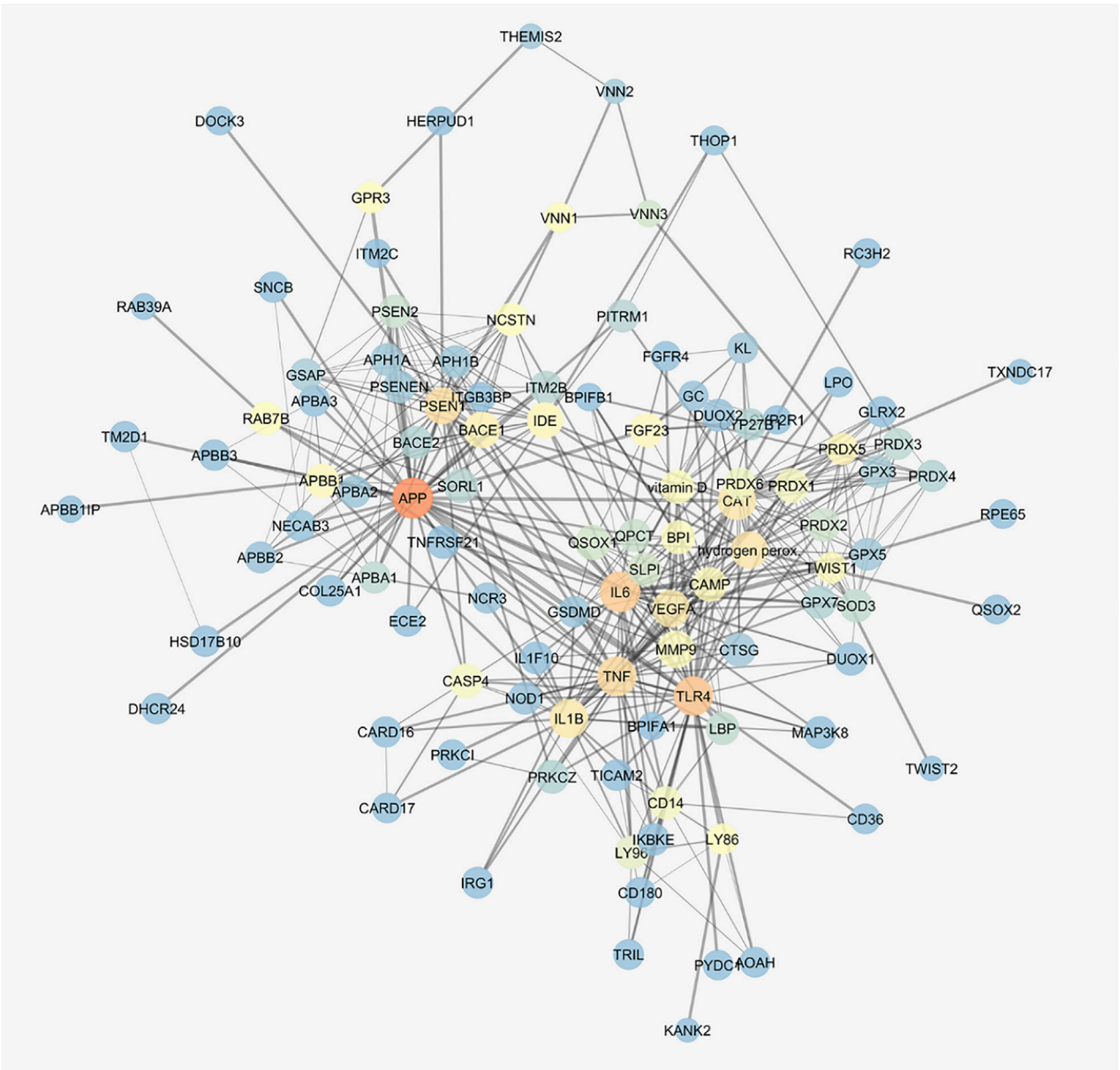

FIGURE 7 | Gene activated by amyloid β, H_2O_2, and LPS are connected. STITCH protein–compound network representing the *in vitro* models. Nodes are represented on the basis of betweenness centrality values (color scale blue < red) and closeness centrality values (node dimension); edge thickness is proportional to edge betweenness values.

Giordano et al., 2020; Micera et al., 2021), involving amyloid-β and oxidative stress, has already been mentioned. As regards as, the LPS challenge is widely used as an experimental model of AMD, involving the activation of Toll-like receptor 4 (TLR-4) and the downstream activation of NFκB (Sung et al., 2019; Hikage et al., 2021), and then triggering the expression of inflammatory cytokines. While, the most potent downstream inflammatory cytokine, TNF-α has been found to promote, in ARPE-19 cells, secretion of proteins involved in AMD pathology, such as complement C3 (An et al., 2008). Worthy of note, antioxidant and anti-inflammatory strategies have been largely explored for treatment of ocular diseases (Bucolo et al., 1999; Shafiee et al., 2011).

As shown by our data, vitamin D_3 and meso-zeaxanthin combination effectively protected cells from damage induced by β-amyloid, H_2O_2, LPS, and TNF-α. However, based on analyzed endpoints, we cannot hypothesize an additive or synergistic effect between vitamin D_3 and meso-zeaxanthin. Specifically, the combination of vitamin D_3 and meso-zeaxanthin was significantly effective, compared to the two single components, in decreasing Il-1β, TNF-α, and VEGF-A (H_2O_2 insult). Moreover, the combination of $1,25(OH)_2D_3$ + meso-zeaxanthin, compared to the

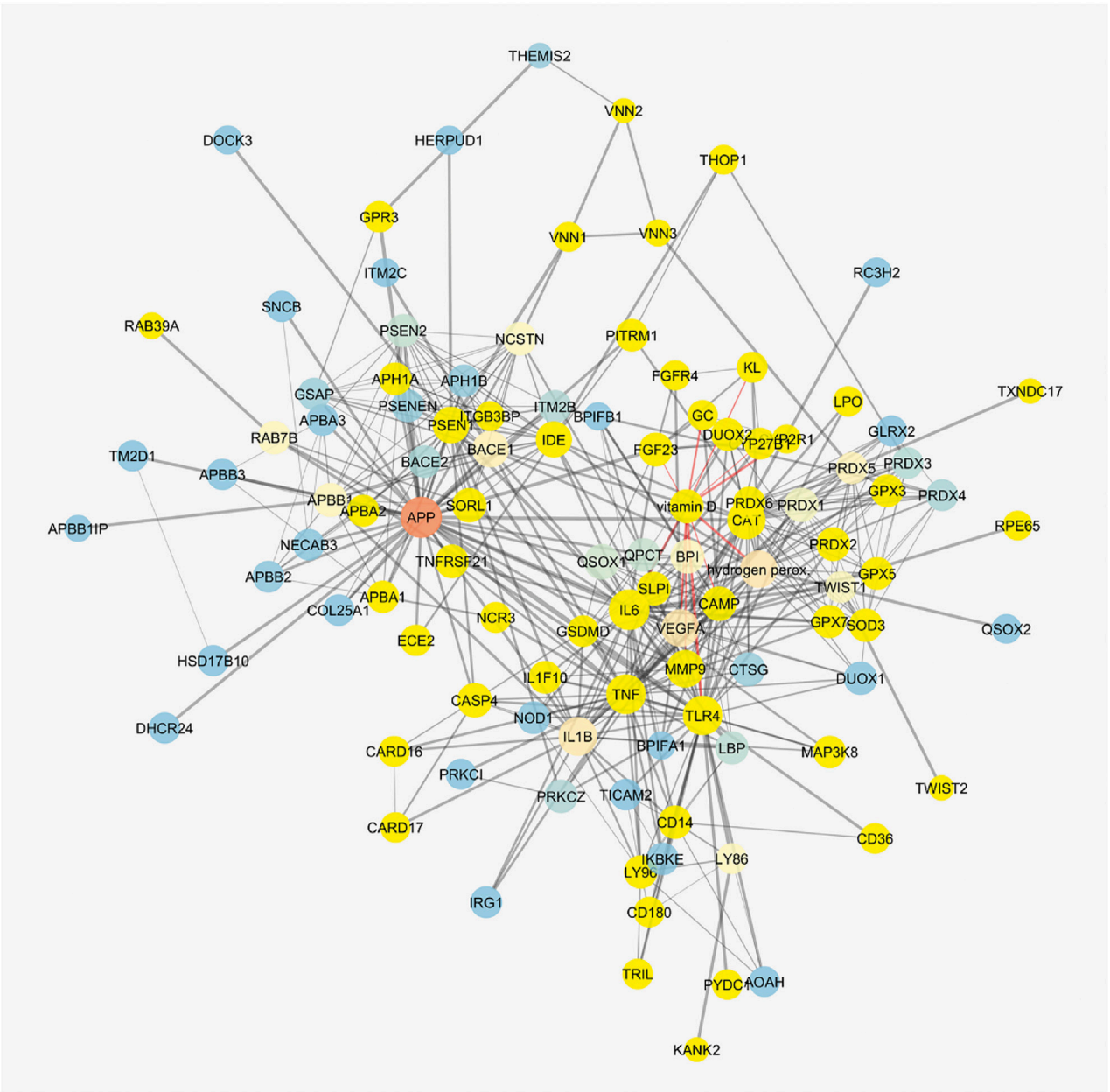

FIGURE 8 | Vitamin D_3–interacting nodes cover most of the STITCH protein–compound network. Red edges highlight direct interactions with vitamin D_3, and yellow nodes represent direct and indirect interactors of vitamin D_3.

two single components, significantly reduced NFκB nuclear translocation, in ARPE-19 cells challenged with H_2O_2, LPS, and TNF-α. While in the β-amyloid model, both vitamin D_3 and the combination with meso-zeaxanthin inhibited NFκB pathway activation but not the meso-zeaxanthin treatment alone.

Our findings about vitamin D_3 activity on ARPE-19 cells challenged with H_2O_2 and LPS are supported by recent findings on $1,25(OH)_2D_3$ antioxidant and anti-inflammatory activity (Fernandez-Robredo et al., 2020; Hernandez et al., 2021). Preclinical and clinical studies evidenced protective effects of vitamin D_3 in Alzheimer disease, an amyloid-β–related pathology (Sultan et al., 2020; McCarty et al., 2021). The link between AMD and AD pathology has been largely documented (Romano et al., 2017), and low-vitamin D_3 levels in serum were linked to progression of AMD, however with small effect (i.e., small adjusted odd ratio) (McKay et al., 2017). We proved for the first time that in ARPE-19 cells, vitamin D_3, meso-zeaxanthin, and their combination protected cells from damage induced by β-amyloid exposure, oxidative stress, and inflammatory stimuli. Recently, it has been demostrated that lutein and meso-zeaxanthin are taken up by ARPE-19 cells via different mechanisms with preferential uptake of

meso-zeaxanthin (Thomas and Harrison, 2016). Additionally, it is known that the enzyme RPE65 converts dietary lutein to meso-zeaxanthin in the retinal pigment epithelium of vertebrates (Shyam et al., 2017). Meso-zeaxanthin is a well-known antioxidant compound that accumulates as other xanthophyll carotenoids in the macula, increasing macular pigments and then protecting pigmented epithelial cells and photoreceptors from photo-oxidative stress (Bone et al., 2007). Up to now, there is an evidence of non-inferiority of meso-zeaxanthin enriched formulation, compared to AREDS2 formulation (Akuffo et al., 2017). On the contrary, non-advanced AMD subjects taking the meso-zeaxanthin–enriched formulation have shown significant higher meso-zeaxanthin and zeaxanthin serum levels and total serum carotenoids, than AREDS2 subjects (Akuffo et al., 2017). Despite large-scale clinical trials that showed the benefits of xanthophyll carotenoids against AMD, recommendations for nutritional interventions are underappreciated by ophthalmologists. Besides the well-known antioxidant activity of meso-zeaxanthin, only few non-ocular studies have reported an anti-inflammatory activity (Firdous et al., 2015; Sahin et al., 2017). Lack of literature findings about meso-zeaxanthin's anti-inflammatory activity was also emerged in our *in silico* analysis. Interestingly, meso-zeaxanthin decreased levels of nuclear p-NFκB and TNF-α secretion in the insulin-resistant rodent model (Sahin et al., 2017); this anti-inflammatory activity has been evidenced also in our experimental settings, since the single treatment with meso-zeaxanthin effectively delivered anti-inflammatory effects.

In conclusion, we hereby provided *in vitro* evidence that vitamin D_3 and meso-zeaxanthin association protected retinal pigmented epithelium from several damages that recapitulate the multifactorial pathogenic mechanisms of AMD. With this regard, vitamin D_3 and meso-zeaxanthin supplementation would be of value in AMD patients, especially for subject diagnosed with early diagnosis of AMD, as already evidenced by several systematic reviews.

DATA AVAILABILITY STATEMENT

The original contributions presented in the study are included in the article/**Supplementary Material**; further inquiries can be directed to the corresponding author.

AUTHOR CONTRIBUTIONS

CB made substantial contributions to conception, design, and interpretation of data. FL, FC, and CP carried out experiments. FL, FC, and CP carried out formal analysis of data. FL, FC, CP, and CB wrote initial draft of the manuscript. CB, CME, and FD reviewed the manuscript critically for important intellectual content and gave final approval of the version to be submitted.

SUPPLEMENTARY MATERIAL

The Supplementary Material for this article can be found online at: https://www.frontiersin.org/articles/10.3389/fphar.2021.778165/full#supplementary-material

REFERENCES

Age Related Eye Disease Study Research Group) (2001). The Age-Related Eye Disease Study System for Classifying Age-Related Macular Degeneration from Stereoscopic Color Fundus Photographs: The Age-Related Eye Disease Study Report Number. *Am. J. Ophthalmol.* doi:10.1016/S0002-9394(01)01218-1

Akuffo, K. O., Beatty, S., Peto, T., Stack, J., Stringham, J., Kelly, D., et al. (2017). The Impact of Supplemental Antioxidants on Visual Function in Nonadvanced Age-Related Macular Degeneration: A Head-To-Head Randomized Clinical Trial. *Invest. Ophthalmol. Vis. Sci.* 58, 5347. doi:10.1167/iovs.16-21192

Albert, D. M., Scheef, E. A., Wang, S., Mehraein, F., Darjatmoko, S. R., Sorenson, C. M., et al. (2007). Calcitriol Is a Potent Inhibitor of Retinal Neovascularization. *Invest. Ophthalmol. Vis. Sci.* 48, 2327. doi:10.1167/iovs.06-1210

Almeida Moreira Leal, L. K., Lima, L. A., Alexandre de Aquino, P. E., Costa de Sousa, J. A., Jataí Gadelha, C. V., Felício Calou, I. B., et al. (2020). Vitamin D (VD3) Antioxidative and Anti-inflammatory Activities: Peripheral and central Effects. *Eur. J. Pharmacol.* 879, 173099. doi:10.1016/j.ejphar.2020.173099

An, E., Gordish-Dressman, H., and Hathout, Y. (2008). Effect of TNF-α on Human ARPE-19-Secreted Proteins. *Mol. Vis.*

Anderson, D. H., Mullins, R. F., and Hageman, L V Johnson, G. S. (2002). A Role for Local Inflammation in the Formation of Drusen in the Aging Eye. *Am. J. Ophthalmol.* 134, 411–431. doi:10.1016/s0002-9394(02)01624-0

Anderson, O. A., Finkelstein, A., and Shima, D. T. (2013). A2E Induces IL-1ß Production in Retinal Pigment Epithelial Cells via the NLRP3 Inflammasome. *PLoS One* 8, e67263. doi:10.1371/journal.pone.0067263

Annweiler, C., Drouet, M., Duval, G. T., Paré, P.-Y., Leruez, S., Dinomais, M., et al. (2016). Circulating Vitamin D Concentration and Age-Related Macular Degeneration: Systematic Review and Meta-Analysis. *Maturitas* 88, 101–112. doi:10.1016/j.maturitas.2016.04.002

Biron, K. E., Dickstein, D. L., Gopaul, R., and Jefferies, W. A. (2011). Amyloid Triggers Extensive Cerebral Angiogenesis Causing Blood Brain Barrier Permeability and Hypervascularity in Alzheimer's Disease. *PLoS One* 6, e23789. doi:10.1371/journal.pone.0023789

Bone, R. A., Landrum, J. T., Cao, Y., Howard, A. N., and Alvarez-Calderon, F. (2007). Macular Pigment Response to a Supplement Containing Meso-Zeaxanthin, Lutein and Zeaxanthin. *Nutr. Metab. (Lond)* 4, 12. doi:10.1186/1743-7075-4-12

Bruban, J., Glotin, A.-L., Dinet, V., Chalour, N., Sennlaub, F., Jonet, L., et al. (2009). Amyloid-β (1-42) Alters Structure and Function of Retinal Pigmented Epithelial Cells. *Aging Cell* 8, 162–177. doi:10.1111/j.1474-9726.2009.00456.x

Bucolo, C., Campana, G., Di Toro, R., Cacciaguerra, S., and Spampinato, S. (1999). σ Recognition Sites in Rabbit Iris-Ciliary Body: Topical σ-1-site Agonists Lower Intraocular Pressure. *J. Pharmacol. Exp. Ther.*

Bucolo, C., Drago, F., Lin, L.-R., and Reddy, V. N. (2006). Sigma Receptor Ligands Protect Human Retinal Cells against Oxidative Stress. *Neuroreport* 17, 287–291. doi:10.1097/01.wnr.0000199469.21734.e1

Buschini, E., Zola, M., Fea, A. M., Lavia, C. A., Nassisi, M., Pignata, G., et al. (2015). Recent Developments in the Management of Dry Age-Related Macular Degeneration. *Opth*, 563. doi:10.2147/OPTH.S59724

Calafiore, M., Copani, A., and Deng, W. (2012). DNA Polymerase-β Mediates the Neurogenic Effect of β-amyloid Protein in Cultured Subventricular Zone Neurospheres. *J. Neurosci. Res.* 90, 559–567. doi:10.1002/jnr.22780

Caruso, G., Benatti, C., Musso, N., Fresta, C. G., Fidilio, A., Spampinato, G., et al. (2021). Carnosine Protects Macrophages against the Toxicity of Aβ1-42 Oligomers by Decreasing Oxidative Stress. *Biomedicines* 9, 477. doi:10.3390/biomedicines9050477

Cascella, R., Ragazzo, M., Strafella, C., Missiroli, F., Borgiani, P., Angelucci, F., et al. (2014). Age-Related Macular Degeneration: Insights into Inflammatory Genes. *J. Ophthalmol.* 2014, 1–9. doi:10.1155/2014/582842

Chew, E. Y., Clemons, T. E., Agrón, E., Sperduto, R. D., SanGiovanni, J. P., Davis, M. D., et al. (2014). Ten-Year Follow-Up of Age-Related Macular Degeneration in the Age-Related Eye Disease Study. *JAMA Ophthalmol.* 132, 272. doi:10.1001/jamaophthalmol.2013.6636

Chew, E. Y., Clemons, T. E., Agrón, E., Sperduto, R. D., Sangiovanni, J. P., Kurinij, N., et al. (2013a). Long-Term Effects of Vitamins C and E, β-Carotene, and Zinc on Age-Related Macular Degeneration. *Ophthalmology* 120, 1604–1611. doi:10.1016/j.ophtha.2013.01.021

Chew, E. Y., Clemons, T. E., SanGiovanni, J. P., Danis, R., Ferris, F. L., Elman, M., et al. (2013b). Lutein + Zeaxanthin and Omega-3 Fatty Acids for Age-Related Macular Degeneration. *Jama* 309, 2005. doi:10.1001/jama.2013.4997

Di Filippo, C., Zippo, M. V., Maisto, R., Trotta, M. C., Siniscalco, D., Ferraro, B., et al. (2014). Inhibition of Ocular Aldose Reductase by a New Benzofuroxane Derivative Ameliorates Rat Endotoxic Uveitis. *Mediators Inflamm.* 2014, 1–9. doi:10.1155/2014/857958

Eandi, C. M., Charles Messance, H., Augustin, S., Dominguez, E., Lavalette, S., Forster, V., et al. (2016). Subretinal Mononuclear Phagocytes Induce Cone Segment Loss via IL-1β. *Elife* 5. doi:10.7554/eLife.16490

Eliassen, A. H., Liao, X., Rosner, B., Tamimi, R. M., Tworoger, S. S., and Hankinson, S. E. (2015). Plasma Carotenoids and Risk of Breast Cancer over 20 Y of Follow-Up. *Am. J. Clin. Nutr.* 101, 1197–1205. doi:10.3945/ajcn.114.105080

Evans, J. R., and Lawrenson, J. G. (2017). Antioxidant Vitamin and mineral Supplements for Slowing the Progression of Age-Related Macular Degeneration. *Cochrane Database Syst. Rev.* 2017. doi:10.1002/14651858.CD000254.pub4

Fernandez-Robredo, P., González-Zamora, J., Recalde, S., Bilbao-Malavé, V., Bezunartea, J., Hernandez, M., et al. (2020). Vitamin D Protects against Oxidative Stress and Inflammation in Human Retinal Cells. *Antioxidants* 9, 838. doi:10.3390/antiox9090838

Firdous, A. P., Kuttan, G., and Kuttan, R. (2015). Anti-inflammatory Potential of Carotenoidmeso-Zeaxanthin and its Mode of Action. *Pharm. Biol.* 53, 961–967. doi:10.3109/13880209.2014.950673

Fisichella, V., Giurdanella, G., Platania, C. B. M., Romano, G. L., Leggio, G. M., Salomone, S., et al. (2016). TGF-β1 Prevents Rat Retinal Insult Induced by Amyloid-β (1-42) Oligomers. *Eur. J. Pharmacol.* 787, 72–77. doi:10.1016/j.ejphar.2016.02.002

Giordano, M., Trotta, M. C., Ciarambino, T., D'Amico, M., Galdiero, M., Schettini, F., et al. (2020). Circulating MiRNA-195-5p and -451a in Diabetic Patients with Transient and Acute Ischemic Stroke in the Emergency Department. *Ijms* 21, 7615. doi:10.3390/ijms21207615

Giurdanella, G., Anfuso, C. D., Olivieri, M., Lupo, G., Caporarello, N., Eandi, C. M., et al. (2015). Aflibercept, Bevacizumab and Ranibizumab Prevent Glucose-Induced Damage in Human Retinal Pericytes *In Vitro*, through a PLA2/COX-2/VEGF-A Pathway. *Biochem. Pharmacol.* 96, 278–287. doi:10.1016/j.bcp.2015.05.017

Green-Gomez, M., Prado-Cabrero, A., Moran, R., Power, T., Gómez-Mascaraque, L. G., Stack, J., et al. (2020). The Impact of Formulation on Lutein, Zeaxanthin, and Meso-Zeaxanthin Bioavailability: A Randomised Double-Blind Placebo-Controlled Study. *Antioxidants* 9, 767. doi:10.3390/antiox9080767

Guillonneau, X., Eandi, C. M., Paques, M., Sahel, J.-A., Sapieha, P., and Sennlaub, F. (2017). On Phagocytes and Macular Degeneration. *Prog. Retin. Eye Res.* 61, 98–128. doi:10.1016/j.preteyeres.2017.06.002

Hageman, G. S., Luthert, P. J., Victor Chong, N. H., Johnson, L. V., Anderson, D. H., and Mullins, R. F. (2001). An Integrated Hypothesis that Considers Drusen as Biomarkers of Immune-Mediated Processes at the RPE-Bruch's Membrane Interface in Aging and Age-Related Macular Degeneration. *Prog. Retin. Eye Res.* doi:10.1016/S1350-9462(01)00010-6

Hernandez, M., Recalde, S., González-Zamora, J., Bilbao-Malavé, V., Sáenz de Viteri, M., Bezunartea, J., et al. (2021). Anti-inflammatory and Anti-oxidative Synergistic Effect of Vitamin D and Nutritional Complex on Retinal Pigment Epithelial and Endothelial Cell Lines against Age-Related Macular Degeneration. *Nutrients* 13, 1423. doi:10.3390/nu13051423

Hikage, F., Lennikov, A., Mukwaya, A., Lachota, M., Ida, Y., Utheim, T. P., et al. (2021). NF-κB Activation in Retinal Microglia Is Involved in the Inflammatory and Neovascularization Signaling in Laser-Induced Choroidal Neovascularization in Mice. *Exp. Cel. Res.* 403, 112581. doi:10.1016/j.yexcr.2021.112581

Holekamp, N. M. (2019). Review of Neovascular Age-Related Macular Degeneration Treatment Options. *Am. J. Manag. Care*.

Hozawa, A., Jacobs, D. R., Steffes, M. W., Gross, M. D., Steffen, L. M., and Lee, D.-H. (2006). Associations of Serum Carotenoid Concentrations with the Development of Diabetes and with Insulin Concentration: Interaction with Smoking. *Am. J. Epidemiol.* 163, 929–937. doi:10.1093/aje/kwj136

Johnson, L. V., Forest, D. L., Banna, C. D., Radeke, C. M., Maloney, M. A., Hu, J., et al. (2011). Cell Culture Model that Mimics Drusen Formation and Triggers Complement Activation Associated with Age-Related Macular Degeneration. *Proc. Natl. Acad. Sci.* 108, 18277–18282. doi:10.1073/pnas.1109703108

Kan, E., Kan, E. K., and Yücel, Ö. E. (2020). The Possible Link between Vitamin D Levels and Exudative Age-Related Macular Degeneration. *Oman Med. J.* 35, e83. doi:10.5001/omj.2020.01

Kassoff, A., Kassoff, J., Buehler, J., Eglow, M., Kaufman, F., Mehu, M., et al. (2001). A Randomized, Placebo-Controlled, Clinical Trial of High-Dose Supplementation with Vitamins C and E, Beta Carotene, and Zinc for Age-Related Macular Degeneration and Vision Loss. *Arch. Ophthalmol.* 119, 1417. doi:10.1001/archopht.119.10.1417

Kauppinen, A., Paterno, J. J., Blasiak, J., Salminen, A., and Kaarniranta, K. (2016). Inflammation and its Role in Age-Related Macular Degeneration. *Cell Mol. Life Sci.* 73, 1765–1786. doi:10.1007/s00018-016-2147-8

Kohen, R., and Nyska, A. (2002). Invited Review: Oxidation of Biological Systems: Oxidative Stress Phenomena, Antioxidants, Redox Reactions, and Methods for Their Quantification. *Toxicol. Pathol.* 30, 620–650. doi:10.1080/01926230290166724

Krebs, I., Glittenberg, C., Ansari-Shahrezaei, S., Hagen, S., Steiner, I., and Binder, S. (2013). Non-responders to Treatment with Antagonists of Vascular Endothelial Growth Factor in Age-Related Macular Degeneration. *Br. J. Ophthalmol.* 97, 1443–1446. doi:10.1136/bjophthalmol-2013-303513

Krohne, T. U., Holz, F. G., and Kopitz, J. (2010). Apical-to-basolateral Transcytosis of Photoreceptor Outer Segments Induced by Lipid Peroxidation Products in Human Retinal Pigment Epithelial Cells. *Invest. Ophthalmol. Vis. Sci.* 51, 553. doi:10.1167/iovs.09-3755

Layana, A., Minnella, A., Garhöfer, G., Aslam, T., Holz, F., Leys, A., et al. (2017). Vitamin D and Age-Related Macular Degeneration. *Nutrients* 9, 1120. doi:10.3390/nu9101120

Lee, V., Rekhi, E., Hoh Kam, J., and Jeffery, G. (2012). Vitamin D Rejuvenates Aging Eyes by Reducing Inflammation, Clearing Amyloid Beta and Improving Visual Function. *Neurobiol. Aging* 33, 2382–2389. doi:10.1016/j.neurobiolaging.2011.12.002

Levy, O., Lavalette, S., Hu, S. J., Housset, M., Raoul, W., Eandi, C., et al. (2015). APOE Isoforms Control Pathogenic Subretinal Inflammation in Age-Related Macular Degeneration. *J. Neurosci.* 35, 13568–13576. doi:10.1523/JNEUROSCI.2468-15.2015

Liu, R. T., Gao, J., Cao, S., Sandhu, N., Cui, J. Z., Chou, C. L., et al. (2013). Inflammatory Mediators Induced by Amyloid-Beta in the Retina and RPE *In Vivo*: Implications for Inflammasome Activation in Age-Related Macular Degeneration. *Invest. Ophthalmol. Vis. Sci.* 54, 2225. doi:10.1167/iovs.12-10849

Maj, E., Filip-Psurska, B., Milczarek, M., Psurski, M., Kutner, A., and Wietrzyk, J. (2018). Vitamin$_3$D Derivatives Potentiate the Anticancer and Anti-angiogenic Activity of Tyrosine Kinase Inhibitors in Combination with Cytostatic Drugs in an A549 Non-small Cell Lung Cancer Model. *Int. J. Oncol.* doi:10.3892/ijo.2017.4228

Majewski, S., Skopinska, M., Marczak, M., Szmurlo, A., Bollag, W., and Jablonska, S. (1996). Vitamin D_3 Is a Potent Inhibitor of Tumor Cell-Induced Angiogenesis. *J. Investig. Dermatol. Symp. Proc.*

McCarty, M. F., Dinicolantonio, J. J., and Lerner, A. (2021). A Fundamental Role for Oxidants and Intracellular Calcium Signals in Alzheimer's Pathogenesis-And How a Comprehensive Antioxidant Strategy May Aid Prevention of This Disorder. *Ijms* 22, 2140. doi:10.3390/ijms22042140

McKay, G. J., Young, I. S., McGinty, A., Bentham, G. C. G., Chakravarthy, U., Rahu, M., et al. (2017). Associations between Serum Vitamin D and Genetic Variants in Vitamin D Pathways and Age-Related Macular Degeneration in the European Eye Study. *Ophthalmology* 124, 90–96. doi:10.1016/j.ophtha.2016.09.007

Merle, B. M. J., Silver, R. E., Rosner, B., and Seddon, J. M. (2017). Associations between Vitamin D Intake and Progression to Incident Advanced Age-Related

Macular Degeneration. *Invest. Ophthalmol. Vis. Sci.* 58, 4569. doi:10.1167/iovs.17-21673

Micera, A., Balzamino, B. O., Di Zazzo, A., Dinice, L., Bonini, S., and Coassin, M. (2021). Biomarkers of Neurodegeneration and Precision Therapy in Retinal Disease. *Front. Pharmacol.* 11. doi:10.3389/fphar.2020.601647

Millen, A. E., Voland, R., Sondel, S. A., Parekh, N., Horst, R. L., Wallace, R. B., et al. (2011). Vitamin D Status and Early Age-Related Macular Degeneration in Postmenopausal Women. *Arch. Ophthalmol.* 129, 481. doi:10.1001/archophthalmol.2011.48

Nolan, J. M., Meagher, K., Kashani, S., and Beatty, S. (2013). What Is Meso-Zeaxanthin, and where Does it Come from? *Eye* 27, 899–905. doi:10.1038/eye.2013.98

Nowak, J. Z. (2006). Age-related Macular Degeneration (AMD): Pathogenesis and Therapy. *Pharmacol. Rep*.

Parekh, N., Chappell, R. J., Millen, A. E., Albert, D. M., and Mares, J. A. (2007). Association between Vitamin D and Age-Related Macular Degeneration in the Third National Health and Nutrition Examination Survey, 1988 through 1994. *Arch. Ophthalmol.* 125, 661. doi:10.1001/archopht.125.5.661

Parks, W. C., Wilson, C. L., and López-Boado, Y. S. (2004). Matrix Metalloproteinases as Modulators of Inflammation and Innate Immunity. *Nat. Rev. Immunol.* 4, 617–629. doi:10.1038/nri1418

Pennington, K. L., and DeAngelis, M. M. (2016). Epidemiology of Age-Related Macular Degeneration (AMD): Associations with Cardiovascular Disease Phenotypes and Lipid Factors. *Eye Vis.* 3. doi:10.1186/s40662-016-0063-5

Platania, C. B. M., Di Paola, L., Leggio, G. M., Leggio, G. L., Drago, F., Salomone, S., et al. (2015). Molecular Features of Interaction between VEGFA and Anti-angiogenic Drugs Used in Retinal Diseases: A Computational Approach. *Front. Pharmacol.* 6. doi:10.3389/fphar.2015.00248

Platania, C. B. M., Leggio, G. M., Drago, F., Salomone, S., and Bucolo, C. (2018). Computational Systems Biology Approach to Identify Novel Pharmacological Targets for Diabetic Retinopathy. *Biochem. Pharmacol.* 158, 13–26. doi:10.1016/j.bcp.2018.09.016

Platania, C. B. M., Maisto, R., Trotta, M. C., D'Amico, M., Rossi, S., Gesualdo, C., et al. (2019). Retinal and Circulating miRNAexpression Patterns in Diabetic Retinopathy: An In Silico and *In Vivo* Approach. *Br. J. Pharmacol.* doi:10.1111/bph.14665

Platania, C., Fisichella, V., Fidilio, A., Geraci, F., Lazzara, F., Leggio, G., et al. (2017). Topical Ocular Delivery of TGF-B1 to the Back of the Eye: Implications in Age-Related Neurodegenerative Diseases. *Ijms* 18, 2076. doi:10.3390/ijms18102076

Romano, G. L., Platania, C. B. M., Drago, F., Salomone, S., Ragusa, M., Barbagallo, C., et al. (2017). Retinal and Circulating miRNAs in Age-Related Macular Degeneration: An *In Vivo* Animal and Human Study. *Front. Pharmacol.* 8. doi:10.3389/fphar.2017.00168

Sahin, K., Orhan, C., Akdemir, F., Tuzcu, M., Sahin, N., Yilmaz, I., et al. (2017). Mesozeaxanthin Protects the Liver and Reduces Cardio-Metabolic Risk Factors in an Insulin Resistant Rodent Model. *Food Nutr. Res.* 61, 1353360. doi:10.1080/16546628.2017.1353360

Sesso, H. D., Buring, J. E., Norkus, E. P., and Gaziano, J. M. (2004). Plasma Lycopene, Other Carotenoids, and Retinol and the Risk of Cardiovascular Disease in Women. *Am. J. Clin. Nutr.* 79, 47–53. doi:10.1093/ajcn/79.1.47

Shafiee, A., Bucolo, C., Budzynski, E., Ward, K. W., and López, F. J. (2011). *In Vivo* ocular Efficacy Profile of Mapracorat, a Novel Selective Glucocorticoid Receptor Agonist, in Rabbit Models of Ocular Disease. *Invest. Ophthalmol. Vis. Sci.* 52, 1422. doi:10.1167/iovs.10-5598

Shyam, R., Gorusupudi, A., Nelson, K., Horvath, M. P., and Bernstein, P. S. (2017). RPE65 Has an Additional Function as the Lutein Tomeso-Zeaxanthin Isomerase in the Vertebrate Eye. *Proc. Natl. Acad. Sci. USA* 114, 10882–10887. doi:10.1073/pnas.1706332114

Sultan, S., Taimuri, U., Basnan, S. A., Ai-Orabi, W. K., Awadallah, A., Almowald, F., et al. (2020). Low Vitamin D and its Association with Cognitive Impairment and Dementia. *J. Aging Res.* 2020, 1–10. doi:10.1155/2020/6097820

Sung, I. S., Park, S. Y., Jeong, K.-Y., and Kim, H. M. (2019). Investigation of the Preventive Effect of Calcium on Inflammation-Mediated Choroidal Neovascularization. *Life Sci.* 233, 116727. doi:10.1016/j.lfs.2019.116727

Thomas, S. E., and Harrison, E. H. (2016). Mechanisms of Selective Delivery of Xanthophylls to Retinal Pigment Epithelial Cells by Human Lipoproteins. *J. Lipid Res.* 57, 1865–1878. doi:10.1194/jlr.M070193

Thurnham, D. I., Trémel, A., and Howard, A. N. (2008). A Supplementation Study in Human Subjects with a Combination Ofmeso-Zeaxanthin, (3R,3′R)-zeaxanthin and (3R,3′R,6′R)-lutein. *Br. J. Nutr.* 100, 1307–1314. doi:10.1017/S0007114508971336

Wang, A. L., Lukas, T. J., Yuan, M., Du, N., Tso, M. O., and Neufeld, A. H. (2009). Autophagy and Exosomes in the Aged Retinal Pigment Epithelium: Possible Relevance to Drusen Formation and Age-Related Macular Degeneration. *PLoS One* 4, e4160. doi:10.1371/journal.pone.0004160

Zając-Pytrus, H., Pilecka, A., Turno-Kręcicka, A., Adamiec-Mroczek, J., and Misiuk-Hojło, M. (2015). The Dry Form of Age-Related Macular Degeneration (AMD): The Current Concepts of Pathogenesis and Prospects for Treatment. *Adv. Clin. Exp. Med.* 24, 1099–1104. doi:10.17219/acem/27093

Conflict of Interest: The authors declare that the research was conducted in the absence of any commercial or financial relationships that could be construed as a potential conflict of interest.

Publisher's Note: All claims expressed in this article are solely those of the authors and do not necessarily represent those of their affiliated organizations, or those of the publisher, the editors, and the reviewers. Any product that may be evaluated in this article, or claim that may be made by its manufacturer, is not guaranteed or endorsed by the publisher.

frontiers in Pharmacology

BRIEF RESEARCH REPORT
published: 28 January 2022
doi: 10.3389/fphar.2021.760507

Recombinant Human Nerve Growth Factor (Cenegermin)–Driven Corneal Wound Healing Process: An Evidence-Based Analysis

Chiara Bonzano[1,2]*, *Sara Olivari*[1,2], *Carlo Alberto Cutolo*[1,2], *Angelo Macrì*[2], *Daniele Sindaco*[1,2], *Davide Borroni*[3], *Elisabetta Bonzano*[4,5] *and Carlo Enrico Traverso*[1,2]

[1]Eye Clinic, Department of Neuroscience, Rehabilitation, Ophthalmology, Genetics, Maternal and Child Health, University of Genoa, Genoa, Italy, [2]IRCCS San Martino Polyclinic Hospital, Genoa, Italy, [3]Cornea Unit, Royal Liverpool University Hospital, Liverpool, United Kingdom, [4]Department of Radiation Oncology, IRCCS San Matteo Polyclinic Foundation, Pavia, Italy, [5]PhD School in Experimental Medicine, University of Pavia, Pavia, Italy

OPEN ACCESS

Edited by:
Mario Damiano Toro,
Medical University of Lublin, Poland

Reviewed by:
Bijorn Omar Balzamino,
GB Bietti Foundation (IRCCS), Italy
Ignacio Alcalde,
Instituto Universitario Fernández-Vega, Spain

***Correspondence:**
Chiara Bonzano
oculistabonzano@gmail.com

Specialty section:
This article was submitted to Experimental Pharmacology and Drug Discovery, a section of the journal Frontiers in Pharmacology

Received: 18 August 2021
Accepted: 13 December 2021
Published: 28 January 2022

Citation:
Bonzano C, Olivari S, Cutolo CA, Macrì A, Sindaco D, Borroni D, Bonzano E and Traverso CE (2022) Recombinant Human Nerve Growth Factor (Cenegermin)–Driven Corneal Wound Healing Process: An Evidence-Based Analysis. Front. Pharmacol. 12:760507. doi: 10.3389/fphar.2021.760507

Purpose: To evaluate anterior segment optical coherence tomography (AS-OCT) to detect the wound healing process as per monitoring the effectiveness of cenegermin to treat moderate to severe neurotrophic keratoplasty.

Methods: A retrospective chart review was realized to identify patients treated with cenegermin at the Clinica Oculistica, University of Genoa, Italy. All patients underwent careful examinations at baseline and follow-up visits. AS-OCT scans centered on the minimum corneal thickness (CT) area were always performed. We compared findings of AS-OCT with the findings from the slit-lamp examination. A linear regression analysis was used to evaluate factors associated with corneal healing. A further analysis, including a control group treated with 50% autologous serum (AS), was done to investigate and compare the efficacy of cenegermin.

Results: Data from 16 eyes were studied. The average patients' age was 60.9 ± 21.1 years; five (31.2%) eyes experienced persistent epithelial defect and 11 (68.8%) eyes had neurotrophic corneal ulcer. The average reepithelialization time was 3.9 ± 0.5 weeks in the cenegermin group versus 5.9 ± 1.9 weeks in the AS group ($p < 0.01$). The AS-OCT scans revealed an average CT at the thinnest point of 276.3 ± 74.1 µm before treatment with an average increase of 176.5 ± 60.3 µm at the end of the cenegermin treatment (B = −0.15; $p = 0.035$). The AS-OCT percentage increase in corneal thickness between the two groups was statistically significant ($p < 0.02$).

Conclusion: Understanding the cascade of events involved in the nerve growth factor–driven corneal wound healing process is clinically meaningful for the clinician. AS-OCT is an effective tool for systematic anterior segment imaging, allowing the detailed detection of the front-to-back layered corneal structure for quantitative analysis and monitoring of the healing process.

Keywords: cenegermin, neurotrophic keratoplasty, corneal diseases, ocular pharmacology, pharmacological targets, anterior segment optical coherence tomography (AS-OCT), rh-NGF, autologous serum

INTRODUCTION

Several ocular and systemic diseases have been associated with damage to the fifth cranial nerve axons, from the trigeminal nucleus to the corneal nerve endings, possibly resulting in the development of neurotrophic keratoplasty (NK) (Dua et al., 2018).

Among the multitude of causes of NK, herpetic keratoplasty (herpes simplex and herpes zoster viral infection) are the most common, followed by intracranial space-occupying lesions or neurosurgical procedures that damage the trigeminal ophthalmic branch (Sacchetti and Lambiase, 2014).

Other ocular causes of NK include chemical burns, physical injuries, corneal dystrophy, chronic use of topical medications (topical anesthetics, timolol, betaxolol, sulfacetamide, and diclofenac sodium), and anterior-segment surgery involving nerve damage (Semeraro et al., 2014). Additional systemic conditions associated with corneal nerve impairment are diabetes mellitus (DM), multiple sclerosis, congenital syndromes, and leprosy (Sacchetti and Lambiase, 2014).

Corneal blindness is the fourth leading cause of blindness worldwide (Jeng and Ahmad, 2021); however, nearly 80% of all cases are avoidable and reversible (Jeng and Ahmad, 2021). Thus, treating corneal diseases such as trauma or keratoplasty represents an urgent or emergent care issue for ophthalmologists. For these reasons, more evidence on new and recent drugs for conservative treatment is highly required, especially in such a crucial time where there is a restriction regarding access to surgical corneal treatments (Toro et al., 2020).

Cenegermin is a novel recombinant human nerve growth factor (rh-NGF) recently approved to treat moderate to severe NK (European Medicines Agency, 2021). Cenegermin eye drop proved to be safe and successful in regenerating corneal integrity in two phase-II clinical trials (Bonini et al., 2018a; Bonini et al., 2018b). The understanding of the cascade of events involved in the NGF-driven corneal wound healing process and the evaluation of how corneal wound healing affects corneal biomechanics and optics are crucial to improving the outcome of the treatment.

Anterior segment optical coherence tomography (AS-OCT) is a noninvasive instrument for systematic anterior segment imaging, allowing the detection of the front-to-back layered corneal structure with sufficient detail to make a quantitative analysis. There have been reports on the assessment of corneal thickness (CT) (Muscat et al., 2002; Ishibazawa et al., 2011); AS-OCT also contributes to the diagnosis of anterior eye diseases, monitoring of pathological conditions, and their healing process (Nubile et al., 2011; Mastropasqua et al., 2017; Venkateswaran et al., 2018; Kowalczyk et al., 2020). OCT technology is also widely used for posterior segment imaging; several studies have shown its effectiveness in disease monitoring with good intra-session reproducibility even in case of corneal pathologies (Reibaldi et al., 2012), as well as in detecting the onset of possible treatment-related complications (Ceravolo et al., 2020; Arumuganathan et al., 2021). Furthermore, it is commonly used as a screening tool for not only ocular diseases but also systemic diseases (Chisari et al., 2019; Carnevali et al., 2021; Koman-Wierdak et al., 2021; Wiest et al., 2021; Zweifel et al., 2021). Recently, AS-OCT has been introduced as a valid tool to optimize the classification of Stage 3 NK (Mastropasqua et al., 2019). The use of AS-OCT for the corneal morphological analysis in patients treated with cenegermin has yet to be described. Our study aims to evaluate AS-OCT to detect the wound healing process as per monitoring the efficacy of cenegermin. A further analysis, including a control group, was performed to investigate and compare the efficacy of cenegermin.

MATERIALS AND METHODS

A retrospective chart review was performed to identify patients treated with topical cenegermin eye drops at the Clinica Oculistica, University of Genova, Italy. To evaluate the ability of AS-OCT in detecting the wound healing process as per monitoring the efficacy of cenegermin, the AS-OCT data were compared with an historical control group of patients affected by NK who received standard conventional treatment, 50% autologous serum (AS) eye drops, since 2018 at the same institution.

Patients Inclusion and Exclusion Criteria

The inclusion criteria were unilateral Stage 2 or 3 NK refractory to one or more conventional treatments for at least 2 weeks, evidence of decreased corneal sensitivity, and the presence of negative corneal cultures, which were taken at admission to our department before the treatment. Finally, only patients with at least 12 months of follow-up after treatment were included.

The diagnosis of NK was established using the Mackie classification: Stage 2 [persistent epithelial defect (PED)] or Stage 3 [neurotrophic corneal ulcer (NCU)]. According to Mastropasqua et al., 2019, the Stage 3 enclosed Stage 3A (corneal ulceration with stromal thinning ≤50% of the total CT) and Stage 3B (corneal ulceration with stromal thinning ≥50% of the total CT). During the treatment period with cenegermin, therapeutic contact lens application and additional topical treatments were discontinued. In addition, possible impending perforation or surgical management needs, and active ocular infection or inflammation unrelated to NK were considered as the exclusion criteria, as were pregnancy and breastfeeding. The same eligibility criteria were applied to enclose the 16 historical controls.

Data Collection

All patients underwent a complete ophthalmic evaluation before starting the treatment and at each follow-up visit on a weekly basis for 8 weeks. Clinical assessment included slit-lamp (NIKON FS-3V Zoom Photo slit-lamp) examination implemented with corneal epithelial fluorescein staining, epithelialization times weekly monitoring, and AS-OCT (RTVue-100 applied anterior corneal module; Optovue, Fremont, CA). The size (mm) and depth (μm) of NK were recorded. Corneal hypoesthesia was confirmed using a Cochet–Bonnet aesthesiometer. At the first and at each follow-up visit, several AS-OCT scans were performed: pachymetric map, horizontal raster scan centered on the thinnest area of the cornea (17 horizontal scans within a height of 6 mm), cross-line (horizontal and vertical 8.00-mm

scans), and line mode (horizontal 8.00-mm scans) on the area of minimum thinning. All scans were centered in the same area at the different visits. We identified the thinnest part of the cornea and measured the corneal and stromal thickness of this portion using the caliper tools that were built into the RTVue-100 system.

Intervention

In the treatment group, we used a sterile, preservative-free ophthalmic solution containing 0.002% (0.02 mg/ml) of the active ingredient, cenegermin (Oxervate®, Dompé Farmaceutici Spa, Milan, Italy). It was packaged in a carton of seven multidose vials (1.0 ml). The patients were instructed to use one vial per day before being discarded and to keep the remaining vials in the carton refrigerated between 2°C and 8°C until the time of use. The scheduled treatment was one drop, six times a day at 2-h intervals for 8 weeks.

In the control group, we used 50% AS eye drops. All patients were screened for blood-borne infections, including syphilis, Hepatitis B and C, and HIV serology before the preparation of AS eye drops. Venipuncture was performed at the antecubital fossa under aseptic conditions to collect 100 ml of whole blood into sterile containers. These were left standing for 2 h to ensure complete clotting. The blood was then centrifuged for 15 min at 3000 RPM. The serum was then separated in a sterile manner and diluted to 50% using saline solution. Patients were recommended to keep the serum at 4°C. We suggested using a bottle for 1 week and administering this six times daily for 8 weeks. Additionally, this group received a prophylactic topical antibiotic (Exocin, Allergan), twice a day. The patients were seen regularly every 7 days for 8 weeks.

Outcome Measures

- Corneal healing (time frame: at Week 8)

The primary outcome of this study was to achieve complete corneal healing of PED or NCU at Week 8, defined as no corneal fluorescein staining in the area of PED or NCU.

- Quantitative analysis and monitoring of the healing process (time frame: at Week 8)

The secondary end point was to assess the CT, stromal, and epithelial changes through AS-OCT (RTVue-100) and to register any adverse reactions to drug or any disease recurrence with at least 12 months of follow-up.

Statistical Analysis

We compared the results of the AS-OCT scans with the biomicroscopic findings. The variables were summarized with mean and standard deviation for continuous variables and absolute value and percentage for frequency of categorical variables. In addition, a univariate linear regression analysis was performed to identify variables associated with the percentage change of CT by AS-OCT at the thinnest point. A standard statistical two-tailed paired *t* test was used to estimate the statistical significance of the differences between groups. All statistical analyses were performed with Stata version 15.1 (StataCorp LP, College Station, TX). The alpha level (type I error) was set at 0.05 for all analysis.

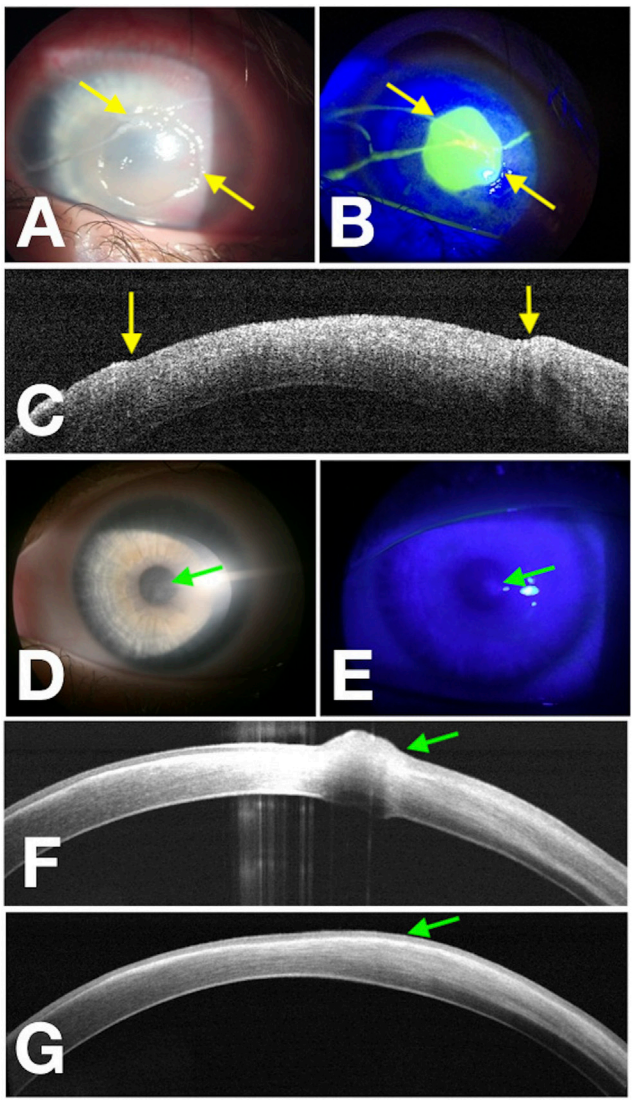

FIGURE 1 | Corneal wound healing of pediatric NK (rh-NGF Case 1) imaged with a multimodal approach. Yellow arrows point at the edges of the epithelial fronts in the photograph obtained at baseline with diffuse white light **(A)**, with fluorescein staining (green) photograph obtained under cobalt-blue light illumination **(B)**, and points to the epithelial edges in the OCT scan over the thinnest area at baseline **(C)**. **(D–F)** Images acquired at the end of the treatment at Week 8, and the green arrows show a residual paracentral corneal epithelial hyperplasia. About 1 month later, OCT scan **(G)** reveals complete regression of the corneal epithelial hyperplasia.

RESULTS

Affected Eyes in the Cenegermin Group

There were 11 female and five male patients with a mean age of 60.9 ± 21.1 years (range, 7–88 years) in the cenegermin group. In this group, five (31.2%) eyes experienced PED and 11 (68.8%) eyes had NCUs to varying degrees. According to the substages of NK, at Stage 3 of the Mackie's classification suggested by Mastropasqua et al. (2017), seven were Stage 3A and four were Stage 3B.

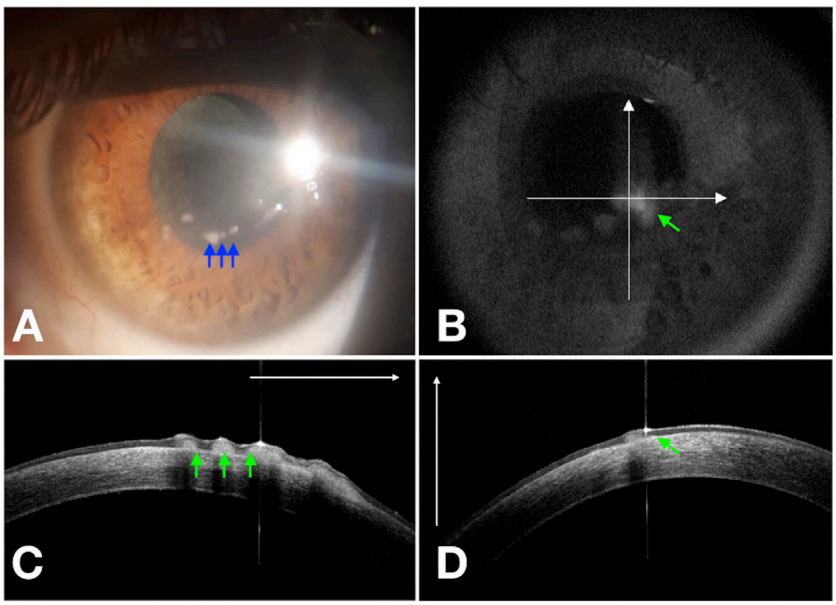

FIGURE 2 | Residual corneal epithelial hyperplasia (blue arrows) of NK (rh-NGF Case 4) at Week 8 **(A)**. Cross-line OCT **(B)** confirms the epithelial hyperplasia (green arrows) in the horizontal **(C)** and vertical **(D)** scans.

Affected eyes with PED: one recurrent herpetic epithelial lesion despite antiviral therapy, one epithelial defect after surgical treatment for acoustic nerve neuroma refractory to previously tarsorrhaphy, one PED developed on a previously transplanted cornea, one PED occurred in a child affected by a diffuse midline glioma, and one developed in the context of severe dry eye concomitant to corneal anesthesia.

Affected eyes with NCU: a cornea ulcer subsequent to a severe alkali burn, three recurrent herpetic stromal ulcers, and one NCU developed on a previously transplanted cornea in a diabetic patient. Four NCU occurred in eyes previously underwent surgical retinal detachment repair (Pars Plana Vitrectomy and endolaser). One NCU developed in the context of systemic polyneuropathy, and one occurred after a long-term topical glaucoma medication concomitant to corneal hypoesthesia.

All patients were treated by cenegermin eye drops six times a day. A total of 16 eyes of 16 patients healed completely with minimal scarring. There was no recurrence in these patients during the 12 months of follow-up time. Three eyes affected by PED (60% of PED) experienced epithelial hyperplasia regressed within the following month (**Figure 1** and **Figure 2**). The demographic data, etiologies, stages of NK before the treatment, and percentage increase in CT after cenegermin administration are summarized in **Table 1**.

Affected Eyes in the Autologous Serum Group

In the control group, there were 11 female and five male patients, and the mean age was 67.2 ± 18.4 years (range, 13–86 years). There were five (31.2%) PED and 11 (68.8%) NCU, with only two in Stage 3B.

Affected eyes with PED: three recurrent herpetic epithelial lesions, one PED developed in the context of corneal hypoesthesia, and one occurred after a long-term topical glaucoma medication.

Affected eyes with NCU: one recurrent herpetic stromal ulcer, one NCU developed on a previously transplanted cornea, and one NCU refractory to previously amniotic membrane transplantation. Two NCU occurred in eyes that had previously undergone surgical retinal detachment repair (Pars Plana Vitrectomy and endolaser) and two NCU resulting from post-surgical trigeminal nerve injury. One NCU developed in systemic polyneuropathy, and three NCU developed in the context of severe dry eye disease.

We administered 50% AS eye drops six times a day. A total of 16 eyes of 16 patients healed completely with minimal scarring. The follow-up time was 12 months, and the defect recurred after the suspension of therapy in four (25%) patients during the follow-up period. The demographic data, etiologies, stages of NK, and percentage increase in CT in the AS control group are summarized in **Table 1**.

As in the literature data (Bonini et al., 2018a; Bonini et al., 2018b), the most common cause of NK in our patients was herpes simplex keratoplasty, followed by ocular surgery, neurosurgical trigeminal damage, and severe dry eye disease (**Table 2**).

Additionally, three patients reported associated systemic conditions: DM, systemic polyneuropathy, and diffuse midline glioma, respectively.

Slit-Lamp Monitoring of the Cornea Healing Process

The epithelialization was screened by fluorescein staining test on slit-lamp examination. The mean time for closure of the

TABLE 1 | Ocular and demographic characteristics of the treated cases and the control group, *measured by AS-OCT.

	N	Age	Gender	Eye	Underlying cause	NK (stage)	Healing time (weeks)	Post-TP CT* (%)
					rh-NGF			
						PED		
	1	7	M	OS	Neurosurgical procedure	2	3	73.2
	2	47	M	OD	Neurosurgical procedure	2	4	31.9
	3	88	F	OD	Herpetic eye disease	2	3	20.6
	4	46	F	OD	Corneal hypoesthesia	2	4	54.8
	5	74	F	OS	keratoplasty	2	4	50
mean ± SD		*52.4 ± 31.1*					*3.6 ± 0.5*	*46.1 ± 20.5*
						NCU		
	6	76	F	OD	DM/keratoplasty	3 (IIIa)	5	53
	7	64	M	OD	Herpetic eye disease	3 (IIIa)	3	81.5
	8	76	F	OS	Herpetic eye disease	3 (IIIa)	4	73.2
	9	58	F	OS	Ocular surgery	3 (IIIa)	4	69.5
	10	45	M	OD	Ocular surgery	3 (IIIa)	5	96.2
	11	86	F	OS	Polyneuropathy	3 (IIIa)	3	62
	12	39	M	OD	Ocular surface injury (Chemical burn)	3 (IIIa)	4	65.3
	13	61	F	OD	Ocular surgery	3 (IIIb)	4	85
	14	53	F	OD	Ocular surgery	3 (IIIb)	4	90.4
	15	79	F	OS	Glaucoma medication (drops)	3 (IIIb)	4	85.6
	16	75	F	OS	Herpetic eye disease	3 (IIIb)	4	74
mean ± SD		*64.7 ± 15*					*4 ± 0.5*	*75.9 ± 13.1*
PED + NCU		***60.9 ±21.1* (*7–88*)**					***3.9 ±0.5***	***66.6 ±20.7***
					AS			
						PED		
	1	81	M	OS	Herpetic eye disease	2	8	14
	2	68	F	OD	Corneal hypoesthesia	2	7	10
	3	70	F	OD	Herpetic eye disease	2	7	13.9
	4	61	F	OD	Glaucoma medication (drops)	2	3	9.5
	5	80	F	OS	Herpetic eye disease	2	5	9.1
mean ± SD		*72 ± 8.5*					*6 ± 2*	*11,3 ± 2.4*
						NCU		
	6	69	F	OD	Severe dry eye	3 (IIIa)	3	12.4
	7	77	F	OS	Severe dry eye	3 (IIIa)	4	15
	8	86	M	OS	Ocular surgery	3 (IIIa)	8	16
	9	74	F	OS	Herpetic eye disease	3 (IIIa)	8	18
	10	84	F	OD	Ocular surgery	3 (IIIa)	8	17
	11	47	M	OD	Neurosurgical procedure	3 (IIIa)	7	23.9
	12	53	F	OS	Polyneuropathy	3 (IIIa)	6	11
	13	56	M	OS	keratoplasty	3 (IIIa)	4	19
	14	77	F	OD	Severe dry eye	3 (IIIa)	5	16
	15	13	M	OS	Ocular surgery	3 (IIIb)	3	18
	16	79	F	OD	Neurosurgical procedure	3 (IIIb)	8	13
mean ± SD		*65 ± 21.5*					*5.8 ± 2.1*	*16.3 ± 3.6*
PED + NCU		***67.2 ±18.4* (*13–86*)**					***5.9 ±2***	***14.7 ±4***

n=number, SD=standard deviation, PT CT (%)= post-treatment percentage increase in corneal thickness*

corneal lesion was 3.9 weeks ± 0.5 (range: 3–5 weeks) and 5.9 weeks ± 1.9 (range: 3–8 weeks) for the cenegermin group and AS group, respectively. The difference in epithelialization times between the two groups was statistically significant ($p < 0.01$).

Then in the cenegermin group, we clinically observed that the cornea healing was faster in patients younger than 75 years, but it was not statistically significant ($p > 0.05$).

In the AS control group, we observed a 25% recurrence rate compared with no recurrence in the cenegermin group.

During the first phase of NK healing, opaque slit-lamp scar tissue with high reflectivity on AS-OCT, looking different from the normal corneal stroma, was detected (**Figure 3**). At first, corneal epithelial hypertrophy filled the thinning area. Then scar tissue formed, and the corneal stroma thickness gradually improved. Second, when the scar tissue disappeared on slit-lamp examination, AS-OCT still detected an increased reflectivity of the anterior stroma at the corneal lesion site (**Figure 4**). In three PED, epithelial hyperplasia co-occurred with reepithelialization. It was appreciable with both the slit-lamp (**Figure 1D,E** and **Figure2A**) and AS-OCT (**Figure 1F** and **Figure 2C**). Finally, within a month, it resolved in all three cases and was no longer detectable (**Figure 1G**).

TABLE 2 | Participant baseline characteristics demonstrating that there were no significant differences in patient demographics between the treatment and historical control groups.

Baseline characteristics	rh-NGF (*n* = 16 eyes)	As (*n* = 16 eyes)	*p* Value
Age (years), mean ± SD (range)	60.9 ± 21.1 (7–88)	67.2 ± 18.4 (13–86)	0.13
Sex			0.67
Male	5 (31.2%)	5 (31.2%)	
Female	11 (68.8%)	11 (68.8%)	
Diagnosis			
Neurosurgical procedure	2	2	
Ocular surgery	4	3	
keratoplasty	2	1	
Herpetic eye disease	4	4	
Corneal hypoesthesia	1	1	
Ocular surface injury (chemical burn)	1	—	
Glaucoma medication (drops)	1	1	
Polyneuropathy	1	1	
Severe dry eye	—	3	

n = number, SD = standard deviation.

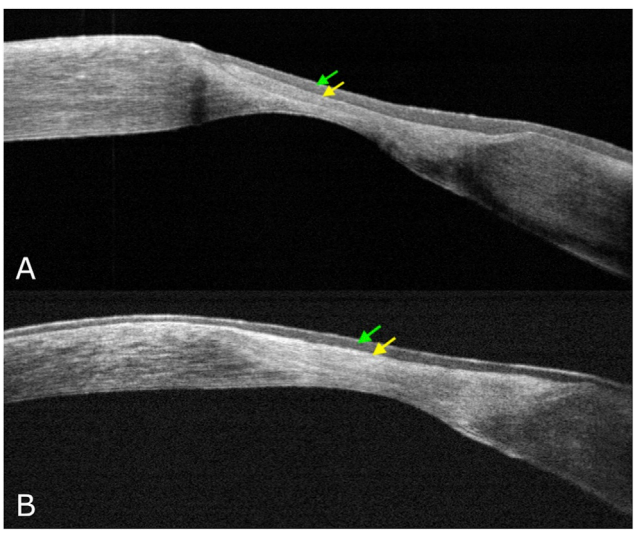

FIGURE 3 | Corneal wound healing AS-OCT detail. First corneal epithelial hypertrophy filled the thinning area, then scar tissue formed **(A)**, and the corneal stroma thickness gradually improved **(B)** (green arrow points to corneal epithelium; yellow arrow points to corneal stroma).

AS-OCT Analysis and Monitoring of the Cornea Healing Process

AS-OCT scans revealed an average CT in the thinnest point of 276.3 ± 74.1 μm at baseline and an average increase in CT of 176.5 ± 60.3 μm at the end of the cenegermin treatment (Week 8). Linear regression showed that the percentage increase of CT at the end of treatment with cenegermin was associated with the pre-treatment CT (B = −0.15; $p = 0.035$) (**Graph 1**). **Table 3** shows the results of the regression analysis. No other variables such as demographic factors or the epithelial defect area were associated with changes detected by AS-OCT.

Compared with the control group, AS-OCT data showed that the average percent change in CT detection was 66.6% [95% confidence interval (CI), 20.6–96.2] in the cenegermin treatment group and 14.7% (95% CI, 9.1–23.9) in the control group. The difference of percentage AS-OCT increase in cornea thickness between the two groups was statistically significant ($p < 0.02$) (**Graph 2** and **Graph 3**).

No side effects were observed in patients who received cenegermin or AS eye drops. Furthermore, there were no serious complications such as infectious keratoplasty that were encountered during the entire study period.

DISCUSSION

Of our cohort of patients, herpetic keratoplasty was the leading cause of corneal innervation impairment. Neurological and ocular surgical procedures, DM, and chronic glaucoma medication were other conditions involved in the disease pathogenesis.

We showed that baseline CT significantly correlates with post-treatment CT increase. The lower the baseline stromal thickness, the more significant was the effect of cenegermin in restoring CT.

Keratocytes, collagen fibrils, and proteoglycans are essential components of the corneal stroma (Hassell and Birk, 2010). Corneal transparency is guaranteed thanks to the uniform distribution of collagen lamellae (Maurice, 1957; Meek, 2009). This primary ultrastructure could be compromised during the wound healing process, giving way to a progressive swelling and a subsequent corneal opacity, identified as a scar on slit-lamp examination. It means decreased visual acuity in clinical practice, and AS-OCT could detect it as hyper-reflective scar tissue (McCally et al., 2007; Kamma-Lorger et al., 2009; Alafaleq et al., 2021). Type 3 collagen expression is initially significantly improved during the corneal healing process (Cintron et al., 1988). It is synthesized and deposited primarily by fibroblasts; however, it is easily broken down during tissue remodeling (Wilson et al., 2012). The scar tissue formation is probably due to the fibrotic cellular responses and an abnormally large fibril diameter formation (Wilson et al., 2012). First, the scar tissue appeared opaque, as seen with the slit lamp, and had a

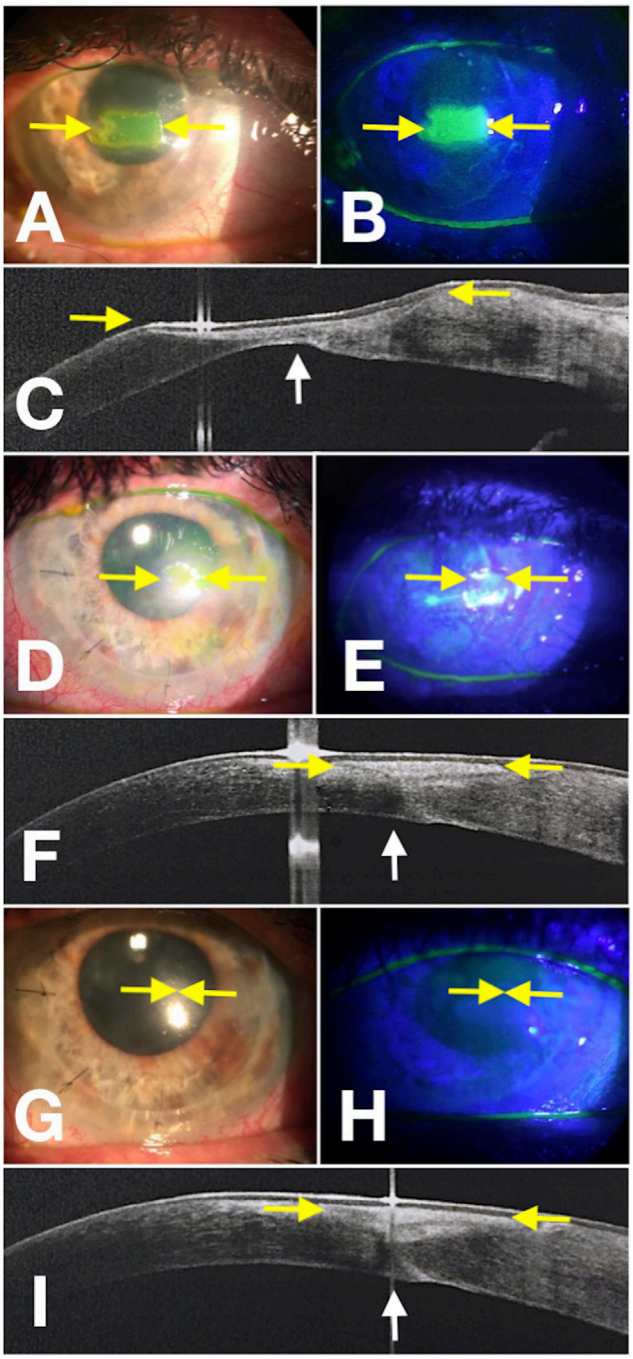

FIGURE 4 | Corneal wound healing of neurotrophic corneal ulcer (rh-NGF Case 6) imaged with a multimodal approach. Yellow arrows point at the edges of the epithelial fronts in the photograph obtained at baseline with diffuse white light **(A)**, with fluorescein staining (green) photograph obtained under cobalt-blue light illumination **(B)**, and points to the ulcer area in the OCT scan detected over the thinnest area at baseline **(C)**. **(D–F)** Images show the progression at Week 4, and the yellow arrows point to the epithelial edges. **(G–I)** Images were acquired at the end of the treatment at Week 8. The white arrows point to the change in CT detected by the AS-OCT scan **(C,F,I)**.

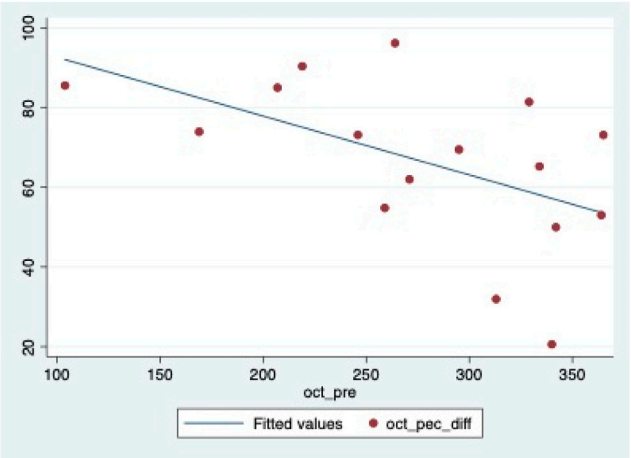

GRAPH 1 | Scattergram representing the association between pre-treatment CT and gain in CT at the end of the treatment.

TABLE 3 | Linear regression analysis. Outcome: percentage change in CT at the end of cenegermin treatment.

	Coefficient	95% CI	*p*-value
Age, years	–0.35	–0.88 to 0.18	0.179
Gender, female	–9.35	–33.60 to 14.90	0.422
Healing time, weeks	4.88	–14.12 to 23.87	0.591
Area pre-treatment, mm^2	0.04	–0.15 to 0.24	0.631
CT pre-treatment, μm	–0.15	–0.28 to –0.02	0.035

high signal on AS-OCT, looking different from the normal corneal stroma. Second, the scar tissue disappeared on slit-lamp examination, suggesting that the cornea healing process had switched from an acute wound healing stage to a remodeling one. Utsunomiya et al. (2014) had stated that a long-term AS-OCT hyper-reflectivity persists even when the cornea clears up on slit-lamp examination, and they supposed it could be due to the scar tissue's incapacity to come back to the original arrangement.

The characteristic of scar tissue is an abnormal alignment of the collagen fibrils, directly associated with the tissue's transparency (Zhou et al., 2017). In our case series, we also observed that the younger the patient was, the faster the scar tissue formation, and the less time-consuming the process was to restore transparency. It is only a clinical remark, and there is no statistical significance for the small number of patients. It could mean an age-related cornea healing capacity, confirming age-related changes in the human cornea described in the literature (Marr, 1967; Alvarado et al., 1983; Faragher et al., 1997; Berlau et al., 2002; Roszkowska et al., 2004; Niederer et al., 2007; Gipson, 2013; Bonzano et al., 2021). Mechanisms underlying an age-related slowdown of collagen synthesis in damaged stroma have not been fully delineated yet.

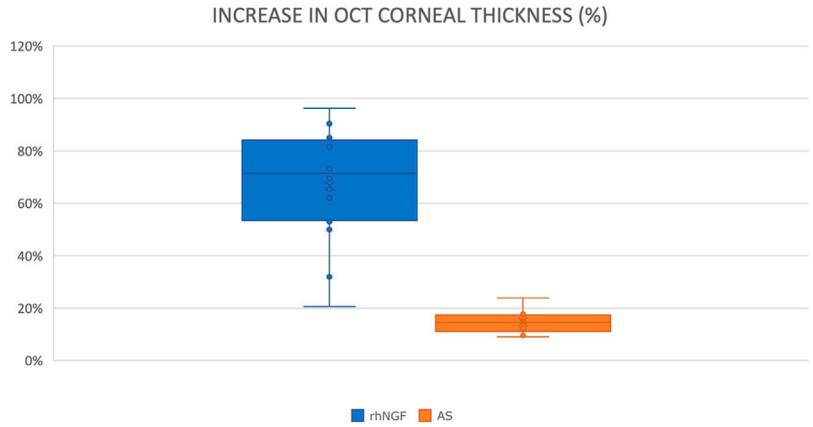

GRAPH 2 | Box plot representing the difference of percentage AS-OCT increase in corneal thickness between the cenegermin (rh-NGF) group and the AS group.

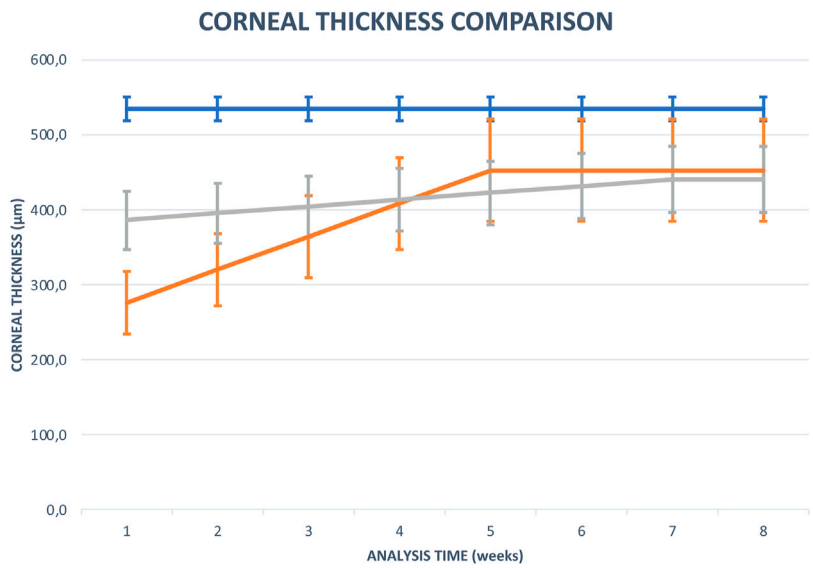

GRAPH 3 | Comparison chart of the mean CT at each time point during the treatment period (8 weeks) between the cenegermin group (orange line), the AS group (gray line), and 16 healthy corneas (blue line).

Both cenegermin and AS eye drops proved to be effective in treating NK from different etiologies. Thanks to its biomechanical and biochemical properties, similar to natural tears (Geerling and Hartwig, 2002), the serum has gained wide acceptance in treating ocular surface disorders unresponsive to conventional medical treatment (Tsubota et al., 1999; Matsumoto et al., 2004; Bonzano et al., 2018). Epithelial growth factors such as vitamin A, fibronectin, epidermal growth factor, transforming growth factor b, substance P, and insulin-like growth factor-1 in serum could explain its efficacy in healing cornea lesion, which is usually associated with an already compromised ocular surface (Matsumoto et al., 2004).

Cenegermin in our patients proved to heal the NK faster than the AS and prevent NK recurrence in the 12-months follow-up. According to literature data, this could be explained thanks to the ability of cenegermin in inducing corneal recovery by restoring sensory nerve supply (Bonini et al., 2018b; Pflugfelder et al., 2020).

Both treatments proved to heal NK within 8 weeks in our patients, but with different mechanisms: AS seems to restore the ocular surface providing some neural healers when administered (Matsumoto et al., 2004) and, in four cases, it required to be continued over time to maintain healing; cenegermin, by addressing the underlying cause, induces recovery of corneal nerves, and then it seems to ensure a stable framework even when discontinued with less risk of recurrence (Sacchetti et al., 2021). As recently reported by Pflugfelder et al. (2020), variables such as disease stage, time since diagnosis, and underlying

etiologies did not significantly affect the healing status. Furthermore, in our patients, as reported in the literature, no initial NK lesion size (Pflugfelder et al., 2020) impacted significantly; conversely, the pre-treatment cornea thickness detected by AS-OCT was associated with the percentage increase of CT. Therefore, monitoring the healing improvements in terms of thickness and transparency of the cornea by AS-OCT could help understand the corneal healing response to cenegermin.

We used RTVue-100 for AS-OCT that is a spectral-domain OCT that was developed for the retinal analysis. This instrument uses an 840-nm wavelength beam. We are aware that other specialized AS-OCTs by using a 1310-nm wavelength could be more performing (Georgeon et al., 2021). Anyway, RTVue-100 allowed us to detect detailed scans of the corneal healing process and its improvements over time. Thanks to its dedicated caliper tool, it also allowed us to accurately document changes by measuring the stromal thickness at the thinnest part. AS-OCT is an effective tool for systematic anterior-segment imaging, allowing the detailed detection of the front-to-back layered corneal structure for quantitative analysis and monitoring of the healing process (David et al., 2021). Using AS-OCT granted us quantitative monitoring of structural changes in NK treated by cenegermin, obtaining a better understanding of rh-NGF–driven corneal wound healing process.

DATA AVAILABILITY STATEMENT

The raw data supporting the conclusion of this article will be made available by the authors, without undue reservation.

ETHICS STATEMENT

This study was conducted in accordance with the Declaration of Helsinki. The protocol was reviewed and approved by the institutional independent ethics committee (code 0782019). Written informed consent from the participants was not required to participate in this study in accordance with the national legislation and the institutional requirements. However, the details of the study were explained to the patients and written informed consent was obtained from the individuals for the publication of any potentially identifiable images or data included in this article.

AUTHOR CONTRIBUTIONS

BC: designed and directed the study. CB, SO, AM, and DS: acquisition and interpretation of data for the work. CC and EB: provided critical feedback and statistical analysis. CB, DB, EB, and CT: review and editing of the final manuscript. All authors reviewed the manuscript and agreed with its content.

REFERENCES

Alafaleq, M., Knoeri, J., Boutboul, S., and Borderie, V. (2021). Contact Lens Induced Bacterial Keratitis in LCD II: Management and Multimodal Imaging: a Case Report and Review of Literature. *Eur. J. Ophthalmol.* 31 (5), 2313–2318. doi:10.1177/1120672120968724

Alvarado, J., Murphy, C., and Juster, R. (1983). Age-Related Changes in the Basement Membrane of the Human Corneal Epithelium. *Invest. Ophthalmol. Vis. Sci.* 24 (8), 1015–1028.

Arumuganathan, N., Wiest, M. R. J., Toro, M. D., Hamann, T., Fasler, K., and Zweifel, S. A. (2021). Acute and Subacute Macular and Peripapillary Angiographic Changes in Choroidal and Retinal Blood Flow post-intravitreal Injections. *Sci. Rep.* 11 (1), 19381. doi:10.1038/s41598-021-98850-8

Berlau, J., Becker, H. H., Stave, J., Oriwol, C., and Guthoff, R. F. (2002). Depth and Age-Dependent Distribution of Keratocytes in Healthy Human Corneas: A Study Using Scanning-Slit Confocal Microscopy *In Vivo*. *J. Cataract Refract Surg.* 28 (4), 611–616. doi:10.1016/s0886-3350(01)01227-5

Bonini, S., Lambiase, A., Rama, P., Filatori, I., Allegretti, M., Chao, W., et al. (2018). Phase I Trial of Recombinant Human Nerve Growth Factor for Neurotrophic Keratitis. *Ophthalmology* 125 (9), 1468–1471. doi:10.1016/j.ophtha.2018.03.004

Bonini, S., Lambiase, A., Rama, P., Sinigaglia, F., Allegretti, M., Chao, W., et al. (2018). Phase II Randomized, Double-Masked, Vehicle-Controlled Trial of Recombinant Human Nerve Growth Factor for Neurotrophic Keratitis. *Ophthalmology* 125 (9), 1332–1343. doi:10.1016/j.ophtha.2018.02.022

Bonzano, C., Bonzano, E., Cutolo, C. A., Scotto, R., and Traverso, C. E. (2018). A Case of Neurotrophic Keratopathy Concomitant to Brain Metastasis. *Cureus* 10 (3), e2309. doi:10.7759/cureus.2309

Bonzano, C., Cutolo, C. A., Musetti, D., Di Mola, I., Pizzorno, C., Scotto, R., et al. (2021). Delayed Re-epithelialization after Epithelium-Off Crosslinking: Predictors and Impact on Keratoconus Progression. *Front. Med.* 8, 657993. doi:10.3389/fmed.2021.657993

Carnevali, A., Giannaccare, G., Gatti, V., Battaglia, C., Randazzo, G., Yu, A. C., et al. (2021). Retinal Microcirculation Abnormalities in Patients with Systemic Sclerosis: An Explorative Optical Coherence Tomography Angiography Study. *Rheumatology (Oxford)* 60 (12), 5827–5832. doi:10.1093/rheumatology/keab258

Ceravolo, I., Oliverio, G. W., Alibrandi, A., Bhatti, A., Trombetta, L., Rejdak, R., et al. (2020). The Application of Structural Retinal Biomarkers to Evaluate the Effect of Intravitreal Ranibizumab and Dexamethasone Intravitreal Implant on Treatment of Diabetic Macular Edema. *Diagnostics (Basel)* 10 (6), E413. doi:10.3390/diagnostics10060413

Chisari, C. G., Toro, M. D., Cimino, V., Rejdak, R., Luca, M., Rapisarda, L., et al. (2019). Retinal Nerve Fiber Layer Thickness and Higher Relapse Frequency May Predict Poor Recovery after Optic Neuritis in MS Patients. *J. Clin. Med.* 8 (11), 2022. doi:10.3390/jcm8112022

Cintron, C., Hong, B. S., Covington, H. I., and Macarak, E. J. (1988). Heterogeneity of Collagens in Rabbit Cornea: Type III Collagen. *Invest. Ophthalmol. Vis. Sci.* 29 (5), 767–775.

David, C., Reinstein, D. Z., Archer, T. J., Kallel, S., Vida, R. S., Goemaere, I., et al. (2021). Postoperative Corneal Epithelial Remodeling after Intracorneal Ring Segment Procedures for Keratoconus: An Optical Coherence Tomography Study. *J. Refract Surg.* 37 (6), 404–413. doi:10.3928/1081597X-20210225-02

Dua, H. S., Said, D. G., Messmer, E. M., Rolando, M., Benitez-del-Castillo, J. M., Hossain, P. N., et al. (2018). Neurotrophic Keratopathy. *Prog. Retin. Eye Res.* 66, 107–131. doi:10.1016/j.preteyeres.2018.04.003

European Medicines Agency (2021). EU/3/15/1586 | European Medicines Agency. Available at: https://www.ema.europa.eu/en/medicines/human/orphan-designations/eu3151586 (Accessed July 6, 2017).

Faragher, R. G., Mulholland, B., Tuft, S. J., Sandeman, S., and Khaw, P. T. (1997). Aging and the Cornea. *Br. J. Ophthalmol.* 81 (10), 814–817. doi:10.1136/bjo.81.10.814

Geerling, G., and Hartwig, D. (2002). Autologous Serum-Eye-Drops for Ocular Surface Disorders. A Literature Review and Recommendations for Their Application. *Ophthalmologe* 99, 949–959. doi:10.1007/s00347-002-0661-6

Georgeon, C., Marciano, I., Cuyaubère, R., Sandali, O., Bouheraoua, N., and Borderie, V. (2021). Corneal and Epithelial Thickness Mapping: Comparison of Swept-Source- and Spectral-Domain-Optical Coherence Tomography. *J. Ophthalmol.* 2021, 1–6. doi:10.1155/2021/3444083

Gipson, I. K. (2013). Age-Related Changes and Diseases of the Ocular Surface and Cornea. *Invest. Ophthalmol. Vis. Sci.* 54 (14), ORSF48. doi:10.1167/iovs.13-12840

Hassell, J. R., and Birk, D. E. (2010). The Molecular Basis of Corneal Transparency. *Exp. Eye Res.* 91 (3), 326–335. doi:10.1016/j.exer.2010.06.021

Ishibazawa, A., Igarashi, S., Hanada, K., Nagaoka, T., Ishiko, S., Ito, H., et al. (2011). Central Corneal Thickness Measurements with Fourier-Domain Optical Coherence Tomography versus Ultrasonic Pachymetry and Rotating Scheimpflug Camera. *Cornea* 30 (6), 615–619. doi:10.1097/ICO.0b013e3181d00800

Jeng, B. H., and Ahmad, S. (2021). In Pursuit of the Elimination of Corneal Blindness: Is Establishing Eye Banks and Training Surgeons Enough. *Ophthalmology* 128 (6), 813–815. doi:10.1016/j.ophtha.2020.06.042

Kamma-Lorger, C. S., Boote, C., Hayes, S., Albon, J., Boulton, M. E., and Meek, K. M. (2009). Collagen Ultrastructural Changes during Stromal Wound Healing in Organ Cultured Bovine Corneas. *Exp. Eye Res.* 88 (5), 953–959. doi:10.1016/j.exer.2008.12.005

Koman-Wierdak, E., Róg, J., Brzozowska, A., Toro, M. D., Bonfiglio, V., Załuska-Ogryzek, K., et al. (2021). Analysis of the Peripapillary and Macular Regions Using OCT Angiography in Patients with Schizophrenia and Bipolar Disorder. *J. Clin. Med.* 10 (18), 4131. doi:10.3390/jcm10184131

Kowalczyk, M., Toro, M. D., Rejdak, R., Załuska, W., Gagliano, C., and Sikora, P. (2020). Ophthalmic Evaluation of Diagnosed Cases of Eye Cystinosis: A Tertiary Care Center's Experience. *Diagnostics (Basel)* 10 (11), 911. doi:10.3390/diagnostics10110911

Marr, M. (1967). Zur Altersabhngigkeit der Heilung von Hornhautepitheldefektenngigkeit der Heilung von Hornhautepitheldefekten. *Albrecht von Graefes Arch. Klin. Ophthalmol.r Klin Exp. Ophthalmol.* 173 (3), 250–255. doi:10.1007/bf00410848

Mastropasqua, L., Massaro-Giordano, G., Nubile, M., and Sacchetti, M. (2017). Understanding the Pathogenesis of Neurotrophic Keratitis: The Role of Corneal Nerves. *J. Cel Physiol* 232 (4), 717–724. doi:10.1002/jcp.25623

Mastropasqua, L., Nubile, M., Lanzini, M., Calienno, R., and Dua, H. S. (2019). *In Vivo* microscopic and Optical Coherence Tomography Classification of Neurotrophic Keratopathy. *J. Cel Physiol* 234 (5), 6108–6115. doi:10.1002/jcp.27345

Matsumoto, Y., Dogru, M., Goto, E., Ohashi, Y., Kojima, T., Ishida, R., et al. (2004). Autologous Serum Application in the Treatment of Neurotrophic Keratopathy. *Ophthalmology* 111, 1115–1120. doi:10.1016/j.ophtha.2003.10.019

Maurice, D. M. (1957). The Structure and Transparency of the Cornea. *J. Physiol.* 136 (2), 263–286. doi:10.1113/jphysiol.1957.sp005758

McCally, R. L., Freund, D. E., Zorn, A., Bonney-Ray, J., Grebe, R., de la Cruz, Z., et al. (2007). Light-Scattering and Ultrastructure of Healed Penetrating Corneal Wounds. *Invest. Ophthalmol. Vis. Sci.* 48 (1), 157–165. doi:10.1167/iovs.06-0935

Meek, K. M. (2009). Corneal Collagen-Its Role in Maintaining Corneal Shape and Transparency. *Biophys. Rev.* 1 (2), 83–93. doi:10.1007/s12551-009-0011-x

Muscat, S., McKay, N., Parks, S., Kemp, E., and Keating, D. (2002). Repeatability and Reproducibility of Corneal Thickness Measurements by Optical Coherence Tomography. *Invest. Ophthalmol. Vis. Sci.* 43 (6), 1791–1795.

Niederer, R. L., Perumal, D., Sherwin, T., and McGhee, C. N. (2007). Age-related Differences in the normal Human Cornea: A Laser Scanning *In Vivo* Confocal Microscopy Study. *Br. J. Ophthalmol.* 91 (9), 1165–1169. doi:10.1136/bjo.2006.112656

Nubile, M., Dua, H. S., Lanzini, M., Ciancaglini, M., Calienno, R., Said, D. G., et al. (2011). *In Vivo* analysis of Stromal Integration of Multilayer Amniotic Membrane Transplantation in Corneal Ulcers. *Am. J. Ophthalmol.* 151 (5), 809–822. doi:10.1016/j.ajo.2010.11.002

Pflugfelder, S. C., Massaro-Giordano, M., Perez, V. L., Hamrah, P., Deng, S. X., Espandar, L., et al. (2020). Topical Recombinant Human Nerve Growth Factor (Cenegermin) for Neurotrophic Keratopathy: A Multicenter Randomized Vehicle-Controlled Pivotal Trial. *Ophthalmology* 127 (1), 14–26. doi:10.1016/j.ophtha.2019.08.020

Reibaldi, M., Uva, M. G., Avitabile, T., Toro, M. D., Zagari, M., Mariotti, C., et al. (2012). Intrasession Reproducibility of RNFL Thickness Measurements Using SD-OCT in Eyes with Keratoconus. *Ophthalmic Surg. Lasers Imaging* 43 (6 Suppl. l), S83–S89. doi:10.3928/15428877-20121001-04

Roszkowska, A. M., Colosi, P., Ferreri, F. M., and Galasso, S. (2004). Age-Related Modifications of Corneal Sensitivity. *Ophthalmologica* 218 (5), 350–355. doi:10.1159/000079478

Sacchetti, M., Komaiha, C., Bruscolini, A., Albanese, G. M., Marenco, M., Colabelli Gisoldi, R. A. M., et al. (2021). Long-term Clinical Outcome and Satisfaction Survey in Patients with Neurotrophic Keratopathy after Treatment with Cenegermin Eye Drops or Amniotic Membrane Transplantation. *Graefes Arch. Clin. Exp. Ophthalmol* [Epub ahead of print]. doi:10.1007/s00417-021-05431-6

Sacchetti, M., and Lambiase, A. (2014). Diagnosis and Management of Neurotrophic Keratitis. *Clin. Ophthalmol.* 8, 571–579. doi:10.2147/OPTH.S45921

Semeraro, F., Forbice, E., Romano, V., Angi, M., Romano, M. R., Filippelli, M. E., et al. (2014). Neurotrophic Keratitis. *Ophthalmologica* 231 (4), 191–197. doi:10.1159/000354380

Toro, M., Choragiewicz, T., Posarelli, C., Figus, M., and Rejdak, R. (2020). Early Impact of COVID-19 Outbreak on the Availability of Cornea Donors: Warnings and Recommendations. *Clin. Ophthalmol.* 14, 2879–2882. doi:10.2147/OPTH.S260960

Tsubota, K., Goto, E., Shimmura, S., and Shimazaki, J. (1999). Treatment of Persistent Corneal Epithelial Defect by Autologous Serum Application. *Ophthalmology* 106, 1984–1989. doi:10.1016/S0161-6420(99)90412-8

Utsunomiya, T., Hanada, K., Muramatsu, O., Ishibazawa, A., Nishikawa, N., and Yoshida, A. (2014). Wound Healing Process after Corneal Stromal Thinning Observed with Anterior Segment Optical Coherence Tomography. *Cornea* 33 (10), 1056–1060. doi:10.1097/ICO.0000000000000223

Venkateswaran, N., Galor, A., Wang, J., and Karp, C. L. (2018). Optical Coherence Tomography for Ocular Surface and Corneal Diseases: A Review. *Eye Vis. (Lond)* 5 (1), 13. doi:10.1186/s40662-018-0107-0

Wiest, M. R. J., Toro, M. D., Nowak, A., Baur, J., Fasler, K., Hamann, T., et al. (2021). Globotrioasylsphingosine Levels and Optical Coherence Tomography Angiography in Fabry Disease Patients. *J. Clin. Med.* 10 (5), 1093. doi:10.3390/jcm10051093

Wilson, S. L., El Haj, A. J., and Yang, Y. (2012). Control of Scar Tissue Formation in the Cornea: Strategies in Clinical and Corneal Tissue Engineering. *J. Funct. Biomater.* 3 (3), 642–687. doi:10.3390/jfb3030642

Zhou, H. Y., Cao, Y., Wu, J., and Zhang, W. S. (2017). Role of Corneal Collagen Fibrils in Corneal Disorders and Related Pathological Conditions. *Int. J. Ophthalmol.* 10 (5), 803–811. doi:10.18240/ijo.2017.05.24

Zweifel, S. A., Foa, N., Wiest, M. R. J., Carnevali, A., Zaluska-Ogryzek, K., Rejdak, R., et al. (2021). Differences between Mycobacterium Chimaera and Tuberculosis Using Ocular Multimodal Imaging: A Systematic Review. *J. Clin. Med.* 10 (21), 4880. doi:10.3390/jcm10214880

Conflict of Interest: The authors declare that the research was conducted in the absence of any commercial or financial relationships that could be construed as a potential conflict of interest.

Publisher's Note: All claims expressed in this article are solely those of the authors and do not necessarily represent those of their affiliated organizations, or those of the publisher, the editors, and the reviewers. Any product that may be evaluated in this article, or claim that may be made by its manufacturer, is not guaranteed or endorsed by the publisher.

Advantages of publishing in Frontiers

OPEN ACCESS
Articles are free to read for greatest visibility and readership

FAST PUBLICATION
Around 90 days from submission to decision

HIGH QUALITY PEER-REVIEW
Rigorous, collaborative, and constructive peer-review

TRANSPARENT PEER-REVIEW
Editors and reviewers acknowledged by name on published articles

Frontiers
Avenue du Tribunal-Fédéral 34
1005 Lausanne | Switzerland

Visit us: www.frontiersin.org
Contact us: frontiersin.org/about/contact

REPRODUCIBILITY OF RESEARCH
Support open data and methods to enhance research reproducibility

DIGITAL PUBLISHING
Articles designed for optimal readership across devices

FOLLOW US
@frontiersin

IMPACT METRICS
Advanced article metrics track visibility across digital media

EXTENSIVE PROMOTION
Marketing and promotion of impactful research

LOOP RESEARCH NETWORK
Our network increases your article's readership